CLASSIFICATION AND GENETIC ANALYSIS OF HUMAN FACIAL FEATURES

Michelle Caroline McCulley

December 2000

Thesis submitted for the degree of
Doctor of Philosophy in the University of London

MRC Human Biochemical Genetics Unit
The Galton Laboratory
University College London
University of London

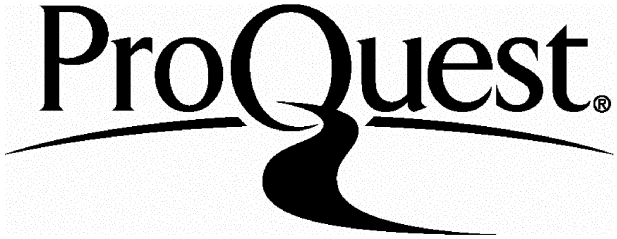

ABSTRACT

This thesis considers normal person to person variation in facial features, as opposed to aberrant variation usually classified as dysmorphology. An attempt has been made to categorise the face simply, as a combination of a relatively small number of variable components, in an attempt to reduce the complexity of individual appearance and make the face more amenable to genetic analysis.

Three-dimensional facial data have been collected from over 1000 individuals, both unrelated individuals and family groups, using two types of optical surface scanner and the merits of these systems were evaluated. Methods of analysing the data were investigated, a traditional landmark approach was used for direct measurement of various facial dimensions and novel techniques exploring properties of surface geometry were used to delineate the face into areas of similar shape to facilitate discrete classification.

Aspects of midline features including the chin cleft and nose were classified into discrete categories and analysed at both the population and family level. When tested for Mendelian segregation in available family data (two-parent plus offspring families), the nose band classification fitted to an autosomal dominant model of inheritance (40 families) and the chin cleft fitted to an autosomal co-dominant model (49 families studied).

The majority of subjects analysed were normal individuals but a small set of patients (n=14) with Medullary Sponge Kidney (MSK) were investigated in order to explore face scanning as an objective diagnostic tool. Minor asymmetry of the face, previously described in MSK, was assessed using two landmark-based approaches but was not found to be significant compared with matched controls.

The analysis and measurements made to establish phenotypic classification of the face have enabled preliminary genotype-phenotype association studies to be performed. Polymorphisms in 2 candidate genes were typed and analysed in a set of up to 97 scanned unrelated subjects where DNA had been collected. Although no significant associations were found this demonstrated the practical feasibility of such an approach for identifying genes responsible for facial variation.

This project provides a novel perspective on addressing the complexity of the genetics of facial variation. The classifications described in this thesis have made aspects of individuality amenable to association and family studies and open the way for the development of larger-scale initiatives to identify genes responsible for facial appearance.

ACKNOWLEDGEMENTS

I would like to thank Professor David Hopkinson for allowing me the opportunity to work with him on this project. His enthusiasm, advice and friendship have made the duration of this thesis thoroughly enjoyable. I am also very grateful to Dr David Whitehouse and Professor Yvonne Edwards for their time, experience and advice. I must also thank all my colleagues in the lab, especially Wendy Putt and Ira Islam for their help and patience.

This thesis would not have been possible without the co-operation of the UCL Medical Graphics and Imaging group of Dr Alf Linney, and Professor Jim Moss. I am especially grateful to Dr Robin Richards for his excellent support and advice on all aspects of scanning and analysis and for allowing me to use his CLOUD software. I am also grateful to Dr Robin Hennessy for providing the LSMVIEW software.

A special thank-you must also be given to my family and friends especially my mum for putting up with me for the last three months, and my brother James for keeping me sane. Last, but by no means least I want to thank Ramsey for his love and encouragement as well as for reading this thesis.

This work was supported jointly by the Medical Research Council and the Forensic Science Service of the UK Home Office.

CONTENTS

FIGURES

Chapter 5

Chapter 6

Chapter 7

Chapter 8

TABLES

Chapter 6

Chapter 7

Chapter 8

Abbreviations

bp	base pair
cDNA	complementary deoxyribonucleic acid
CI	Confidence Interval
DNA	deoxyribonucleic acid
dNTP	deoxynucleoside triphosphate
EDTA	ethylenediaminetetraacetic acid
EST	expressed sequence tag
EtBr	Ethidium Bromide
g	grams
HBGU	Human Biochemical Genetics Unit
HLS	hand held laser scanner
kb	kilobase
lsm	laser scan multiple; data from fixed scanner
M	molar
Mb	Megabases
MGI	Medical Graphics and Imaging
mm	millimetre
mM	millimolar
MRC	Medical Research Council
mRNA	messenger ribonucleic acid
ng	nanograms
nt	nucleotides
obj	object(wavefront) file; export data from hls
PCR	polymerase chain reaction
psi	pounds per square inch
RNA	ribonucleic acid
SDS	sodium dodecyl sulphate
SI	shape index
SSCP	single strand conformation polymorphism

STA	surface type analysis
TBE	tris/borate/EDTA buffer
TEMED	N, N, N^1, N^1-tetramethylethylenediamine
Tm	melting temperature
Tris	2-amino-2 (hydroxymethyl)-propane-1, 3-diol
UCL	University College London
UTR	un-translated
UV	ultraviolet
v/v	volume to volume
w/v	weight per volume
µg	microgram
µl	microlitre
µM	micromolar
°C	degrees centigrade
3D	Three dimensional

CHAPTER 1

Introduction

The overall aim of this thesis is to attain some understanding of the relationship between the variation in facial appearance and the underlying genetic constitution. Although humans are extremely complex it is possible to view our genome as an extensive series of simple assembly instructions that progressively act to generate a complex organism. Genes are the starting points; the genes encode proteins, which in turn contribute specific qualities to cells such as polarity, adhesion, reception to signals, and metabolism. In normal development a cell lineage becomes established, cells interact and morphogenesis, histogenesis and growth result in the complex phenotype. It is from deploying a relatively limited range of basic cell properties in various ways that a vast range of complex phenotypes can be built.

This project has taken advantage of recent developments in both Medical Physics (3D image capture and analysis) and Human Genetics (gene identification and function analysis). Information from these separate disciplines has been combined in this thesis to produce basic groundwork towards making the face more amenable to genetic analysis. The remainder of this introduction is organised into two parts; the first chapter is focused on the description of methods of analysis (including physical techniques as well as an

account of normal variation) while the second chapter concerns the biology of the face (including anatomy, embryology, and abnormal development).

The appearance of the human face has been fundamental to both biological and social functioning since the origin of the species. There are several obvious and basic functions of the face, which have evolved in humans and other primates to a great extent. The face is the focal point for communication contributing to speech, expression, emotion and recognition as well as being the hub for nutrition, respiration and the special senses. Our ability to recognise and identify other individuals is dependent on finely tuned analysis of person to person variation in facial features, which makes us each unique.

The genetic elements of facial features were inadvertently recognised well before the actual concept of genes was documented and it is common for parents and other relatives to recognise and comment on familial features in a newborn baby. Kin resemblance, recognition of 'identical' twins, anthropometric studies and racial stereotypes of different populations are all indirect attempts at defining the genetic basis for normal variation in the human face.

From the late nineteenth century the study of phenotypic variation and heredity in man went into overdrive with statistical analysis of numerous traits, both quantitative and qualitative brought under scrutiny. These are exemplified by the range of topics

investigated by Francis Galton and include studies of twins (Galton 1875), transmission of acquired habits (Galton 1889), eugenics (Galton 1909), fingerprints (Galton 1891), and his famous publication Heredity Genius (Galton 1869). The turn of the century also brought a renewed interest in the phenotypic variation of human faces, in particular facial pathology and dysmorphology, coinciding with the rediscovery of Mendelian laws. There was a well-known dispute between Galton and Bateson, a Mendelian geneticist, concerning the genetic aetiology of physical deformities. Galton believed that characteristics such as cleft lip and palate were signs of physical and racial degeneracy where as Bateson attributed such characteristics to Mendelian inheritance (cited by Melnick 1997). Galton gave much thought to the inheritance of physical attributes in normal subjects, and actively encouraged members of the general population to record their personal information relating to growth and development (including height, eye colour and temperament) in a family album termed 'Record of Family Faculties' (Galton 1884).

This century several attempts have been made to try to classify and describe various aspects and individuality of the head and face for clinical, anthropological and forensic purposes. For instance, Galton devised a method of numeralising facial profiles for individual identification; a subject's profile could be described by four quintets of numbers referring to both physical measurements and subjective features of their profile (Galton 1910). Early work carried out on the

genetic basis of morphological variation in general (Osborne and De George 1959) used twin studies, not dissimilar to those carried out by Galton, concentrating on the problem of heredity versus environment. This study found that generally anthropometric measurements showed the strongest genetic component when the measurements were taken along the longitudinal axis, i.e. height measurements. They concluded that the following measurements were good measures of 'genetic only' influences in both sexes: upper face height, nose height, head height, and bigonial breadth. More recent studies (Devor 1987), concentrating on the face as a singular complex object, addressed the problem caused by gene-environment interactions and used more complex statistical approaches based on measurements of face width and height in an attempt to identify and define heritability of craniofacial dimensions. They concluded that it was very difficult to differentiate the gene-dependent component of facial similarity from other environmentally dependent factors.

Much of the work done on facial classification has been based on measurements between an extensive repertoire of landmarks, described in detail in many books (Hrdlicka, 1920; Farkas, 1994). Such measures have been used, directly or to produce average faces in numerous studies including analysis of dysmorphology (Zumpano et al 1999), facial asymmetry (Shaner et al 2000), sexual dimorphism (Rao and Suryawanshi 1998), ethnic variation in facial form (Miyajima 1996), and attractiveness (Perrett et al 1998). While there

is relatively little change in the positioning of anatomical landmarks used, methods incorporating thin plate splines have been developed to increase the repertoire of points available for analysis, especially where there are no obvious anatomical landmarks (Bookstein 1997).

There are numerous techniques for statistical interpretation of landmark data sets, aside from straightforward calculations of angles and distances, popular methods include; Procrustes analysis (Mosier 1939), deformation/transformation grids (Thompson 1917 Bookstein 1977) and Euclidean distance matrix analysis (EDMA) (Lele 1993). These methods explore variability within and between data sets by estimating average shape, looking at shape change and provide information on the direction and extent of shape change between data. Such methods have been applied to clinical pathology, to try to describe the physical difference between normal and abnormal and aid diagnosis and management of dysmorphology. Applications include studies of sexual dimorphism (Ferrario et al 1994), abnormal craniofacial growth (Richtsmeier and Lele 1990), cleft lip and palate (McAlarney and Chiu 1997), and malocclusion of the mandible (Singh et al 1998). These approaches have also been applied in anthropological studies of human evolution (Bookstein et al 1999), as well as in studies of related individuals (Byard et al 1985).

Genetics has advanced at a phenomenal rate: on 25th June 2000 the two groups working on sequencing the whole human genome, Human Genome Project and Celera Genomics, jointly

announced that they had completed initial sequencing of the human genome ahead of schedule. The fully finished high quality sequence is expected to be available within three years. Methods for genetic analysis such as whole genome scans now mean that the task of linking genes with facial features is not so formidable as previously envisaged. With the sequence practically known more efforts will be focused on identifying and characterising genes and gene products. Extensive work on a range of model organisms, has provided us with an understanding of the 'building block' genes, such as the Hox genes, which are considered to be a broadly conserved developmental starting point in chordates (Veraksa et al 2000). The advances made in understanding the effects of these genes, their products and interactions have benefited the understanding of human development. The genetic basis of a large number of human pathological and dysmorphological conditions is now known with at least 40 craniofacial syndromes having a well-defined genetic aetiology (Winter 1996).

Advances in computer technology have led to the development of a 3D optical surface scanner that is used to record, with a high degree of accuracy, the surface shape of the face (Arridge et al 1985). The scan data provide a permanent record of facial morphology and this, coupled with the development of new shape analysis software, has meant that now it is possible to view variation in human face shape in a number of new and different ways. This, together with

progress in human genetics, increases the feasibility of linking facial phenotype with DNA genotype.

1.1 Analysis of facial features

The fascination with the analysis and description of the human face is reflected in a vast amount and range of literature. There are many books devoted to this subject including; The Face (McNeil 1998), In the Eye of the Beholder (Bruce and Young 1998), About Face (Cole 1997), The Human Face (Liggett 1974) and Biology and Cognitive Development: The case of face recognition (Johnson and Morton 1991). These together with additional information have been sourced to provide a brief history of the quantification of human facial features.

1.1.1 Historical introduction of interest in the face

From ancient to modern times the face has been the subject of wonder. Egyptian artists used grid systems in order to draw heads to ideal proportions (cited by Robins 1994), and these ancient methods are not greatly dissimilar to those described by Moorrees et al (1976) to aid cephalometric analysis.

Ancient Greeks were interested in formulating rules to define beauty. They used geometry to record and analyse basic dimensions and proportions of the face (Beardsley 1966). Aristotle made reference to this when defining genus: 'APART FROM SUPERFICIAL CHARACTERS, THE ESSENTIAL DIFFERENCES BETWEEN SPECIES ARE MERELY

DIFFERENCES OF PROPORTION, OF RELATIVE MAGNITUDE OR OF EXCESS AND DEFECT'.

Pythagoros, Plato, Euclid and other eminent figures identified the 'golden section' which they believed were the proportions that produced optimum visual harmony. These ratios were thought to be centred on the number 1.618, or its reciprocal 0.618, which also describes the ratio of successive numbers in the series described by the Italian mathematician Leonardo Fibonacci (cited by Ricketts 1982); it is also referred to as phi. Early Japanese Buddhists also believed there was a number which described perfect proportions, for them it was 1.414 or the square root of two (Nakajima et al 1985).

In medieval times superstitions focused on the occult, and subjects such as fortune and character depiction through phrenology and facial features are well documented. These interests in phrenology and physiognomy have persisted up until relatively recent times; continuing through the eighteenth (Laveter 1789), nineteenth (Cross 1817), and twentieth (Burr 1935) centuries. Modern studies analogous to these works include efforts to map cognitive function (Terrazas and McNaughton 2000) and studies of recognition and perception of facial expression (Hassin and Trope 2000).

The renaissance period brought the integration of art and science and a resurgence of efforts to describe mathematically facial form and beauty. Leonardo da Vinci's treatise on painting (published after his death, Parigi 1651), entitled 'Trattato della pittura' included

a guide to artists addressing the problem of accurately representing the face. The book focused on describing various ratios and proportions of the human face. For example it shows how the face could be broken up into four main parts; the forehead, nose, mouth and chin. Da Vinci acknowledged the complexity of the nose and rationalised its description using three variable properties (straight, concave and complex) which in various combinations gives a gradually more complex structure. Leonardo's so-called grotesque heads are also closely linked with this treatise. They have been described as caricatures; but actually, they are variations of the human face in its gradations between the extremes of beautiful and ugly, normal and abnormal, dignified and vulgar. They also relate to anatomical-physiological studies, in which old age is contrasted with youth.

Da Vinci's work inspired the German mathematician and artist, Albrecht Durer, to produce very detailed studies of human proportion. Durer came to the conclusion that the face resembled a multifaceted formation, consisting of small geometric areas, which are joined in various angles. After his death in 1528, his major work 'Four books on human proportions' was published, giving systems for measurement and guides to the proportions of different parts of the body including the head (Durer 1528).

Both Da Vinci and Durer were interested in transformation. For example, Da Vinci's works included detailed drawings showing the

transformation of a lion head into that of a man. These ideas inspired the Scotsman D'arcy Thompson to describe his transformation grids, which provided a primer to many of the modern methods of statistical interpretation of variation between two forms. Thompson observed that there only a few generic shapes repeatedly used by nature. These shapes are greatly modified by slight variations in their physical and chemical environment during growth and development. He drew two different species of crab, and superimposed a grid over each and by mathematical transformation of the co-ordinates showed how a great variety of crab shapes might be produced from just one generic crab pattern (Thompson 1917). This pioneering work, which basically involved recording the differences between forms as distortions in co-ordinate grids, was very hard to reproduce up until recently when Bookstein (1977) introduced the concept of biorthogonal grids.

The face has also been important in the field of forensic science as a tool for identification and more controversially as an index of criminality. Cesare Lombroso, an Italian physician, psychiatrist and criminologist, caused an uproar with the publication of his book 'L'uomo delinquente' (Criminal Man 1911). In this work, Lombroso used Darwinian ideas of evolution to explain criminal behaviour. He measured and compared the heads of living and executed criminals against the skulls of apes, prehistoric humans and 'primitive' peoples. From his comparisons he concluded that criminals were victims of atavism and although he gradually came to think that

social factors were also significant in criminal disposition he still believed that at least forty percent of criminals were prisoners through their biological inheritance.

In mid-nineteenth century France, work carried out by Alphonse Bertillon was not so far removed from e-fit descriptions used for criminal identification today (Rhodes 1956). In 1882 Bertillon began using his system of criminal identification, on offenders detained at Paris's Palais de Justice. Essentially, the Bertillon system entailed photographing the subject looking directly at the camera, then in profile with the camera centred upon the right ear. Besides the two photographs, the height of the subject was recorded, together with the length of a foot, an arm and an index finger. By the early 1890s, Bertillon's techniques proved extremely useful and there are elements of this system still being used by police forces and immigration authorities around the world. Sir Francis Galton also experimented with photography and worked with Bertillon on recording both the face and the fingerprints of criminals. Galton also developed a technique for producing composite photographs, in order to generate an average criminal face and also an average family face to illustrate similarity in resemblance (Galton 1878).

Copies of photographic images were expensive to produce and postal services were unreliable, whereas measurements could be transmitted by telegraph. This prompted Galton to devise his method

of numeralising profiles in order to provide a means of communicating a good likeness of an individual via telegraph using a series of numerical couplets (Galton 1910). This described an individual appearance, in profile, in a format ideal for communication, illustrated in Figure 1.1.

The variations in facial features across populations have been much studied professionally by anthropologists. Standard measurements for sexes, ethnic groups, ages (Farkas and Munroe 1987) and normal asymmetries (Farkas and Cheung 1981) as well as growth standards and collections of normal physical measurements, (Hall et al 1989) from extensive descriptions of anthropometric measurements, have been collected. Such detailed anthropological records of facial dimensions have facilitated detailed reconstruction from skulls (Tyrrell et al 1997).

In addition to morphological interest in the face there is also a large body of literature on more dynamic aspects of the face such as emotion, recognition, perception, psychology and attractiveness. Darwin considered the cross-cultural perception of facial expression and emotion in his book entitled the 'The expression of emotion in man and animals', recently edited by Paul Ekman (Darwin, Edited by Ekman 1999). Human emotion and facial expression has been a focus for many psychological studies for example the famous experiments carried out by Charles Bell using electrical stimuli to artificially induce emotion in a subject.

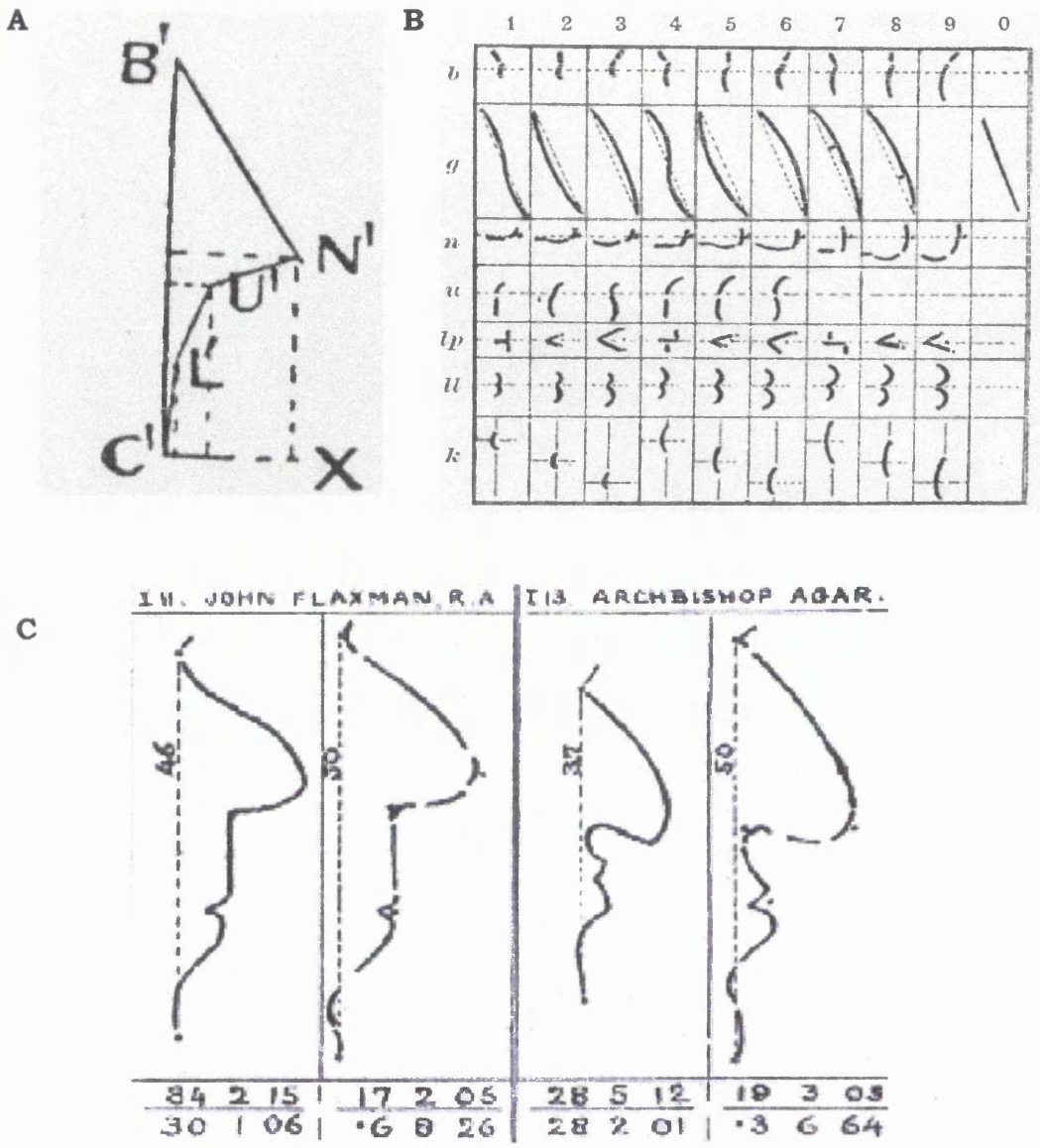

Figure 1.1 Galton's numeralised profiles for classification and recognition. A -anatomical landmarks used to make various facial height and width measurements. B - morphological description of facial parts. C - facial profiles standardised for size and described numerically. (Reproduced from paper by Galton, 1910)

The profile is written as follows: $\frac{\text{Nx n Ny}}{\text{Ux u Uy}} : \frac{\text{Lx lp Ly}}{\text{.b g ll k}}$ **. Nx, Ux and Lx are vertical measurements taken from the respective landmarks to the dropped perpendicular X, and Ny, Uy and Ly are horizontal measurements taken from the respective landmarks to the line B'C'(A). n describes the morphology under the nose, u describes the curvature of the area under the nose onto the upper lip, lp describes the protrusion of the upper and lower lips at rest, b describes the frontonasal curvature, g describes the profile of the nose, ll describes the size of the lips and k describes the curvature between the end of the lower lip and the mandible.**

Facial expression is an important variable for a large number of studies on human interaction and communication and has become a measure frequently used in numerous studies as many neurological and psychiatric disorders involve aberrations in expression, perception, or interpretation of facial action. Analysis of inappropriate facial expressions may provide evidence for the location and type of brain lesions, for example, recent work has shown that individuals with Huntington disease are very poor at recognising emotion, in particular disgust (Sprengelmeyer et al 1996).

There is a long history of research into face recognition and interpretation. However, as this present study is concerned with objective quantification of the structural features of the face as opposed to dynamically dependent properties, the fields of face recognition and interpretation are not developed further.

1.2 Methods for measurement of the face

1.2.1 Anthropometry

Anthropometry literally means 'measure human'. Anthropometry has been extensively applied in clinical analysis (Ward and Jamison 1991), especially of craniofacial dysmorphologies and in assessment of pre- and post-operative surgery to the head and neck (Farkas et al 1993). The primary goal in assessing craniofacial dysmorphology is to determine the morphological deviation from 'normal'. Patients are matched for age, sex and ethnicity and compared with a normal population. Generally the normal range is

taken as the mean value plus or minus two standard deviations, with the optimal range falling within one standard deviation (Farkas 1987).

In order to provide a quantitative assessment Farkas described a comprehensive set of 47 landmarks, a combination of classical anatomical landmarks as well as additional measuring points, to make linear and angular measurements of the head and face (Farkas 1994). Detailed measurements provide an adjunct to more subjective methodology. This is particularly relevant in the field of dysmorphology where there is a heavy reliance on the experienced clinician to recognise the overall 'gestalt' of a pathological facial phenotype. In order to acquire anthropometric measurements, callipers and measuring tape are used and the data are recorded directly from the subject. The main sources of error in this method arise from the inaccurate identification of landmarks, relative sizes of measurements (smaller distances have proportionally larger error), improper measuring and inadequate use of the measuring equipment (Jamison and Ward 1993). Additional drawbacks are that the subject is required to sit still for a long period of time while the measurements are being made and only one representation of the face is produced.

1.2.2 Photogrammetry

Photogrammetry depends on the collection of data from standard photographs. It is convenient and widely used in the medical sector (Kohout et al 1998; Bishara et al 1995). The main difficulty with photogrammetry is the accurate identification of the landmarks. Subtle variations in lighting or in the position of the subject when photographed make it very difficult to make accurate comparisons. It depends upon very careful standardisation of the size of the photograph and views of the subject (Nechala et al 1999). In a comparative study of 62 measurements, taken from photographs and living subjects, only 26 of the measurements were reliable from the photographs when compared to the 'living' subject (Farkas et al 1980). The best results from photographs were attained when the landmarks were placed physically on the face of the subjects.

1.2.3 Stereophotogrammetry

When the left and right eyes view the same image from their slightly different vantage points the brain perceives the image in terms of depth as well as lateral and vertical position. This is the basis of binocular vision and is exploited in stereophotogrammetric techniques that use two or more cameras at a fixed distance apart, to record the same object from slightly different viewpoints. The main problem for the analysis of facial surfaces is that it is difficult to represent parts of the face where there are no obvious features to register such as the cheeks and forehead. Companies such as

Cyberware and Tricorder have made significant progress in generating 3D images of the face from advanced stereophotogrammetric techniques. In one case, six cameras record the data. To help with the alignment of images from each camera, a pattern of speckled light points is projected onto the surface of the face. The location of the pattern from all vantage points is referenced to provide a 3D image. This technique has been used in several recent studies of the face including studies of facial asymmetry (Shaner et al 2000) and growth (Ras et al 1996).

Moiré photography is another non-invasive projection technique for obtaining 3D information from the face. It involves offsetting the light source and placing a light refracting transparent grid system in front of the face. The light projects through the grid twice, first on to the facial surface and then back through the grid to be captured by a camera. This generates an interference pattern of dark and light lines (fringes), each fringe represents a set of points equidistant from the grid. The fringes appear as a series of contour plots of similar depth on the facial surface. This has been used to evaluate craniofacial surgical correction (Chen and Iizuka 1995) and to generate normal facial measurements (Zhang et al 1990).

1.2.4 Recording 3D landmarks

These methods of 3D data capture rely on recording the x, y, z co-ordinates of each landmark to attain a spatial relationship between landmarks. The full description of the location of the

landmark requires information on both the position and the orientation of the point in relation to the body. There are currently two methods; contact and non-contact. Contact techniques involve the positioning of a stylus at each individual landmark point, which although precise is very slow and therefore not practical for collection of comprehensive data sets. Optical surface scanning in contrast is a very rapid non-contact method for 3D data collection and is described in more detail below. Computerised tomography (CT) is another method applied to collect 3D data from the head, but because of it's invasive nature it is not practical for this project and so is not considered further.

Optical Surface scanner

The optical surface scanner was designed and built in response to the growing need for clinicians to be able to objectively monitor the outcome of reconstructive surgery in 3-D (Moss et al 1988). The system allows thousands of 3D co-ordinates to be recorded in seconds (Arridge et al 1985).

The fixed laser scanner records the surface co-ordinates of the face using a low-grade laser beam that is fanned out into a line and projected onto the surface of the face. The line is distorted by the shape of the face and is recorded by a CCD camera. Two mirrors are arranged in such a way that the camera can view the laser line from two opposite angles, this prevents loss of the signal caused by occlusion. In order to get a surface scan of the face the individual is

rotated on a platform under computer control. The data set collected from one scan normally consists of about 40 000 x, y, z co-ordinate points lying on the surface of the face. The accuracy of the data is recorded with a precision better than 0.5mm. The reproducibility and accuracy of the data from fixed laser scanners has been analysed (Aung et al 1995; Bush and Antonyshyn 1996).

There is now a wide range of optical surface scanners/3D digitisers available which have applications in surgery, clinical studies, prosthetics, forensics, archaeology, psychology and art. From a practical point of view the recent development of portable 3D laser scanners is particularly relevant. One version, the HLS hand held laser scanner works on the same principle as the fixed optical surface scanner but has a transmitter-receiver device that records the position of the laser light source relative to the object being scanned. Portable scanners have widened applications into various fields such as 3D animation and digitisation for film production. The precise method and format for data acquisition varies with the scanner used, this is expanded in Chapter 3.

1.3 Methods of analysis

It is important to record accurately differences and similarities between face shapes. Most of the mathematical methods for describing the shape of the face are dependent on anatomically defined landmark points. Apart from the problem of identifying homologous points on different sides of the face and amongst

individuals, landmark analysis also excludes a majority of what we perceive as the face, i.e. the surface between landmark points.

1.3.1 Inter landmark distances

Landmark co-ordinates can be used to determine the relationship between points using basic mathematics principles:
If Landmark A is (x^1, y^1, z^1) and Landmark B is (x^2, y^2, z^2) then the distance between the two landmarks can be calculated as follows:

$$\text{distance } \overline{12} = \sqrt{(x_1 - x_2)^2 + (y_1 - y_2)^2 + (z_1 - z_2)^2}$$

Where distance 12 is the distance between two points; 1 and 2.
Similarly the angular relationship between point can be calculated by first calculating the distance between the points and then using trigonometry:
If Landmark A is (x^1, y^1, z^1) and Landmark B is (x^2, y^2, z^2) and Landmark C is (x^3, y^3, z^3) then the angle between the three landmarks can be calculated as follows:

$$\text{angle } \overline{123} = \frac{(\overline{12}^2 + \overline{23}^2 - \overline{31}^2)}{2(\overline{12} \times \overline{23})}$$

A technique applied for analysis of facial asymmetry using basic trigonometry has been described where a set of 13 landmarks are placed on the face and used to make 13 triangles each side of the face covering the surface area of the face. The area of each of these

triangles is then calculated and compared with the corresponding triangle on the opposite side of the face (Moss et al 1991).

The majority of work analysing facial data has been dependent on the description of the integrated difference of a set of homologous landmarks between two data sets. Principal component analysis, Procrustes analysis and Euclidean distance matrix analysis (EDMA) are methods commonly used to explore configurational changes between landmark data sets.

These methods of analysis provide a statistic for the description of shape variation when trying to separate data sets into groups, on the basis of pathology, sex, age or ethnic variation (Dean et al 2000; Singh et al 1998; Hanihara 1997; Richtsmeier and Lele 1990). The major drawback with these methods is the difficulty of accurate and reproducible placement of landmarks in homologous positions on different subjects. This is very hard to accomplish with an extremely variable shape such as the face and additional methods have been introduced to cope with this problem through creation of 'pseudo' landmarks, essentially interpolated from the anatomical landmarks, to increase the repertoire of points (Bookstein 1997). However an approach relying on overall configurational differences is problematic when trying to assess individual variation in terms of discrete facial components or in assessing heritability of features.

1.3.2 Eigen faces and Neural Networks

Much of the work in computer recognition of faces has focused on detecting individual features such as the eyes, nose, mouth, and head outline, and defining a face model by the position, size, and relationships among these features. These systems use automated or semi-automated face recognition strategies which model and classify faces on the basis of normalised distances and ratios among points such as the eye corners, mouth corners, nose tip, and chin point (Craw et al 1987).

Recently, automated approaches have focused more on the overall configuration, or gestalt-like nature of facial recognition with the development of techniques such as eigenfaces and neural networks (Haxby et al 2000). The eigenface technique breaks up the face into component parts (these can be up to 100 isolated regions of the face or combinations of features) and searches a database of faces for a match. A neural network is a processing device, either an algorithm, or actual hardware, designed to work similarly to animal brains. Most neural networks have some sort of "training" rule whereby the weights of connections are adjusted on the basis of presented patterns so that the neural networks effectively learn from examples. Neural networks used for face identification have properties similar to those of neurones in regions of the primate visual cortex that respond selectively to faces. This approach depends

on the availability of a large number of labelled examples of face types that can be used for training the network.

Both neural networks and eigenface techniques have been successful in pilot studies for finding and recognising faces, lip-reading, sex classification, and expression recognition. The eigenface technique has been successfully applied to databases containing up to 8,000 face images and is reported to achieve recognition rates greater than 90% (Turk and Pentland, 1991). Neural networks have also been reported to perform well in tasks such as human sex determination from face images (Golomb et al 1991).

1.3.3 Surface segmentation

With the development of 3D data capture techniques such as the optical surface scanner there was an opportunity to describe complete surface morphology without losing information between landmark points. Surface type analysis methods were developed that could break up a surface into component shape types. Methods described use differential geometry and patch-fitting algorithms (Stokely and Wu 1992) at a selected patch surrounding each data point to calculate mean (H) and Gaussian curvature (K) properties across the surface. The mean and gaussian curvatures relate to the intrinsic and extrinsic properties, the stretching and bending properties, of a surface. The theory is well described by several authors (Besl and Jain, 1985; Koenderink and van Doorn, 1992). The mean and Gaussian curvature values can then be used to segment

the surface on the basis of eight primitive surface types that can be colour coded to facilitate interpretation (Besl and Jain 1986).

This has been applied to 3D facial data obtained from the laser scanner with the aim of providing a quantitative description of the face (Coombes et al 1992) and also to describe differences in patients faces pre- and post- surgery (Coombes et al 1990). The x,y,z co-ordinates from the laser scan can be used to compute mean (H) and gaussian (K) curvatures across the surface of the face to produce the surface type at each data point. The data point is then colour coded on the basis of the surface type value and segments the face into regions of similar shape.

The Shape Index value takes this classification scheme further to capture the notion of the local shape of a surface and attribute a numerical value (Dorai and Jain 1997). The Shape Index scale ranges from 0 to 1 and provides a continuous gradation between convex, saddle and concave surface shapes using a large numerical vocabulary to describe intermediary shapes and subtle shape variations. Like the surface type method, the Shape Index value is calculated from the 3D data co-ordinates and displayed graphically through colour coding to represent the local shape of the surface.

1.4 Normal Adult appearance

Studies of facial recognition attempt to achieve what pigeons can be trained to do and babies can do so as early as 3 hours after birth and what the human brain does on a daily basis (Johnson and

Morton, 1991). Many distinctions that we regularly make between individuals are based on very complex recognition of a certain gestalt. Very subtle variation in size, shape and skin tone allow us to determine properties about a persons face both individually subjective and with a high degree of accuracy.

1.4.1 Facial Similarities

'WE KNOW THAT CHILDREN MOST RESEMBLE THE FATHER ONLY WHEN THE MOTHER HAS A VERY LIVELY IMAGINATION AND LOVE FOR OR FEAR OF THE HUSBAND.'

Lavater, 18th century.

The idea of family resemblance in appearance is not new or unusual. The problem of obtaining a quantitative estimate of the resemblance between sibs can be dated back to 1875 (Galton 1875) and correlation studies of twins have continued since for an extensive repertoire of characteristics both qualitative and quantitative (Eaves et al 1999; Burke and Healy 1993).

Very few facial features have been documented as being inherited in a simple manner following a Mendelian pattern of inheritance. Although through family records and photos it is possible to trace particular features through the generations, this is particularly the case in royal families which are often well documented for many generations through portraits and sculptures. However most royal families through the ages have advocated a form of inbreeding so that the monarch line is kept 'pure'. Thus it has not

been uncommon for first cousin, aunt-nephew, and uncle-niece marriages to occur.

Portraits of European monarchs often display striking similarities between related members of the family, possibly reflecting the reduction in genetic heterogeneity. From the 13th to the 20th century the Habsburg royal family was powerful in Europe. Artists unwittingly documented the effect of successive generations of inbreeding in this family through portraits (Hodge 1977). The phenotypes portrayed on canvas aided compilation of an extensive Habsburg family pedigree with 409 members, 23 generations and 13 families (Wolff et al 1993). This pedigree displays one of very few examples of simple autosomal dominant Mendelian inheritance of a facial feature, the prognathic mandible. The prognathic mandible was observed in 9 successive generations of the family and although it appeared to be transmitted as an autosomal dominant trait the male members were documented as more severely affected.

In addition to the genetic study of a classical facial trait there are numerous documented instances of more individual facial traits in OMIM (McKusick-Nathans 2000). This includes lip pits, chin dimples, ear lobe attachment and hair line but in most cases evidence is anecdotal and the judgement about the genetic basis is uncertain.

1.4.2 Facial Differences

The most obvious genetic difference between males and females is the chromosomal constitution, females being the homogametic sex 46, XX and males the heterogametic sex, 46, XY. The Y chromosome is believed to contain relatively few active genes (Graves 1998), the most important in sex determination being the SRY gene, often referred to as the male determining gene. This gene is clearly involved in gonadogenesis but whether or not it is the only gene responsible for male/female physical differences is unresolved.

The task of distinguishing gender from static facial cues alone, in the absence of hairstyle, makeup and other cues is more difficult, though humans still perform quite well (Burton et al 1993). There are general differences between the sexes thought to be an important factor in aiding sex differentiation. The muscles of the female face are generally less substantial and better hidden by fatty tissue, and the female nose is proportionately smaller, wider and more concave with the bridge of the nose often being depressed. These less robust, less mobile features are believed to make the female face appear youthful and childlike, qualities postulated to be associated with femininity (Ligget 1974).

Sexual dimorphism in humans is not as marked as in some other primates (Masterson and Hartwig 1998). The actual difference between male and female faces is relatively difficult to quantify, as its basis is likely to be very complex reflecting subtle growth,

development and endocrine variations. Sexual dimorphism is generally either difficult to measure or expressed in terms of an index; such as protrusion of the mandible or craniofacial index. However there are comprehensive data available on human sex differences (Keen 1950; Farkas 1994).

From birth, the height of the midface, from eye level to the level of the nostrils, grows steadily up until adolescence, more so than the rest of the face. There is little sexual difference in skull size up until puberty by when 90% of the adult cranial size is attained (Humphrey 1998). A feature associated with a younger face is that a young child's nose is generally small, wide and concave with a sunken bridge, the nose develops along with the growth of the midface until adolescence. Adolescence brings about further change in face shape, the onset of puberty in males bringing about growth and definition of the mandible, and in females the loss of 'puppy fat' resulting in a more womanly face (Enlow and Hans 1996).

Dermal changes are mainly responsible for the change in appearance that we associate with older age, the loss of elasticity, pigmentation spots, thinning and wrinkling of the skin. Wrinkles often first appear on the transverse lines of the forehead, along the line between the outer mouth and the nose and around the eye area. In terms of ageing and genetics relatively little is known, however, there are a number of congenital pathological conditions that are

associated with premature ageing, such as Cockayne syndrome (Nance and Berry 1992).

The most noticeable differences between faces are generally attributed to differences in ethnic background; this is an overall gestalt of features rather than a singular feature. Many studies have been carried out on establishing craniofacial standards for different ethnic populations (Richardson 1980; Chung et al 1982 Shalhoub et al 1987; Huang et al 1998; Farkas 1994). Ideas as to why different ethnic groups have evolved with distinct facial phenotypes have included the hypothesis of environmental adaptation (Carey and Steegmann 1981). That is that during the course of evolution wide and flat faces like the Mongoloid faces were selected for in cold climates as a face type with no 'jutting parts' is defended more easily from the cold. The incidence of other facial variations such as sutural variants as well as non-metric variants has also been closely looked at in different populations (Berry and Berry 1967).

Differences in pigmentation provides the most pronounced visual differences between individuals of different ethnic origin and much work has been done to try to understand the genetic basis of skin colouration (Robins 1973; Nichols 1973). Such works conclude that the genetic basis of skin and eye pigmentation is likely to be extremely complex involving considerable number of genes. However recent studies have associated the melanocyte-stimulating hormone receptor gene with pale skin and red hair (Valverde et al 1995).

CHAPTER 2

Biology of the face

The aim of this section is to bring together the anatomy, embryology and development of the human face in order to appreciate the complexity of the processes underlying normal facial variation. An understanding of normal and abnormal development can then allow us to postulate candidate genes for facial features on the basis of known function, expression pattern and timing. The major sources of reference for this section were Gray's Anatomy (38th Edition 1995), Human Embryology (Larsen 1997), OMIM (McKusick-Nathans 2000) and London Dysmorphology Database (Winter and Baraitser 1998).

2.1 Anatomy of the face

Anatomy is the science of the structure of animals, which began as a descriptive language for physicians. Comparative anatomy has provided us with the basis for our knowledge on the course of hominid evolution and has been essential to biological classification and ordering of organisms. In terms of the face there is, broadly speaking, a universal blueprint conserved in mammals. Generally this blueprint comprises two horizontally placed eyes above a central nose and mouth with a degree of bilateral symmetry evident (Butler 2000).

Typical vertebrate features such as the presence of a notochord, segmented axial musculature and a head are believed to

have developed in response to an active life involving predation in the course of evolution. Jaw development and the development of sophisticated sensory organs, necessitating a larger brain, also exerted evolutionary change on the shape of the skull resulting in the characteristic human head shape, arranged vertically as opposed to horizontally. The evolutionary adaptations and changes of the human face also reflect the important modifications necessary for the development of complex speech, the lowering of the larynx and lengthening of the pharynx and the highly developed muscles of the lips, cheeks, mouth and tongue. The arrangement of human facial features is a reflection of sensory, dietary and linguistic adaptations made in the course of evolution so although we perceive each person as being individual the underlying design of the human face is identical.

The mandible and cranium together make up the skull, the cranium comprising the mid- and upper facial skeleton. The skull is the most elaborate part of the vertebrate skeleton, adaptations having been made through the process of evolution in order to accommodate the brain and sensory organs. Protection of the brain from external impact is a major function of the skull as well as continual buffering against stresses of the powerful axial and masticator muscles. The rigidity of the cranium also provides a protected and isolated environment for cerebral circulation. The facial skeleton (Fig 2.1) comprising the supraorbital region and orbital cavities, nose and

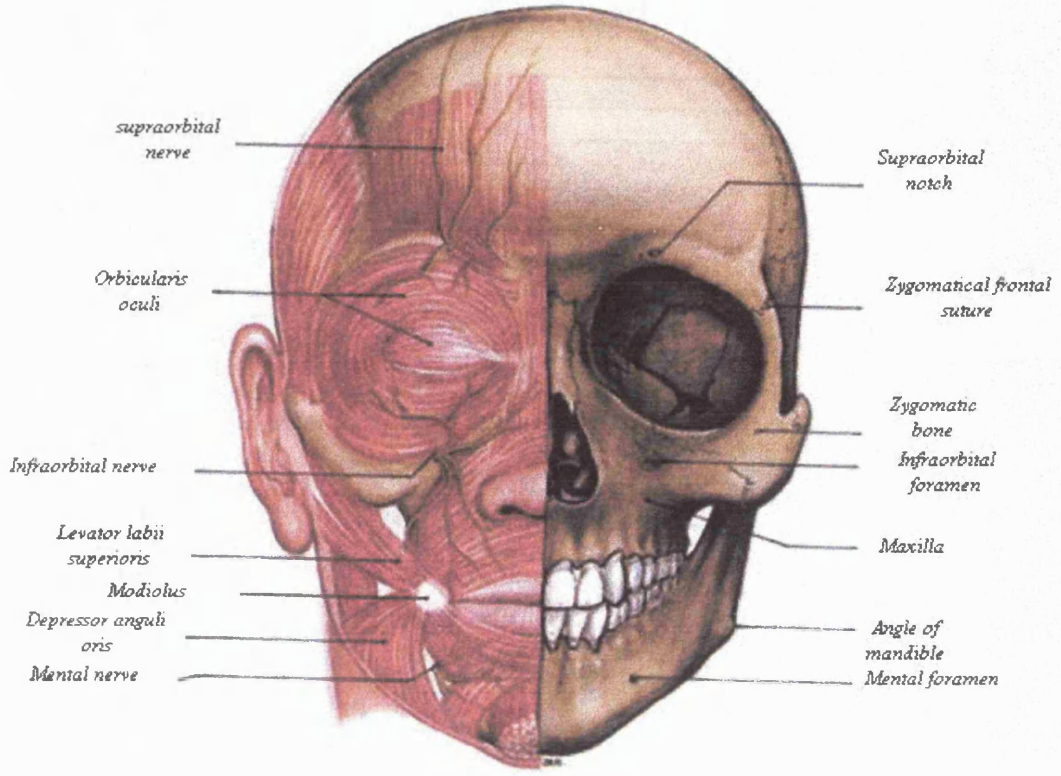

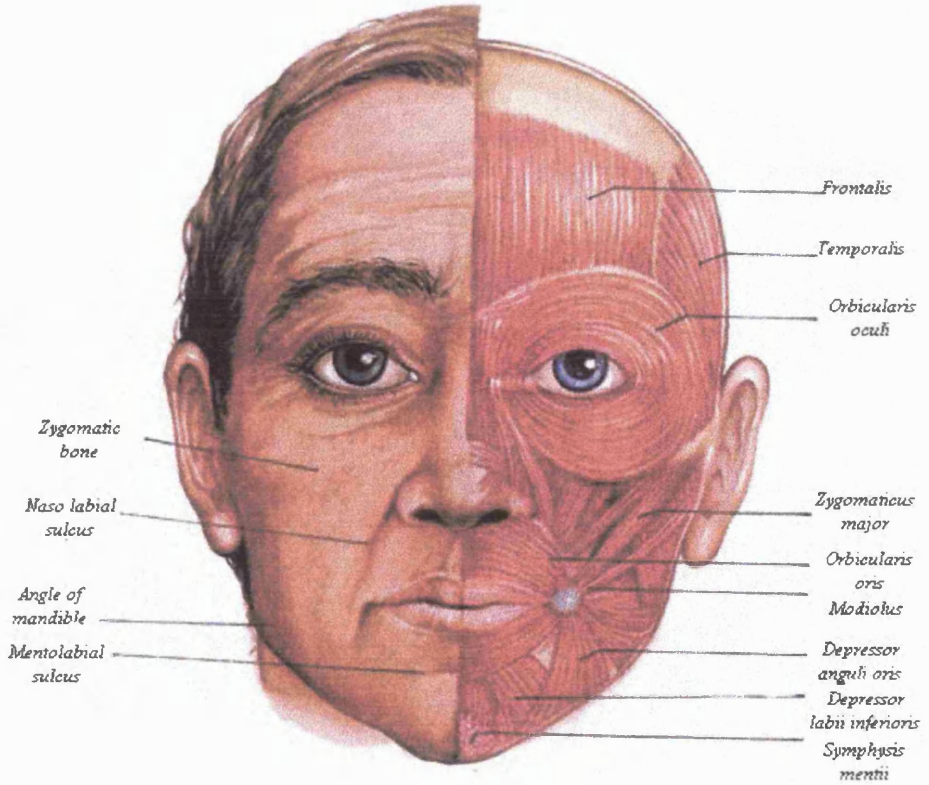

Figure 2.1 (top) Skeletal and musculature components of the face. Figure 2.2 Superficial and musculature components of the face (reproduced from Gray's Anatomy).

nasal cavity and the upper and lower jaws may be crudely divided into upper, mid and lower facial regions respectively. While each of the regions has an independent function they all have a considerable influence on the overall integrated morphology of the facial skeleton, the lower face/mandible perhaps contributing the greatest effect to individual face shape.

Aside from the skeletal contribution to variation in facial appearance one must also consider the contribution made by the facial musculature. The muscles of the head are crudely divided as craniofacial and masticators (Fig 2.2). Craniofacial muscles, often referred to as the muscles of facial expression, include the orbital margins and eyelids, the outer nose and nostrils, the lips, cheeks and mouth, scalp and skin of the neck. The masticator muscles are mainly concerned with movements of the temporomandibular joint necessary for eating but they are also involved in facial expression.

2.2 Embryological development of the face

Development of the face begins around the 4th week of embryological development and by the 8th week a human face is apparent. Subtle differences in relative growth rates and timing of fusion of the facial processes (see below), variations in structural and extracellular matrix proteins and the mechanical effects of underlying structures, such as the brain and developing teeth, all appear to contribute to the individuality of each person.

The head is a composite structure, the end product of a substantial number of contributions from a range of cell lineages. The mesenchyme is the source of the major lineage involved in craniofacial development and in itself is derived from one of two origins: the neural crest and the mesoderm. The neural crest derived mesenchyme makes a proportionately larger contribution to the development of the head. The cranial ganglia, odontoblasts, corneal stromal fibroblasts, fascia of muscles, dermis, melanocytes, smooth muscle (associated with major blood vessels) and the greater part of the skeletal tissue are all derived from a population of cells which emerge from the neural tube during neuralation. The mesodermal derived mesenchyme contributes to the development of angiogenic tissue, otic capsule, bones of occipital region, striated muscle and a limited amount of connective tissue.

The structures of the face develop from 5 primordia, which are active centres for mesenchymal growth and are derived from migrating neural crest cells:

- The frontonasal prominence
- Left and right maxillary prominence
- Left and right mandibular prominence

At the start of the 4th week of embryological development the first overt sign of morphogenesis is obvious in the lifting up of the anterior end of the embryonic axis from the surrounding extraembryonic tissues, this event is termed the head fold. By the end of the 4th week

the frontonasal mass (comprising mainly of neural crest cells) emerges and either side of it the olfactory placodes become apparent.

Along the embryonic axis from the anterior end, is a series of five paired branchial arches, numbered 1, 2, 3, 4 and 6. The specialisation of each arch is characteristic of modern vertebrate development; in terms of craniofacial development we are only really concerned with arches 1(mandibular) and 2(hyoid). The mandibular and maxillary prominences are derived from the first branchial arch. The hyoid or second branchial arch lies caudal to the first and grows ventrally to meet and fuse in the midline. In terms of the development of facial musculature it is often generalised that the muscles of mastication are derived from the first arch and the muscles of facial expression are derived from the second arch.

Early on in development cephalic neural crest cells, derived from the posterior midbrain-hindbrain, populate the branchial arches. During migration these cells undergo an epithelial to mesenchymal transition and then interact with both epithelial and mesodermal cell populations within the arches leading to the formation of craniofacial bones, cartilage and connective tissues. It is believed that the precise expression of transcription factors plays an important role in guiding neural crest cells during migration and in orchestrating their differentiation.

During the sixth week of development the olfactory placodes begin to thicken and the medial and lateral nasal swellings grow and

begin to surround the nasal placode ectoderm so that the placodes lie at the base of shallow nasal pits. The frontonasal mass at this point grows forward and downward. In the seventh week there is a crucial time point when the lateral and medial nasal processes contact the maxillary processes. The ectoderm remodels so as to produce a continuous epithelium and three processes on either side of the face contribute the cheeks and the alae of the nostrils to the fully developed face. At the same time the frontonasal mass grows to provide tissue between the medial nasal processes, the intermaxillary process, and the midfacial tissue which includes most of the nose and the philtrum (Fig 2.3).

2.3 Molecular biology of facial development

The progression of vertebrates from stem chordates has involved the diversification of fins and limbs, the elaboration of the endoskeleton, cephalization, increased sensory organs and neural processing. In the course of evolution early vertebrates underwent a major behavioural explosion and started to occupy most ecological domains, the emergence of the first chordates, the jawless fish coincided with the arrival of the neural crest cells (Northcutt and Gans 1983). These multi-potent precursor cells originate from the neural crest after closure of the neural tube in vertebrate embryos. After closure of the neural tube the neural crest cells migrate and populate diverse regions of the embryo.

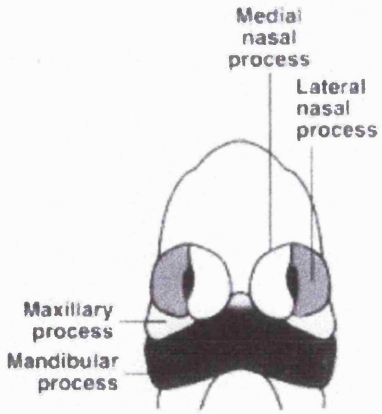

Early 6th week

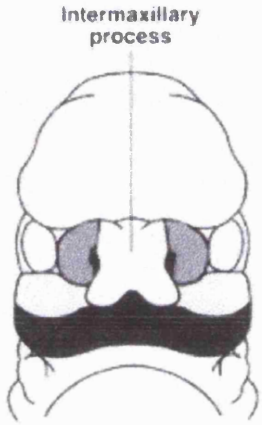

Late 7th week

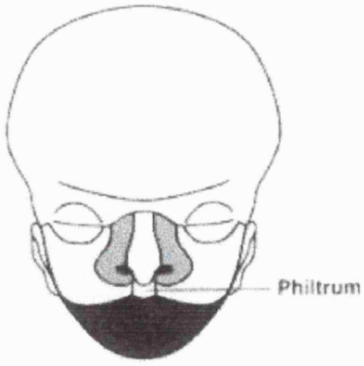

10th week

Figure 2.3 Early embryonic development and fusion of the facial processes (modified from Larsen's Human Embryology)

Cells and tissues derived from the neural crest include the peripheral nervous system, endocrine glands, pigment cells, teeth, pharyngeal arches and most of the bones and cartilage which make up the skull and jaw. The crest cell population becomes more heterogeneous with time as the cells migrate ventrally and encounter different conditions at different sites. The neural crest cells have an in-built developmental mechanism for generating a diversity of cell types, cell arrangements and capacity to respond to a wide variety of conditions. The cranial neural crest cells can also adapt to changes in the size and shape of the brain, sense organs and branchial arches as they all lie in their migration path (Le Douarin et al 1994). Recent work has shown that cranial neural crest cells do not follow a fixed predetermined plan in patterning of facial tissues; rather, patterning is maintained by passive transfer of positional information from the hindbrain to the periphery (Trainor and Krumlauf 2000).

The molecular genetics of early neural crest formation can be seen as 3 main stages (LaBonne and Bronner-Fraser 1999). Stage one is the formation of the neural crest; this involves the closure of the neural tube and requires the interaction of numerous genes including BMP, Wnt, FGF, and MSX-1. The second stage is the expression of genes at the neural crest which establish the patterning and migration fate of the neural crest cells, genes acting at this stage include the transcription factors SNAIL, ZIC, PAX and MSH. The third

stage is neural crest cell migration which involves genes such as Rho-family GTPases and cell adhesion molecules such as cadherins.

Cranial neural crest cells migrate to populate the first branchial arch and eventually differentiate into multiple cell lineages in the maxilla and mandible during craniofacial morphogenesis. The development and differentiation of neural crest cells within the branchial arches relies upon the action of numerous transcription factors which guide migrating cells and later play a role in lineage determination expansion and differentiation. Many genes have been reported to be involved in branchial arch development, Dlx-1 and Dlx-2 (Qiu et al 1997, Thomas et al 2000), Goosecoid (Boucher et al 2000), Fgf8 (Tucker et al 1999), Endothelin-1 and Endothelin receptor A (Clouthier et al 2000) have all recently been associated with defects in cephalic neural crest derived skeletal elements. The mandible is predominantly affected and overlapping phenotypes were observed in the knockout animals studied (zebrafish, mouse and chick).

Normal development of the head is the result of an extremely complex sequence of tightly co-ordinated pathways during growth and morphogenesis. At the cell level, position and timing are critical and sensitive to perturbation.

2.4 Abnormal facial development

Bearing in mind the complexity of craniofacial development and the necessity for immense precision it is hardly surprising that a

large proportion of all major birth defects involve the head and face. The majority of human syndromes involving the craniofacial complex are not restricted to the head and are associated with more widespread defects. The degree to which the face is affected is hugely variable and not only varies between conditions but also within a given syndrome. It is often the case that the distinction between 'normal' and 'abnormal' is not clearly definable. It is conceivable that an overlap exists between the extremities of the 'normal' range and 'abnormal' range.

Over the last decade many genes that are causally related to different categories of human craniofacial malformation have been identified (reviewed by Winter 1996). Classification of craniofacial malformations based on clinical phenotypes is sometimes quite different from the genetic findings in patients. For example, different mutations in a single gene can cause distinct syndromes, and mutations in different genes can cause the same or similar syndromes. Winter classifies craniofacial defects into five main groups on the basis of associated pathology:

i. Craniosynostoses
ii. Syndromes with brain defects
iii. Syndromes associated with cardiac malformations
iv. Syndromes associated with premature ageing
v. Multiple congenital anomalies

In this section a similar approach is taken, concentrating on the type of pathological disruption rather than gene families. Here syndromes largely affecting the face are considered and are subdivided on the following criteria:

i. Craniosynostoses
ii. Branchial arch-derived structures affected
iii. Midline and epithelial fusion defects
iv. Overall syndromic effect.

Among the genes that have been identified *MSX2, FGFR2, TWIST, SHH,* and *TCOF1* are considered in detail in this section to illustrate how signalling molecules, transcription factors, and growth factor receptors can all be involved in the complex signalling network controlling craniofacial development. It is important to emphasise that several of pathological conditions mentioned could fall under more than one of the groups. However, to reduce the complexity, they are only listed once.

2.4.1 Craniosynostoses

Craniosynostoses are conditions where the skeletal defect is largely confined to the craniofacial area. The growth function of the cranial sutures terminates prematurely when they differentiate into bone too early; this prevents the continuation of growth of the cranium and the brain. As a result of the increased intracranial pressure, the shape of the cranium can become distorted and cause neuropathological damage. The Crouzon, Pfeiffer and Saethe-Chotzen

syndromes are all examples of skeletal dysplasias that are predominantly localised to the head. Some of the genes reported to cause craniosynostosis as a primary feature when disrupted are summarised in Table 2.1; these include *MSX2, FGFR1, FGFR2, FGFR3,* and *TWIST*.

Craniosynostoses are generally inherited as autosomal dominant conditions. A single amino acid substitution in the homeobox of the human MSX2 gene has been associated with the dominantly inherited, craniofacial disorder Boston type craniosynostosis (Jabs et al 1993). Mouse models have shown that skull development is very sensitive to Msx2 dosage. A mutation that increases the binding affinity of Msx2 for its target sequence leads to an effective increase in Msx2 dosage and results in the pathological phenotype (Liu et al 1999). Synostosis of the sagittal suture of the forming skull bones generally involves enhanced osteoblast activity and enhanced bone growth associated with localised fusion of the parietal bones at one or more sites. Msx2 gene dosage influences the number of proliferative osteogenic cells in the growth centres of the developing skull. It is thought that over-expression of *MSX2* in the sutures of the skull may keep the osteoblastic cells in a proliferative, undifferentiated state for longer. This in turn increases the osteoprogenitor pool resulting in over-growth of the parietal bones into the sutural space.

Chromosome Location	Condition	OMIM	gene
4p16	Muenke syndrome	600593	FGFR3
5q34-35	Boston craniosynostosis	123101	(MSX2)
7p21	Saethre-Chotzen - acrocephalosyndactyly	101400	TWIST
8p11	Pfeiffer syndrome	101600	(FGFR1)
10q25-26	Pfeiffer syndrome	101600	(FGFR2)
10q25-26	Crouzon (craniofacial dysostosis)	123500	(FGFR2)
10q25-26	Apert syndrome	101200	(FGFR2)
10q25-26	Jackson-Weiss syndrome	123150	(FGFR2)

Table 2.1 Summary of genes, chromosome location and OMIM entry number known to be associated with common craniosynostosis syndromes (McKusick 2000).

In contrast to these studies, families have also been reported with enlarged parietal foramina that have either deletions of the whole *MSX2* gene or mutations in the homeodomain (Wilkie et al 2000). The homeodomain binds DNA that in turn regulates transcription of other genes, hence *MSX2* basically acts as a transcription factor. This suggests that both loss and gain of function of the *MSX2* gene affects the differentiation of osteogenic cells in the superior cranium.

Because loss and gain of function of *MSX2* have been associated with extreme pathological phenotypes, it is also conceivable that disruption of this gene, with a relatively mild degree of loss or gain of function could explain aspects of normal variation. One of the features of Boston type craniosynostosis is a prominent forehead or bossing of the forehead. The *MSX2* gene could be considered as a possible candidate gene for features that are predominantly skeletal, particularly localised to sutures of the skull, such as the brow area.

Three members of the fibroblast growth factor receptor (FGFR) family have been associated with craniosynostosis; *FGFR 1*, *FGFR 2*, and *FGFR 3* (Wilkie 1997). The FGFRs relay extracellular signals from the fibroblast growth factors to the cytoplasm and play an important role in limb and craniofacial development. Several distinct fibroblast growth factors (FGFs) bind to each FGFR and both FGFs and FGFRs are widely expressed in organogenesis, so it is feasible that signalling

may be dependent on the coincidental expression of certain FGFs and FGFR isoforms in particular developing sites. Apert syndrome is a distinctive malformation syndrome resulting in craniosynostosis and severe syndactyly of the hands and feet. The condition is caused by mutation of the *FGFR 2* gene (Wilkie et al 1995). The majority of mutations found in Apert syndrome patients are in the portion of the gene coding for the immunoglobulin like domains needed for ligand binding and receptor activation (Park et al 1995).

The phenotype of the condition varies in severity depending on the specific location of the mutation in the gene, possibly reflecting the varied patterns of expression of the fibroblast growth factors (Lajeunie et al 1999). Mutations in *FGFR 2* have also been associated with other craniosynostotic conditions where there is a different clinical presentation; Crouzon, Pfeiffer and Jackson Weiss syndromes (Meyers et al 1996). The fact that different mutations in the *FGFR 2* gene can result in different phenotypes suggests that the mechanisms of signalling are not uniform throughout the whole body. A subtle difference in conformation between the different mutated forms of FGFR 2 protein could tip the balance towards a greater abnormality of signalling in a particular site, e.g. limb or head, and lead to a more severe phenotype localised to that body part. It is also possible that mutation elsewhere in the gene could have an even more subtle effect and result in minor degrees of normal facial variation.

Mutations in the *TWIST* gene have been associated with the human craniosynostosis syndrome Saethe Chotzen (Howard et al 1997). *TWIST* encodes a nucleolar protein that belongs to a family of transcription factors, which contain a basic helix-loop-helix (bHLH) domain. Mutation of the gene leads to loss of function of the product but there has been no genotype-phenotype association between mutation and clinical manifestation (Gripp et al 2000). A recent study has suggested that the loss of TWIST protein function in patients could arise through protein degradation and lack of ability to localise in the correct nuclear location (El Ghouzzi et al 2000). As there is no obvious association between genotype and phenotype it is harder to postulate a direct role for *TWIST* in normal facial variation. Other studies have suggested that there is an overlap in the expression patterns of mouse Twist and Fgfr2, Twist preceding Fgfr2 expression during suture formation (Johnson et al 2000). If these genes both act in the same pathway in humans then this could explain both the vast heterogeneity observed in craniosynostoses and the apparent lack of genotype-phenotype correlation observed in Saethe Chotzen patients.

2.4.2 Arch Defects

These defects arise as a result of a problem in migration of the neural crest cells, branchial arch growth, or in the correct specification of the arch fate. Although this type of defect can result from exposure to teratogens in the first 6 weeks of development several are known to have a genetic aetiology. The first arch

predominantly contributes to the bony structures of the developing lower face and abnormalities generally involve the maxilla and the mandible, a common feature being a dysmorphic lower face with micrognathia (underdeveloped jaw). The zygomatic arches can also be affected, as can the orbits, ears and palate.

Treacher Collins is an autosomal dominant inherited form of a common type of first arch defect collectively grouped as mandibulofacial dystoses. The Treacher Collins phenotype is very heterogeneous and ranges from a fatal form due to breathing obstruction, to a very mild facial phenotype with only minimal facial changes to the jaw size and angle.

Mutations in *TCOF1* have been associated with Treacher Collins syndrome (Wise et al 1997). Currently more than 50 mutations, resulting in truncation of the protein product, have been identified throughout the gene. The phenotypic severity does not appear to correlate with the location of the mutation (Edwards et al 1997). It is believed that dosage level of the correct protein product is important, as peak expression of the gene coincides with early craniofacial morphogenesis (Dixon et al 1997) with reduced levels of the protein producing the abnormal phenotype. It has been postulated that the role of *TCOF1* is to shuttle proteins involved in ribosome assembly between the cytoplasm and the nucleus and hence affect the rate of protein translation, but why this predominantly affects only first arch structures is unknown (Marsh et al 1998).

2.4.3 Midline and epithelial fusion defects

This class of defect is often a reflection of failure of growth, contact, fusion and remodelling of the facial processes. This largely affects the developmental events that produce the upper face and hence often results in unilateral and bilateral clefting of the lip and palate. These events can be isolated or syndromic and are complex in their aetiology, and often are the result of embryonic exposure to teratogens.

An early reference to midline defects can be seen in Homer's Iliad with the mention of the one eyed Cyclops, now medically referred to as holoprosencephaly. The majority of genes identified to date, shown to be responsible for midline defects, are those largely involved in the overall bilateral patterning and symmetry during early embryonic development (Table 2.1). Midline defects of the face are a result of either impaired forebrain development, or insufficient frontonasal mass and intermaxillary processes. They manifest phenotypically in the holoprosencephalies; these range from mild, as seen in foetal alcohol syndrome (Chan 1999) through to extreme phenotypes. Mildly affected individuals may present with facial features such as a short upturned nose, a shallow or absent philtrum, highly arched palate, and a short retracted lower jaw. Severe forms of holoprosencephaly present with craniofacial and forebrain pathology (Nanni et al 2000).

Chromosome Location	Condition	OMIM	gene
2p21	Holoprosencephaly, type-2	157170	SIX3
4q25-26	Rieger syndrome	180500	PITX2
7q36	Holoprosencephaly, type-3	142945	SHH
13q32	Holoprosencephaly, type-5	603073	ZIC2
18p11.3	Holoprosencephaly, type-4	142946	TGIF
21q22.3	Holoprosencephaly, type-1	236100	HPE1
Xp22	Opitz syndrome	300000	MID1

Table 2.2 Genes, chromosome location and OMIM entry number known to be associated with midline defects (Wallis and Muenke 2000[2], McKusick 2000).

A number of genes have been identified as having a role in midline patterning. Mutations of *SHH* in humans causes a loss of midline tissue (rather than an expansion) resulting in holoprosencephaly (Nanni et al 1999). Opitz syndrome (OS) is an inherited disorder with midline defects not restricted to just the head. The condition is genetically heterogeneous in that it has been linked to two separate chromosomal locations, Xp22 and 22q11.2 (Robin et al 1995). *MID1* (midline 1) is on Xp22 and is believed to be a candidate gene for Opitz syndrome (Quaderi et al 1997). *MID 1* belongs to a family of transcription regulators (B-box) that have been implicated in fundamental processes such as body axis patterning and control of cell proliferation. The X-linked Opitz syndrome also presents with mental retardation and a rare example of Mendelian inheritance of cleft lip and palate, the phenotype is more severe in males than in females.

Now that a number of genes involved in midline development have been discovered it may be possible to look at these genes for subtle mutations or polymorphisms to explain some aspects of normal facial variation in features such as the nose, the philtrum and eye-spacing.

2.4.4 Syndromic defects with facial involvement

This category includes conditions with a genetic/heritable basis but where an abnormal face is the not the primary problem area but a consequence of the generalised pathology. These include conditions

resulting from abnormalities of vascularization, storage disorders, multiple congenital abnormalities and chromosomal anomalies.

Vascularisation defects occur as a result of disruptions in the development of the blood vascular system in the head and neck area, localised ischaemia and tissue necrosis affecting normal craniofacial development. The hemifacial microsomias, such as the dominantly inherited Goldenhar syndrome, are the most common of this category. Here a vascular disturbance may result in reduced size, dysmorphology or complete absence of the following features: the mandible, temporomandibular joint, associated muscles, outer and inner ear associated with hearing loss. While this syndrome has been reported to follow dominant segregation (Kaye et al 1992), it is not without exception and like many heterogeneous pathologies can also arise through exposure to teratogens in early development.

There are many cases where the face can be indirectly affected through deficiency or excess of a toxic metabolite. Progressive coarsening of the face is observed in many lysosomal storage disorders and is the result of an accumulation of a storage product for example Alpha-Mannosidase B deficiency (Gotoda et al 1998). Haematological abnormalities such as X-linked alpha thalassaemia also give rise to characteristic dysmorphic faces (McPherson et al 1995), as do endocrine abnormalities such as Cushing Disease (Blevins et al 1992).

Gross chromosomal aneuploidies as well as Turner syndrome and Klinefelter syndrome all have distinctive aspects to the facial appearance (Epstein 1990; Corvo et al 1988; Brown et al 1993). Perhaps the most obvious is Trisomy 21 (Down syndrome) where there is the characteristic flat 'moon' face, or Mongoloid appearance. Here the condition is the result of all or part of chromosome 21 being present in three copies. From this one could postulate that the Down syndrome critical region could therefore contain genes either directly or indirectly involved in facial morphogenesis (Richtsmeier et al 2000).

Other chromosomal anomalies with a facial phenotype include syndromes resulting from large deletions such as DiGeorge, Velo-Cardio-Facial, and Conotruncal anomaly face syndrome where the critical deleted region is 1.5mb on chromosome 22 (Driscoll 1994). Characteristic features of these syndromes include abnormalities of the heart, thymus, parathyroid and mild craniofacial dysmorphologies.

The fact that facial anomalies can result from a vast range of pathology is a reflection of the complexity of embryonic development. Appreciating the numerous ways in which these abnormal facial phenotypes can arise can allow a better understanding of the molecular processes governing normal development.

2.5 Candidate genes for normal facial variation

It is clear from a consideration of the literature on the genes and gene products associated with the development of the human face that there are many potential candidates that could be studied for an association with a particular facial trait in the general population. As this pilot project progressed and DNA samples began to be assembled from individuals who had participated in the facial scanning, a small-scale study of two specific human genes was initiated. The details of the results of this molecular study are given in Chapter 7 but it seems more appropriate to provide relevant background information here including details of the genes and the criteria used to decide that these were sensible choices for this study.

Endothelin 1 (ET1), sometimes referred to as the Preproendothelin gene, belongs to a family of structurally similar vasoconstrictor peptides. There are three members in the family, *ET-1, ET-2* and *ET-3,* and in each case the mature peptide is 21 amino acid residues long (Inoue et al 1989). Each endothelin binds and activates two related receptors, and the Endothelin receptor A (*ETRA*) and B (*ETRB*) which belong to the seven membrane-spanning G-protein coupled receptor family.

The *ET-1* gene is located on chromosome 6 and comprises five exons and four introns spanning 5.5kb. All of the mature peptide sequence is contained in exon 2. The *ETRA* gene is on chromosome 4 and spans more than 40kb, containing 8 exons and 7 introns. The

biosynthesis of *ET-1*, to produce a mature peptide that can bind to the ETA receptor occurs in 2 stages. The 212 amino acid (aa) pre-proendothelin is cleaved by a furin-like protease at sites that contain paired basic amino acids. This produces 'Big ET-1', which is cleaved again, this time by the protease ECE-1, to produce the biologically active peptide that is a ligand for the endothelin receptors (Fig 2.4).

Because the endothelins have been identified as potent vasoconstrictors they have been studied extensively as candidates for pathology of the heart (Tiret 1999; Cambien et al 1999). However, recent work suggests a role for endothelin in the normal development of neural crest-derived structures. Mice homozygous for a null mutation of ET-1 show severe craniofacial anomalies including a marked reduction of the mandibular bone and a hypoplastic jaw in the tissues that are derived from the first branchial arch (Kurihara et al 1994). A similar pattern of abnormalities is seen when the ETA receptor gene is disrupted and includes severe jaw and throat abnormalities. The ETA deficient mice also have heart defects and die shortly after birth from breathing obstruction (Clouthier et al 1998). Mice deficient for the enzyme ECE-1 also have very similar craniofacial and cardiac anomalies suggesting that the ET-1/ECE-1/ETA pathway is critical for normal face and heart development.

The precise role of the ET-1/ECE-1/ETA pathway in neural crest development is not yet known but it may be necessary for migration, proliferation or differentiation. However, it is clear from the

Human Preproendothelin-1 protein (212 residues)

MDYLLMIFSLLFVACQGAPETAVLGAELSAVGENGGEKPTPSPPWRLRRS
KRCSCSSLMDKECVYFCHLDIIWVNTPEHV VPYGLGSPRSKRALENLLPT
KATDRENRCQCASQKDKKCWNFCQAGKELRAEDIMEKDWNNHKKGKDCSK
LGKKCIYQQLVRGRKIRRSSEEHLRQTRSETMRNSVKSSFHDPKLKGKPS
RERYVTHNRAHW*

FURIN-LIKE PROTEASE

Big Endothelin-1 (38 aa)

CSCSSLMDKECVYFCHLDIIWVNTPEHVVPYGLGSPRS

ENDOTHELIN CONVERTING ENZYME (ECE-1)

Mature Endothelin-1 (21 aa)

CSCSSLMDKECVYFCHLDIIW

Endothelin Receptor A Endothelin Receptor B

Figure 2.4 Two-stage synthesis of the endothelin-1 peptide. The yellow highlighted sequence is the big endothelin 1 peptide. The green highlighted sequences are target sites for action of the proteases.

mouse knock-out work that the ET-1/ECE-1/ETA pathway is crucial for normal development of the first and second branchial arches.

Barni et al (1998) have hypothesised that ET-1 promotes branchial arch development during weeks 11-12 of human embryological development, coinciding with development of the face. It is envisaged that the action of ET-1, mediated by ETA and ECE-1, together with the different patterns of expression in different cell compartments leads to a differential response to cell proliferation and bone formation. The phenotype of ET-1 -/- mice has considerable similarity to mandibular abnormalities shown in human syndromes where the first branchial arch is affected such as Treacher Collins (OMIM154500) and Pierre Robin syndrome (OMIM 261800). The fact that both the face and the heart are affected highlights similarities with the cardio-facial conditions collectively grouped as CATCH 22 (Wilson et al 1993).

2.6. Methods of genetic analysis

Mapping studies and identification of mutations in genes that cause craniofacial defects enables some understanding of the pathways involved in the development of the face and may help to identify candidate genes responsible for normal person to person variation. These approaches have been employed to identify genes responsible for both complex and simple pathology.

It has been estimated that Humans are 99.9% genetically identical; this corresponds to a difference of one nucleotide per

thousand out of the total 3000 million nucleotides, meaning an average of 3 million differences between any two individuals. Therefore without the recent rapid progress made in gene identification, function and expression studies along with progress made in sequencing and single nucleotide polymorphism (SNP) identification, the process of identifying genes responsible for human variation in facial features would have been an impossibly difficult task to undertake.

Complex genetics focuses on individual variation in continuous traits. These are graded series of phenotypes from one extreme to another with no clearly distinguishable subsets and where there are often elements of gene-environment and gene-gene interaction. These traits include height, weight, and IQ. Complex traits are often multifactoral; the phenotype being dependent on environmental and numerous genetic factors. Also, in contrast to traits which follow a simple Mendelian pattern of inheritance the genes contributing to complex traits have relatively small effects, and act in concert: as such they cannot be easily identified through segregation analysis.

Very few facial features have been documented as being inherited in a simple manner following a Mendelian pattern of inheritance. Furthermore, it is likely that the genetic mechanisms underlying inheritance of normal facial features are complex in order to account for the immense person to person variability. It is assumed that the inheritance of quantitative characters depends on

combinations of genes that are subject to the same laws of transmission as simple trait loci. Therefore through the analysis of large families, and breaking down the complexity of phenotypes into simple component parts, the effect of each contributory gene may be ascertained. For example, if the face were to be categorised into 20 polymorphic features and each of the 20 features had 3 phenotypes, this alone would account for 3^{20} or 3486784401 facial combinations. This simple calculation ignores variability due to other factors such as age, ethnic background, sex, and weight.

Practical considerations

When trying to identify genes responsible for particular phenotypes there are broadly speaking two strategies that can be used, linkage or association analysis.

Linkage analysis-linkage looks at physical relationships between loci. The underlying aim is to see how often a marker locus and a trait locus is separated by meiotic recombination. The number of informative meioses required to detect linkage is dependent on the recombination rate: with no recombinants it is estimated that 10 meioses are sufficient to detect linkage whereas with a recombination fraction of 0.3, 85 would be required in order to get the same level of significance. The approach depends on collecting family data from large pedigrees or numerous small pedigrees and looking for linkage between the scored phenotype and known genetic markers. The efficacy with which linkage can be used to map traits is variable and relies in part upon the type of markers used and how densely they are spaced throughout the genome (Kruglyak 1999; Collins et al 1999; Wang et al 1998; Schafer & Hawkins 1998).

Problems associated with linkage include the need for informative meioses and complete specification of a genetic model of the trait being mapped, including modes of inheritance, segregation data, and estimates of gene frequencies and penetrance [Mueller and Cook 1996; Lathrop, Terwilliger & Weeks 1996; Spence and Hodge 1996; Wright Carothers & Pirastu 1999; Wang 2000]. Other problems include locus heterogeneity and false recombinants [Whittemore and Halpern 2001]. Model-free methods of linkage analysis have also been developed, including the important sib-pair analysis approach, where efforts are focused on looking at chromosome segments shared by affected individuals. In this method a limiting feature is the need to collect large enough numbers of sib pairs to achieve statistical significance, especially where genetic heterogeneity is a problem. Overall, linkage analysis has been the major method for identifying loci that determine single gene disorders or conditions in which relatively few genes determine phenotype. Many of the craniofacial disorders cited in this section were identified using a linkage approach.

Association analysis- allelic association studies look at the relationships between alleles, either in affected families or across populations of affected and unaffected individuals, to see to what extent an allele at a particular marker locus is associated more frequently than random expectation with a trait. Association between an allele and a trait can arise either because the allele causes the trait directly or is very closely linked to an allele that does. Allelic association analysis is an essential tool in determining the genetic basis of complex disorders/traits where linkage analysis is difficult. A major problem with association studies is population stratification, which arises largely from ethnic diversity, but age and gender may also exert an influence. Thus in case/control studies it is extremely important to select a suitably unbiased control cohort. [Schork et al 2001]. Another problem with association is that the statistical analysis is often not suitably stringent with reference to the number of questions asked, such as the number of loci tested. Thus the Bonferroni correction, which takes this into account, should always be applied ($p= 0.05/n$ where n is the number of questions asked). Due to the problem of finding suitable controls, association methods with internal controls are now often used (Lander and Schork 1994). For example, TDT (transmission distortion test) uses nuclear families with one or more affected offspring and one parent heterozygous at the marker locus under investigation. This test compares the frequency with which the parental alleles are transmitted to offspring with the trait/disorder. Deviations from the 50:50 ratio of transmission indicate an association (Spielman et al 1993). Such methods have been successful in identifying genes for complex disorders such as diabetes [Reed et al 1997).

Association analysis has also been used to great effect when a strong 'candidate gene' has been proposed for a particular phenotype [eg. polycystic ovary syndrome Urbanek et al 1999]. Such genes are usually selected on the basis of the function of the gene product, the pattern of expression during development or studies of animal models systems. Such explorations are best carried out using several markers since some negative results might occur, if for example the marker polymorphism has arisen subsequent to the trait or has been separated by recombination.

It is believed that for complex disorders, an approach combining linkage analysis and association studies is desirable. One of the main goals of the genome project after completing the sequencing of the genome is the systemic identification of common variants in all genes, a project that will greatly facilitate future association studies (Lander 1996). Such studies can be very complex, especially if there are several functional polymorphisms in a particular gene but the most important aspect of any study is the accurate classification and assignment of phenotypes.

With the complete sequence of the human genome now within sight it is possible to carry out procedures, such as whole genome scans, to facilitate the task of gene hunting through linkage analysis. A genome wide approach for mapping complex phenotypes would involve developing dense maps of SNPs throughout the genome in order to detect susceptibility genes through linkage disequilibrium (Zhao et al 1998). A computer simulation has recently led to the questioning of the merits of this approach (Kruglyak 1999). In addition to the complete sequence, an STS map of the human genome has been produced along with an SNP database under way (Bentley 2000). It is believed that for complex disorders, an approach combining linkage analysis and association studies is desirable. One of the main goals of the genome project after completing the sequencing of the genome is the systemic identification of common variants in all genes, a project that will greatly facilitate future association studies (Lander 1996). Such studies can be very complex, especially if there are several functional polymorphisms in a particular gene but the most important aspect of any study is the accurate classification and assignment of phenotypes.

2.7 Aims and objectives

The aim of this thesis is to classify normal human facial variation suitable for genetic analysis. The eventual aim is to link facial appearance with underlying genetic constitution. During the course of this thesis the human genome project reached preliminary

completion, making this aim more plausible. Additionally there has been an almost exponential explosion in technology, rapid processing and manipulation of 3D data. The project described in this thesis has attempted to harness developments in both these disciplines to provide groundwork for future studies.

Objectives

- Collect facial data and DNA from unrelated and related subjects and thus provide a resource for long term studies
- Explore and validate methods for analysing data
- Identify polymorphic facial phenotypes and devise objective procedures for classification based on qualitative and quantitative data.
- Analyse population data for frequency and distribution of identified phenotypes and use to generate genetic hypotheses
- Analyse family data to determine if classified phenotypes follow patterns of simple mendelian segregation
- Investigate facial asymmetry in a specific medical condition, Medullary Sponge Kidney (MSK), and compare with normal subjects.
- Explore relationship between normal genetic polymorphisms in candidate genes and facial phenotypes.

CHAPTER 3

Materials and Methods

This chapter provides details of the materials and methods used to collect and analyse the data assembled in this thesis. Information is provided on recruitment of subjects, two types of optical surface scanner and software used to collect and analyse the 3D face data described in Chapters 4, 5, and 6 as well as the materials and processes used to generate the molecular data presented in Chapter 7.

3.1 Data set

Initially subjects were recruited randomly in UCL. They mainly comprised students of at least eighteen years of age. This meant that the face was close to fully-grown and also that the subjects could give written consent to participate in the project. A consent form approved by the UCL ethics committee was filled out by each participant, DNA in the form of a blood or buccal sample were obtained where possible as well as personal information.

Some of the early volunteers were approached at a later date for two reasons; the first was to generate a data set where face data had been collected from the same subjects at a year interval and secondly to begin collection of family data. As the focus of the project shifted towards collection of family data, various strategies were employed to encourage family participation. These involved gimmicks

such as offering subjects their face image as a printout, T-shirt transfer or screen saver. Numerous other volunteers also emerged from various media broadcasts related to the project on the television and radio and in newspaper articles. Other initiatives to target family groups included weekend scanning at Whiteleys Art gallery in the Bayswater shopping centre and also weekly scanning in the 'Live Science' arena in the new Wellcome Wing of the Science Museum from July to December 2000. These projects both made use of the portable optical surface scanner described in section 3.2 and enabled us to double the number of family groups collected.

Participants were requested to fill out a questionnaire providing personal information including age, gender, ethnicity, relevant trauma/operations to the face, place of birth etc (Table 3.1). The completed information sheet was assigned the same number as the subject's scan to ensure anonymity of the data. The information was collated in a Microsoft Access database in order to make the data more accessible for further analysis e.g. stratification of the data for ethnicity, sex or age. The extent to which the information sheets were completed was extremely variable and not all subjects provided all the personal information requested.

Where possible DNA samples were collected from participants. This was not practical in public arenas such as the Science Museum and Whiteleys Gallery. Prof. Hopkinson took a 20ml intravenous blood sample, collected in a Na-EDTA tube, from volunteers (stored at

CONFIDENTIAL

CONSENT FORM [investigator's file copy]

Title of Study: Genetic analysis of Human Facial Features

Chief Investigator : Professor David A. Hopkinson

To be completed by the volunteer: **Please delete as necessary**

1. Have you read the information sheet about this study? YES/NO
2. Have you had an opportunity to ask questions and discuss this study? YES/NO
3. Have you received satisfactory answers to all your questions? YES/NO
4. Have you received enough information about this study? YES/NO
5. **Do you understand that you are free to withdraw from this study**
   - *** at any time** **YES/NO**
   - ***without giving a reason** **YES/NO**
6. **Do you agree to take part in this study?** **YES/NO**

Signed ..... Date .....

Investigators Signature . . . . . Date .....

About You:

Last Name _____ First Name(s) _____

Sex: _____ Date of Birth: _____ Place of Birth: _____

Ethnic Origin: _____Ethnic origin of parents:_____

_____

Are you Left Handed? Yes/No

Any operations or dental work that has affected your appearance: Yes/No (If Yes, please give details overleaf)

Tel. Number/email _____

May we contact you for further information if needed? Yes/No

For office use only:

Date: Number: File names: DNA: Saliva/Blood

All proposals for research using human subjects are reviewed by an ethics committee before they can proceed. This proposal was reviewed by the Joint UCL/UCLH Committee on the Ethics of Human Research.

Table 3.1 Example consent form and information sheet used

-70°C until required). Buccal samples were taken, in the form of 0.9% saline solution mouthwashes and buccal swabs (placed in 1.5ml of 0.05mM EDTA; 0.5% SDS) and stored at 4°C for up to two weeks. Dr Mark Thomas (Dept. of Biology, UCL) provided guidelines for collection and precipitation of DNA from buccal samples (personal communication).

3.2 Optical surface scanners

3D face data were collected from all participants using either a fixed or a portable optical surface scanner. Both scanners work on the principles described in Chapter 2.

3.2.1 Fixed scanner

Collaboration with UCL Medical Physics and Bioengineering department meant that it was possible to access the fixed optical surface scanner housed in the UCH maxillofacial unit. Due to its location, this system was largely used to collect data from students and staff in UCL. The equipment was operated as described in the User's Guide, provided by the Department of Medical Physics.

The scanner was located in a small room where it was possible to control the lighting and air conditioning. The equipment consisted of a rotatable chair, camera and monitor, two mirrors, laser light source, processor and computer. The scanner was operated from a DOS program run from a standard PC. It was possible to adjust the interval and region of data capture from this program. The light intensity was adjusted according to background lighting as well as

the skin tone of the subject using the video gain but generally was operated at the recommended middle-range signal saturation of 125 (max. a-d conversion = 255). Fig 3.1 illustrates the apparatus used.

3.2.2 Portable scanner

The Polhemus FastSCAN™ Handheld Laser Scanner (HLS) system was purchased through DHA (Duncan Hynd Associates Ltd), their Handbook of Instructions for installing the software and operating the scanner system (including settings for scanning, creating export files and calibration) was followed in the standard recommended manner. This apparatus comprised a scanner wand, receiver and transmitter device, processor and laptop PC with HLS operational software. Fig 3.2 illustrates the HLS equipment. As with the fixed scanner it was possible to adjust the camera 'sensitivity' to compensate for different lighting conditions and skin tone. This was achieved by changing the sensitivity setting on the wand on a scale from 1 to 5, 5 being the most sensitive. For normal operation a setting of 4 was used.

The HLS software settings could be adjusted for data capture parameters and data export parameters. It was essential to save HLS scans in a .obj export format that could be recognised by the software used for analysis. The export file is defined by the 'clipping' margin, this is the stringency used when meshing separate scan sweeps obtained from the system. A broad clipping margin (4mm) produces less stringent and smoothed data where as a narrow clipping margin

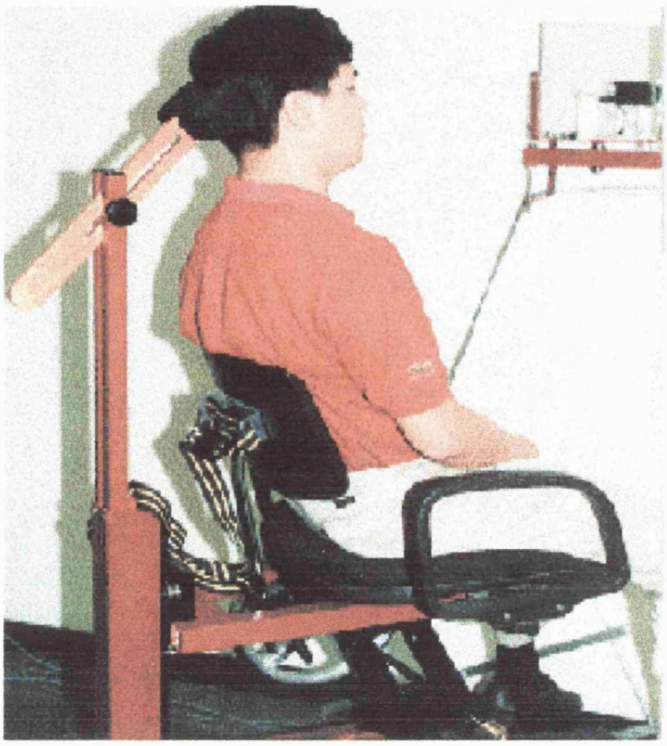

Figure 3.1 The MGI laser scanner. The subject sits on a chair that is rotated under computer control. A low-power laser line illuminates the face and is viewed by a camera from 2 different directions using two wall-mounted mirrors. The acquisition takes a few seconds to obtain a full-face scan comprising approximately 40 000 x, y, z data points.

(Image obtained from Medical Graphics and Imaging homepage http://www.medphys.ucl.ac.uk/mgi/)

A

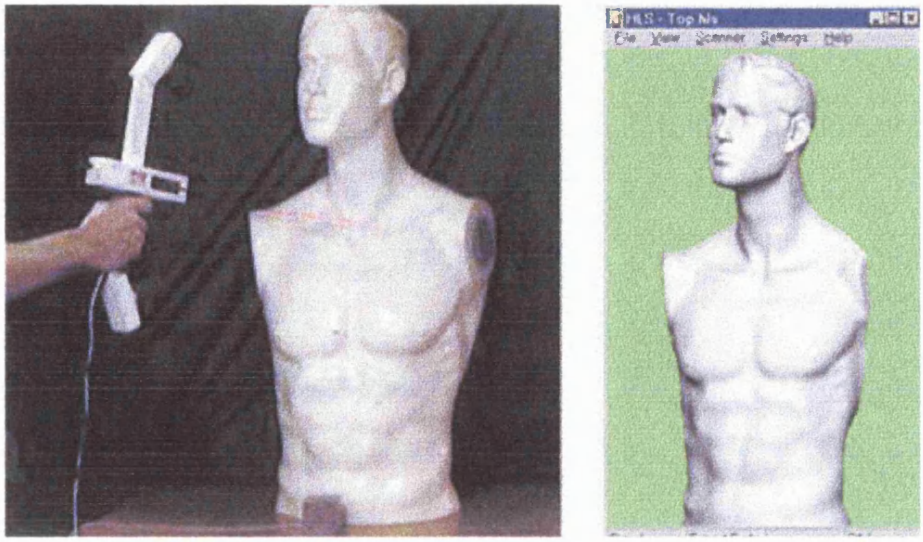

B

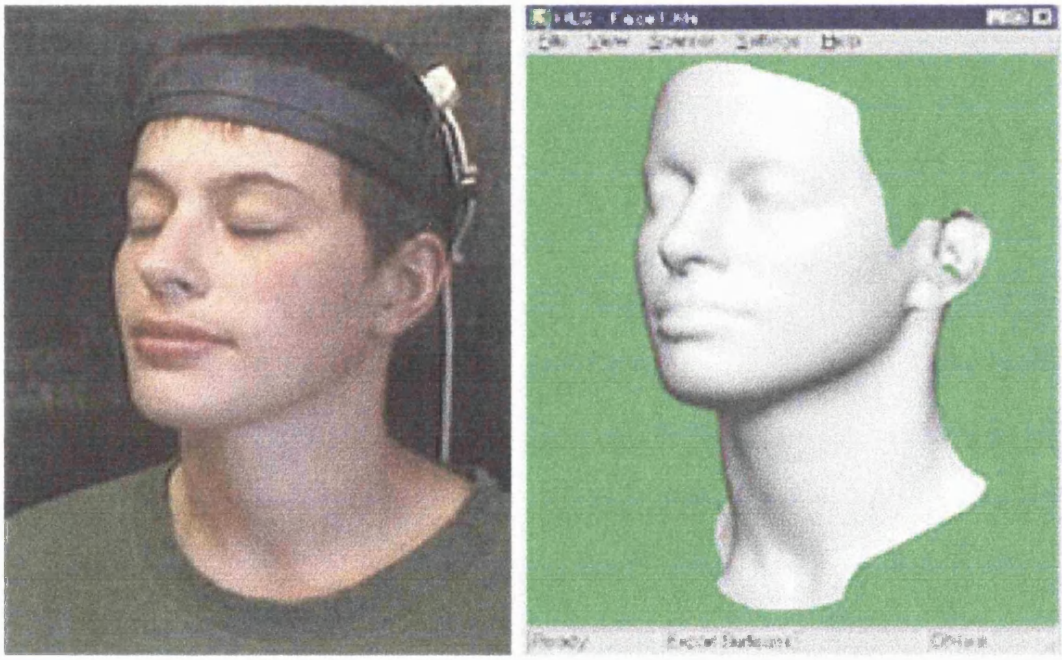

Figure 3.2 HLS equipment. A- Scanner wand and results observed on the computer screen from scanning a model. B- scanning of a 'live' subject which requires additional receiver device on the headband to compensate for subtle movement.

(Images are reproduced from the Polhemus website: http://www.polhemus.com)

(0.5mm) preserves finer detail, generally the 2mm recommended clipping margin was used.

3.3 Software

Most of the data analysis was carried out using CLOUD and LSMVIEW. Other software was used for statistical data and for the analysis of molecular data.

3.3.1 CLOUD

This program was kindly provided by Dr Robin Richards (UCL Medical Physics and Bioengineering Dept.) and largely used for viewing raw scan data, placing anatomical landmarks on the 3D scan and calculating distances and angles between defined points. The software could be used on .lsm files by the fixed scanner as well as .obj files generated by the HLS scanner. An additional use of CLOUD was to 'pseudo-scan' .obj files, which converted them into .lsm files, and this allowed direct comparison of the calculated surface segmentation files derived by the two types of scanner (Chapter 4).

3.3.2 LSMVIEW

Dr R. Hennessy developed this program in the MRC HBGU. This software made use of Surface Type analysis (STA) (Coombes et al 1990) and Shape Index (SI) (Koenderink and Van Doorn 1992) surface segmentation, mentioned in Chapter 1, and their direct application to the analysis of 3D face data. In order to view the surface segmentation the HK file had to first be calculated and this

took approximately 30 minutes per face scan using a standard PC. The HK file is a calculation of the mean (H) and gaussian (K) curvature at each data point obtained from the scan of the face and is used to generate both STA and SI segmentations. The program selects a circular patch with 10mm radius around each data point to calculate the local shape properties. The effects of altering the shape and size of the patch of points are discussed in Chapter 4. LSMVIEW was used to view the calculated HK file loaded onto the 3D face scan.

A 2D face map of the SI and STA analyses could be projected from .lsm data, but not .obj data, using LSMVIEW. A 2D face map allowed a specific SI value to be estimated at a point on the face. This was used in the classification of chin cleft (Chapter 4). As .obj files derived from the HLS scanner could not be projected into 2D face maps (unless converted into .lsm files by 'pseudo-scanning') an alternative method of grading shape variation was devised by changing the STA threshold function from the default parameter of 0.005 to 0.05. This generates STA patterns, which accentuate the more curved mid-face features as opposed to flatter features, and thus was extremely valuable in categorising the chin cleft feature (Chapters 4 and 5). Generally speaking there was good correlation between classifications using the STA and the SI analysis (Chapter 4).

3.3.3 Other software

Statistical analysis was carried out in Microsoft Excel using standard statistical formula for F tests, T tests, Correlation,

Covariance, Chi-square analysis, and calculation of mean, standard deviation, and 95% confidence interval values. The Chiprob program from GCG was used to obtain a probability associated with Chi-square analysis and the 2 by 2 program from GCG was used to carry out Fishers exact test. For analysis of molecular data, 'Amplify' was used to check primer sequence and GCG MAP sequence analysis programs used to identify restriction enzyme sites in variant sequences. All GCG programs were accessed through HGMP.

3.4 Molecular analysis

This section provides brief details on the standard techniques and materials used to produce the data presented in Chapter 7.

3.4.1 Materials

Standard reagents:

Analar grade reagents were purchased from BDH/Merck, Fisons and Sigma.

Enzymes:

Restriction enzymes were purchased from New England Biolabs. The *Taq* polymerase used for PCR was from Advanced Biotechnologies and the Thermo Sequenase from Amersham Life Science

Electrophoresis reagents:

Agarose was from BRL and Nusieve low melting point agarose from FMC Bioproducts. 40%(w/v) acrylamide and 2%(w/v) bisacrylamide were from BIO-RAD. 19:1 acrylamide/bisacrylamide solution was

from Severn Biotech, APS (ammonium persulphate) was from BIO-RAD and TEMED (N, N, N', N' – tetramethylethylenediamine) was from BDH.

Miscellaneous

dNTPs were purchased from Amersham Pharmacia Biotech UK. Gel extraction and PCR clean up kits came from Qiagen. The 1kb DNA marker used to estimate the size of DNA fragments in agarose gels was bought from Gibco, BRL.

Commonly used Solutions:

10 x TBE: 890mM TrisHCL, 890mM Boric Acid, and 20mM EDTA

1 x TE: 10mM TrisHCL, 1mM EDTA, at pH7.5

6 x Loading Buffer: 30% Glycerol, 1 x TE, 0.05% bromophenol blue

All solutions were made using distilled water. The water used in SSCP and PCR was further irradiated by ultraviolet light (MilliQ plus 185) and autoclaved.

3.4.2 Methods

Glassware used was sterilised by autoclaving (15psi, 121°C for 20-25 minutes), as were commonly used solutions. Autoradiography was carried out by exposure of MR-1 X-ray film (Kodak) at room temperature overnight for ^{33}P labelled sequencing.

DNA preparation

I. Islam (MRC HBGU, UCL) prepared DNA from blood and buccal samples using standard procedures outlined by Grimberg et al (1989)

for the isolation of genomic DNA from blood samples and a phenol extraction procedure for buccal samples (Dr M. Thomas, Dept. Biology, UCL personal communication).

PCR Amplification

All reactions used 10 x Buffer V (Promega Formula: 500mM KCl, 100mM Tris-HCl; pH 8.3 at 25°C, 15mM $MgCl_2$, 1% TritonX-100) from Advanced Biotechnologies. Reactions were carried out using; ~50-200ng of genomic DNA with 50pmoles of forward and reverse primers (details of primer design and sequence is given in Chapter 7), 0.2mM dNTPs, 1 x Buffer V and 1µl of *Taq* all in a final volume of 100µl, made up with sterile distilled water. Reaction mixes were also prepared where the DNA was substituted with sterile water to monitor for DNA contamination. The reaction mixes were prepared in 0.5ml eppendorf tubes, vortexed and amplified using a Phoenix PCR machine (with a heated lid). The standard cycling conditions for up to 35 cycles were: denaturation at 96°C for 30 seconds, annealing for 30 seconds and extension at 72°C for 30 seconds. Initially, the annealing temperature used was calculated as T_m – 4°C, where T_m is the melting temperature whereby approximately equal proportions of the DNA are annealed and dissociated. T_m was calculated from the primer sequence using the following equation:

T_m = 69.3 +0.41 (%G+C content of primer)-(650/length of primer)

After an initial PCR, annealing temperatures were decreased or increased to achieve specific amplification of the desired PCR

product, the optimum PCR cycling conditions for each exon of ET1 and ETRA are listed in Table 3.2. Once optimum conditions were established PCRs were carried out in microtitre plates rather than eppendorf tubes to facilitate the handling of greater numbers of samples. For microtitre plates the Perkin Elmer PE9700 PCR machine was used.

Agarose gel electrophoresis and recovery of DNA fragments

DNA fragments were resolved in 1.0-6.0% agarose gels. Generally a 1.5% agarose gel was used for electrophoresing PCR products and this was made by dissolving 0.75g of agarose in 50ml of 1x TBE buffer solution with 1µl ethidium bromide (at a concentration of 100ngml^{-1}). The gels were poured into 8 x 10cm flatbed moulds and when set, run at 10Vcm^{-1} in 1x TBE buffer solution. To enable visualisation of the DNA fragments, by ultra-violet transillumination, ethidium bromide was also added to the buffer solution. 3% and 6% gels were used to obtain better resolution of the DNA bands if diagnostic restriction enzyme digestion had been used on the PCR product.

Single stranded conformation polymorphism (SSCP)

SSCP analysis was carried out using Hoefer (SE 600) vertical electrophoresis units. The gels were 16x14 cm and were made by mixing the appropriate volumes of 40% acrylamide and 2% bis-acrylamide, in 0.5 x TBE, with 0.16% (v/v) TEMED and 4% (w/v) ammonium persulfate to polymerise the gel as well as 50% glycerol

Primer name and sequence 5'→ 3'	Anneal temp.	Additional
ET- F1 taaagggcacttgggctgaagg **ET- R1** ccgagacttacaagtcaacgag	56	30 cycles
ET- F2 tttgaggagacatcccccactg **ET- R2** gtggagccagcgctaatgaatg	57	30 cycles
ET- F3 ggaataggtgtgtccatgtgtc **ET- R3** tgataggaaggagttcaggagg	51	35 cycles, extension temp. 60°
ET- F4 ctatcatggtactgccttcctg **ET- R4** aggctgctggcatcactgactg	58	30 cycles
ET- F5 aaagttcacaaccagattcagg **ET- R5** gggaactccttaacctttcttg	53	30 cycles
ETA2AF agcagcacaagtgcaataagag **ETA2AR** agtctgctgtgggcaatagttg	54	35 cycles
ETA2BF atttggtcctacccagcaatg **ETA2BR** catttgtggttacttcctacc	52	35 cycles, denature held for 45 sec, anneal held for 60 sec
ETA3F actgtgtctccttctttcagc **ETA3R** aagggaaagaaccacattacc	53	35 cycles
ETA4F ttcaggtacagagcagttgc **ETA4R** tgtggcattgagcatacagg	52	35 cycles, denature held for 45 sec, anneal held for 60 sec
ETA5F tcactttgaagttctaccaag **ETA5R** catgatgttatgggatttacc	50	30 cycles
ETA6F cactttcctttagcgtcgag **ETA6R** gcgagtacacaggatcatac	53	30 cycles
ETA7F ttgctctagtttcttactgc **ETA7R** tgaaaaatcatcttacctgg	55 49	5 cycles, anneal held for 45 sec 30 cycles
ETA8F gtctgttccttcccccagtc **ETA8R** gcatttcttcttgggtgtgg	56	35 cycles

Table 3.2 Primer sequence and optimal annealing temperature used to amplify the desired sequence from ET-1 exons 1-5 and ETRA exons 2-8. All reactions were carried out using Buffer V. Unless stated otherwise each denaturation, annealing, and extension stage was each held for 30 seconds, per cycle.

solution (if required) to achieve a gel of desired cross-linker composition. The volumes of acrylamide and bis-acrylamide were altered to achieve the required %T (total amount, in grams of monomers, of acrylamide and bisacrylamide per 100ml) and %C (total amount of bisacrylamide in the total amount of monomers). Generally two types of gel were made, with 12% T 2% C and 10%T 1.5%C.

To prepare the sample for loading onto the gel 1μl PCR product was added to 4μl SSCP loading buffer (95% formamide pH 7.0, 0.02M EDTA, 0.05% bromophenol blue in sterile distilled water) and 3μl water and mixed well. The mix was then incubated at 96°C for 7mins to denature the DNA and plunged into a bucket of ice before loading immediately onto the gel with a long tip pipette. A 1kb DNA ladder and a non-denatured sample were run on each gel. The gels were electrophoresed in 0.5 x TBE (also used to flush out the wells before loading the mixture) at room temperature.

A number of parameters were varied to optimise the SSCP analysis of each PCR product. These were percentage of acrylamide and bis-acrylamide, addition of glycerol and the length of the run (volt-hours). Table 3.3 summarises the final SSCP conditions chosen for maximum resolution of each of the 5 exons of ET-1 and for exons 2 to 8 of ETRA respectively (all experiments were carried out at room temperature).

Silver Staining

The DNA banding patterns were revealed by silver staining as follows:

ET-1	Gel Composition	glycerol	Volts/hours	Example
Exon1	12%T 2%C	✗	170 volts for 17 hours	Fig 7.1 C
Exon 2	12%T 2%C	✗	350 volts for 4 hours	Fig 7.2 B
Exon 3	12%T 2%C	✗	170 volts for 17 hours	Fig 7.3 C
Exon 4	12%T 2%C	✗	190 volts for 17 hours	Fig 7.4 C
Exon 5	12%T 2%C	✗	180 volts for 17 hours	Fig 7.5B
ETRA	**Gel Composition**	**glycerol**	**Volt/hours**	**Example**
Exon 2 (5')	12%T 2%C	✓	130 volts for 19 hours	Fig 7.6 A
Exon 2 (3')	12%T 2%C	✓	140 volts for 17.5 hours	Fig 7.6 D
Exon 3	12%T 2%C	✗	350 volts for 4 hours	Fig 7.7 B
Exon 4	12%T 2%C	✓	350 volts for 4 hours	Fig 7.8 C
Exon 5	12%T 2%C	✓	350 volts for 5 hours	Fig 7.9 C
Exon 6	12%T 2%C	✗	140 volts for 18 hours	Fig 7.11 B
Exon 7	12%T 2%C	✓	350 volts for 4 hours	Fig 7.10 B
Exon 8	12%T 2%C	✓	160 volts for 18 hours	Fig 7.12 C

Table 3.3 SSCP conditions chosen to achieve optimal resolution of bands for exons 1-5 of ET-1 and exons 2-8 of ETRA.

The gels were fixed by washing for 2 x 3.5min in a 10% ethanol 0.5% acetic acid solution, with agitation throughout, then incubated in a freshly made 0.1% aqueous solution of silver nitrate for 2 washes of 7 min and 6 min, with continuous agitation. After brief washes (x2) in water the developing solution (1.5% sodium hydroxide with 0.01% sodium borohydride and 0.4% formaldehyde) was applied. After 3-10 min the developer was removed, the timing being determined by the intensity of band development. The gel was finally rinsed in water and dried on a vacuum drier at 83°C for 1.5 hours.

Preparation of PCR products for sequencing

When variant banding patterns were observed on SSCP analysis the remainder of the corresponding PCR product was cleaned up for DNA sequence analysis either directly using the QIAquick PCR purification kit or QIAquick gel extraction kit, after cutting out the desired product band from an agarose electrophoresis gel using a sharp scalpel. The protocol suggested by the manufacturers was followed without alteration for both methods.

DNA sequencing

PCR products were sequenced using the dideoxynucleotide chain-termination method (Sanger et al 1977), using the Amersham Thermo sequenase radiolabelled terminator cycle sequencing kit according to the manufacturers instruction in conjunction with the Amersham Pharmacia radioactive labels (Revidue ^{33}P labelled terminators).

2μl Thermosequenase DNA polymerase was mixed with 2μl of 10 x reaction buffer (260mM Tris-HCl, pH9.5, 65mM $MgCl_2$), 2.5pmol of primer and approximately 50-500ng of DNA made up to a final 20μl volume with distilled water. Four 4.5μl aliquots were mixed with 2.5μl of A, C, T and G termination mixes (each termination mix comprised 7.5μM dATP, dCTP, dGTP, dTTP with 0.0752μM (0.2252 μCi) of the appropriate chain terminators [α- ^{33}P] ddNTP (1500Ci/nmol)). The reactions were covered with 30μl paraffin oil and then cycled on a PCR machine for 40 cycles of: 95°C for 30 sec, 60°C for 30 sec and 72°C for 1min 30 sec. After single strand amplification 4μl of stop solution (95% formamide, 20mM EDTA, 0.05% bromophenol blue, 0.05% xylene cyanol) was added to each reaction and the mixture removed from under the layer of mineral oil. Each sample was then denatured at 95°C for 5-6min, before loading 1.2μl of each mix onto the sequencing gel.

Electrophoresis was carried out using Biorad sequencing apparatus and a denaturing polyacrylamide gel. The gel was prepared containing 42g Urea, 15ml acrylamide mix [ACCU gel 19:1, 40%(19:1) acrylamide: bisacrylamide solution), and 5ml 20 x Glycerol tolerant buffer (GTB)[216g Tris-HCL, 72g Taurine, 4g EDTA in 1litre] made up to 100ml with distilled water. 40ml of this solution was poured into the casting tray to seal the bottom of the gel and the remaining 60ml was used to cast the gel. Prior to pouring, 160μl of 20%APS and 100μl TEMED was added to the casting tray mix and 120μl of

20%APS and 120µl TEMED were added to the gel mix. The gel was poured and allowed to set overnight. The gel was pre-run in 1 x GTB at 50 watts to warm the gel to 50°C. The samples were denatured in an oven at 80°C prior to loading on the gel using a 48-well shark's tooth comb. The gel was electrophoresed for approximately 2-2.5hrs at a constant 50°C (40-50W). After disassembly of the apparatus, the gel was transferred to Whatmann paper and dried in an 80°C oven for 45 min. The gel was exposed to X-ray film overnight at room temperature in a light-tight black box.

DNA modification

Restriction enzyme digests were performed using the provided incubation buffers and carried out according to the manufacturers instruction either in a water bath at 37°C or 65°C.

CHAPTER 4

General aspects of data collection and evaluation

The aim of this thesis is to classify normal human facial variation and generate systems that are suitable for genetic analysis. Hence the first objective was to establish a reliable method for collecting facial data from volunteer subjects. Then came the investigation of suitable methods, using conventional and novel approaches for the analysis and classification of facial features. This chapter provides an overview of the initial data collection procedure and the general analysis of the face data together with the study of specific polymorphic facial features.

3D face data has been collected with two types of optical surface scanner. These data are briefly assessed from the point of view of quality and also in terms of the feasibility of achieving the outlined objectives. Quantitative and qualitative methods of facial classification are explored and investigate particular features as well as general properties of the face; their relative merits and applications for genetic analysis are discussed. The quantitative approach takes two lines, that of an overall judgement of the symmetry of the face as well as analysis of a localised feature in terms of the degree of protrusion of the mandible. Qualitative methods are described which provide an objective classification of several midline features. The

chapter concludes with an evaluation of the reproducibility of these analytical procedures.

4.1 Collection of 3D data sets

3D surface data from the face were collected from randomly recruited volunteers using the two types of optical surface scanner, described in Chapter 3.

4.1.1 Scan data from fixed optical surface scanner

More than 600 individuals were scanned using the fixed optical surface scanner. Four separate scans were made of each individual; full face, mid face and one of each ear (Fig 4.1). The height of the chair was adjusted to maximise the area of the face scanned. The individual was aligned vertically against the headrest and asked to close their eyes. The chair was rotated manually to check that the fanned laser stripe projected vertically along the midline profile of the face. The video gain was adjusted according to background lighting and skin tone, generally to around 125 units, but slightly higher for subjects with darker skin tone. The full-face scan began at the left ear and the chair was rotated anticlockwise 250° under computer control to finish approximately at the right ear, capturing data at one-degree intervals.

The mid-face scan was taken 30° either side of the midline with data captured at every 0.25° (Fig 4.2). The raw data for each scan was saved as a Laser Scan Multiple file (.lsm), this file records the x, y, z

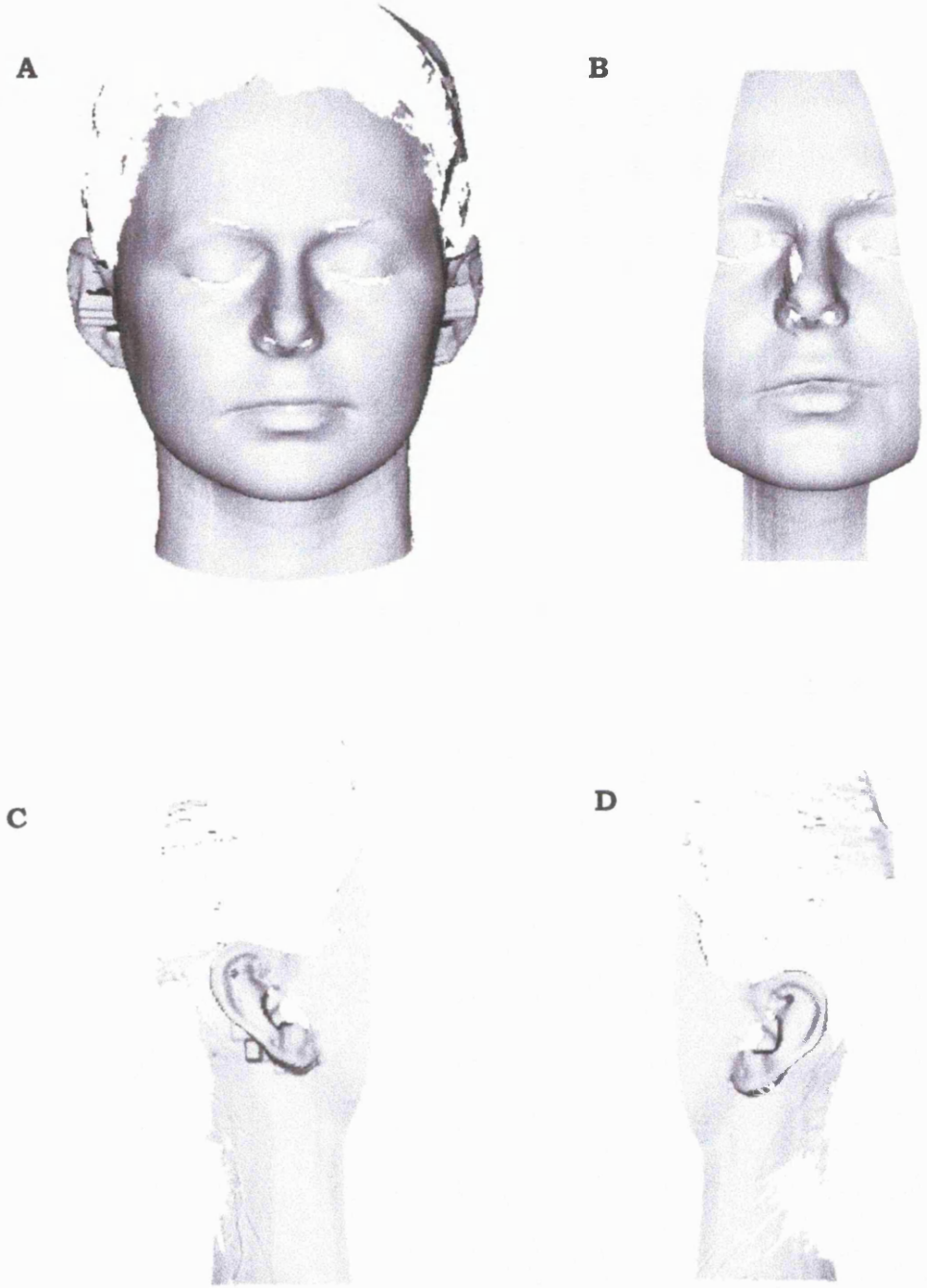

Figure 4.1 Raw data (.lsm) obtained from fixed optical surface scanner A- Full-face (f) scan, B- Mid-face (n) scan, C- Right ear (r) scan, D- Left ear (l) scan.

A

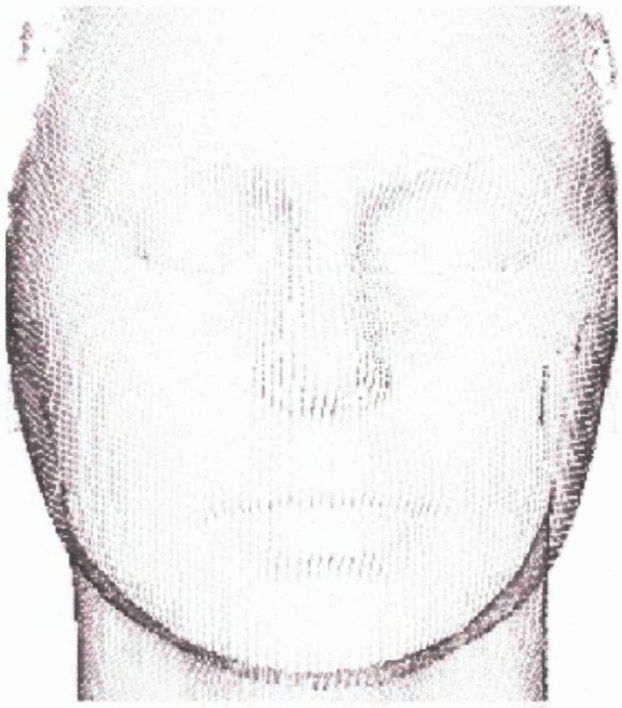

B

Figure 4.2 A- Density of data points collected from a full-face scan, where the data are collected at 1° intervals on rotation of the subject. B- Density of data points collected from a mid-face scan, data collected at 0.25° intervals as subject is rotated

co-ordinates of the 40,000 data points collected from a scan. Ears were scanned at the same resolution as the full face scans.

4.1.2 Scan data from HLS

The hand held laser scanner works on the same principle as the fixed system. The main difference between the two systems is that the fixed scanner records data in vertical stripes, at approximately one-degree intervals around the face from left ear to right ear, and the HLS captures information, at a similar density, as a blanket of points from each sweep made with the wand. It is not essential to align the subject carefully before scanning since the integrated tracking system determines the position and orientation of the wand during each sweep across the surface of the face. The computer simultaneously reconstructs the 3D face on the screen.

It was found that three overlapping sweeps covering the left and right sides of the face as well as the mid face region provided sufficient data. Optimum data was obtained with the wand about 30 cm from the subject. In general, in subdued lighting, the sensitivity level 4 was used to collect data with the HLS; if the subject had darker skin tone then a higher sensitivity was used.

The HLS software was used to mesh the data from three sweeps and delete overlapping points to produce an 'export' file comprising 30-40, 000 data points (Fig 4.3). The export file was in Wavefront or object file (.obj) format and could be viewed and manipulated with other software such as CLOUD and LSMVIEW.

A

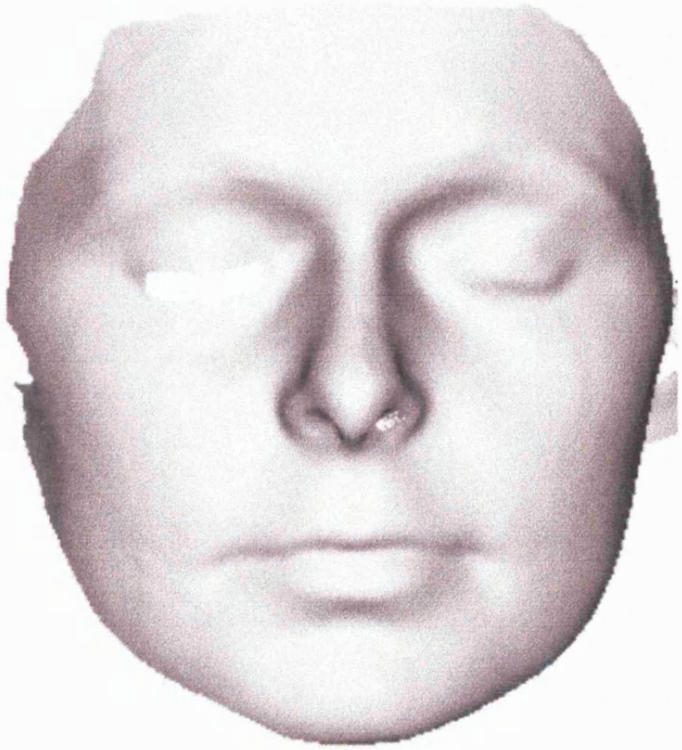

B

Figure 4.3 Data obtained from the Hand-held Laser Scanner (HLS) displayed in Wavefront (Object–obj) format. A- Complete export scan, B- Display showing data points collected.

The density of data was shown to vary according to the speed at which the sweep was performed. Slower sweeps generated denser data sets but required more care in maintaining smooth movement of the wand.

4.1.3. Evaluation of scan data

Data were collected using both scanners. For both systems adjusting the scanner settings could influence data quality. For subjects with dark skin the data were obtained by increasing the laser intensity and hence the sensitivity of the scanner. In general the slower the scans the better the evenness of data capture. However, if a scan was too slow there was an increased risk of movement in the subject. Additionally, with the HLS system, a slow speed often resulted in a stuttered appearance due to the difficulty of maintaining a consistent wand speed. For scans of young children, who have a tendency to move, it was found that faster scans were better.

a) Fixed scan

The main drawback of this system for our study was the lack of portability. This became more of an issue as the focus of the project shifted to recruitment of families. Specific problems included subject alignment, headrest distortion, and a lengthy re-calibration procedure. It was very important to align the laser stripe along the facial midline of each subject as the scanner captures data in vertical profiles. Thus, any deviation from midline alignment resulted in

uneven data collection and occlusion. Problems also arose if the subject moved in between alignment and scanning and when a precise facial midline could not be identified, for example when a subject had a 'crooked' nose. A further problem with subject alignment arose if the head was pressed too far back or forward because the headrest was badly adjusted. The fixed scanner sometimes required calibrating which is a lengthy process. Hence it was very important to ensure the scanner calibration was not disturbed.

b) Portable scanner

The acquisition of the hand held scanner allowed greater mobility for data collection and in a short time it provided a significant increase in the number of family data sets collected. We have found that the major problem with the HLS system is the sensitivity of the receiver-tracking system to the presence of heavy metals, such as iron in building structures and furniture. This results in distorted and ineffective meshing of scan sweeps. It was found that the minimal precautions were to have the subject seated on a non-metallic chair at least a metre from all surrounding computer equipment and any other metallic objects and wiring. Subjects were asked to remove jewellery and watches from the hand that held the tracking device. Metallic distortion proved more of a problem than we had originally anticipated and in some instances it was not always easy to determine the source of the interference. In

environments where the scans were of consistently poor quality when meshed together, we found that increasing the clipping margin for meshing provided a less distorted export file. However through making the meshing less stringent, the number of data points was reduced and hence too the data quality/sensitivity.

The HLS system also appeared to be much more sensitive to movement related distortion than the fixed scanner; slight movement of the eyes, relaxation of the mouth and swallowing were all relatively common occurrences in between scan sweeps of overlapping areas and this led to distortion. These problems were offset however by the speed with which the scan could be repeated, in less than a minute, without the need to realign the subject.

4.2 Summary of 3D data collected

Facial data from about 1000 subjects were collected, summarised in Table 4.1. The individuals were very heterogeneous with respect to geographical/ethnic origin; and very few subjects actually originated from the local London area. 693 unrelated subjects could be classified on the basis of ethnicity as stated on the completed information sheet. The majority of these were European Caucasians (n=584). Individuals of African (n=18), Indian (n=50), Chinese (n=27) and Middle Eastern (n=14) origin were also examined. These classifications were very broad: African included people from Africa and the Caribbean; Middle Eastern included people from Iran, Iraq, Kuwait and Syria; Chinese included subjects of Hokkien

Total Data Collected (unrelated) N= 928	750 subjects from initial recruitment 408 female 342 male 55 subjects from Whiteleys project 123 subjects from Science Museum project
Family Groups Collected N = 133	78 family groups initially collected 17 groups recruited from Whiteleys project 38 groups recruited from Science museum 57 two parent groups (1-8 offspring)
Ethnic Origin: 5 groups N = 693	European N = 584 Indian N = 50 Chinese N = 27 African N = 18 Middle Eastern N =14
Ages: N= 669	24 subjects over 75 33 subjects 66-75 49 subjects 56-65 85 subjects 46-55 121 subjects 36-45 203 subjects 26-35 127 subjects 16-25 27 subjects aged 15 and under
DNA Collected from unrelated Caucasians	78 Blood samples 115 Buccal swab samples
DNA collected from complete two parent families	2 families: all blood samples 2 families: mixture of blood and saliva samples 6 families: all saliva samples

Table 4.1 Face and DNA data collected throughout the project

background; Indian included individuals from Sri Lanka, and the European group comprised individuals from Britain and the whole of Europe including eastern Europe.

Data were obtained from over 133 family sets comprising 473 subjects. These ranged from cousins, sib pairs, twins, to 'complete' families (two parents and children). 78 family groups were recruited by direct approach, the projects held at Whiteleys and the Science Museum provided an additional 55 family groups. Altogether there were 57 'complete' families with between one and eight offspring.

The ages of the volunteers ranged from 8-90 years; 80% of volunteers were aged between 15 and 55 with an average age of about 35.

4.3 Analysis of 3D data

Initial examination of the 3D scan data suggested subtle person to person variation could be identified. For example, the raw data revealed that even with the absence of important recognition cues such as skin tone, hair, and eye colour it was possible to judge the approximate age, sex and ethnicity of individuals from a simple front or side view of the 3D image.

The data were then looked at in various general ways to highlight those areas of the face that showed the greatest apparent person to person variation. For example, crude image processing techniques were employed on 2D images of the face scans. Using

such methods, the left and right sides of the face were compared in a set of subjects to investigate variability in facial symmetry (Fig 4.4A).

The data were also used to generate a 'depth map' of contours based on the z co-ordinate values derived from an aligned scan. The variability of these patterns was used, for example, to look at variation in chin shape (Fig 4.4 B) but it became clear that the patterns produced were very dependent on alignment of the 3D image before generating the depth map.

The facial profile was also analysed in a set of subjects in the way described by Galton (1910) using his combination of measurements and subjective criteria (Fig 4.4C).

In this way numerous facial traits that appeared to be amenable to classification were identified. However whilst encouraging, these early analyses tended to be rather subjective, and more objective and rigorous methods of classification were therefore sought. Traditional methods such as anthropometry as well as newer techniques based on properties of surface curvature were thus investigated for reliability and reproducibility.

4.3.1 Anthropometrical analysis of 3D data

All anthropometric measurements were carried out using the program CLOUD generously provided by Robin Richards. CLOUD allowed placement of landmarks and calculation of angles and distances between points. The focus for quantitative analysis was

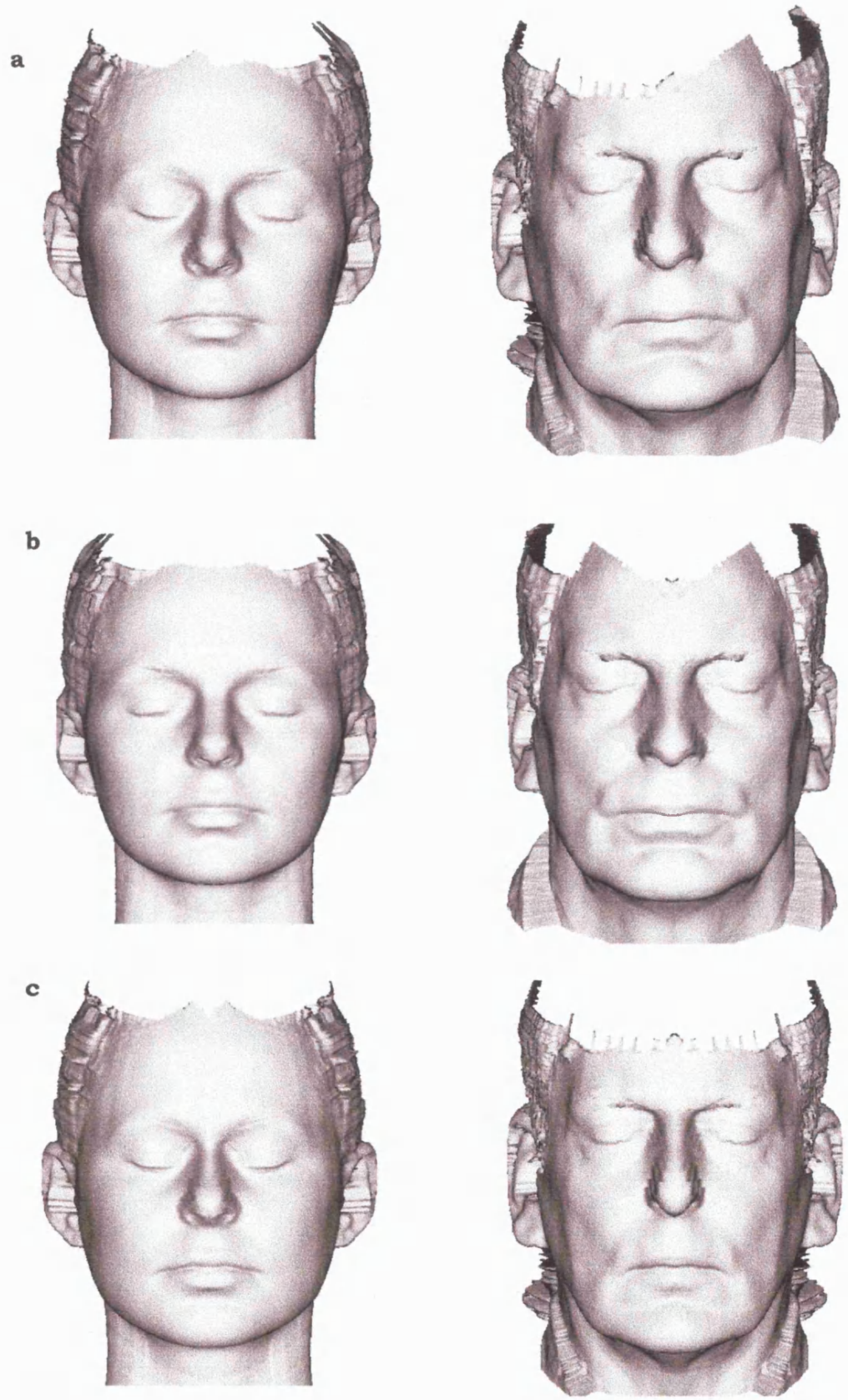

Figure 4.4 A. Crude analysis of facial asymmetry on 2D image from scan data of two subjects. a- Raw scan data, b- image made from the left side of the face paired with the left mirror image, c- image made from the right side of the face paired with the right mirror image.

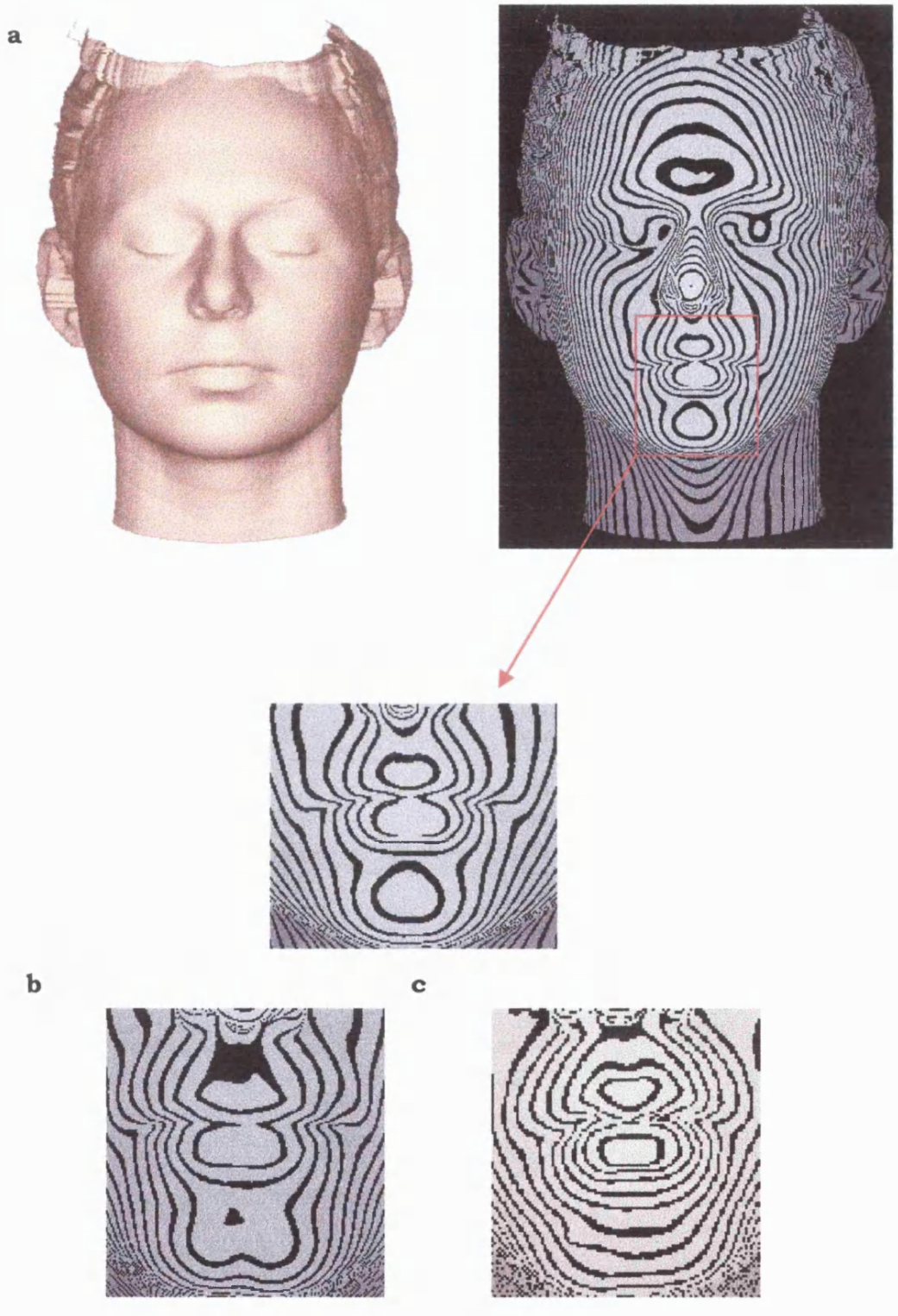

Figure 4.4 B. Raw scan data with z-co-ordinate based 'depth-map' applied. a- Area marked in red is magnified to illustrate pattern associated with chin shape; b and c illustrate same region in two other unrelated subjects.

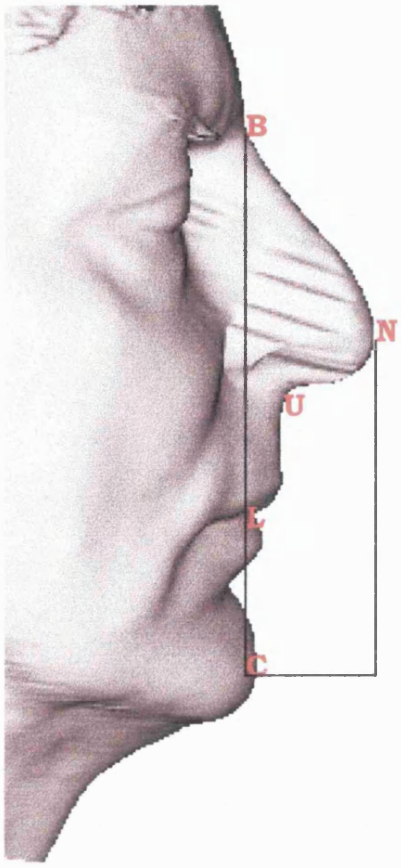

$$\frac{32\ \ 8\ \ 17}{25\ \ 1\ \ 3} : \frac{14\ \ 5\ \ 1}{.7\ \ 8\ \ 41}$$

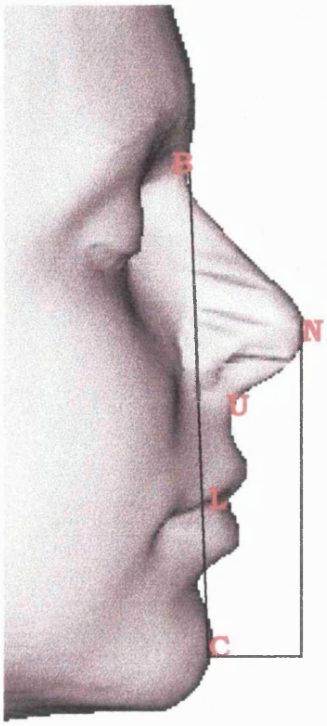

$$\frac{34\ \ 5\ \ 12}{29\ \ 6\ \ 3} : \frac{15\ \ 3\ \ 2}{.6\ \ 0\ \ 52}$$

Figure 4.4 C. Numeralised classification of facial profile using the method described by Galton (1910). Measurements of the face are standardised by making the distance between landmarks B and C equal 50mm. Five facial landmarks are used together with seven subjective criteria to produce a set of numbers unique to each person describing the relative proportions of the facial profile (full details are given in Chapter 2, Fig 2.1)

initially the whole face to investigate symmetry followed by a more local study leading to an estimate of jaw protrusion.

a) Triangle area method

A method used to judge asymmetry of patients with hemifacial microsomia (Moss et al 1991) was utilised to analyse minor facial asymmetry. This method involved the placement of 19 facial landmarks (Fig 4.5A) onto the 3D face scan. These landmarks were used to make 13 symmetrical triangles on both the left and right sides covering the surface of the 3D face (Fig 4.5B). The lengths of each side of each triangle were used to calculate the area from the following equation:

AREA =SQRT (S (S-A)(S-B)(S-C)), WHERE S=(A +B +C)/2 OR PERIMETER/2.

The area of each triangle was then compared to the corresponding triangle on the other side of the face to estimate the variability and extent of facial asymmetry. This method was used in a study to investigate facial asymmetry in individuals with a heterogeneous kidney disorder. These data are presented in section 6.2.

b) Jaw protrusion

A receding mandible or retrognathia is a feature of many craniofacial disorders and there are numerous reported angles and measurements describing various aspects of the jaw morphology. In order to estimate the degree of protrusion of the jaw three centrally located landmarks were chosen, these were the nasion (n), pogonion (pg), and subnasale (sna). The nasion was determined as the

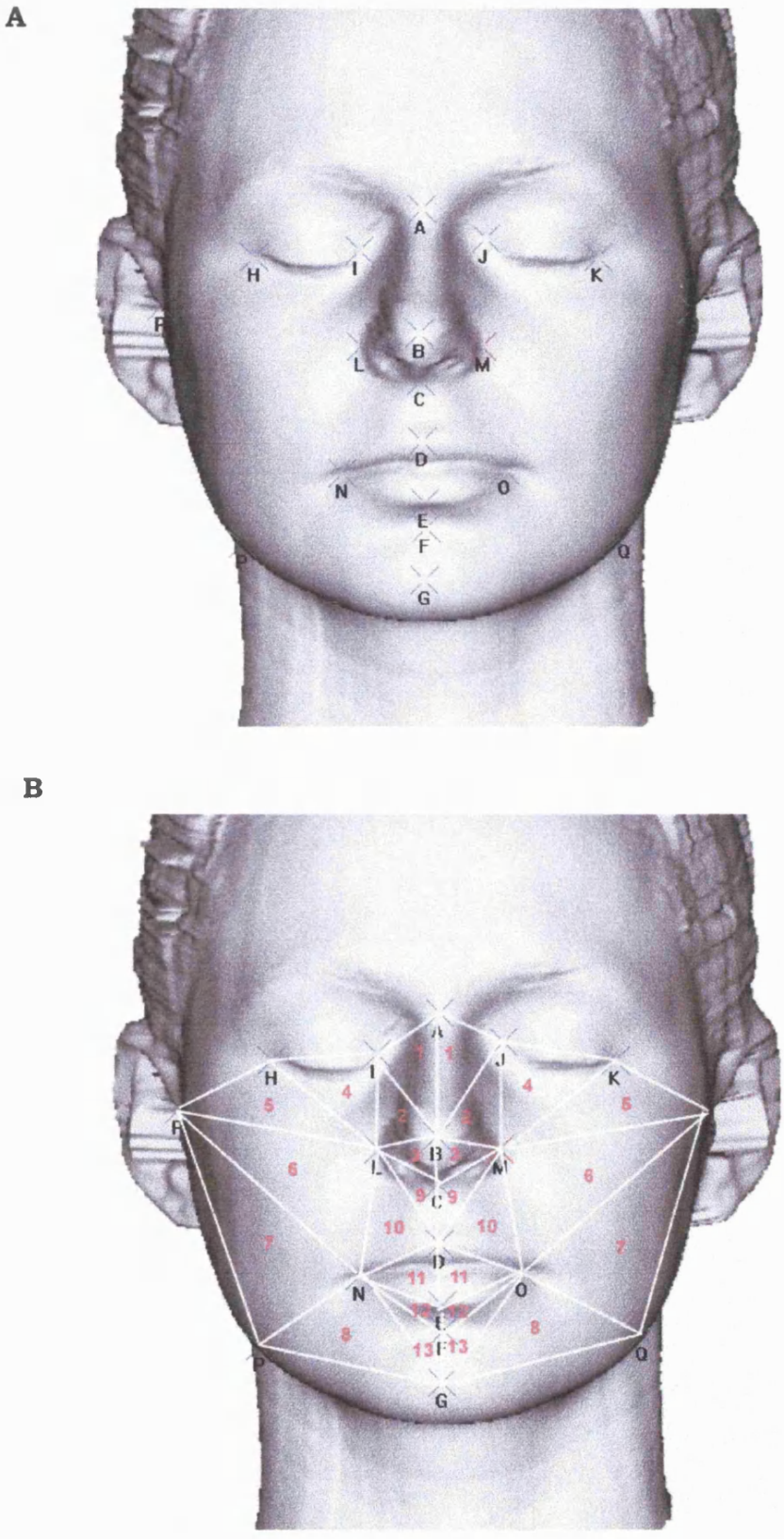

Figure 4.5 Triangle area method used to estimate facial asymmetry. A. 19 landmarks used to form triangles covering the surface of the face. B. 13 triangles on left and right sides of the face used to estimate facial asymmetry.

minimum point in the midline of the nasofrontal suture. The pogonion was located on the most prominent anterior midpoint of the chin and the subnasale the midpoint where the lower border of the nose and the upper lip meet (Fig.4.6A). The angle N-SNA-PG (Fig 4.6B) was calculated using the x, y, z co-ordinates and the formulae described in Chapter 2. This feature was scored in a subset of the scanned population and also in families where the offspring were over 16, the data are presented in section 6.1.

4.3.2 Surface Analysis and segmentation of 3D data

A surface segmentation output file was generated on each face scan using the LSMVIEW program. This calculates the mean (H) and Gaussian (K) curvatures, measures of the extrinsic and intrinsic surface curvature. Segmentation using the H and K parameters provided an eight-colour surface type analysis (STA) (Fig. 4.7a), the colour relating to the positive or negative values of the H and K parameters (Fig. 4.7b). The STA method of analysis colour codes the laser-scanned image on the basis of the degree of curvature, the more positive curvature (convex) describing a peak shape and the more negative curvature (concave) describing a saddle valley shape. This information is added to the 3D view of the facial surface to generate segmentation of the face where areas of similar shape are delineated by the same colour (Fig 4.7).

These values are also used to compute Koenderink's modified Shape Index (SI)(Koenderink and Van Doorn 1992), which allows

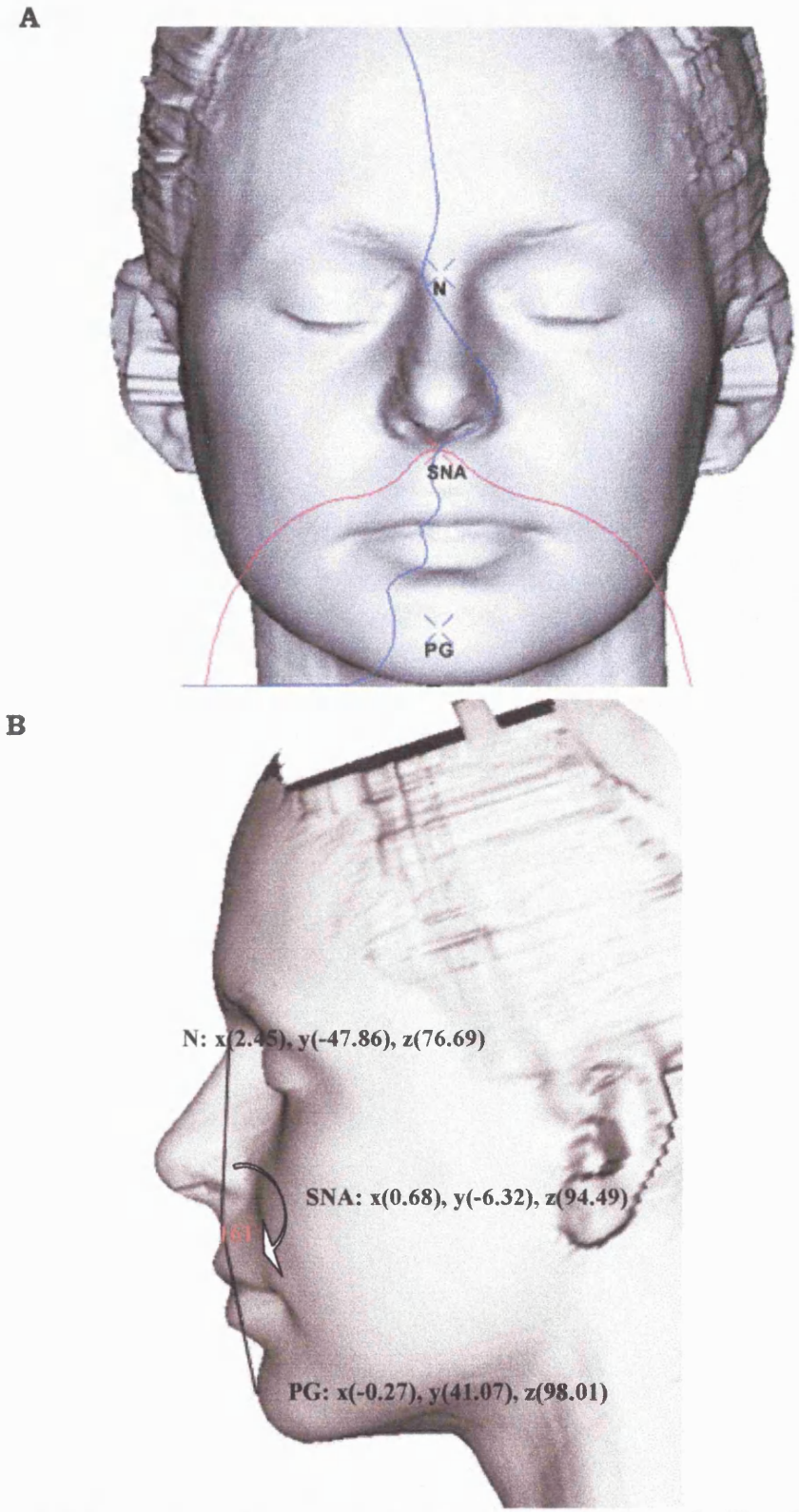

Figure 4.6 Measurement used to estimate jaw protrusion. A. The three landmarks chosen were nasion (N), subnasale (SNA) and pogonion(PG). B. The 3D co-ordinates of these landmarks were used to calculate the included angle N SNA PG using basis trigonometric formulae.

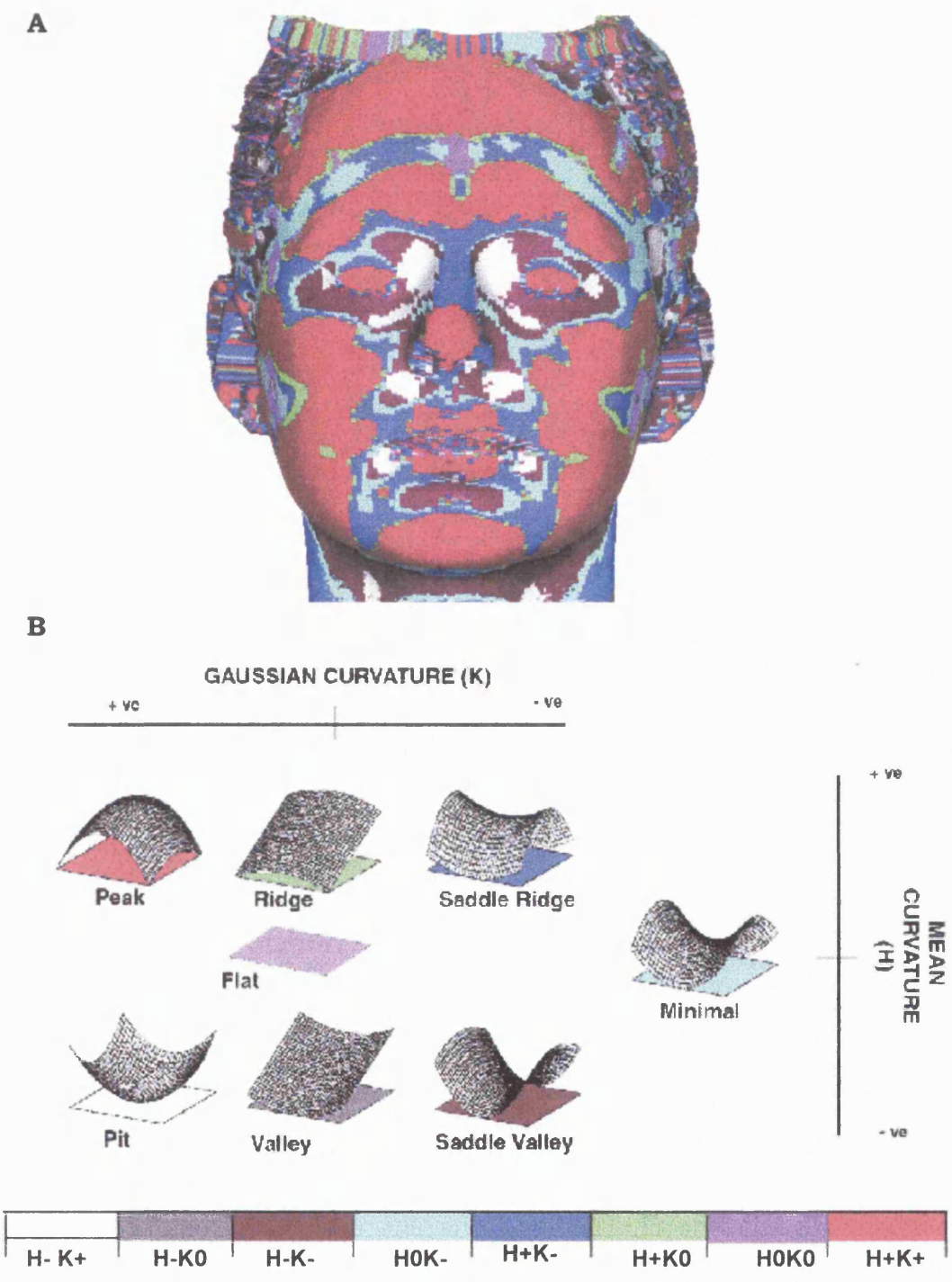

Figure 4.7 STA surface analysis of 3D data. A. Colour coded segmentation of the face calculated from raw 3D scan data, independent of orientation of the subject. B. Colour segmentation is calculated from mean (H) and gaussian (K) curvature values.

colour coded segmentation and also provides a continuous numerical scale on which surface shape is described (Fig 4.8). This allows a single numerical shape index value to be obtained at each data point on a scan. The facial surface is segmented on the basis of the average shape of a patch of points surrounding each data point. The total range of all possible shapes is described on a continuous scale from zero to one. This scale is subdivided into 9 colours that represent the range of shapes from spherical cup (SI value of zero) to spherical cap (SI value of one)(Fig 4.8B). Midpoint shape types for each colour-coded category are shown in Fig 4.8C. The colour scheme ranges from cold colours (green/blue) to warm colours (yellow/red) to visualise and distinguish convex from concave shapes (Fig 4.8A).

From looking at the 3D rendered face with both the STA and SI colour segmentations it is possible to refine description of several familiar facial features by using the component shape types. For example with the STA segmentation (Fig 4.7A) the nose can be described as saddle ridge with a peak at the tip. The Shape Index provides further segmentation (Fig 4.8A), with the nose described as spherical cap at the tip surrounded by dome, then ridge along the length of the nose and saddle ridge at the top of the nose and around the nasion landmark.

It is possible for the data obtained using the fixed scanner to be 'unwrapped' and displayed as a 2D face map (Fig 4.9). This facilitates the exploration of local surface variation using curvature profiles,

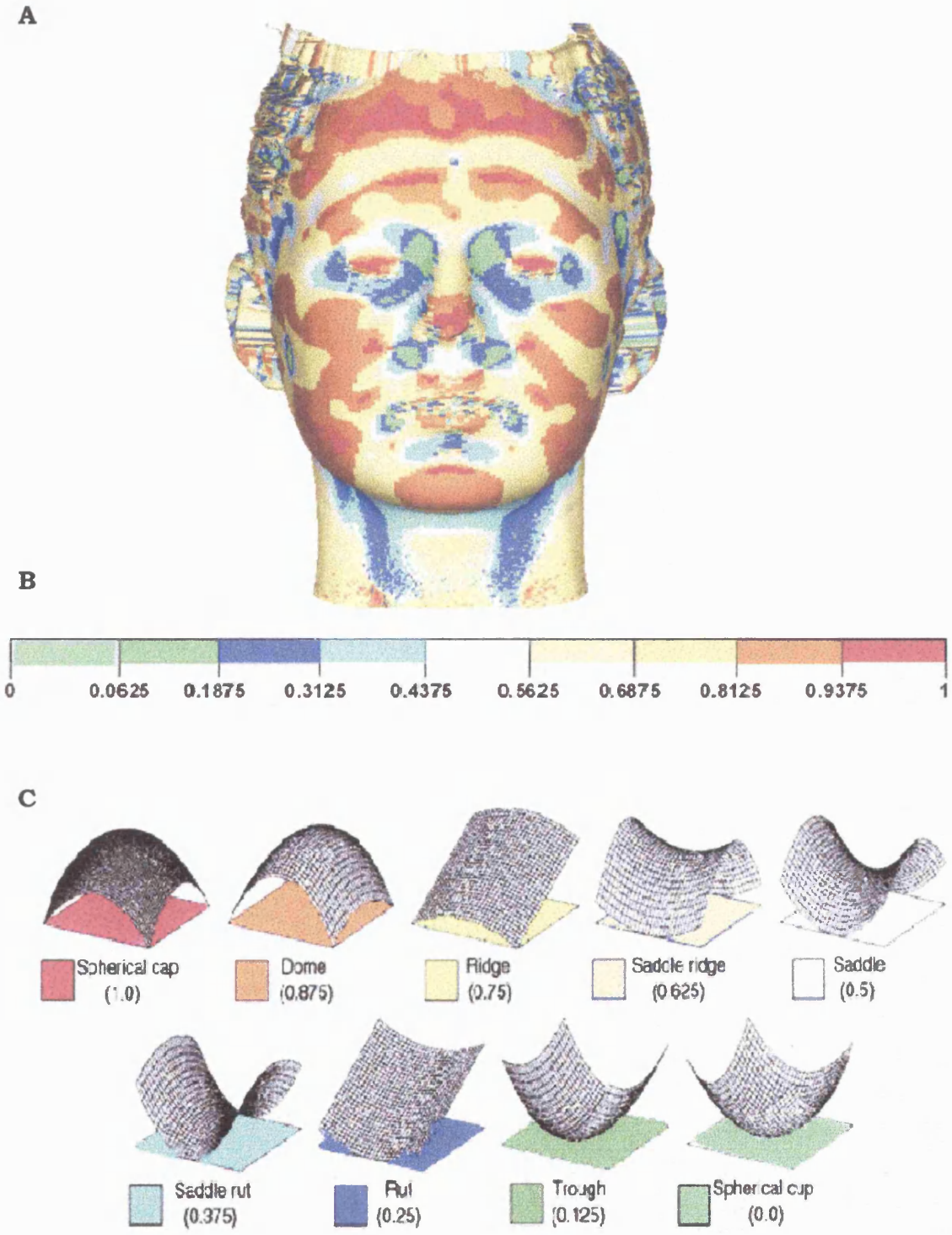

Figure 4.8 Koenderink's Shape Index (SI) surface segmentation
A. Segmentation applied to 3D face data. B. Numerical scale describing range of shapes, from concave spherical cup (SI value zero) through to convex spherical cap (SI value one). C. Example of shape types that represent the midpoint value of each of the shape index categories in between spherical cap and spherical cup.

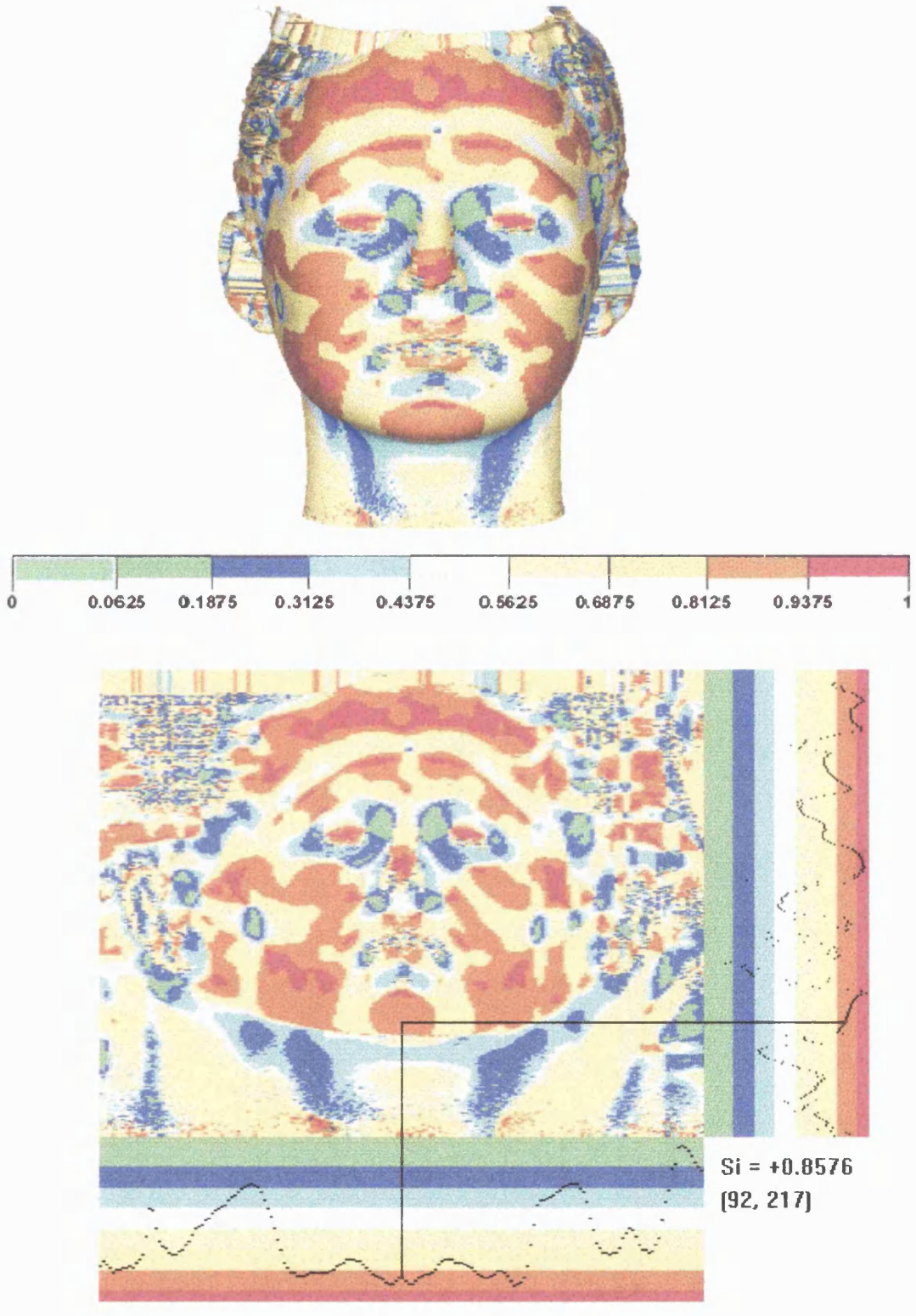

Figure 4.9 3D face data with SI surface segmentation. Data from the fixed scanner can be, unwrapped to produce a 2D colour coded face map of each data point collected. SI value at specific points on the face can be explored using the vertical and horizontal profile functions, for example, at the point on the chin where the two profiles intersect, a SI value of 0.8576 is given.

horizontal and vertical through the point of interest and records the co-ordinate location and SI value at a given point. Data from the HLS scanner can not be directly transformed into a 2D face map due to the inherent triangular data format of the .obj file. However it was found by simulating a rescan of the .obj file to make it into a .lsm file that it could then be unwrapped. This has the effect of slightly smoothing the data but was used for data evaluation study and is discussed further in section 4.5.

4.3.3 Features identified using surface segmentation

The rest of this chapter considers three variable facial features that appear to be discrete traits. These were first identified in a test panel of twenty randomly selected subjects using either SI or STA to examine the surface segmentation patterns.

a) Chin cleft

Variation in chin clefting is dependent on the local face shape, and hence on the underlying jaw and the overlying tissue layers. It is necessary to take this into account in order to produce an accurate classification. The SI value was chosen since it appeared to be more informative than STA. The SI surface segmentation of the data was selected and converted into the 2D face map so that the profile function, could be used to identify the chin cleft as a dip between two peaks (Fig. 4.10).

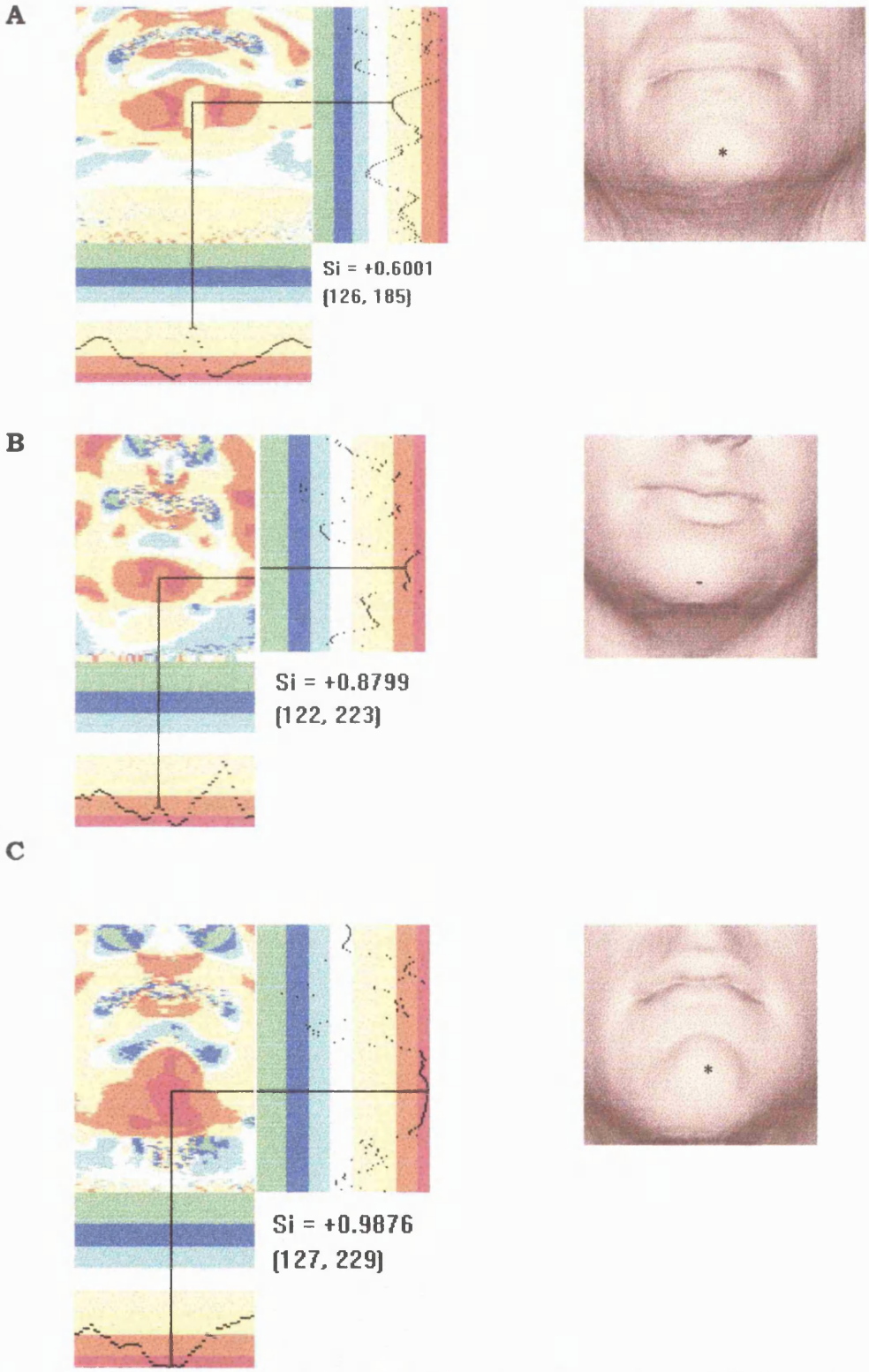

Figure 4.10 SI colour surface segmentation and scan data of three male chins with varying degrees of chin cleft. A Strong chin cleft, has a low SI value of 0.60 at the highlighted point, B. weaker chin cleft has a value of 0.88 at the highlighted point, C. No chin cleft detectable, so attributed an arbitrary score of 1.

The lowest value at the dip was taken to be the magnitude of the chin cleft and the SI value at this point was recorded. A low SI value was indicative of a strong chin cleft (Fig 4.10 A) and a high SI value represented a weaker cleft (Fig 4.10 B). Some subjects completely lacked a dip and displayed no variation across the chin surface (Fig 4.10 C). These individuals were classified as 'no cleft' and assigned an arbitrary value of 1 (high SI values, between 0.9375 and 1, on the shape index scale correspond to the least concave shape type; spherical cap). This initial classification produced two distinct phenotypes: cleft and no cleft although at this stage the possibility of subdividing the cleft category into weak and strong cleft was recognised.

Data files from the portable scanner could not be directly converted into face maps so an alternative method was determined by thresholding the STA segmentation (Chapter 3). Using this system the same classification of chin clefts was obtained, for example the same three chins shown in Fig 4.10 using the SI segmentation are shown in Fig 4.11 using the STA method of analysis

b) Nose Band

The STA surface segmentation was applied to the full-face scans. A discrete variation in nose profiles was scored according to the presence or absence of a red band across the bridge of the nose. The presence of the red band appears to correspond to a local convexity of the nasal profile but this can be very slight and not easily discernible from the raw data or on the 'live' face (Fig. 4.12).

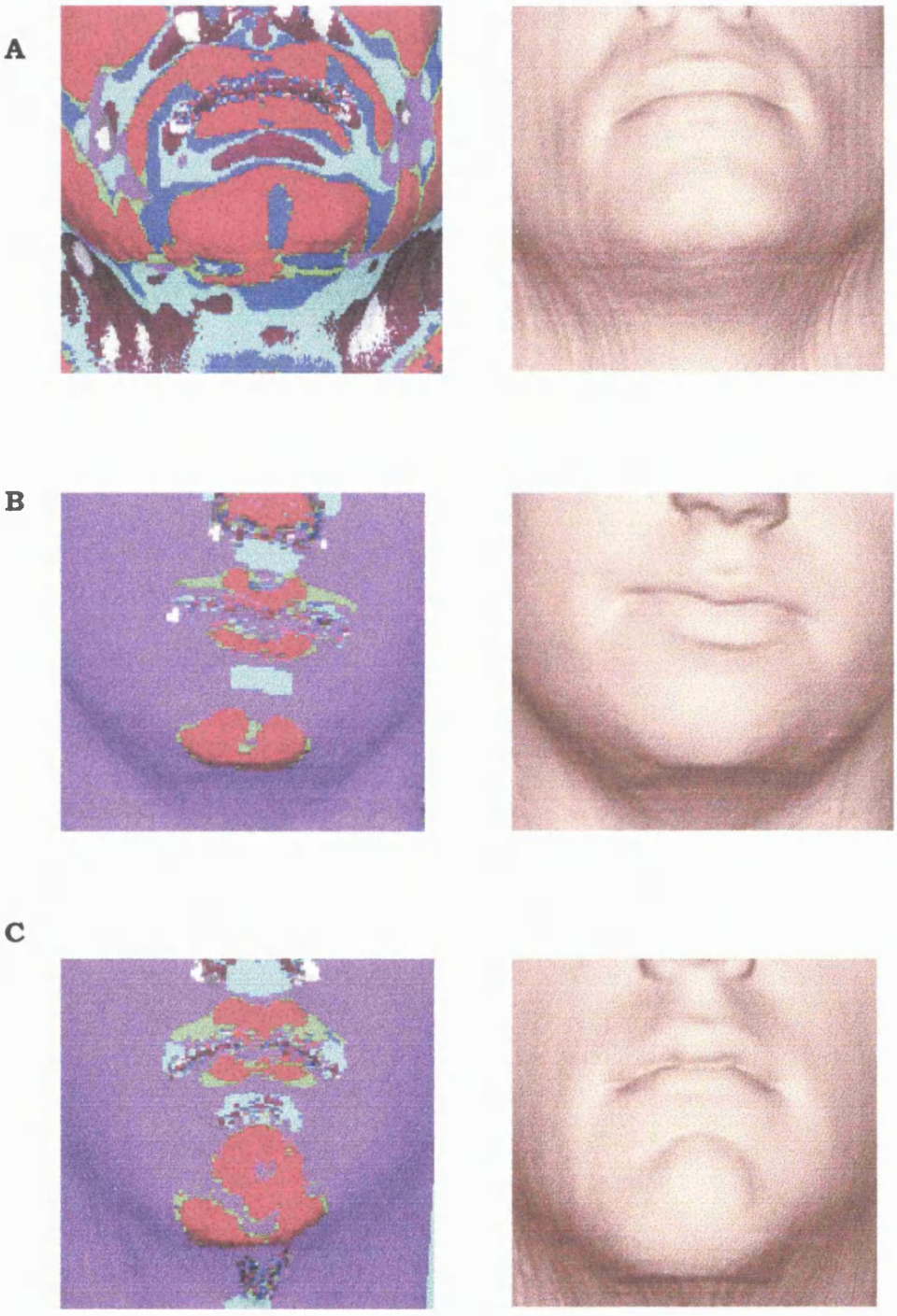

Figure 4.11 STA colour surface segmentation and scan data of same three male chins with varying degrees of chin cleft. A Strong chin cleft, apparent without thresh-holding data B. weaker chin cleft, cleft only becomes apparent upon thresh-holding C. No chin cleft detectable even with thresh-holding, so attributed an arbitrary score of 1.

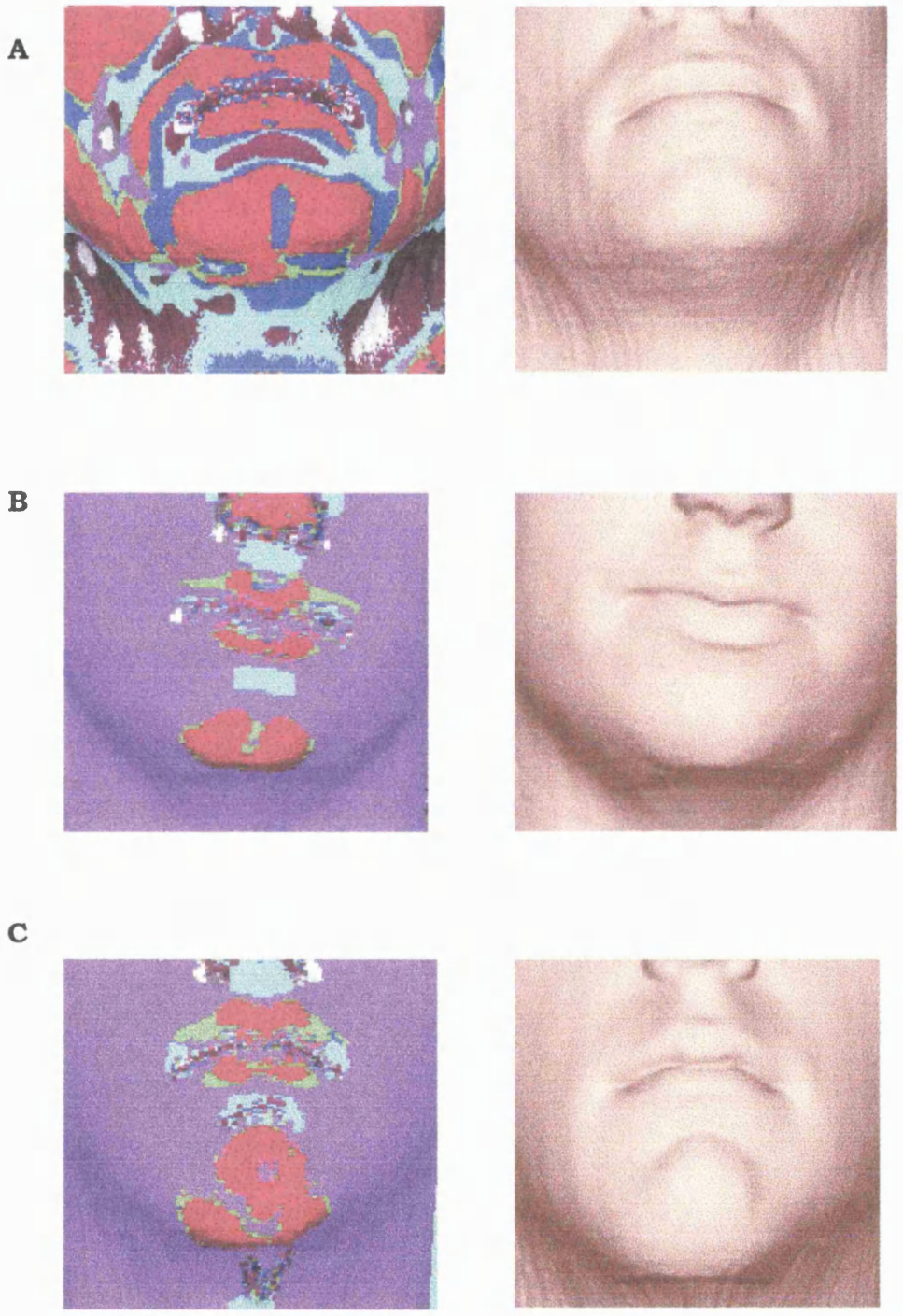

Figure 4.11 STA colour surface segmentation and scan data of same three male chins with varying degrees of chin cleft. A Strong chin cleft, apparent without thresh-holding data B. weaker chin cleft, cleft only becomes apparent upon thresh-holding C. No chin cleft detectable even with thresh-holding, so attributed an arbitrary score of 1.

A. Banded

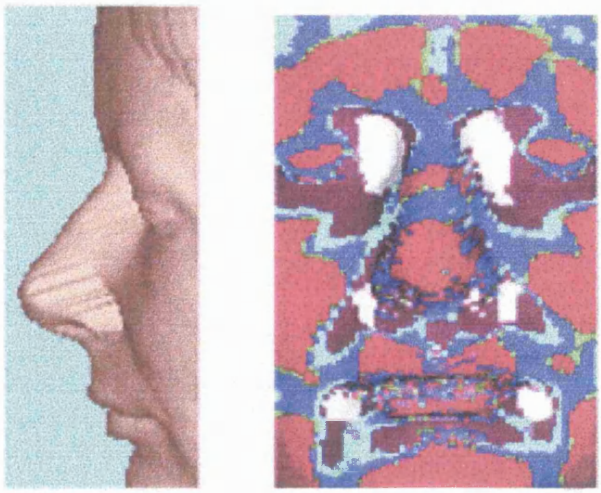

B. Non-banded

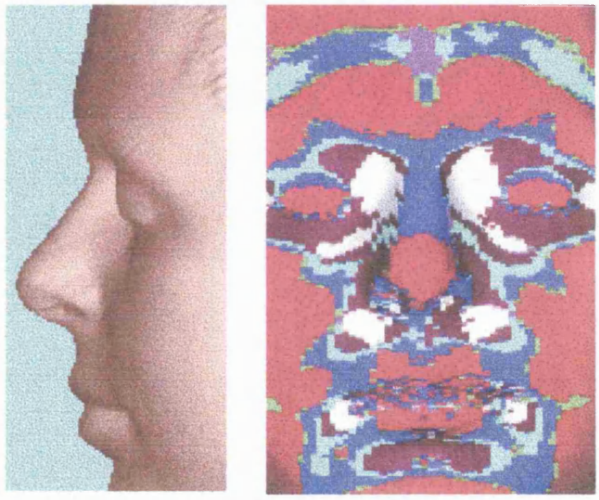

Figure 4.12 STA surface segmentation and scan data of two female noses. A. Banded phenotype, the red band across the nose is indicative of humping in the nose profile, B. Non-banded phenotype, no band across the nose, the nose has a straight profile.

Individuals with a red band were termed 'banded' and individuals without a red band were termed 'non-banded' (Fig. 4.12). This feature was scored in population and family data sets, and is discussed in section 5.2.

c) Brow

The brow produces complex and highly variable surface segmentation patterns that have proved difficult to classify. Variability was initially observed in two families where there appeared to be evidence for segregation of specific brow patterns. Four different banding patterns were discernible (Fig 4.13 A). Type 1 had a continuous band across the forehead, Type 2 the band was divided at the centre, Type 3 there was no apparent band, Type 4 the band was divided into four blocks. A relatively infrequent variation of the Type 4 brow pattern showed continuation of the outer blocks of the brow band curving onto the eye (Fig 4.13 B).

4.4 Consideration of age and ethnicity

Data from subjects of different ethnic backgrounds as well as from children of different ages were analysed for the effects of age and ethnicity on facial morphology.

a) Age

Data from six male subjects were collected over a minimum of four years around the age of puberty (11-19). Similar general trends

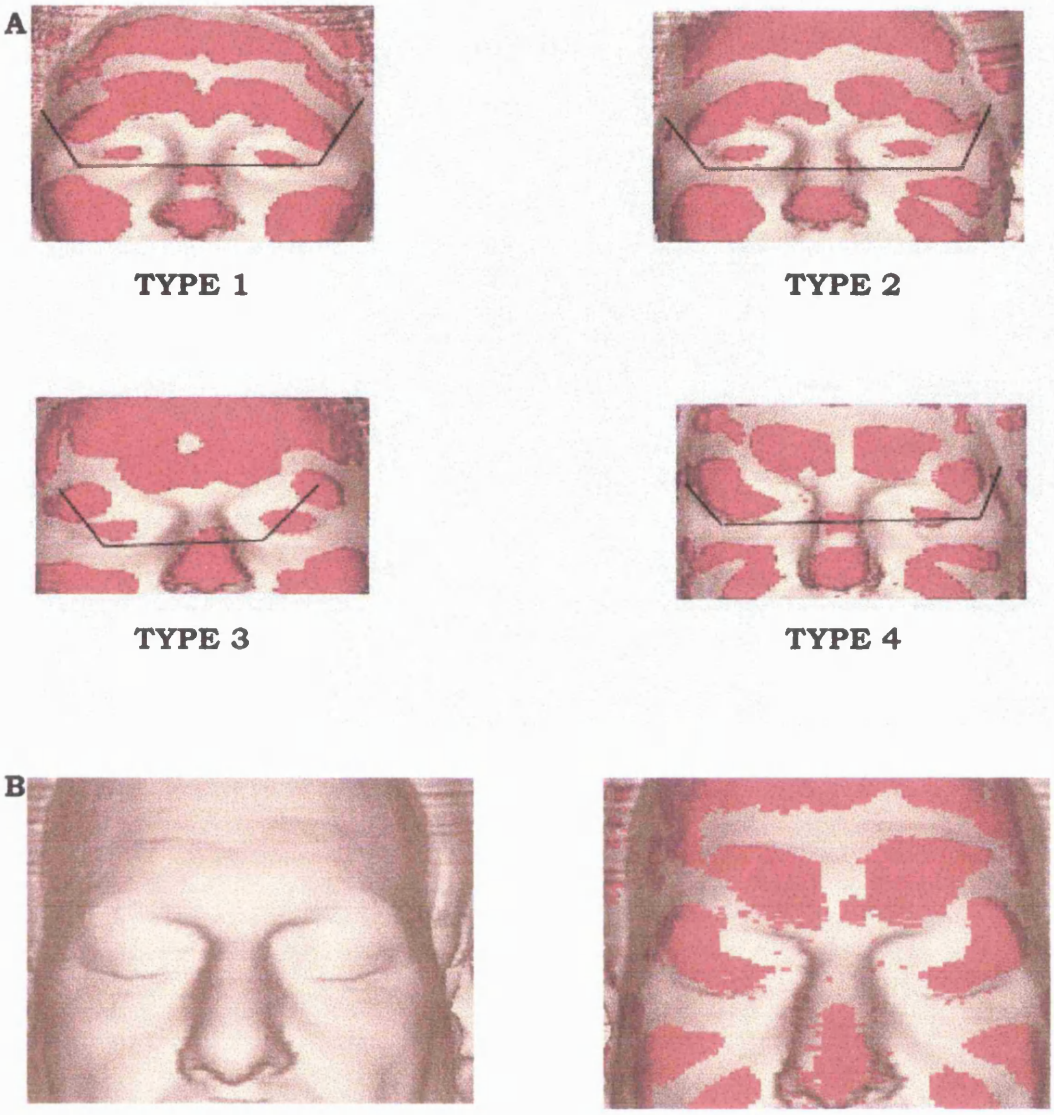

Figure 4.13 STA classification showing variation of the brow, only the peak (red) of the STA is shown for clarity. A. Four individuals with differing brow patterns; Type 1 phenotype is a continuous red band across the brow, Type 2 phenotype the band is divided into two, Type 3 phenotype the band is absent, and Type 4 phenotype shows the band divided into four. B. Raw data and peak of STA classification illustrating variation of the Type 4 phenotype where the outer blocks of the brow band continue round onto the eyes.

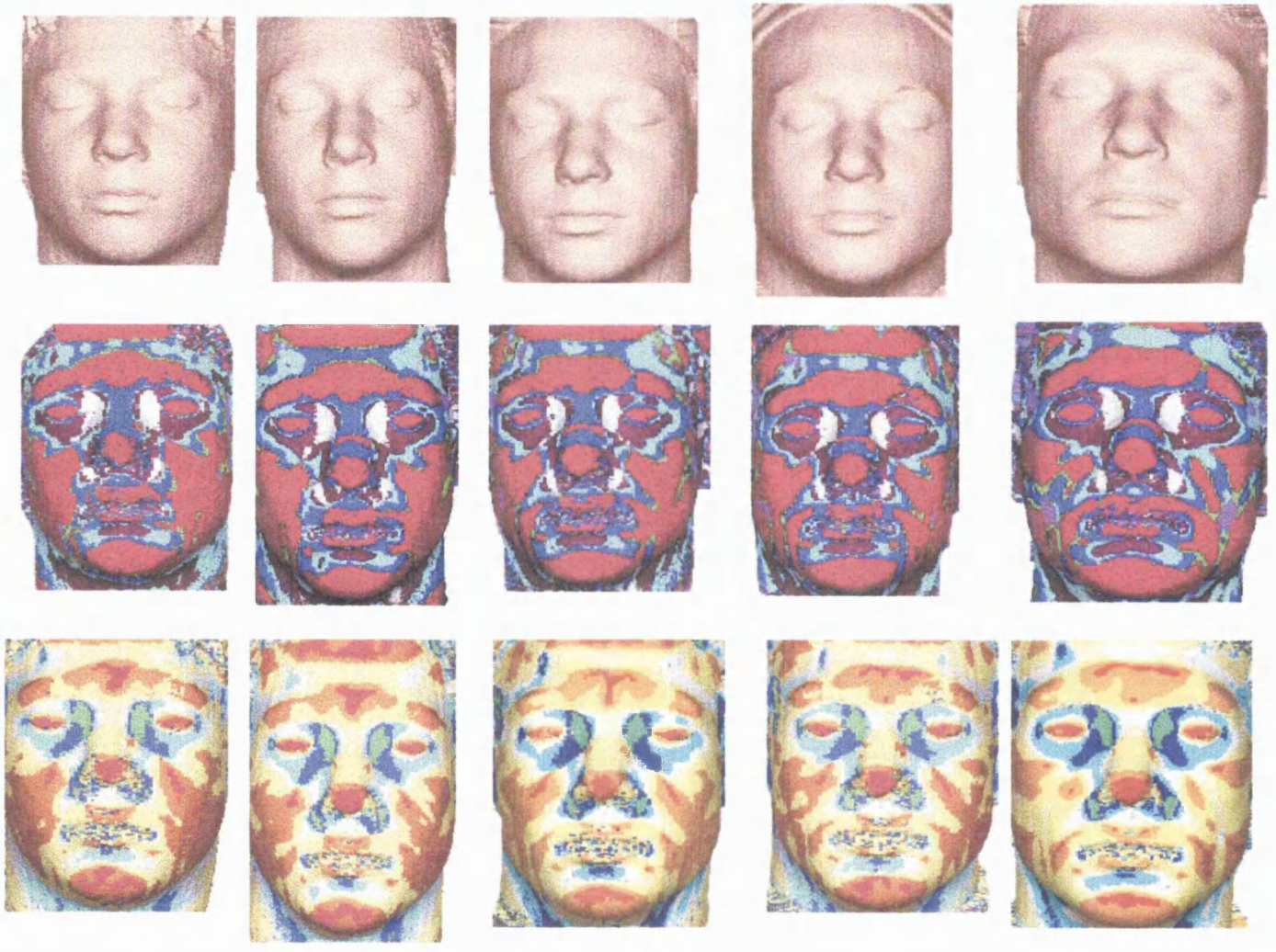

Figure 4.14 Raw data, STA and SI surface segmentation file of male subject scanned at ages 11, 13, 15, 17, 19 (left to right).

were observed in all subjects and are illustrated in Fig 4.14 which shows data collected from one subject at two-year intervals from 11-19 years (kindly made available to me by Prof. Moss). The most noticeable change in midline features is the appearance of the red band across the bridge of the nose at age 13 on the STA display. Generally the midline features did not show as much variation as areas of the face such as the cheeks, which reflect the loss of facial fat associated with adolescence. It is interesting to note the effect that age has on the SI surface colour segmentation. The SI shows a progressive decrease in convexity of the facial surface with age illustrated by change in colour composition from red/orange to yellow/white.

The chin cleft, nose band and jaw angle classifications were carried out on this subject at each age (Table 4.2). The nose band trait became constant at the age of 13 and the chin cleft value altered fairly little throughout the growth period. The jaw angle measurement in contrast seemed to be quite variable with respect to age and showed stability only in the final two scans between ages 17-19.

b) Ethnic origin

A small survey of faces from different ethnic groups, which comprises individuals of African, Chinese, Indian, European and Middle Eastern origin was carried out (Fig 4.15). The segmentation patterns are very complex but it is possible to see similarities and differences between each subject. The surface segmentation provides

Age	Chin cleft	Nose band	Jaw angle
11	0.89	2	157.7
13	0.87	1	158.7
15	0.87	1	161.2
17	0.87	1	163.1
19	0.86	1	163.3

Table 4.2 Comparison of classification scores for chin cleft, nose band and jaw angle in same male subject scanned at ages 11, 13, 15, 17 and 19.

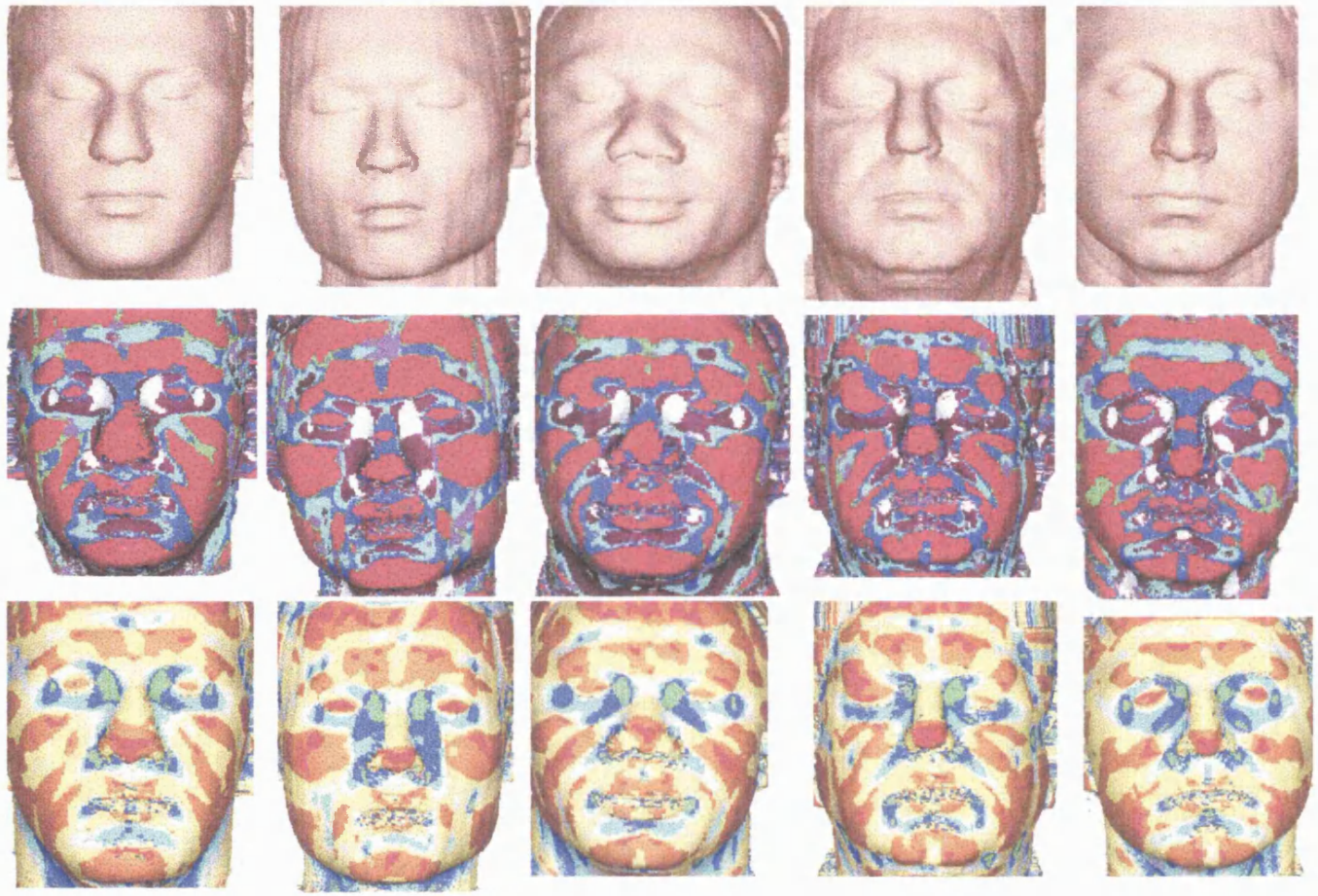

Figure 4.15 Raw data, STA and SI surface segmentation of five male faces of different ethnic backgrounds (from left to right: Middle Eastern, Chinese, African, European, Indian).

a novel view of the face drawing only on structural differences and similarities.

4.5 Evaluation of data

To investigate the reproducibility of the scan data and to compare the data generated by the two types of scanner, 17 subjects were scanned twice by the fixed scanner at approximately a one-year interval and also scanned using the HLS system. Scan data of the same subject from the two different scanners along with STA and SI colour segmentation are displayed in Figure 4.16.

It is apparent that the pattern of STA and SI segmentation is very similar in the data obtained from the two scanning systems. The main differences appear over the cheeks whereas the greatest similarity is around the midline structures. Table 4.3 compares the data from the fixed scan (two at a year interval) and the HLS scan in 17 subjects. To obtain the direct comparison of the SI chin cleft values, the HLS .obj files were 'pseudo-scanned' on the computer using the CLOUD software to make them into .lsm files in order to project into a 2D-face map. There is good agreement between the data from scans repeated after a year with the fixed scanner and the scans taken with the HLS scanner. Therefore it was decided that data collected from the fixed scanner and/or the HLS system could be combined with confidence.

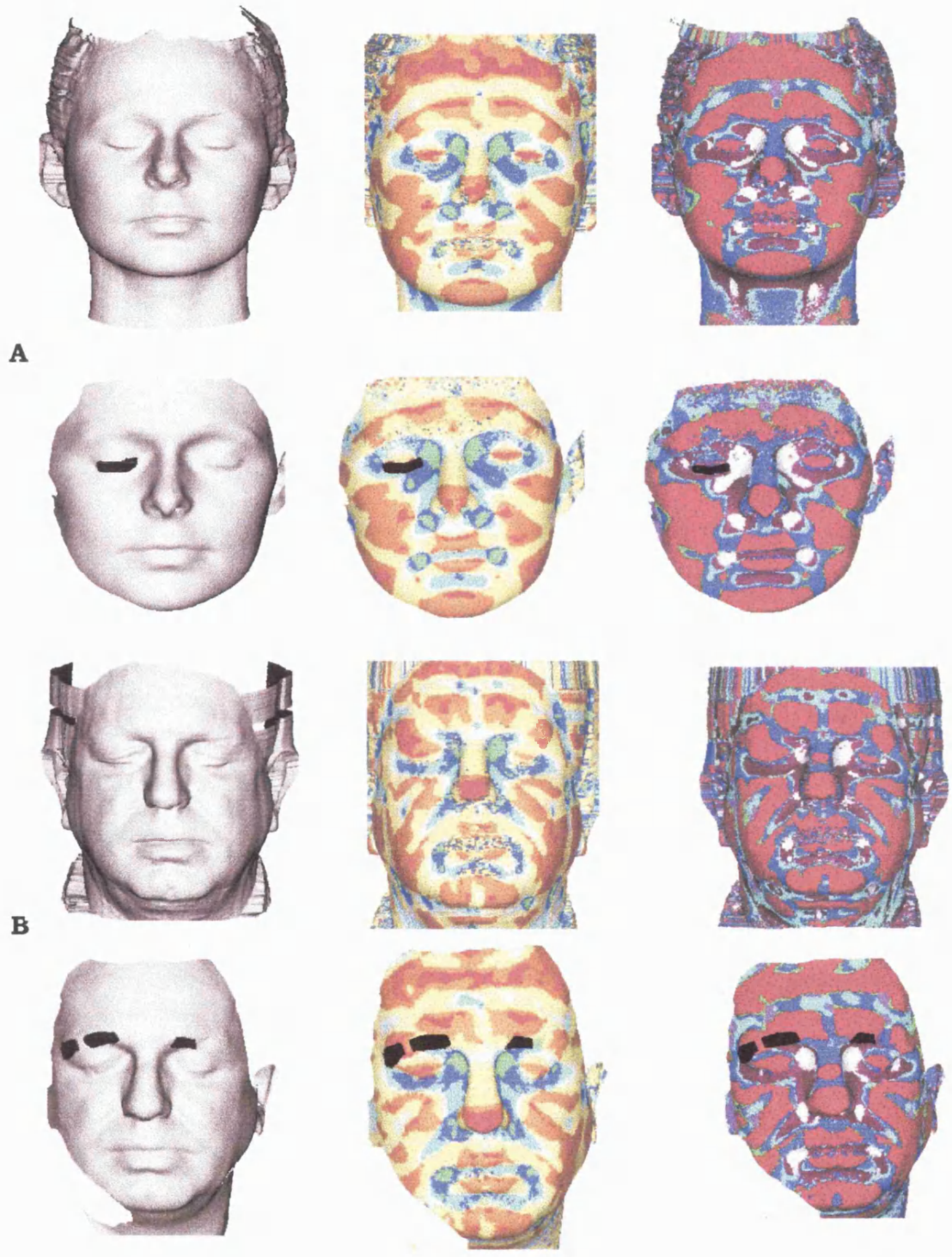

Figure 4.16. Comparison of raw data and surface segmentation (SI and STA) of facial data recorded using the fixed scanner (upper images) and the HLS system (lower images) in two subjects, A. Female European, B. Male European. It is important to note that on both scans from the HLS there is artefact due to light reflection, in the first subject this is below the right eye and in the other subject this is on both eyebrows. This artefact is not interpreted by the surface segmentation software and is coloured black.

Scan No.	Chin cleft SI [1]			Chin cleft STA [2] threshold			Nose [3]			Jaw protrusion (degrees)		
	fixed		hls[4]	Fixed		hls	fixed		hls	fixed		hls
49	0.78	0.77	0.79	0.025	0.030	0.030	2	2	2	163	165	166
22	0.77	0.76	0.79	0.01	0.02	0.025	2	2	2	153	155	155
10	1	1	1	1	1	1	1	1	1	161	160	163
606	1	1	1	1	1	1	1	1	1	159	160	157
6	1	1	1	1	1	1	2	2	2	171	168	169
38	1	1	1	1	1	1	1	1	1	167	167	166
26	0.85	0.84	0.84	0.05	0.05	0.05	1	1	1	171	171	172
286	0.79	0.79	0.79	0.04	0.04	0.04	1	1	1	164	165	163
67	1	1	1	1	1	1	1	1	1	161	161	161
179	0.82	0.83	0.84	0.04	0.05	0.045	1	1	1	163	163	163
5	0.58	0.59	0.62	0.005	0.005	0.005	1	1	1	164	163	164
17	0.85	0.85	0.86	0.05	0.05	0.05	2	2	2	172	171	172
14	0.89	0.89	0.89	0.05	0.05	0.05	1	1	1	161	161	160
76	0.83	0.83	0.85	0.05	0.05	0.05	2	2	2	161	162	161
89	0.81	0.79	0.82	0.045	0.045	0.045	2	2	2	166	165	163
50	0.87	0.84	0.86	0.04	0.040	0.04	1	1	1	158	158	156
8	0.59	0.62	0.63	0.005	0.005	0.005	1	1	1	169	167	167

Tables 4.3 Comparison of scan data from fixed and portable scanners in seventeen subjects. Two scans were taken from the fixed system after approximately a one-year interval. Comparison made from classifying the previously described traits; Chin cleft (SI and STA), Nose band and Jaw angle. There is very good agreement with the values obtained from repeat scans taken by the fixed scanner and with scans taken from the two different scanners.

Note:

[1] A low SI value is indicative of a stronger chin cleft, an arbitrary value of 1 was assigned where no cleft was apparent.

[2] A STA value of 0.005 indicates that a chin cleft is apparent without thresh-holding, a value of 1 was arbitrarily assigned where there was no visible cleft.

[3] Nose band score; 1 present; 2 absent

[4] In order to classify the chin cleft from the SI value, the HLS scan had to be 'pseudo-scanned' to transform it into the LSM file format, which could be projected as a 2D-face map.

4.5.1 Evaluation of software

One concern was whether the mathematical parameters used might effect the trait classification. The LSMVIEW software calculates the colour coded STA and SI displays by selecting a specified patch of data points as a local area and computing local curvature properties of each data point (or facet in the case of obj files). The default parameter set was a circular patch with 10mm radius, since this was found to be generally informative in representing the shapes of the face. The effects of using a rectangular patch (horizontal and vertical) and a smaller circular patch (8mm and 6mm) were explored in a set of 30 individuals to see whether these changes affected the scoring of the chin cleft trait (Table 4.4).

Surface segmentation files were generated using the dense data sets of the mid-face scans. The SI value for chin cleft in fifteen males and fifteen females (five strong cleft, five weak clefts and five no cleft) was scored under the varying patch parameters.

Changing the radius of the circular patch generally produced the greatest change in SI value. The chin cleft became progressively stronger with decreased patch size. Changing the shape of the patch from a circle to a rectangle produced the most noticeable change in pattern of segmentation (Fig 4.17). Data segmentation generated from 8mm and 6mm patches was generally very speckled and difficult to interpret. Data generated from a vertical rectangular patch were similarly difficult to interpret. The horizontal patch seemed least

	ID	10mm Circular	8mm Circular	6mm Circular	Horizontal Rectangle	Vertical Rectangle
STRONG CLEFT	F251	0.41	0.35	0.33	0.79	0.57
	F285	0.67	0.69	0.65	0.83	0.45
	F417	0.56	0.43	0.35	0.74	0.57
	F5	0.6	0.48	0.38	0.73	0.63
	F537	0.73	0.56	0.35	0.81	0.73
	M105	0.62	0.47	0.35	0.77	0.61
	M11	0.35	0.28	N/A	0.68	0.48
	M136	0.54	0.42	N/A	0.65	0.53
	M238	0.62	0.56	0.51	0.69	0.51
	M248	0.63	0.54	0.46	0.75	0.54
WEAK CLEFT	F165	0.82	0.82	0.78	0.85	0.87
	F285	0.78	0.53	0.48	0.87	0.77
	F518	0.85	0.83	0.79	0.88	0.81
	F200	0.86	0.84	0.78	0.89	0.83
	F33	0.78	0.63	0.66	0.83	0.78
	M27	0.78	0.78	0.72	0.8	0.77
	M399	0.78	0.73	0.69	0.8	0.75
	M559	0.76	0.73	0.69	0.8	0.77
	M129	0.78	0.74	0.66	0.8	0.73
	M488	0.78	0.77	0.72	0.81	0.8
NO CLEFT	F385	1	1	1	1	1
	F203	1	1	1	1	1
	F148	1	0.9	0.85	1	1
	F174	1	1	1	1	1
	F183	1	0.86	0.85	1	1
	M145	1	1	1	1	1
	M162	1	1	1	1	1
	M167	1	1	1	1	1
	M206	1	1	1	1	1
	M259	1	1	0.93	1	1

Table 4.4 Comparison of SI values for chin cleft trait using varying patch parameters to calculate the SI surface segmentation file.

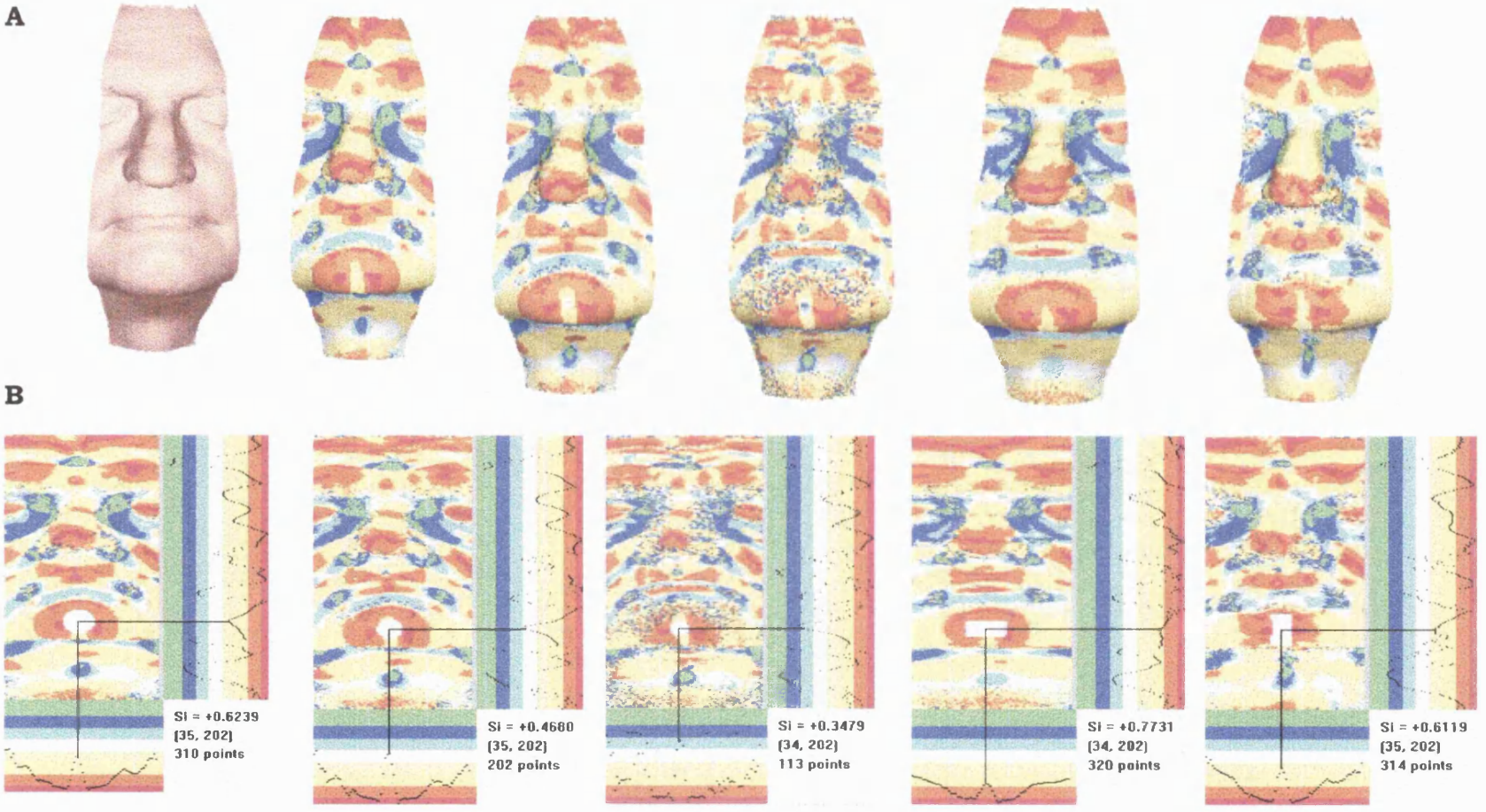

Figure 4.17 Effect of patch size on SI surface segmentation, illustrated on mid-face of male subject 105. A. Raw scan data and files with circular patches (10mm, 8mm and 6mm) and horizontal and vertical patches, B. 2D projection to look at effect of SI value for chin cleft with respective patch shape and sizes.

suited to the analysis of a localised feature as the local neighbourhood of data points, constituting the patch, covered a relatively large and variable area of the chin, which was reflected in the narrow range of values obtained in the subjects analysed. Variations in SI values scored with different patch sizes were similar in males and females but the range of the variability in trait scoring was greatest on a person to person basis. This could reflect individual variation in overall face size and shape. Reduction of the circular patch size allows increased localisation on a specific feature but it became obvious that there was an optimum patch size, below which one should not go because of the intense speckling which occurs. Perhaps if a different population was targeted, such as young children, then it maybe appropriate to take a smaller patch size as standard.

A problem with the STA classification is that size can affect the calculated curvature. For example, although a football and a golf ball are the same shape the curvature on the golf ball is much tighter than on the football. Subtle male-female differences in facial morphology such as fat deposition, muscle formation, mandible width and overall face size will affect the STA segmentation pattern for this reason. Shape Index is independent of size and should provide more reliable classification of features. However, the actual SI values are dependent in part on the patch size chosen. The problem with this is that a 10mm patch on a large face covers a proportionately smaller area than a 10mm patch on a smaller face. Generally speaking females have smaller faces than males, and it is possible that this could affect the reliability of the shape index classification and to some extent explain male-female differences. One way to overcome this problem would be to scale the patch size according to the size of each face; but this would create a further problem of how best to assess the size of the face. Furthermore, these data on overall size are not available from the face scans collected.

Although all the face scans were taken at rest it is also evident from some of the data that 'at rest' in itself can be variable. This is particularly evident with the brow classification where looking at the classifications reveals that creasing of the brow and natural wrinkle lines in this region can affect the outcome of the surface segmentation. While this is difficult to overcome, excluding older-aged subjects could help to minimise this problem, and a program of rescanning might alleviate this problem.

4.5.2 Evaluation of Classifications

For genetic analysis a reliable and reproducible classification of phenotypes is essential. Thus the results from independent observers in classifying these traits (chin cleft, nose band, brow and jaw angle) were compared. Each feature was scored in 100 individuals at least twice. The chin cleft and nose band classification showed high reproducibility (98% and 99 % respectively with same assessor and 93% and 95% with an independent assessor). SI and STA values for chin cleft classifications were investigated in another set of 134 individuals and found to be highly correlated ($r= 0.92$, $p < 0.001$). In the case of the chin cleft the discrepancies were mainly in female subjects that were on the borderline between weak and no cleft. However, on discussion the classification was easily agreed with a clear definition of the phenotype. Similarly discrepancies in nose band classification were easily resolved and largely arose when there was just a slight suspicion of a band or an incomplete band across the nose. The brow phenotype showed relatively high reproducibility by the same assessor (86%) but was lower with an independent assessor (72%). For jaw protrusion there was high reproducibility for same assessor (average standard error between measures = +/-1.1°) and slightly lower for independent assessor (average standard error between measures = +/-2.4°).

CHAPTER 5

Population and family studies of chin cleft and nose band traits

The previous chapter presented a general review of qualitative and quantitative analysis of human 3D face data. Two traits that appeared to be suitable for genetic analysis were chin cleft and nose band, since they were shown to be reliable and reproducibly classifiable facial features. Both of these midline features were deemed to be good candidates for population and family studies, as they appeared to be constant individual characters, largely unaffected by variable background factors such as obesity and periodic water retention. Furthermore, the qualitative nature of the surface segmentation approach as a means of facial classification was shown to provide objectively defined polymorphic traits. Data were therefore collected from family groups as well as a large population of unrelated subjects and classified for chin cleft and nose band phenotypes.

The principle objective of this chapter is to provide an assessment of the genetic aspects of the chin cleft and the nose band phenotypes. A mode of inheritance is postulated for each feature and supporting evidence from family and population data are assembled.

5.1 Chin cleft

Shape Index (SI) and Surface Type Analysis (STA) were used to classify chin cleft as described in the previous chapter. STA was used to classify data exported as object (. obj) files from the portable HLS system.

5.1.1 Population Analysis

459 unrelated subjects, aged 16-70, were scored for chin cleft. The group comprised 402 Europeans (183 males, 219 females), 32 Indians (9 male, 23 female) and 25 Chinese (16 male, 9 female). In each group approximately one third of the individuals were classed as 'non-cleft' (SI value of 1). The 'cleft' category showed a broad range of SI values (Fig 5.1) ranging from 0.15, which signifies a very strong cleft, to 0.90 where the cleft is scarcely discernible. The 'cleft' group was then subdivided according to the extent of the chin cleft. On a scanned face image a cleft with a value of 0.76 or less is generally easily visible from the raw scan data without needing to scrutinise the surface segmentation file. This seemed a logical boundary to subdivide the 'cleft' phenotypes. A SI score less than or equal to 0.76 was classified as 'strong cleft' and a cleft with a value greater than 0.76 was classified 'weak cleft'. Thus three chin cleft phenotypes were defined: no cleft (W), weak cleft (SW) and strong cleft (S).

There appeared to be clear evidence of three chin cleft phenotypes, distinguishing cleft and no cleft was easy using the shape index analysis profile and traversing the surface of the chin looking for an indentation. However separating strong from weak cleft was not so simple. After

considerable experimentation, 0.76 was chosen as the cut-off point and anything above this value was deemed to be a weak cleft. This value was chosen for two reasons: clefts with a value of <0.76 are visible as an indentation in the scan before estimating a shape index value, and 0.76 is close to the mean cleft value of the total population.

The distribution of the phenotypes in the population sample was also analysed using 0.71 and 0.81 as the cut-off values between strong and weak. This leads to marked differences in the calculated frequency of the S allele (from 0.41 to 0.57 respectively). These values generated a much less good fit between observed and expected numbers of chin cleft phenotypes in the population sample than was obtained with the 0.76 cut-off value (Table 5.3). In the family data, altering the cut-off point did not have an obvious effect. There was evidence of both father to son and mother to son transmission with all three cut-off values; arguing against sex-linked inheritance. With all three of the cut-off values tested in detail there were a couple of 'borderline' families that either fitted with the proposed model of inheritance or did not fit on the basis of the cut-off value chosen; in these cases it is difficult to ascertain what the optimum cut-off should have been.

The analysis was also carried out on the premise that there were 2 phenotypes; cleft and no cleft, but when this was investigated the family data did not fit as well to a model of dominant or recessive inheritance as they did to a 3-phenotype model of co-dominance. Generally the data provided the best fit to the autosomal co-dominant inheritance model when the 0.76 cut-off value was used.

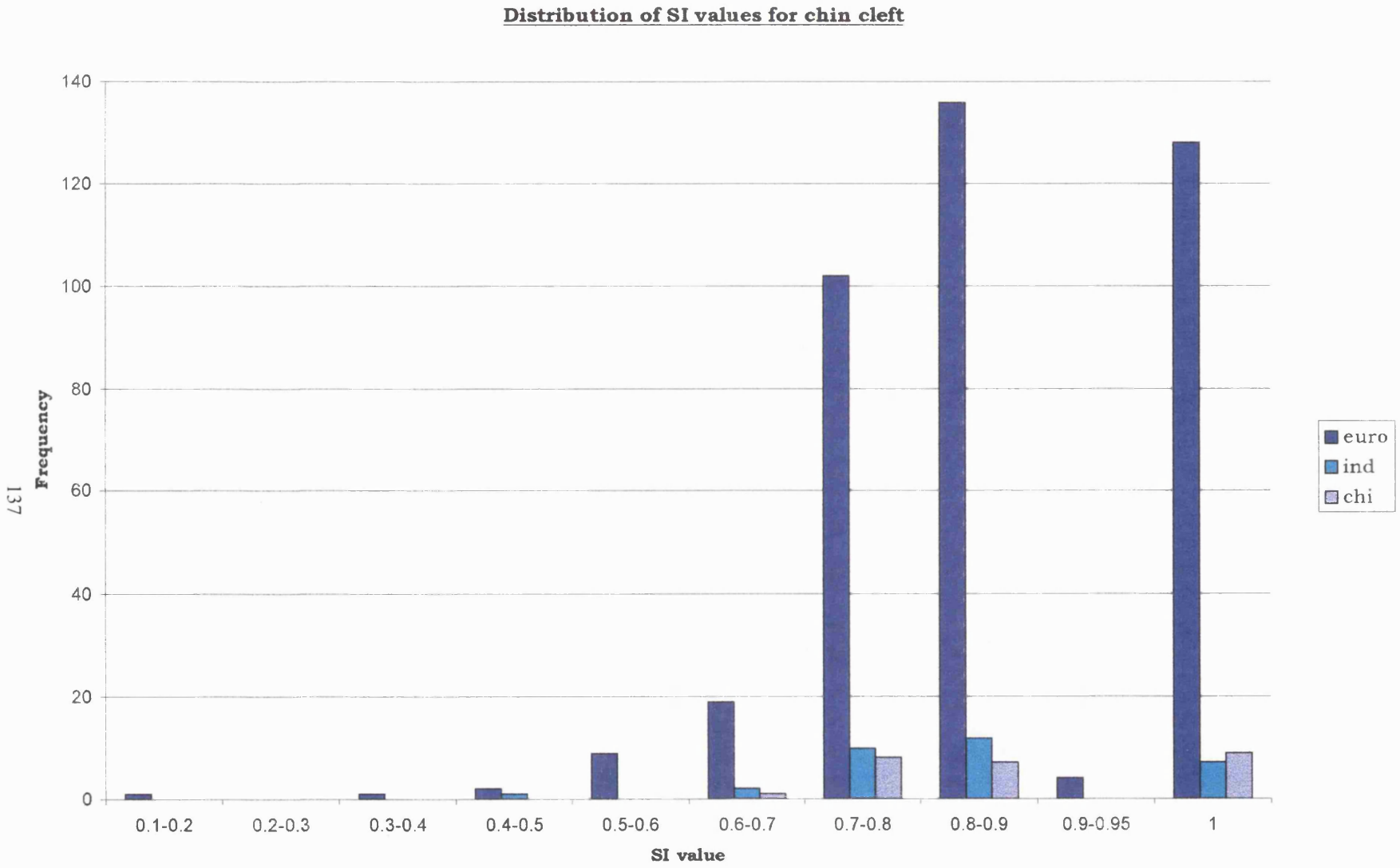

Figure 5.1 Range of SI values for chin cleft, where 1 is arbitrarily assigned to individuals with no cleft.

	European			Indian			Chinese		
	M N=182	F N=220	ALL N=402	M N=9	F N=23	ALL N=32	M N=16	F N=9	ALL N=25
NO CLEFT (W)	**39**	**89**	**128**	**1**	**6**	**7**	**6**	**3**	**9**
frequency as percentage	*21.4*	*40.5*	*31.8*	*11.1*	*26.1*	*21.9*	*37.5*	*33.3*	*36.0*
CLEFT:	143	131	274	8	17	25	10	6	16
frequency as percentage	*78.6*	*59.5*	*68.2*	*88.9*	*73.9*	*78.1*	*62.5*	*66.7*	*64.0*
WEAK CLEFT (SW)	**88**	**111**	**199**	**2**	**13**	**15**	**7**	**5**	**12**
frequency as percentage	*48.4*	*50.4*	*49.5*	*22.2*	*56.5*	*46.9*	*43.8*	*55.6*	*48.0*
STRONG CLEFT (S)	**55**	**20**	**75**	**6**	**4**	**10**	**3**	**1**	**4**
frequency as percentage	*30.2*	*9.1*	*18.7*	*66.7*	*17.4*	*31.2*	*18.7*	*11.1*	*16.0*
Frequency S 'Allele'	**0.54**	**0.34**	**0.43**	**0.78**	**0.46**	**0.55**	**0.41**	**0.39**	**0.4**
Frequency W 'Allele'	**0.46**	**0.66**	**0.57**	**0.22**	**0.54**	**0.45**	**0.59**	**0.61**	**0.6**

Table 5.1. Distribution of the observed chin cleft phenotypes in three ethnic groups; European, Indian and Chinese showing relative frequencies of males, females and combined sexes for each chin cleft phenotype; No cleft, weak cleft and strong cleft.

All three phenotypes were found in varying frequency in both sexes of the three population samples (Table 5.1). In all groups the frequency of weak cleft was higher in females and the frequency of strong cleft was higher in males. In both the European and Indian populations the incidence of no cleft in females was approximately double that found in males. This sex difference is particularly evident in the large European population (χ^2 1df, $p < 0.0001$) but not significant in the Indian or Chinese populations ($p > 0.1$)(Table 5.2).

Despite the marked differences in frequency between males and females, the preliminary family data supported chin cleft as a genetically determined trait. Evidence of father to son transmission argued against X-linked inheritance, similarly mother to son transmission argued against Y-linked inheritance. The occurrence of three phenotypes in both sexes suggested simple autosomal co-dominance as the most likely mode of inheritance. Particularly good support for this hypothesis came from the large family with eight children (Fig.5.2), discussed in more detail along with the rest of the family data in section 5.1.2.

A model of autosomal co-dominance for the chin cleft trait assumes that two alleles, *S* and *W*, give rise to the three phenotypes; S (strong cleft) and W (no cleft), the respective homozygotes, and SW (weak cleft), heterozygous for the two alleles. Based on this hypothesis 'gene' frequencies were estimated by counting the number of individuals of each phenotype (Table 5.1). In all populations the frequency of the *S* allele appeared to be higher in males than in females. In the total European and Chinese population groups the *W* allele (0.57 and 0.60 respectively) is more frequent than the *S* allele

	European		Indian		Chinese	
	M	**F**	**M**	**F**	**M**	**F**
No Cleft (O)	**39**	**89**	**1**	**6**	**6**	**3**
(E)	*57.95*	*70.05*	*1.97*	*5.03*	*5.76*	*3.24*
Cleft (O)	**143**	**131**	**8**	**17**	**10**	**6**
(E)	*124.05*	*149.95*	*7.03*	*17.97*	*10.24*	*5.76*

Table 5.2 Observed and expected numbers of cleft and no cleft in males and females. The expected number is calculated on the assumption that the proportion of cleft and no cleft individuals should not be different in males and females. Chi-square analysis reveals that the difference between the sexes is significant in the large European population ($p < 0.0001$) but not in the other two populations ($p > 0.1$).

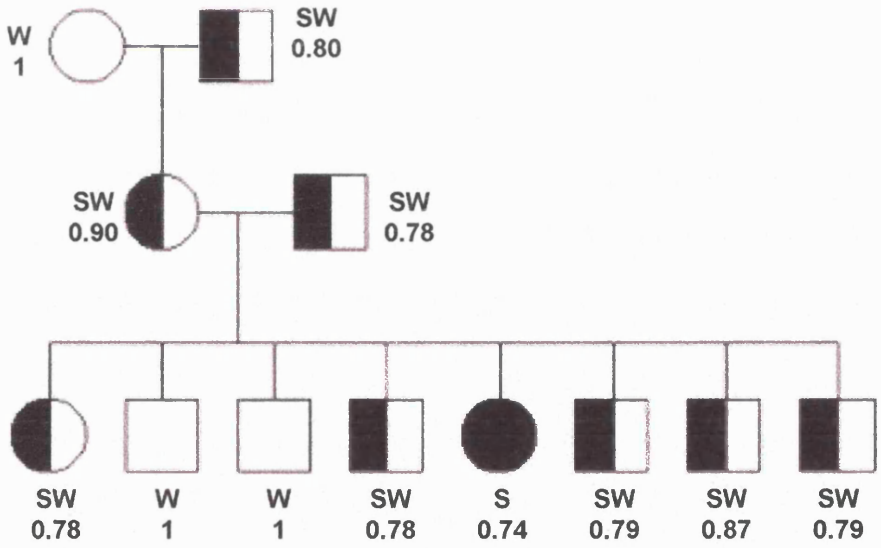

Fig 5.2 Pedigree of large family displaying the chin cleft trait, SI values used to assign phenotypes written below. Individuals with an SI value of 0.76 or below are shaded black and have a strong cleft (S), individuals shaded half black and half white have an SI value higher than 0.76 and are weak cleft (SW), individuals not shaded do not have a cleft (W).

(0.43 and 0.40 respectively) but this is reversed in the Indian population (S=0.55 and W=0.45). However, the population groups are small and heterogeneous for the Chinese and Indian samples and it is difficult to attribute high levels of confidence to these observations. This might indicate that the difference in genetic background between the groups could modify the penetrance of the cleft trait. Clearly more data on other larger population groups would be required to establish this. Nevertheless it is also interesting to note the heterogeneity in the gender differences in the calculated allele frequencies in these population samples. There is a marked gender difference in the European and Indian groups, with the *S* allele appearing much more frequently in males than in females (0.54 v 0.34 and 0.78 v 0.46 in European and Indian males and females respectively), but there is a much less noticeable difference in the Chinese group (0.41 v 0.39).

The expected Hardy-Weinberg proportions were investigated in the European data set. The *S* and *W*, allele frequencies calculated from the frequencies of the three phenotypes; S, SW, W (Table 5.1) were used to test the males, females and total data for deviations from expected proportions given Hardy-Weinberg equilibrium (Table 5.3a). For this calculation, it was assumed that $S = p$ and $W = q$. The expected frequency for strong cleft (S) was calculated as p^2, weak cleft (SW) was calculated as $2pq$ and no cleft (W) was calculated as q^2 (e.g.

	Male S=0.54, W= 0.46		Female S= 0.34, W= 0.66		Total S=0.43, W=0.57	
	O	E	O	E	O	E
No cleft	39	38.5	89	95.8	128	130.6
Weak cleft	88	90.4	111	98.7	199	197.1
Strong cleft	55	53.1	20	25.4	75	74.3
χ^2 Value	0.14		3.16		0.08	

Table 5.3a Observed and expected numbers of the three chin cleft phenotypes. The expected frequencies are calculated from the respective allele frequencies for the male, female and total data set assuming Hardy Weinberg equilibrium. While all three data sets fit expected proportions, the male data and the combined data are a better fit than the female data.

	Male S=0.43, W= 0.57		Female S= 0.43, W= 0.57	
	O	E	O	E
No cleft	39	59.1	89	71.5
Weak cleft	88	89.2	111	107.8
Strong cleft	55	33.7	20	40.7
χ^2 Value	20.3		24.9	

Table 5.3b Observed and expected numbers of the three chin cleft phenotypes. The expected frequencies are calculated from the total population allele frequencies (S =0.43, W=0.57).

	Female S= 0.54, W= 0.46	
	O (n=220)	E (n=220)
No cleft	89 (41%)	46.6 (21%)
Weak cleft	111 (50%)	109.2 (50%)
Strong cleft	20 (9%)	64.2 (29%)

Table 5.3c Observed and expected numbers of the three chin cleft phenotypes in females. The expected frequencies are calculated from the male allele frequencies (S =0.54, W=0.46).

for the male expected distributions; $S = 0.54^2 \times 182$, $SW = 2 \times 0.46 \times 0.54 \times 182$, $W = 0.46^2 \times 182$).

Each of the observed data sets fitted well with expected Hardy-Weinberg distributions calculated from the respective gene frequencies (Table 5.3a). However, if the total population gene frequencies were applied separately, to the female and male data, both the males and the females displayed a large deviation from the expected proportions (Table 5.3b) emphasising the observed sex difference. It is hard to see how a real difference in allele frequencies could occur between males and females. The male data provided a closer fit to Hardy Weinberg proportions than the female data suggesting that males may be more reliably scored. The three phenotypes are observed in both sexes with similar ranges of SI values perhaps indicating that not all females are underscored for the trait but that something about female facial morphology makes classification less reliable. This obvious difference in sex ratio could suggest that the gene for chin cleft manifests in all males but only a proportion of females. Perhaps in some females of a particular genetic background there is a sex-limiting modifying gene that prevents phenotypic expression of the cleft allele.

If the chin cleft phenotype manifests fully in males then the male data could be used to get an estimate of the extent of underscoring in females. Table 5.3c shows a comparison of the observed and expected numbers in females based on the male gene

frequencies. In the strong cleft category there appears to be a 20% deficit with underscoring in cleft females when comparing the observed and expected frequencies. There is a matching 20% excess of females scored in the no cleft category. As it is unlikely that a strong cleft female would be classified as no cleft, we can probably assume that 20% no cleft females are weak cleft and 20% of weak cleft females are strong cleft. Thus overall a female has a one in five chance of being misclassified as W when should be SW and a one in five chance of being misclassified as SW and should be S.

The incidence of mating types in the family data was calculated using the allele frequencies based on the total random population. In families where there was more than one family unit, only one mating pair was counted, leaving 39 unrelated couples. Comparing the observed and expected mating types (Table 5.4) it can be seen that generally there is good agreement (χ^2 gives a value of 5.25 which is not significant, p= 0.38). The main difference arises through a slight deficiency of S x SW matings and a slight excess of W x SW matings in this data set. Overall, the lack of significant deviation of the observed frequencies from the expected suggests that the family data set is a representative sample from the total population.

5.1.2 Segregation Analysis

The distribution of the three phenotypes (S, SW and W) in the population, in the parents of family groups analysed as well as the clear segregation pattern in a large pedigree (Fig 5.2) all support

Mating	Observed number	Expected number
S x S	0	1.3
S x SW	4	7.1
SW x SW	12	9.4
W x S	4	4.7
W x SW	16	12.4
W x W	3	4.1
Total:	39	39

Table 5.4 Observed number of each mating type in family analysis compared to expected number calculated from population allele frequencies (*S*=0.43, *W*=0.57). Gives a χ^2 value of 5.25, showing no significant difference between observed and expected number of mating types (p=0.38).

Mating	Offspring	Strong Cleft (S)	Weak cleft (SW)	No cleft (W)
S x S 1	1	1 (1)		
S x SW 4	6	1 (3)	5 (3)	
S x W 6	13	1	10 (13)	2
SW x SW 14	33	8 (8.25)	17 (16.5)	8 (8.25)
SW x W 19	31		19 (15.5)	12 (15.5)
W x W 5	9		4	5 (9)
TOTAL: **49**	**93**	**11** **(12.25)**	**55** **(48)**	**27** **(32.75)**

Table 5.5 Segregation data from 49 mating pairs producing 93 offspring. Shaded cells indicate where no offspring would be expected and figures in brackets indicate expected phenotype distribution of offspring assuming an autosomal co-dominant model of inheritance.

autosomal co-dominance as a likely mode of inheritance for chin cleft. In the large pedigree presented (Fig 5.2) both parents have the weak cleft phenotype (SW). Assuming Mendelian segregation the expected distribution of phenotypes in the eight offspring would be 2 W (no cleft), 4 SW (weak cleft) and 2 S (strong cleft). The actual observation is 2 W, 5 SW and 1 S, which fits well with the expected.

Detailed segregation analysis was carried out on forty-nine families with 93 offspring using both SI and STA values to classify the cleft trait (Table 5.5). Out of the ninety-three offspring, eighty-six fitted well with the expected segregation pattern for an autosomal co-dominant locus with two alleles, especially in the largest two mating categories; SW x SW and SW x W. The 35 children from matings between two weak cleft parents show segregation very close to the 1:2:1 (S: SW: W) ratio of phenotypes expected (8 strong cleft, 17 weak cleft and 8 no cleft observed). Similarly in the 31 children from the weak cleft by no cleft category the segregation of weak cleft to no cleft phenotypes is close to the expected 1:1 ratio (19 weak cleft and 12 no cleft observed).

There were seven offspring that did not fit with the expected segregation model. In these cases there was no knowledge of illegitimacy. Indeed in three of the seven exceptions the paternal phenotypes were compatible with the offspring but the maternal phenotype was incompatible (Table 5.6). As maternal illegitimacy is very unlikely, and there was no evidence for adoption, these

Mating M x F		Offspring	Strong Cleft (S)		Weak cleft (SW)		No cleft (W)	
			M	F	M	F	M	F
S x S	1	1	1					
SW x S	0	0						
S x SW	4	6	0	1	1	4		
W x S	2	5			1	2		2
S x W	4	8	1		2	5		
SW x SW	14	33	5	3	9	8	4	4
W x SW	10	19			6	4	5	4
SW x W	9	12			3	6	2	1
W x W	5	9			4		1	4
TOTAL:	49	93	7	4	26	29	12	15

Table 5.6 Raw data segregation analysis for chin cleft classification in 49 matings with 93 offspring showing parental and offspring sex. Shaded cells indicate where no offspring would be expected assuming an autosomal co-dominant model of inheritance.

Mating M x F		Offspring	Strong Cleft		Weak cleft		No cleft	
			M	F	M	F	M	F
S x S	1	1	1					
SW x S	0	0						
S x SW	5	9	1	1	2	5		
W x S	2	5			1	4		
S x W	3	5			1	4		
SW x SW	14	33	5	3	10	7	4	4
W x SW	14	26			10	4	5	7
SW x W	9	12			3	6	2	1
W x W	1	2					1	1
TOTAL:	49	93	7	4	27	30	12	13

Table 5.7 Segregation data after analysis and reclassification of 'exceptions' based on logical determination from male offspring phenotypes. For each case only one individual has effectively been changed, in 5 out of 7 cases the maternal genotype was altered and in two cases the phenotype of a female offspring was altered.

disagreements are very likely to arise as a consequence of the lack of penetrance of this trait in females leading to underscoring. For instance, where an S male and W female produced an S male offspring the female's genotype may have been *SW* rather than the apparent *WW*. These factors led to detailed re-analysis of the family data in an attempt to elucidate the apparent bias in scoring females for the chin cleft phenotype.

Each family was assessed individually to see if any other family members could explain any of the seven exceptions in terms of 'non-penetrant' females i.e. genetically or genotype *SS* (strong cleft) when scored phenotypically as SW (weak cleft) or genetically *SW* when the phenotype was scored W (no cleft). This information could come via mothers, daughters or both. For example in the W x W mating category four SW males have arisen; in all of these cases is it likely that the mother has been 'underscored' as W and should in fact be SW. Similarly in the S ^{father} x W ^{mother} mating category, if an S son occurs it suggests misclassification of the W mother, whose genotype should be *SW*.

Re-analysis of data in this way provided explanations for all of the seven offspring that did not fit the expected segregation. In a S ^{father} x W ^{mother} mating, with three offspring; SW ^{male}, SW ^{female}, S ^{male}, it was decided that the maternal phenotype was misclassified and that the genotype should be *SW* on the basis of her S ^{male} offspring. Therefore this puts the family into the S ^{father} x SW ^{mother} category. In

two cases where the exceptions arose from W ^{father} x S ^{mother} mating the maternal phenotype had to be assumed to be correct as S represents full manifestation of the trait. Here the exceptions could be explained by misclassification of a daughter as W, when she was genetically *SW*. In these non-fit families the phenotypes of the daughters were thus reassigned to the SW category. The four remaining exceptions (all SW males) came from W x W matings. If we assume that the male genotype is 100% penetrant then the father and son have been correctly assigned (W and SW respectively) then we must conclude that the mother's genotype is *SW*. These four matings were therefore reassigned into the W ^{father} x SW ^{mother} mating category. The revised classification of mating types and offspring based on these assumptions is shown in Table 5.7.

The practical approach employed to generate the data in Table 5.7 has been that of minimal disruption, thus only one individual in each family was termed as 'misclassified' (i.e. either mother or daughter). This was sufficient to explain all of the seven exceptions. Also, the revised data provides very strong evidence in support of autosomal co-dominance and the observed distribution of the phenotypes amongst the offspring is very close to the expected (Table 5.8).

5.1.3 Further analysis of the chin cleft segregation data

Each family was scrutinised individually in an effort to determine the extent of variability of penetrance and where

Mating	Offspring	Strong Cleft (S)	Weak cleft (SW)	No cleft (W)
S x S **1**	1	1 (1)		
S x SW **5**	9	2 (4.5)	7 (4.5)	
S x W **5**	10		10 (10)	
SW x SW **14**	33	8 (8.25)	17 (16.5)	8 (8.25)
SW x W **23**	38		23 (19)	15 (19)
W x W **1**	2			2 (2)
TOTAL: **49**	**93**	**11** **(13.75)**	**57** **(50)**	**25** **(29.25)**

Table 5.8 Segregation data after analysis and reclassification of 'exceptions'. The data generally fit well to the expected proportions for autosomal co-dominant inheritance.

appropriate to reclassify the deduced female genotype. The ground rules for this analysis were:

1. The clefting trait follows an autosomal co-dominant pattern of segregation
2. The determination of the male phenotype was judged to be unequivocal since it is assumed that the trait is fully penetrant in males.
3. Where the phenotype of male offspring is informative, a corrected maternal genotype may be deduced.
4. Females were assumed to display one step of lack of penetrance and this proceeds in one direction for example: a female W (no cleft) individual could be considered to be genotypically SW (weak), if she had a strong cleft male offspring, but not S. Similarly a SW female could be considered to be S but not W.

Analysis of each pedigree generated four different categories with varying information content and confidence of accurate assignment of the chin cleft phenotypes (Fig 5.3). In each instance, two different types of pedigree are illustrated, but this is not an exclusive list. Categories A and B provide high level of confidence of accurate phenotypic assignment. The category into which any individual family is placed is determined, to a large extent, by the number and gender of offspring in each family.

Category A

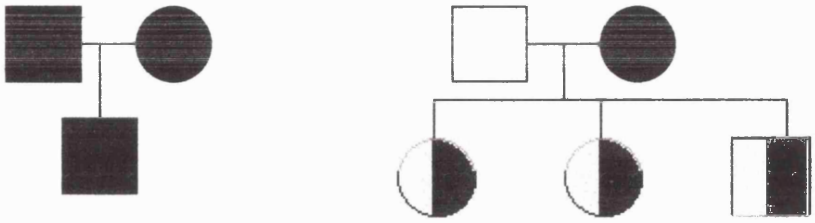

Category B

Category C

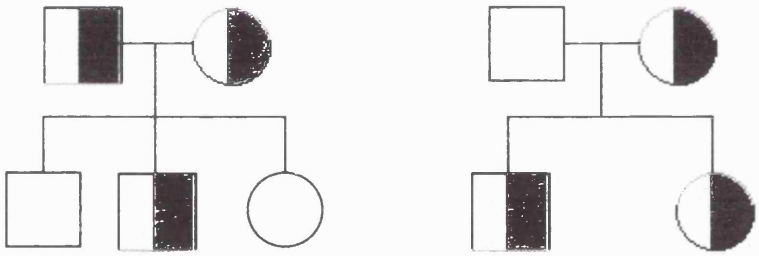

Category D

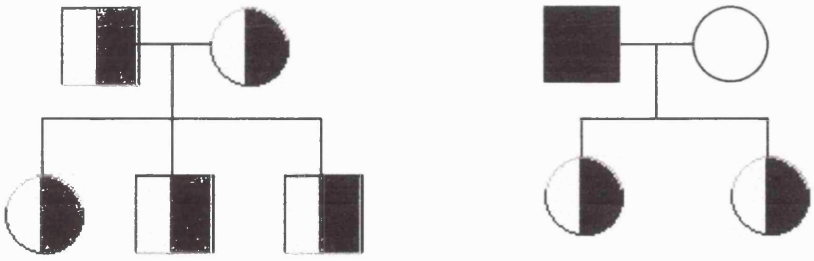

Figure 5.3 Family data collected and classified on the basis of confidence of full manifestation of the trait in female members.

Category A: Full penetrance can be unequivocally assumed in all family members. E.g. S^{father} x S^{mother} ~> S^{m}

W^{father} x S^{mother} ~> SW^{f}, SW^{f}, SW^{m}

In this category a strong cleft male and a strong cleft female produce a strong cleft male offspring. This is the only possible combination of phenotypes and hence genotypes. In this scenario full penetrance is obligatory in the mother. Therefore all male offspring should have the strong cleft phenotype; if a female offspring does not display the strong cleft phenotype then lack of penetrance (of her genotype *SS*) can be assumed. The other family, showing a mating between a W male and an S female, ensures that all offspring are genotypically SW since the S female shows full manifestation of the trait and full manifestation is always assumed in males.

Category B: Full penetrance can be assumed from the phenotype of male offspring. E.g. W^{father} x SW^{mother} ~> W^{m}, SW^{f}

SW^{mother} x SW^{father}~>W^{m}

Here a no-cleft male and a weak cleft female produce a no cleft son and a weak cleft daughter. In this instance, by following the ground rules it is possible to determine that the cleft trait is fully penetrant in both the mother and the daughter. If the mother was partially penetrant and genetically *SS* instead of *SW* then we would expect to see an *S* allele transmitted and fully penetrant in her male offspring. In this instance full penetrance can therefore be assumed. Similarly

in the second situation the no cleft male offspring resulting from two weak cleft parents confirms the maternal phenotype to be correct

Category C: Full penetrance can be assumed in one female member but not both. E.g. SW^{father} x SW^{mother} ~> W^m, SW^m, W^f

W^{father} x SW^{mother} ~> SW^m, SW^f

In the first example the mother can be assumed to be fully penetrant, on the basis of the no cleft son to whom she must have transmitted a *W* allele. As both parents are heterozygous it is possible for any of the three phenotypes (W, SW, S) to manifest in the children. Therefore it is not possible to make an assumption about the penetrance of the trait in the daughter, who could also be non-penetrant when genetically she is *SW*. In the second scenario we can assume full penetrance of the trait in the daughter but it is possible that this pedigree could also arise if the mother was non-penetrant for genotype *SS*.

Category D: Full penetrance cannot be assumed in mother or daughter. E.g. SW^{father} x SW^{mother} ~> SW^f, SW^m, SW^m

S^{father} x W^{mother} ~> SW^f, SW^f

In this case both the parents and all three of the offspring appear heterozygous for the trait. From the ground rules both the father and the two sons can be assumed to be fully penetrant but it is possible that both mother and daughter could be genetically *SS* and thus non-

penetrant. Similarly there is not sufficient information available to be sure of the phenotypes of any of the females in the second scenario.

Looking at the total family data collected, out of the 49 groups, 3 fell into category A, 6 fell into category B, 19 were category C and 20 were category D. However it must be noted that the occurrence of an additional offspring might easily lead to a change from a category D to C or from C to B. Nevertheless analysis of the family data in this way provides an assessment of the problems associated with the variability of penetrance in females.

5.1.4 Summary

The extensive population and family data provides convincing evidence that the chin cleft is determined by a single autosomal locus. The population data suggests that the chin cleft is present in all ethnic groups studied and in the European data set there appeared to be a significant difference in observed frequencies between males and females. The family data suggest that the pattern of segregation for the trait follows simple Mendelian inheritance, though scoring of the trait in females is not straightforward. This is apparent in the raw data collected and evidence becomes stronger when the apparent sex difference in phenotype frequencies is taken into consideration and can be used to explain exceptions to the segregation data. The exceptions to the model of autosomal co-dominance could not be explained by non-paternity in five of the seven cases as the phenotype of the offspring fitted with the paternal

phenotype and not the maternal. As maternal exclusion is very unlikely this suggests misclassification of the female phenotype has occurred.

The previous literature on the chin cleft phenotype, summarised by Mckusick (OMIM: 119000) records the chin cleft as an autosomal dominant Mendelian trait, however, much of the evidence is anecdotal. One of the very early papers (Lebow and Sawin, 1941) records chin cleft in a seven generation 'photo' pedigree. Within this kindred there appeared to be 15 unrelated individuals (7 males and 8 females). Only one of these unrelated individuals, a male, showed the cleft phenotype, therefore it is likely that the trait was underscored in this study and probably only the S phenotype was detected. Within the pedigree there were 10 matings; giving rise to 20 offspring in total, three of these were cleft by no cleft matings, with equal numbers of cleft and no-cleft offspring observed. There were seven no cleft by no cleft matings with 11 no cleft offspring and one cleft offspring. As the photo data is not very detailed, and several male members appear to have facial hair, it is not possible to explain this apparent exception. Nevertheless this study provides very good evidence of segregation of the chin cleft trait in the pedigree presented.

A more recent study (Bhanu and Malhotra 1972) describes the population genetics of chin cleft in India. Once again it is not possible to establish the level of correspondence between this work and the

present study except to note that in this study cleft was defined as anything from 'deep fissure' to 'trace'. A more interesting fact, which emerged from this work however, was that considerable variation in chin cleft frequency was found in different ethnic subgroups of the Indian population. The incidence of chin cleft was reported to vary from 4% to 84%, dependent on the population group observed, and there was also significant variation in the sex ratio of the trait, which is in keeping with the findings from this study.

5.2 Nose Band

The STA classification was used to define the presence or absence of a discrete feature, a 'red' band, corresponding to local concentration of peak on the STA surface segmentation, across the bridge of the nose. This is detailed in section 4.3.2

5.2.1 Population data

In total 582 unrelated individuals were scored comprising 521 European (248 males, 273 females), 36 Indian (9 males, 27 females) and 25 Chinese (9 males, 16 females) subjects. Individuals who had recorded on the information sheet that they had broken their nose were excluded, as were subjects younger than sixteen. Two phenotypes: banded (B) and non banded (b) were found to be frequent in both sexes of all three population samples studied (Table 5.9). The banded phenotype was relatively more common than non-banded in all three population groups and was most frequent (0.76) in the European group. The non-banded phenotype was relatively

most frequent in the Chinese group (0.40). These differences in relative phenotype frequencies suggest there is variation with respect to ethnic background although the Chinese and Indian population sample sizes are rather small to be conclusive. This is echoed in two small groups of African (n=8) and Arabic origin (n=8), not shown here, where in the former the non banded was more common than the banded phenotype and in the latter the banded was the most common phenotype. It would be interesting to investigate larger samples, as well as other ethnic groups, to see if this variation persists.

In all three population groups there appears to be a sex bias with the banded phenotype observed more often in males than females (Table 5.9). This difference was tested in the large European population, and found to be significant ($p< 0.05$ χ^2 2df). The presence of two phenotypes in both sexes could suggest an autosomal mode of inheritance. Two alleles B and b giving rise to the two phenotypes 'banded' (comprising BB homozygotes and Bb) and non banded (comprising bb homozygotes), this assumes that the B allele is dominant to the b allele. The allele frequencies (Table 5.10) were estimated from the frequency of the less common phenotype b. For example, in the total European population, assuming Hardy-Weinberg proportions and B = p and b = q, non banded individuals

	European			Indian			Chinese		
	M N=248	**F N=273**	**TOTAL N=521**	**M N=9**	**F N=27**	**TOTAL N=36**	**M N=16**	**F N=9**	**TOTAL N=25**
Type 1 (Banded)	203	195	398	7	18	25	9	6	15
Phenotype frequency	0.82	0.71	0.76	0.78	0.67	0.69	0.56	0.67	0.60
Type2 (non banded)	45	78	123	2	9	11	7	3	10
Phenotype frequency	0.18	0.29	0.24	0.22	0.33	0.31	0.44	0.33	0.40

Table 5.9 observed number of each nose phenotype: banded (B) and non-banded (b)

	EUROPEAN (N=521)		INDIAN (N=36)		CHINESE (N=25)	
	B	**b**	**B**	**b**	**B**	**b**
ALL	0.51	0.49	0.45	0.55	0.37	0.63
M	0.57	0.43	0.53	0.47	0.34	0.66
F	0.47	0.53	0.43	0.57	0.43	0.57

Table 5.10 Allele frequencies estimated from the non banded phenotype, assuming two alleles *B* and *b* give rise to the two phenotypes B and b, where B is dominant to b.

(bb) represent q^2 so the frequency of q = $\sqrt{246/1042}$ = 0.49 and q is 1-p = 0.51. Thus, in the total European data the B and b alleles were estimated to occur with frequencies of 0.51 and 0.49 respectively. They were similar in the Indian population; 0.45 (B) and 0.55 (b), and slightly different in the Chinese population; 0.37(B) and 0.63(b).

5.2.2 Segregation data

Segregation analysis for the nose band trait was carried out on forty families with 65 offspring (aged sixteen and above). There were no exceptions to the expected segregation pattern for autosomal dominant inheritance where banded (B) is dominant to non banded (b). The expected numbers of each phenotype among the offspring were calculated, along with the expected numbers of mating types (Table 5.11) using the allele frequencies from the whole European population (B=0.51 b =0.49). The distribution of mating types observed was close to that expected from this hypothesis also the observed distribution of the offspring in the banded (Bb and B) and non-banded (b) phenotype categories did not significantly differ from the expected proportions (p = 0.26, χ^2 2.73).

The presence or absence of a red band across the bridge of the nose was immediately evident from the STA display; there were no intermediates or ambiguous cases in the study group. Both population and family data provide strong evidence for a simple genetic basis for the nose banding phenotype. The nose band

				Type B (BB and Bb)		Type b (bb)	
Mating **M x F**	**O**	**E**	**Offspring**	**O**	**E**	**O**	**E**
B x B BB x BB (p^2 x p^2) Bb x BB (2pq x p^2) BB x Bb (p^2 x 2pq) Bb x Bb (2pq x 2pq)	*25*	*23.1*	38	31	33.8 $p^4+2p^3q+2p^3q+¾(4p^2q^2)$ = $p^2(p^2+4pq+3q^2)$ As $p^2+2pq+q^2=1$ and $p+q=1$ can simplify as: $p^2(1+2q)$	7	4.2 $¼(4p^2q^2)$ p^2q^2
B x b *BB x bb (p^2 x q^2)* *Bb x bb (2pq x q^2)*	7	7.3	13	9	8.7 $p^2q^2+½(2pq^3)$ = $pq^2(p+q)$ As $p+q=1$ can simplify as: pq^2	4	4.3 $½(2pq^3)$ pq^3
b x B *bb x BB (q^2 x p^2)* *bb x Bb (q^2 x 2pq)*	6	7.3	9	4	6.0 $p^2q^2+½(2pq^3)$ = $pq^2(p+q)$ As $p+q=1$ can simplify as: pq^2	5	3.0 $½(2pq^3)$ pq^3
b x b *bb x bb (q^2 x q^2)*	2	2.3	5			5	5.0 q^4
Total:	40	40	65	44	48.5	21	16.5

Table 5.11 Segregation analysis for nose profile classification in 40 matings with 65 offspring. Shaded cells indicate invalid result for autosomal dominant model of inheritance where non-banded (b) is recessive to banded (B). Expected frequencies are calculated from the estimated population allele frequencies of B (0.51) and b (0.49). There is very good agreement between the observed and the expected phenotype frequencies in the offspring.

phenotype fits a simple single locus genetic model; with the banded phenotype dominant to the non-banded phenotype. Although the family data are rather small, they provide strong support for the proposed model and the ratio of phenotype distribution in the offspring fits well with expected numbers calculated assuming dominant segregation of the trait.

Considerations when using segregation analysis

Segregation analysis relies on the segregation of alleles by counting phenotypes of offspring from certain mating types in accordance to Mendelian laws [Mueller & Cook 1996). It is particularly useful in determining single gene involvement in complex diseases, genetic heterogeneity and for estimating proportions of families with different types of inheritance. In order for segregation to be observed the trait in question must manifest in different phenotypic forms and within a family a parent must be heterozygous in order to observe segregation of the trait. Additionally families segregating for the trait should be acquired in an unbiased manner; ascertainment is often difficult to resolve and is a particular problem with recessive traits. Both the nose band and the chin cleft traits were amenable to preliminary segregation analysis. However, even these two simple classifications highlighted important considerations associated with segregation analysis including the effects of delayed onset (e.g. development of nose band trait at puberty), variable expression (e.g. male-female variation in frequency of chin cleft), and reduced penetrance, all of which can result in deviation from the expected ratio of offspring,

Support or rejection of a hypothesis can be dependent on sample size, in both cases more family data would have been desirable especially the inclusion of multigenerational large pedigrees to substantiate the hypotheses however, in practice this is very difficult to attain. The analyses presented in this thesis here were based on the assumption that there was a single major locus, responsible for the each trait. Of course this may not be the case and so more complex methods of assessing inheritance of the traits may need to be considered with an expanded data set [Lathrop, Terwilliger & Weeks 1996].. Sophisticated models for complex segregation have been developed to allow for multigene models and the environmental contribution to a phenotype. These techniques combine linkage and segregation analyses to find out which mode of transmission yields the highest lod score; these lods scores, maximised over genetic models are referred to as mod scores (Clerget-Darpoux 1992), this approach has the advantage that it bypasses the ascertainment problem, however, in order for it to be successful the marker must be tightly linked to the trait in order for it to reveal any information. However, these more complex models still suffer the need for very large sample sizes.

CHAPTER 6

Anthropometric assessment of jaw protrusion and facial asymmetry

This chapter describes the use of landmarks to analyse two separate traits; the degree of protrusion of the mandible and assessment of minor facial asymmetry. The jaw angle measurement described in Chapter 4 was made on a subset of the European population in order to see if it were possible to devise a means of classifying the extent of protrusion of the mandible. Various approaches, including the triangle area method also described in Chapter 4, were applied to investigate facial asymmetry in a set of clinical patients with a rare kidney disorder where anecdotal evidence had suggested hemihypertrophy of various body parts including the face (Indridason et al 1996).

6.1 Jaw protrusion

The measurement is described in detail in Chapter 4 but basically involves placement of three midline facial landmarks (nasion, sub nasale, pogonion) to find the included angle n sna pg.

6.1.1 Population data

This feature was scored in 143 unrelated Europeans (72 female, 71 male); genotyped for one or more variants in the candidate

'face genes' described in chapters seven and eight in order to carry out preliminary genotype-phenotype association studies.

The jaw angle values ranged from 148.5° to 177.46° and were found to be normally distributed about a centrally located mean of 164.18°, with a standard deviation of 5.97. The range of values was similar in males and females (150->177° in males and 149->177° in females), as were the mean and standard deviations (163 and 6.12 in males and 165.5 and 5.62 in females).

There does not appear to be a gender difference in the range and frequency of jaw angle values (Fig 6.1) but there does appear to be a slight shift in the male data towards lower values compared to females. On close inspection the male data fit a normal distribution slightly better than the female data. A large sample test on the difference of means between males and females suggested a significant difference between the sexes at the 1% level (z=2.5)(this is discussed further below).

In clinical studies normal and optimal measurements can be defined on the basis of the population standard deviation and mean. The optimal range is defined as measurements that fall within (+/-) one standard deviation of the mean, so the optimal range for these 143 subjects (male and female combined) is between 158.2° and 170.2°. The normal range includes measurements within two standard deviations of the mean, which in this case are between 152.2° and 176.1°. Out of 143 individuals 137 fell within the normal

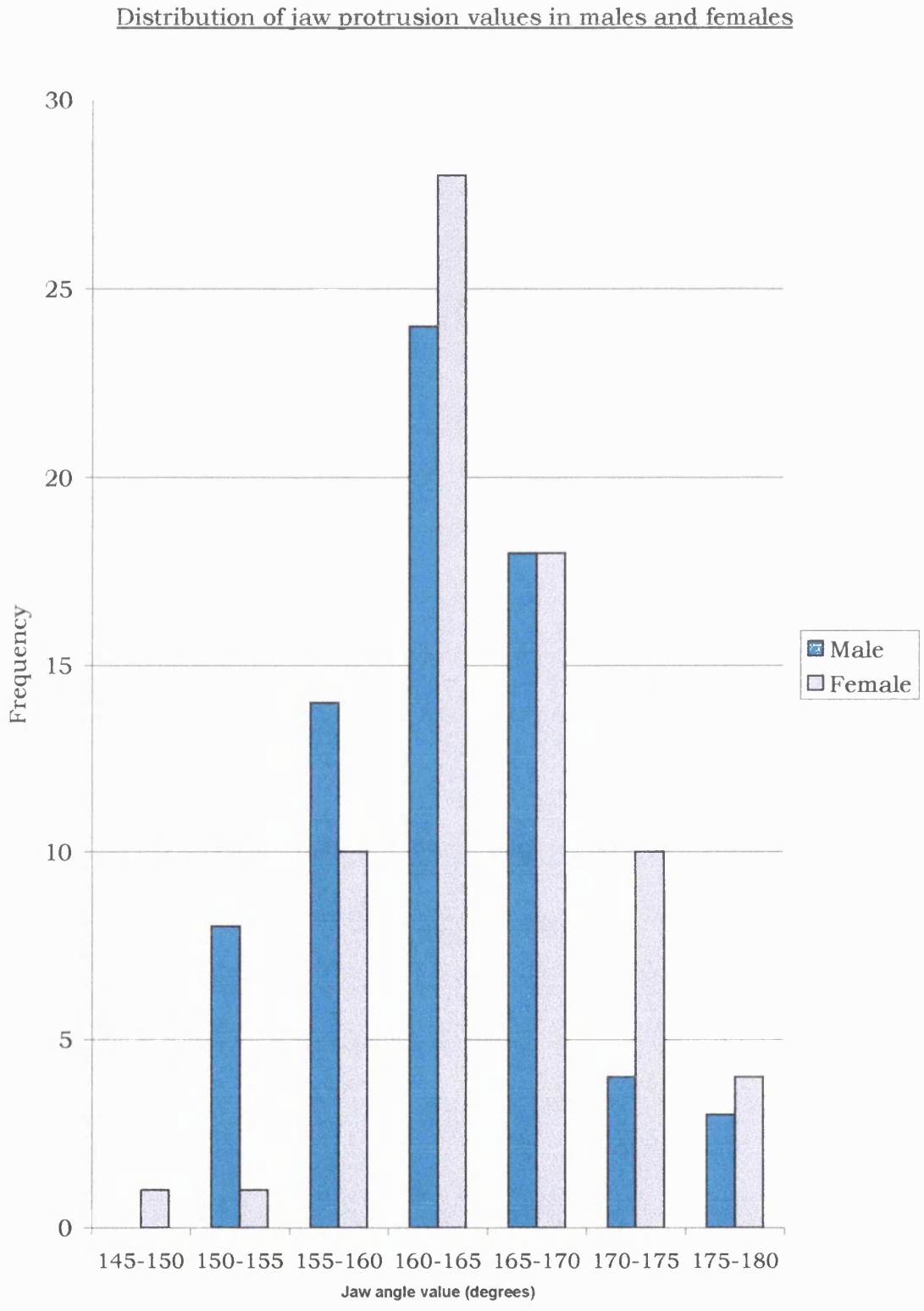

Figure 6.1 Histogram displaying range of jaw protrusion values in male and female unrelated Europeans.

range (four males and two females fell outside this range) and 102 individuals fell within the optimal range (twenty-three males and eighteen females fell outside this range).

The reproducibility of this measurement suggested that on average repeat measures fell within one degree (either plus or minus) of the original measurement. However as the range of values for the jaw angle is relatively small and the standard deviation quite high, it would be difficult to attribute confidence to a classification that subdivided the data into categories on the basis of the standard deviation. Subjects who fell outside of the normal and/or the optimal range could be considered as 'extreme' phenotypes.

Figure 6.2 shows the jaw protrusion measured in nine subjects, the first set of subjects falling within the calculated 'normal' range and the other two sets of subjects falling above and below the normal range. From these images it is quite clear that the shape and projection of the philtrum and upper lip, which affect landmark SNA can have a considerable effect on the measurement attained. While it may seem that this measurement simply assesses jaw protrusion, it is in fact an assessment of the protrusion of the whole of the lower face or the extent of 'flatness' of the face.

6.1.2 Family data

Eighteen mating pairs with 41 offspring were chosen where both parents and at least two adult offspring were scored for the jaw protrusion measurement. The midpoint parental value was calculated

a) Within 'normal' range

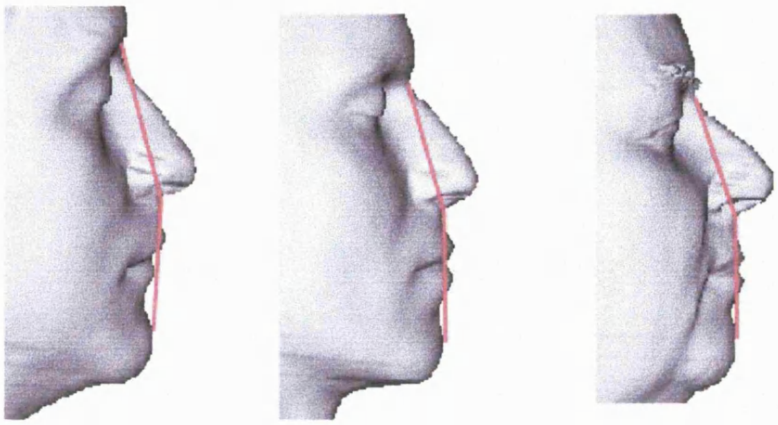

b) Above 'normal' range

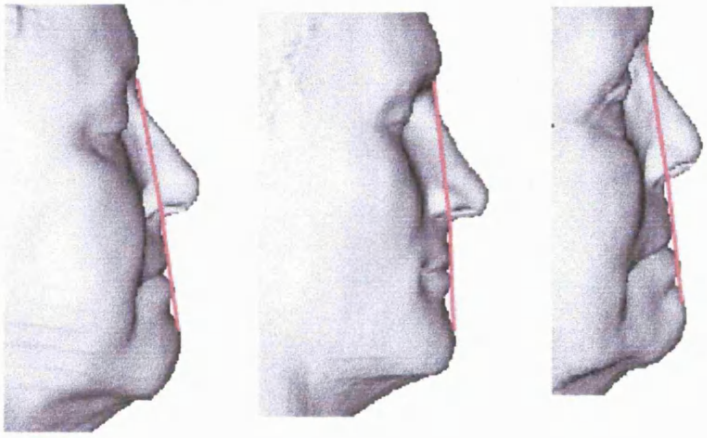

c) Below 'normal' range

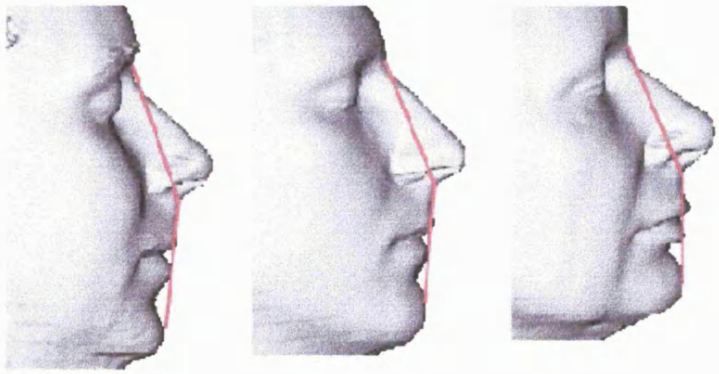

Figure 6.2 Variability of jaw protrusion, the first three subjects have a vale which fits within the calculated normal rang (between 152° and 176°), the other two sets of subjects fall outside of the normal range. Subjects whom fall above the normal have a value > 176°, and subjects whom fall below the normal range have a value which is less than 152°.

for each mating pair and compared with the offspring values (Fig 6.3). The correlation coefficient between the mid-parent and offspring was 0.37 suggesting weak correlation between the data sets (n=41, $p<0.05$). There was no correlation between parental values ($r = 0.07$) nor significant correlation between sib pairs ($r=0.35$, $n= 28$ $p >0.05$).

Correlation analysis was then carried out between parent and offspring and the findings were rather heterogeneous. Mother - daughter pairs produced a positive correlation coefficient of 0.65 ($n=24$, $p<0.001$) whereas father – daughter pairs showed a weak negative correlation ($r = –0.11$) (Fig 6.4). This striking same sex correlation in jaw protrusion was observed with father – son pairs; correlation of 0.59 ($n=17$, $p<0.05$) and there was a low negative correlation between mothers and sons ($n= 17$, $r = –0.12$) (Fig 6.4). Because of the small numbers it was decided to scrutinise the total family data set for more sib pairs and same sex parent/offspring pairs to increase the data set.

Increasing the number of sib pairs did not alter the fact that there was no significant correlation between sib pair values ($n=45$, $r=0.27$, $p>0.05$). Same sex sib pairs were also analysed, in small numbers (n=19 female sib pairs, n=7 male sib pairs), but neither sexes showed significant sib pair correlation (males $r=0.55$, $p=>0.05$, females $r=0.33$, $p=>0.05$). Increasing the father-son set ($n=26$) gave a decreased correlation coefficient ($r=0.42$) but was still significant at the 5% level. Likewise increasing the mother-daughter set ($n=32$)

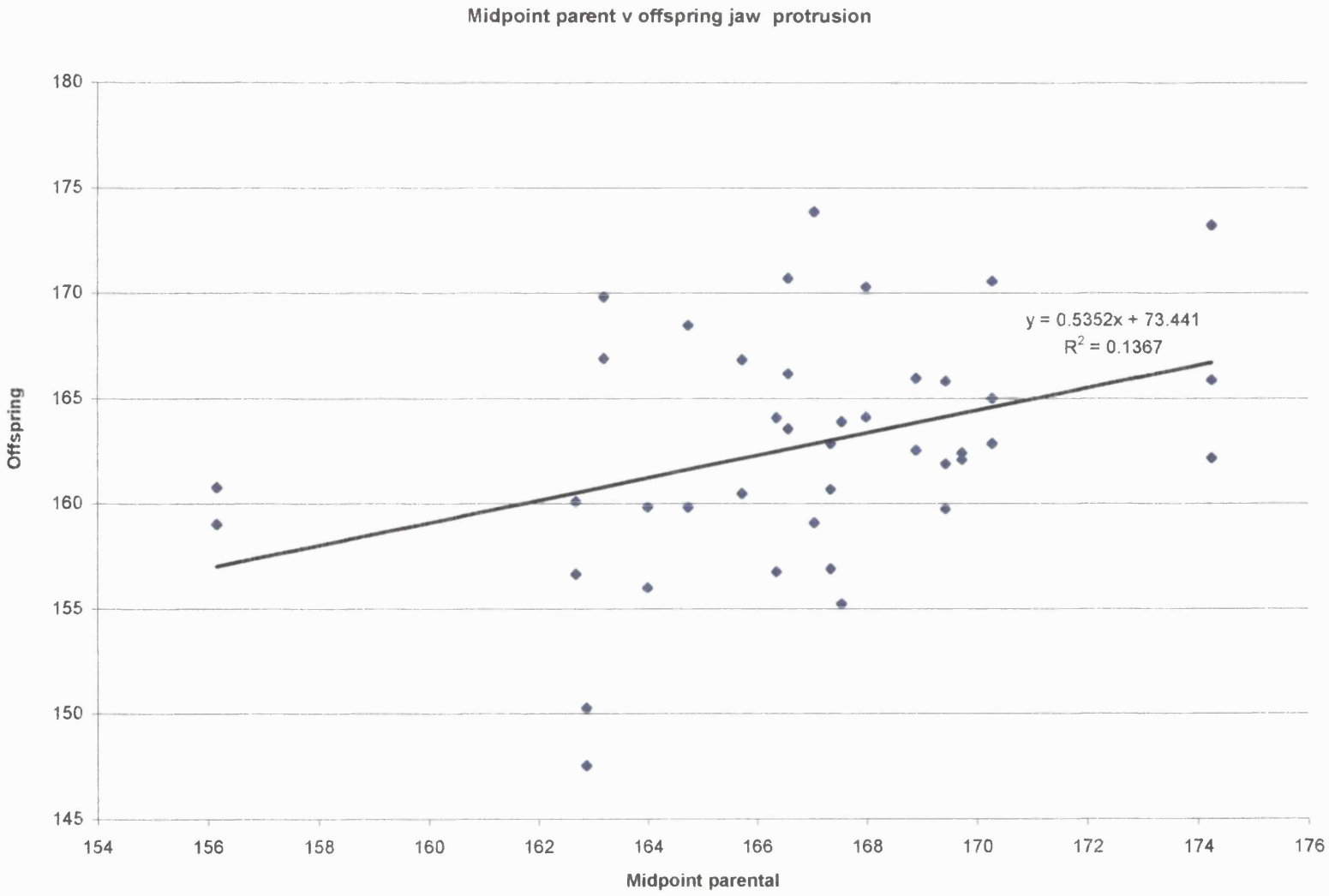

Figure 6.3 Midpoint parental jaw angle value versus offspring jaw angle value, giving a correlation coefficient of 0.37.

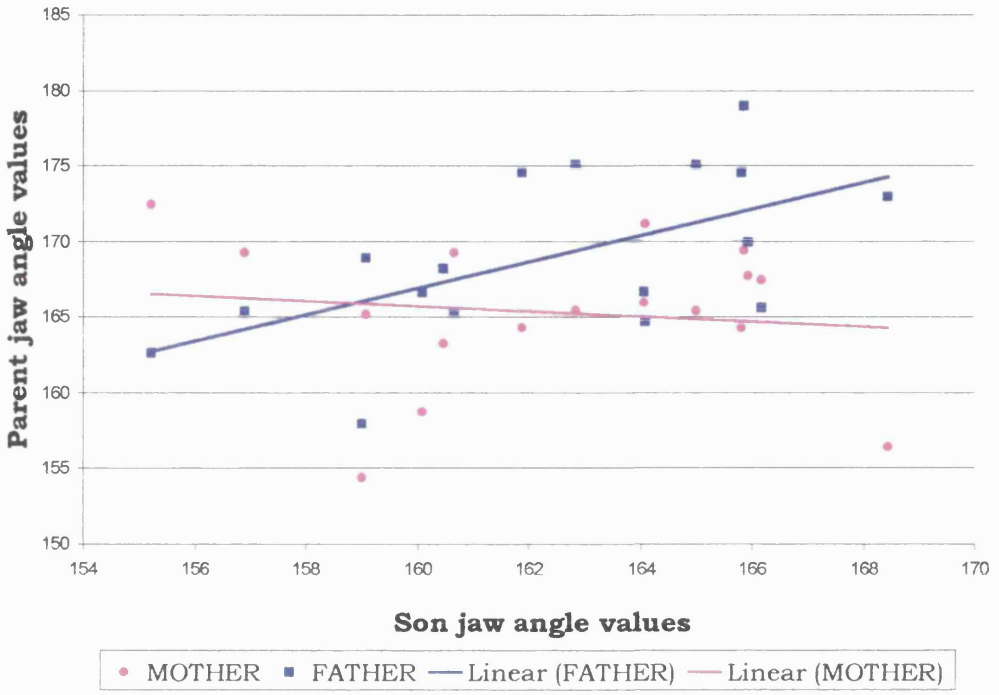

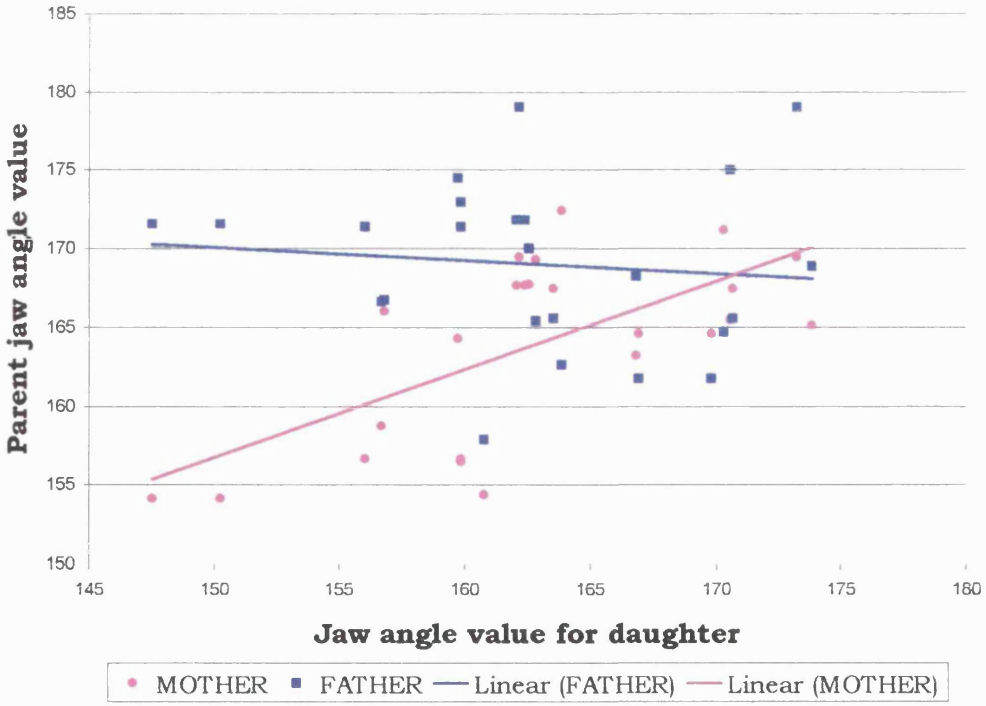

Figure 6.4 A- Correlation between parental jaw angle values and female offspring, 6.4 B- correlation between parental jaw angle values and male offspring.

reduced the correlation coefficient (r=0.59) but remained significant at the 0.1% level. Although the data sets were only slightly increased the trend in same-sex correlation between parent and offspring appeared to persist. This result is interesting and supports the population analysis finding (6.1.1) that suggested that there was a significant difference between mean values for males and females.

It is possible that the observed difference between males and females could arise because of the mentioned difference in the degree of anatomical protrusion of the upper lip. In some individuals the measurement may be a true reflection of mandibular protrusion but in others the landmark SNA and overall 'flatness' of the face might be affecting the value obtained in a disproportionate manner, but this is clearly not random. For example, in the family analysis it is possible that there is genetic similarity between family members, as judged by the correlation, which effectively reduces the heterogeneity of the measurement and makes the male/female difference more apparent. This suggests anthropometric measurements may be too variable and complex and hence not suitable for simple genetic analyses.

Thus, overall in this particular instance the anthropometric measurement being studied provides some evidence of underlying genetic factor. However, unlike the qualitative Shape Index and STA pattern it does not provide a distinctive framework for phenotype classification.

6.2 Medullary sponge kidney (MSK) and facial asymmetry

The diagnosis of medullary sponge kidney (MSK) is based on specific renal function tests and is associated with a somewhat variable clinical presentation (Indridason et al). We were approached, by renal physicians in UCL, to see whether face scanning might provide a low cost non-invasive diagnostic procedure. This idea was based on reports of hemihypertrophy associated with this disorder (Indridason et al). The physicians with whom we collaborated had the impression that in some cases their patients showed subtle abnormal facial development, and asked us to use the scanner and associated software as an objective means of assessment. Thus, the purpose of this study was to assess the facial morphology of a set of MSK patients to see if it is possible to discriminate MSK patients or a subgroup of these patients from normal controls on the basis of anthropometric measurements.

6.2.1 Data set

Prof. Unwin recruited patients from the nephrology department at the Middlesex hospital. Individuals were scanned using the fixed optical surface scanner, in total 14 MSK patients were studied, 6 women and 8 men. A 2D image was also taken with the digital camera of each ear and the face. All of the subjects were of European

origin. Two control sets, matched for age, sex and ethnic background were selected from the database of scanned normal volunteers.

6.2.2 Data analysis

Seven landmarks and eight simple measurements were used in order to assess asymmetry. These measurements were adapted from Burke et al (1971), so they were more suitable for the data obtained from the optical surface scanner as opposed to direct palpation of the subject. The 'Cloud' program was used for location of landmarks and calculation of distances between points. The six landmarks used were; left exocanthion(A), right exocanthion(B), left cheilion(C), right cheilion(D), pronasale(E), nasion(F) (Fig 6.5).

The landmarks were located on each individual and the two matched control groups and the direct distance between the landmarks was calculated. Having made the measurements, the next stage was to compare the left and right sides, this was first done by subtracting the measurement made on the left side from the equivalent measurement made on the right side. The overall differences were calculated (Table 6.1) and in general the measurements made on the left side of the face were slightly larger than those on the right were, for all groups (patients and two control groups). The overall differences were calculated (Table 6.1) and in general the measurements made on the left side of the face were slightly larger than those on the right were, for all groups. This contrasts with a previous study of facial asymmetry in North American Caucasians, (Farkas and Cheung 1981)[1], which reported the right side of the face the largest side,

particularly in measurements made on the upper third of the face. It is possible that the present results reflect a systematic bias in the collection of the data by the fixed surface scanner since the left side of the face is always recorded first. It would be prudent to evaluate this conclusion by using the HLS system to scan the patients, since with this apparatus the scan comprises three random sweeps covering the surface of the face and therefore lateral bias should not occur. It is also possible that the placement of landmarks could bring about this result, especially if there was inaccurate identification of the 'midline' landmark points.

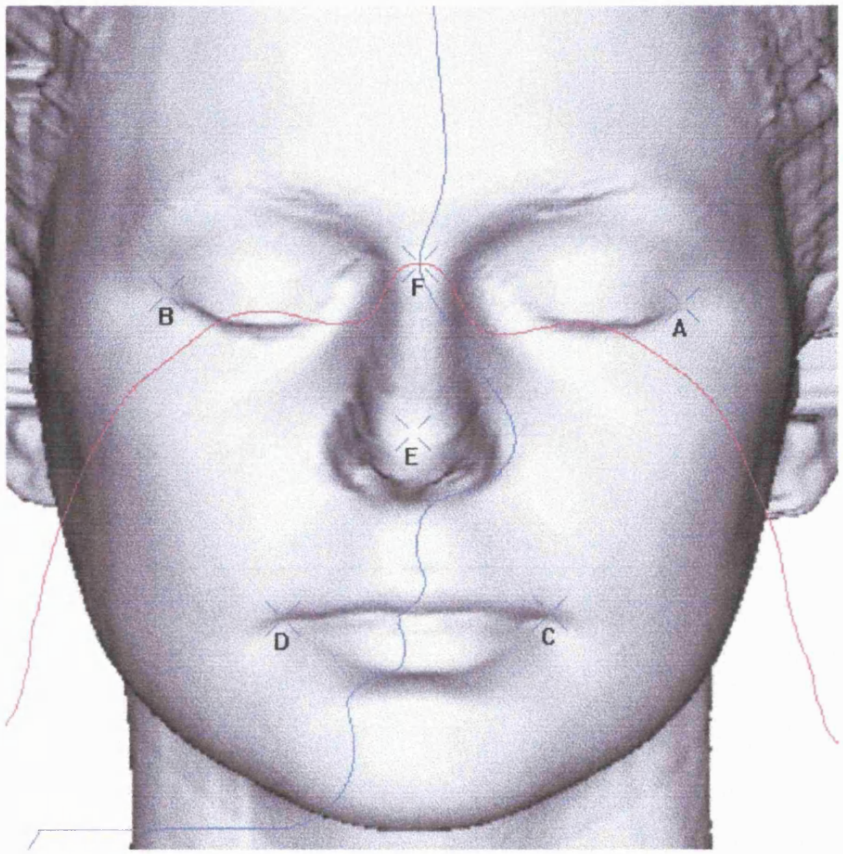

Figure 6.5 Facial landmarks used in initial analysis of facial asymmetry in MSK patients compared to controls.

Mean Measurement (R –L)	MSK Patients	Control 1	Control 2
B>F – A>F	-3.2	-2.0	-1.03
B>E –A>E	-4.6	-2.9	-0.61
B>D –A>C	-1.7	-1.0	0.7
D>E – E>C	0.4	0	-0.7

Table 6.1 Mean left right differences (mm) in four measurements used to estimate facial asymmetry in set of 14 patients with MSK compared to two matched control groups

Mean sum of LR difference squared	MSK Patients	Control 1	Control 2
B>F – A>F	21.9	14.2	4.1
B>E –A>E	38.6	24.5	7.8
B>D –A>C	7.6	12.7	8.8
D>E – E>C	16.4	10.3	2.5

Table 6.2 Mean sum of right-left differences squared used to compare facial symmetry in MSK patients with controls

The sum of the left-right differences squared was also calculated for each individual to get a general view of non-directional asymmetry. The mean values for patients and controls are presented in Table 6.2 and seem to be greater in the patients than in the controls though not significant. These simple analyses did not reflect any striking differences between patients and controls. However, it is interesting to note that the two control groups were quite different in their values, it was therefore decided that further analyses should be carried out using an average of the two matched control groups

In order to look for fluctuating asymmetry a two-tailed T-test was used on the left-right differences squared. Analysis was carried out between patients and the two controls for the four measurements. The T-test on the mean differences squared did not reveal significant difference between the patients and either of the control groups nor between the two control groups. {Patient v Control group 1 T=0.89, d.f=3;p=0.18, Patient v Control group 2 T= 1.42,d.f=3;p=0.22, Control group 1 v Control group 2 T=1.29, d.f=3;p=0.30}

In order to investigate this finding further the triangle area method was employed as a more sensitive technique to assess general facial asymmetry. The landmarks and areas of each of the respective triangles were calculated as described in chapter four. Fig 6.6 illustrates the average area of each of the 13 triangles on the left and right side of the face for the set of MSK patients and the matched controls. From this histogram we can see that the greatest left right difference appeared to occur for triangle 7, however this is similar in both patients and controls probably reflects the trouble in locating the landmark at the tragion (on the edge of the ear) needed to form this triangle. Triangle 8 also shows marked left right difference in area but as this is observed in both patients and controls it is also

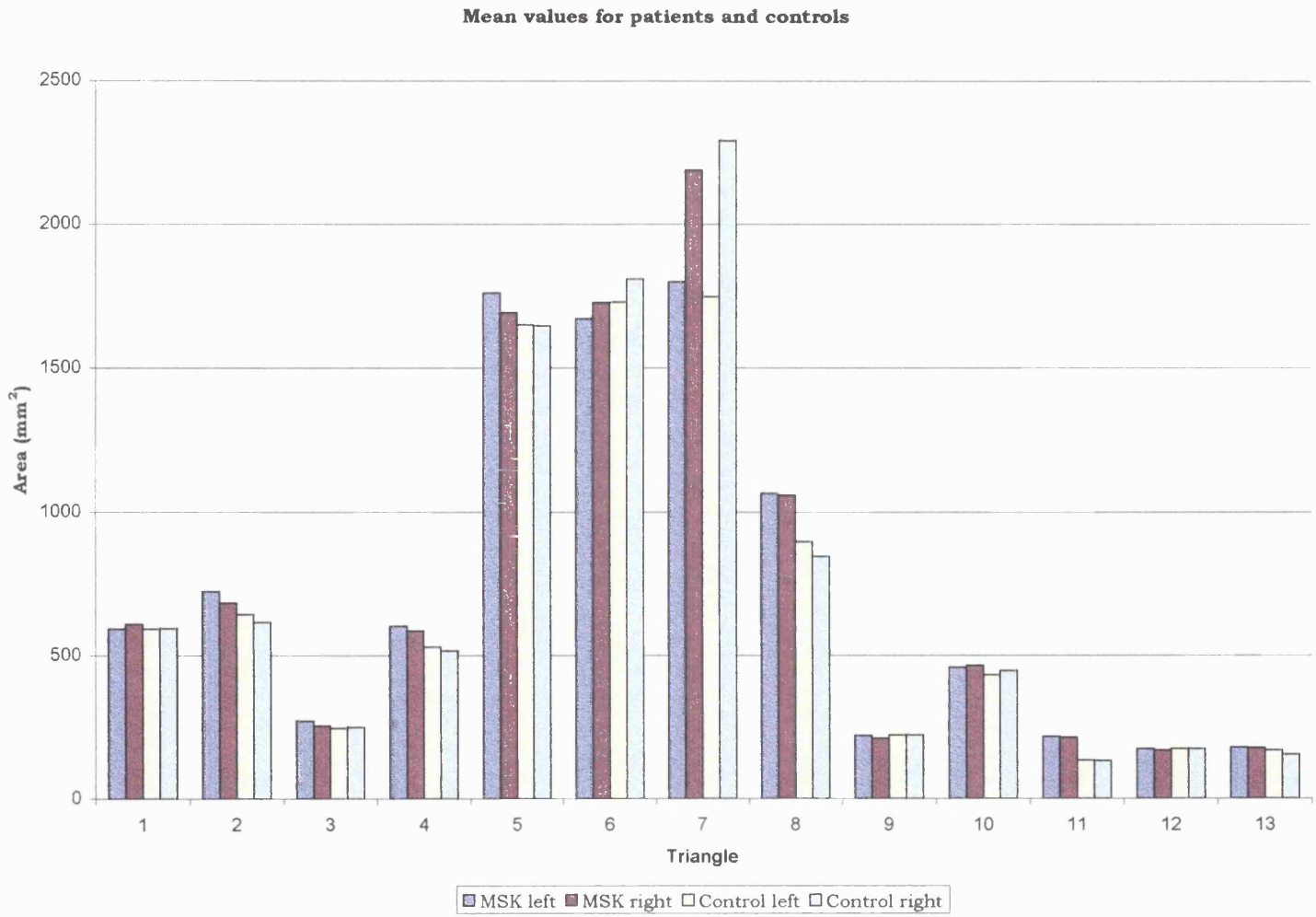

Figure 6.6 Average area of each of the 13 triangles on the left and right side of the face, in a set of MSK patients and matched controls.

likely to reflect poor landmarks. When plotted like this, none of the measurements appeared to reflect left-right differences specific to the MSK patients. Although not a reflection of left-right asymmetry it is interesting to note the difference in mean area between the patients and controls for triangle 11.

The total combined area of the 13 triangles was calculated for the right and left sides of the face for each subject and control to attain an estimate of total left and right face area. With the exception of one subject the area of the left side of the face was larger than the right in both patients and controls. The overall difference in area between left and right sides of the face was not significantly different in patients compared to controls. Fig 6.7 illustrates the total left right difference in area of the face in five MSK patients and their age/sex matched controls.

For each subject the difference between left and right areas of each of the thirteen triangles was calculated. For each triangle this value was analysed by paired t-test, to look for variability in triangle area between the patient data set and the controls. Paired, 2-tailed T-tests did not give significant results for any of the triangles suggesting that there is no heterogeneity of measurements between patients and controls.

The triangle-area method did not reveal any significant facial variation between patients and controls and did not confirm the initial findings from the simple anthropometric analysis suggesting

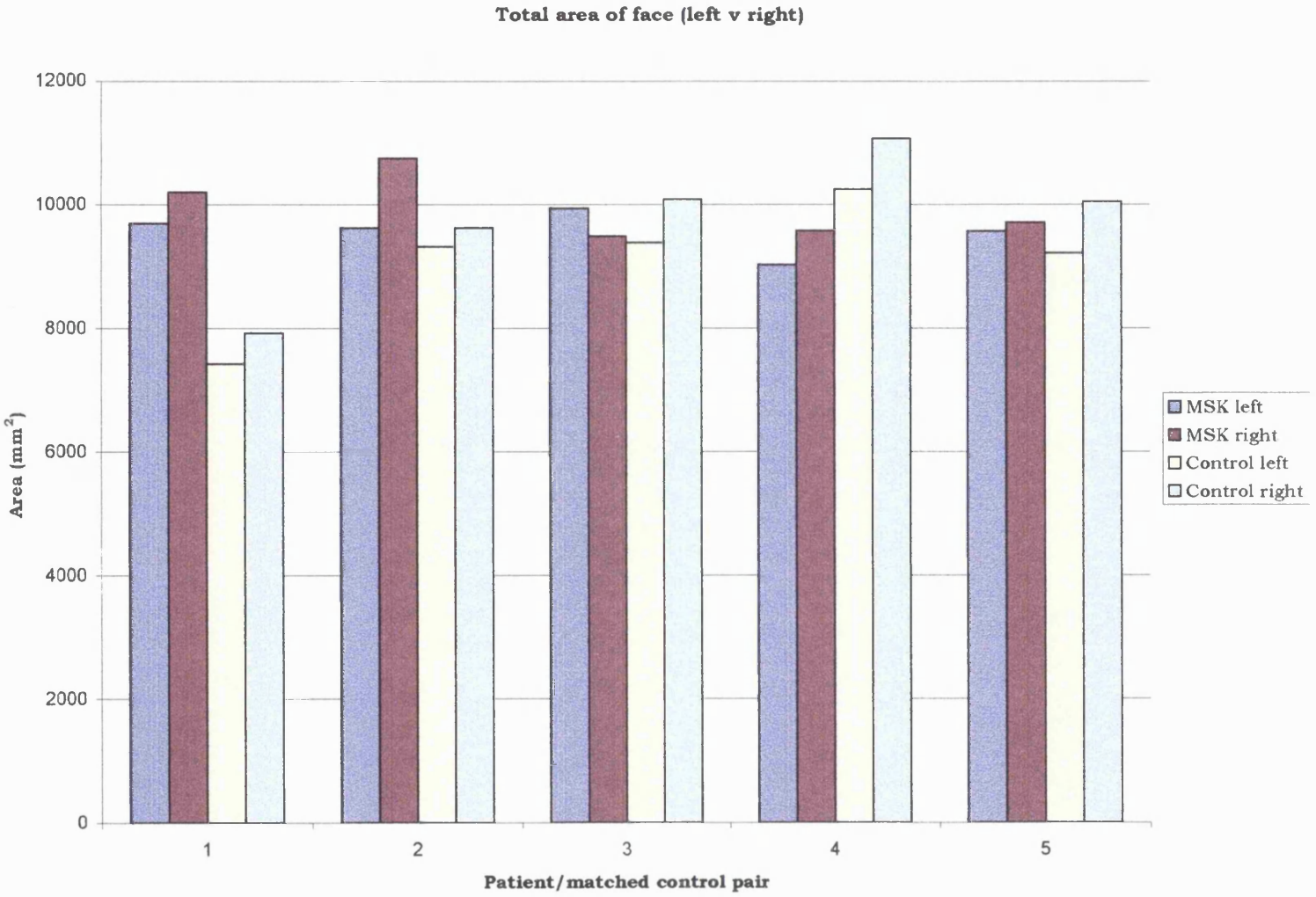

Figure 6.7 Total left-right area difference calculated using triangle area method in five patients and matched controls

these results should be treated cautiously. This study was carried out on 14 patients and matched controls and, although we contacted renal units in other hospitals, further cases of MSK were not forthcoming. Thus it was not possible to increase the number in the data set. This could be a reflection of the relative infrequency of the condition coupled with heterogeneous presentation of the complaint and difficulty in accurate diagnosis of MSK without IVU. However, this was a useful pilot study of 3D face scanning on a small group of patients with variable renal problems associated with MSK. Analysis of the patients' faces in comparison to healthy matched controls did not reveal anything unusual in the symmetry of the face and suggests that the face scanner is not a useful adjunct in MSK diagnosis.

Two systems have been used to analyse facial asymmetry and there are problems and benefits associated with each method. The first method relied on 6 landmarks and 4 measurements to establish a crude index of asymmetry. The landmarks could be identified accurately and were relatively robust, also the measurements were relatively large and the errors proportionately lower. However, only the central area of the face was analysed and there were only two midline points; errors in locating either of these points could have had a significant impact on the overall results. Although a T-test on the raw left-right differences proved to be significant, a T-test specifically investigating fluctuating asymmetry did not highlight significant differences between the patient and control sets.

The triangle area method did not reveal significant differences between patients and controls although it provided comprehensive coverage of the whole of the facial surface. However, the repertoire of landmarks used was more variable in terms of reliability than those used in the crude system. Out of the 19 landmarks there were three that I judged to be particularly unreliable; a central landmark on the pogonion, and the bilateral landmarks on the

mandible and the tragus. It is very likely that the inclusion of these landmarks reduces the overall sensitivity of this approach, particularly as the analysis compounds any inaccuracy by comparing the areas as opposed to direct measurements. In conclusion both of the techniques used have their relative merits and it is difficult to assess which is the best technique. It is also important to recognise that the patient set is small and in itself relatively heterogeneous and only through expanding the data set can a more accurate assessment of reliability be made.

CHAPTER 7

Molecular analysis of ET1 and ETRA as candidate 'face genes'

A long-term objective of this project is to identify genes that underlie the observed variation in normal facial features. One approach to this problem is to investigate 'candidate genes', using genetic variants to look for correlation between genotype and phenotype. This chapter investigates two genes selected as good candidates from a review of literature - Endothelin 1(ET1) and its receptor Endothelin receptor A (ETRA). These are both strong candidate 'face genes' as judged by the following observations;

1. The homozygous mouse knockouts for both genes show severely malformed mandibles (Kurihara et al 1994; Clouthier et al 1998).
2. Expression studies in normal mice find strong expression in the first branchial arch during facial morphogenesis (Barni et al 1998).

The aim of the work described in this section was to investigate the exonic sequence of ET1 and ETRA for genetic variation using PCR-SSCP analysis in DNA from subjects scored for jaw protrusion and chin cleft.

While my work was in progress, a group in France focusing on the endothelins as candidates for cardiac pathology, published information on five polymorphisms in the ET-1 gene (three in 5'

sequence and two in exonic sequence) and five polymorphisms in the ETRA gene (all in exonic sequence)(Cambien et al 1999). These were comprehensive studies, carried out on two separate populations; one Irish and the other French. In a separate study Nicaud et al (1999) looked at the coding regions and 5' flanking sequence of the ETRA gene, identified an additional polymorphism in the 5' flanking region. A summary of these polymorphisms and their precise location is given in Table 7.1.

Since these publications there have been several other studies looking at the association of variant alleles of ET1 and ETRA with various pathologies including; atopic asthma (Mao et al 1999) blood pressure (Tiret et al 1999), and myocardial infarction (Nicaud et al 1999). So far significant association ($p<0.05$) has only been found between the polymorphism in exon 5 of ET1 and blood pressure in overweight subjects (Tiret et al 1999). Neither ET1 nor ETRA have been conclusively linked with human pathology.

The primers and PCR-SSCP conditions used in the present study were designed independently. The polymorphisms in ET1 exon 5, ETRA exon 6 and exon8 were all found independently of the published studies (intronic sequence was not analysed) and no additional variants were found.

7.1 DNA amplification and polymorphism detection

Due to lack of time and resources it was decided to concentrate on translated exon sequence of the two genes rather than the whole

Polymorphisms in ET1	**Position**
T-1398A	5' flanking
G-1396A	5' flanking
T-1370G	5' flanking
+/- A, nt. 138	exon 1 5' UTR
G in. 1 -46 A	intron 1 (46th bp. before exon 2)
T in. 2 -37 C	intron 2 (37th bp. before exon 3)
G 862 T : Lys198Asp	exon 5 codon 198
Polymorphisms in ETRA	**Position**
A 231 G	exon 1 5' UTR
C 1471 T silent	exon 6 codon 323
A 1507 G silent	exon 6 codon 335
C 1856 G	exon 8 (3' UTR 70 bp. 3' to stop codon)
C 3008 T	exon 8 (3' UTR 1222nd bp. after stop codon)
T +52 C	3' flanking (52bp after 3' end of mRNA)

Table 7.1 Published polymorphisms in ET-1 and ETRA (Cambien et al 1999, and Nicaud et al 1999) (UTR- Untranslated sequence)

gene sequence. This was done on the premise that variants found in the coding sequence would be more likely to produce a significant change in the protein structure and possibly cause a phenotypic effect rather than variants found in non-translated sequence. Primers of 20-24 nucleotides long were designed to amplify each of the five exons of the ET1 gene and exons 2-8 of the ETRA gene (ETRA exon 1, which is entirely 5' UTR, was not analysed). The primers were designed so they would anneal at a position within intron sequence approximately 20 basepairs (bp) from exon sequence. Where possible, the primers were approximately 50% G/C content, with a G or a C at the 3' end; the members of a pair of primers were matched for length and G/C content. All primer pairs were checked using the computer program Amplify to ensure only one product and no primer dimers would be produced. Primers were chosen to give PCR products ranging in size from 134-393 base pairs (Table 7.2).

Each exon and intron/exon boundary was PCR amplified and subjected to SSCP analysis in order to search for DNA polymorphisms. Initially DNA from 18 subjects was used so that optimum PCR and SSCP conditions could be established. Four different SSCP conditions were tried routinely to achieve best resolution of bands and to increase the likelihood of detecting additional variants. In brief, the variable conditions were gel composition, buffer pH, running time and voltage. PCR and SSCP conditions are summarised in Tables 3.2 and 3.3 in Chapter 3.

Primer Name	Primer Sequence 5'⟶3'	[1]Tm - 4°C	Product Size (bp)
ET- F1	taaagggcacttgggctgaagg	58	229
ET- R1	ccgagacttacaagtcaacgag	56	
ET- F2	tttgaggagacatcccccactg	58	265
ET- R2	gtggagccagcgctaatgaatg	58	
ET- F3	ggaataggtgtgtccatgtgtc	56	294
ET- R3	tgataggaaggagttcaggagg	56	
ET- F4	ctatcatggtactgccttcctg	56	328
ET- R4	aggctgctggcatcactgactg	60	
ET- F5	aaagttcacaaccagattcagg	53	393
ET- R5	gggaactccttaacctttcttg	54	
ETA2AF	agcagcacaagtgcaataagag	54	265
ETA2AR	agtctgctgtgggcaatagttg	56	
ETA2BF	atttggtcctacccagcaatg	54	274
ETA2BR	catttgtggttacttcctacc	52	
ETA3F	actgtgtctccttctttcagc	54	168
ETA3R	aagggaaagaaccacattacc	52	
ETA4F	ttcaggtacagagcagttgc	53	189
ETA4R	tgtggcattgagcatacagg	53	
ETA5F	tcactttgaagttctaccaag	50	184
ETA5R	catgatgttatgggatttacc	50	
ETA6F	cactttcctttagcgtcgag	53	167
ETA6R	gcgagtacacaggatcatac	53	
ETA7F	ttgctctagtttcttactgc	49	134
ETA7R	tgaaaaatcatcttacctgg	47	
ETA8F	gtctgttccttcccccagtc	57	290
ETA8R	gcatttcttcttgggtgtgg	53	

Table 7.2 Sequence of the primers designed to amplify each of the translated exons of ET1 and ETRA.

[1] Tm = 69.3 + (0.41 x A) – 650/B
Where A = %G/C of primer and B = length (nt.) of primer

Initially PCR-amplified DNAs from 18 subjects were analysed under the four different conditions and then, PCR products from up to a further 35 subjects were analysed using SSCP conditions judged to give optimal resolution.

PCR products showing variant SSCP patterns were sequenced to investigate whether a DNA change underlay the variation. Where variants were found MAP analyses of the wild type and variant sequences were compared in order to look for changes in restriction enzyme sites that could be used for rapid genotyping.

7.2 SSCP analysis of ET1

The five exons of endothelin –1 were PCR amplified and analysed by SSCP analysis. Fig. 7.1 A shows the sequence of the exon 1 PCR product with the translation initiation codon highlighted in green. Fig. 7.1 B and C show typical SSCP analyses of this product under two different electrophoretic conditions. The gel in Fig 7.1B (10%T, 1.5%C, plus glycerol) shows three bands, the central band slightly broader than the others suggesting that it may be a doublet. Fig 7.1 C shows the same samples run on a gel with different bisacrylamide composition (12%T and 2 %C glycerol omitted). In this gel the bands are more widely separated and more sharply resolved. The doublet is resolved into two bands so that four bands of relatively equal intensities, with the third band slightly weaker, are seen. A four-banded pattern suggests that both the forward and reverse strands of DNA have two stable confirmations under these

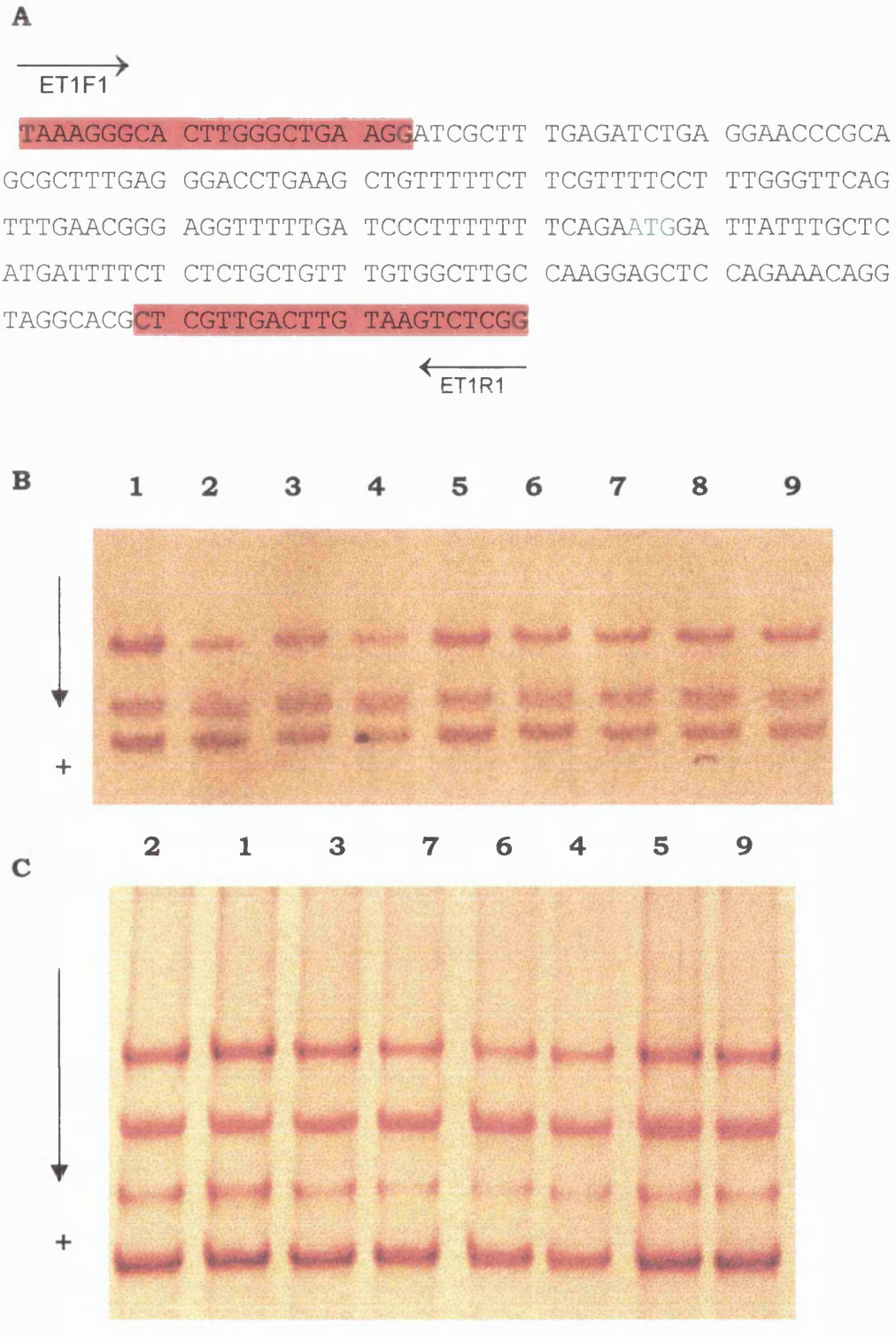

Figure 7.1 SSCP analysis of ET1 exon 1. A-the sequence amplified, the primers are highlighted in red and the translation initiation codon is marked in green. B-SSCP gel: 10%T 1.5% C, plus 5% glycerol, C-SSCP gel: 12%T 2% C. Samples were run for 17hours at 170 volts on both gels.

conditions. DNA from a total of 57 individuals was analysed using the conditions shown in Fig 7.1C and no variants were observed.

Fig. 7.2 A shows the sequence of ET1 exon 2 PCR product and Fig. 7.2 B and C typical SSCP analyses. Both gels, which differ only in their bisacrylamide composition (12%T, 2 %C and 10%T, 1.5%C respectively) show similar banding patterns comprising two pairs of bands. The gel with higher cross-linker composition appears to give slightly better resolution (Fig 7.2B). As for exon 1, the four-banded pattern seen here suggests that each strand of DNA has two stable confirmations under these conditions. In total 50 individuals were analysed and no polymorphism was identified.

Fig. 7.3 A shows the sequence of ET1 exon 3. The gel in Fig. 7.3 B shows three bands, the central band is broader and more intense than the outer two, Fig 7.3 C shows the same samples run on a gel which is the same composition as B except 5% glycerol has been omitted from the gel. In this case the bands are much more sharply resolved and four bands are apparent. This suggests that each DNA strand has two stable conformations, the higher mobility set of bands is more intense than the slower two suggesting that these conformations are relatively favoured. Samples 5 and 7 in Fig 7.3 B show an unusual pattern, the bands are in the same relative positions but differ in intensity. This variation is not typical of a genuine variant pattern and indeed re-analysis of the same samples using the same conditions failed to replicate this result (not shown).

A

ET1F2 →

TTTGAGGAG ACATCCCCCA CTGACCTGCT CTTTCTCTCC CCAGCAGTCT
TAGGCGCTGA GCTCAGCGCG GTGGGTGAGA ACGGCGGGGA GAAACCCACT
CCCAGTCCAC CCTGGCGGCT CCGCCGGTCC AAGCGCTGCT CCTGCTCGTC
CCTGATGGAT AAAGAGTGTG TCTACTTCTG CCACCTGGAC ATCATTTGGG
TCAACACTCC CGAGTAAGTC TCTAGAGGGC ATTGTAACCC TATTCATTCA
TTAGCGCTGG CTCCAC

← ET1R2

B

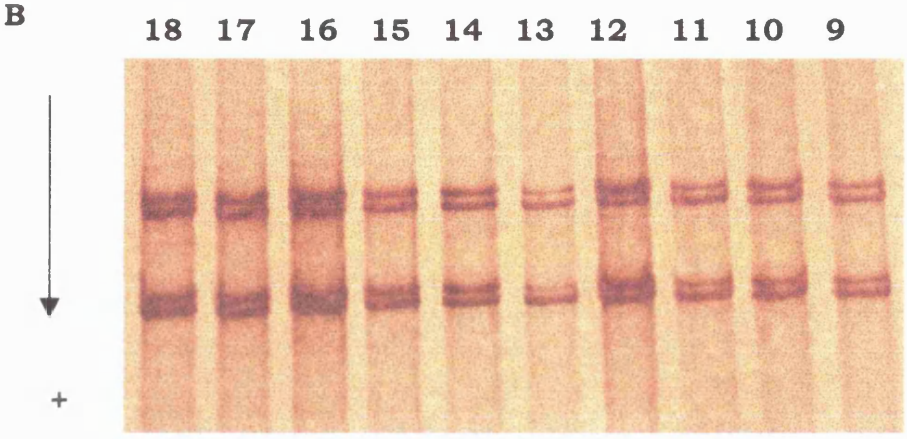

C

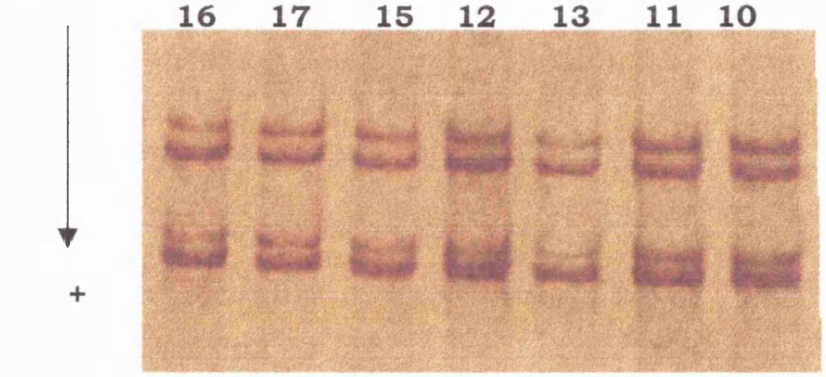

Figure 7.2 SSCP analysis of ET1 exon 2. A- the sequence PCR amplified, the primers are highlighted in red, B-SSCP gel 12.5% T 2% C, C- SSCP gel 10% T 1.5%C. Samples were run for 4 hours at 350 volts on both gels.

A

ET1F3 →

GGAAT AGGTGTGTCC ATGTGTCATT TTAAAGACTA TTAATTACAC
TAATATAGTT TCTTTCTCTC TTTGGATAAT AGGCACGTTG TTCCGTATGG
ACTTGGAAGC CCTAGGTCCA AGAGAGCCTT GGAGAATTTA CTTCCCACAA
AGGCAACAGA CCGTGAGAAT AGATGCCAAT GTGCTAGCCA AAAAGACAAG
AAGTGCTGGA ATTTTTGCCA AGCAGGAAAA GAACTCAGGT GAGCAGAAAC
ACCTTTGCTT TTCAATCAGT TTAACAGCCT CCTGAACTCC TTCCTATCA

← ET1R3

B

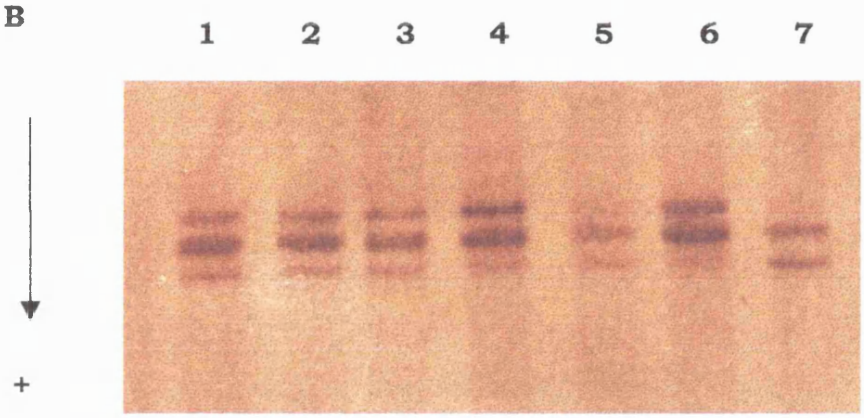

C

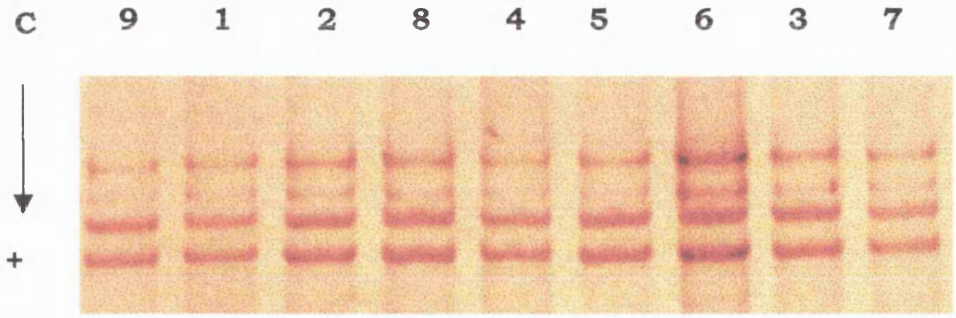

Figure 7.3 SSCP analysis of ET1 exon 3, A-sequence amplified, the primers used are highlighted in red, B-SSCP gel 10% T 1.5% C plus 5% glycerol, C-SSCP gel 12% T 2% C. Samples on both gels were run for 17 hours at 170 volts.

This kind of result sometimes occurs if there is unequal loading of the samples and in the gel shown samples 5 and 7 seem to be rather weak compared to the other samples. PCR products from a total of 53 individuals were analysed using the conditions shown in C and no variants were found.

Fig. 7.4 shows the analysis of exon 4. The denatured DNA resolved into a four-banded pattern in which the bands with the greatest and least mobilities were well resolved and the intermediate bands less resolved. In some instances the intermediate bands appear variable in intensity, e.g. compare samples 10, 15, 16 and 17 on gel B. This variability was not consistent on re-analysis by SSCP with running time extended from four hours to 19 hours (Fig 7.4C). Nevertheless in order to ensure no sequence variation was overlooked samples 10, 15, 16 and 17 on gel B were sequenced and no sequence differences found. The observed variation in banding pattern might suggest that two of the DNA conformations are highly similar and interchangeable. It might be possible to identify electrophoretic conditions that may help to stabilise the conformations, perhaps by altering the pH or cross linker composition (Kukita et al 1997). In total 58 individuals were analysed and no polymorphisms were observed.

Fig. 7.5 shows the analysis of exon 5, B shows a typical SSCP analysis of the exon 5 PCR product; five samples (6, 7, 9 10 and 11) show three-banded patterns while five others (2, 3, 4, 5 and 8) show

A

ET1F4 →

CTATCAT GGTACTGCCT TCCTGTTTTA GAGAGACTAA CAGAGACATT
GAAAGTCAGG GTAAAGCTGA ATATAACATT GCTGAAATGT TTTTCCTTGT
GTATTTTAAC AGGGCTGAAG ACATTATGGA GAAAGACTGG AATAATCATA
AGAAAGGAAA AGACTGTTCC AAGCTTGGGA AAAAGTGTAT TTATCAGCAG
TTAGTGAGAG GAAGAAAAAT CAGAAGAAGT TCAGAGGAAC ACCTAAGACA
AACCAGGTAA GAGGGAAGGA AGAAAAATTA GGTAAGAGGT TCACAAGAAC
AACTAGCCCC AGTCAGTGAT GCCAGCAGCC T

← ET1R4

B

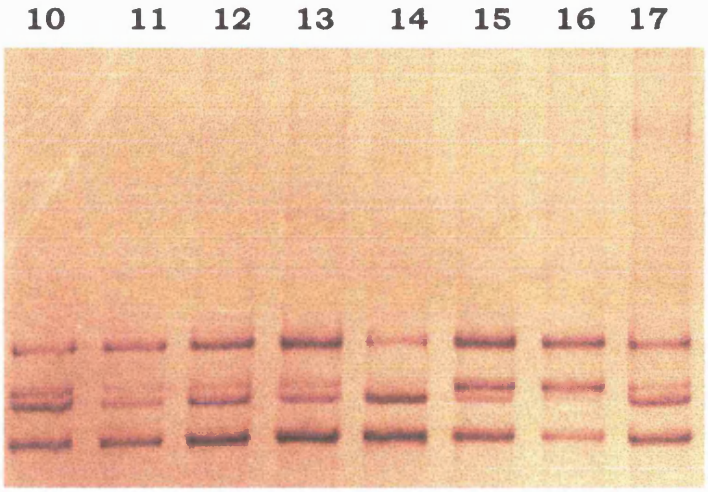

C

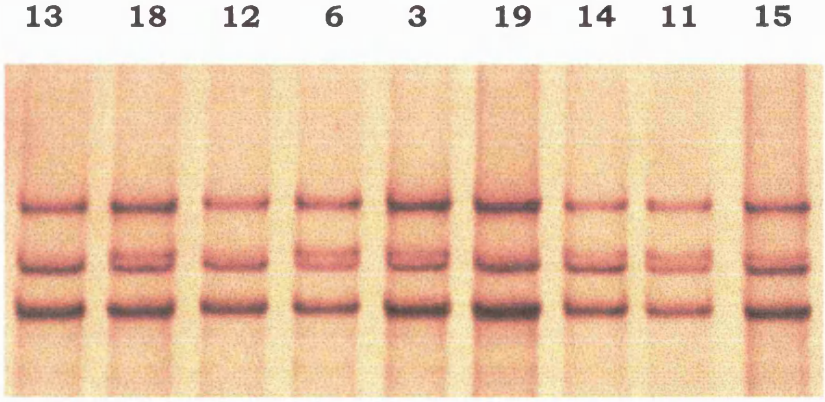

Figure 7.4 SSCP analysis of ET1 exon 4. A-the sequence amplified, the primers used are highlighted in red, B-SSCP gel with bisacrylamide composition: 12% T 2% C, with the samples run for 4 hours at 350 volts. C-samples run on an SSCP gel with the same composition as in B but electrophoresed for longer period of time; 17 hours at 190 volts.

A

ET1F5 →

AAAGTT CACAACCAGA TTCAGGTTTT GTTTGTGCCA GATTCTAATT
TTACATGTTT CTTTTGCCAA AGGGTGATTT TTTTAAAATA ACATTTGTTT
TCTCTTATCT TGCTTTATTA GGTCGGAGAC CATGAGAAAC AGCGTCAAAT
CATCTTTTCA TGATCCCAAG CTGAAAGGCA AGCCCTCCAG AGAGCGTTAT
GTGACCCACA ACCGAGCACA TTGGTGACAG ACCTTCGGGG CCTGTCTGAA
GCCATAGCCT CCACGGAGAG CCCTGTGGCC GACTCTGCAC TCTCCACCCT
GGCTGGGATC AGAGCAGGAG CATCCTCTGC TGGTTCCTGA CTGGCAAAGG
ACCAGCGTCC TCGTTCAAAA CATTCCAAGA AAGGTTAAGG AGTTCCC

← ET1R5

B

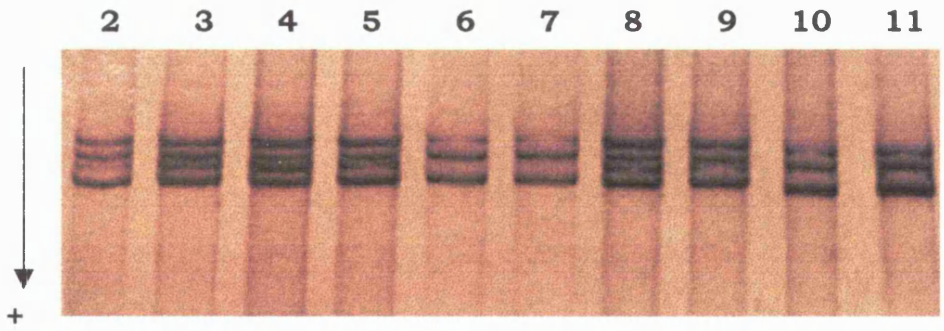

Figure 7.5 Analysis of ET1 exon 5. A-the sequence amplified, the primers are highlighted in red, and the sequence shown in Fig 7.6C is highlighted in yellow. The sequence variant is underlined in blue and the translation stop codon is written in red. B-SSCP gel 12% T, 2% C, run for 4 hours at 350 volts

four-banded patterns. Two of each type were selected for sequence analysis. This showed that each sample with a four-banded pattern was heterozygous for a G to T change at nucleotide position 862 (Fig 7.5C – the sequence is highlighted in yellow in Fig 7.5A), this is the same as that found by Cambien et al (1999). The three-banded samples were homozygous for the published nucleotide sequence (G at nt. 862). The G 862 T variant causes an amino acid change Lys to Asn at residue 198 (Fig 7.5C) thereby exchanging a positively charged amino acid (lysine) with a neutral amino acid (asparagine).

The base change also leads to the loss of a Cac 8I restriction enzyme site the published sequence (G) has a Cac 8I site and the variant (T) does not. Therefore it was possible to genotype the remainder of the face-scanned panel by direct restriction enzyme digest of the PCR product (Fig 7.5D). Samples homozygous for the G862 allele (1, 4, 7 12, 13 and 14 in Fig 7.5D) showed two bands on the digest (176 bp and 217 bp in size) and individuals homozygous for the T862 allele showed one uncut band of 393 bp (not shown). Heterozygous individuals therefore showed three bands on a restriction digest (samples 2, 3, 5, 6, 8, 9, 10 and 11 on Fig 7.5D). In total 78 European subjects were genotyped, the allele frequencies were estimated as 0.80 for the G862 allele and 0.20 for the variant T862 allele (Table 7.3). Allele frequencies were also calculated in a small population samples of Japanese (n=42) and African (n=26)

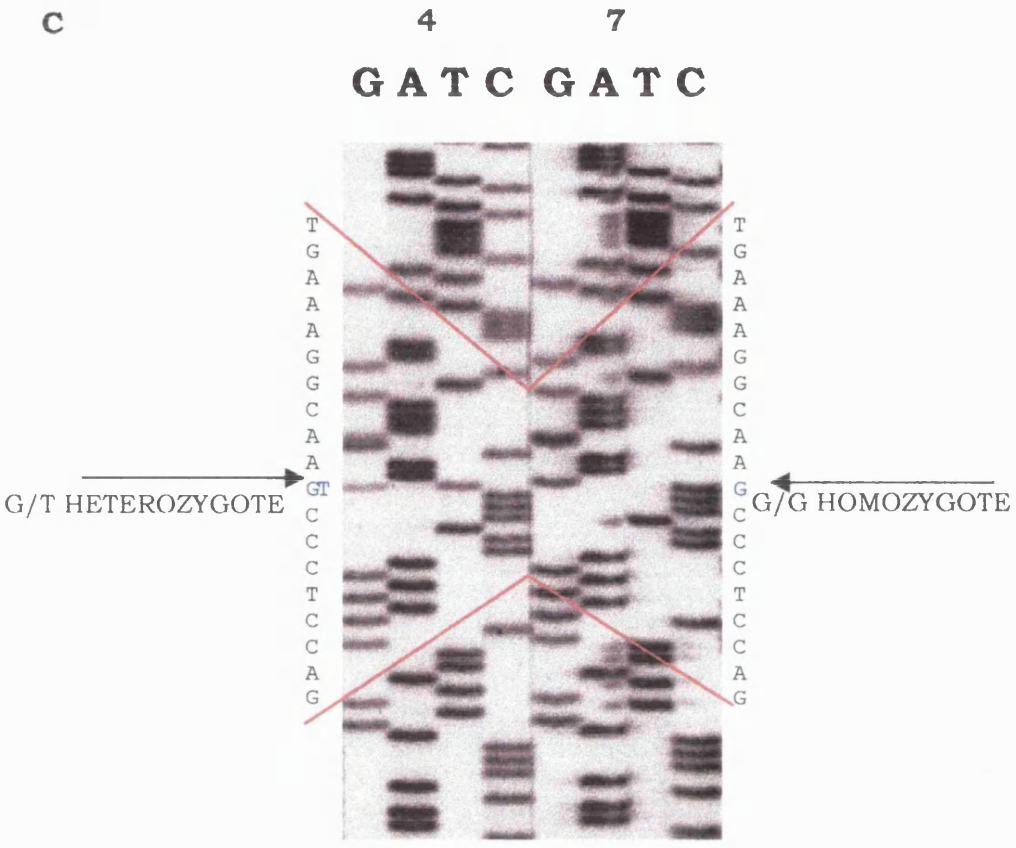

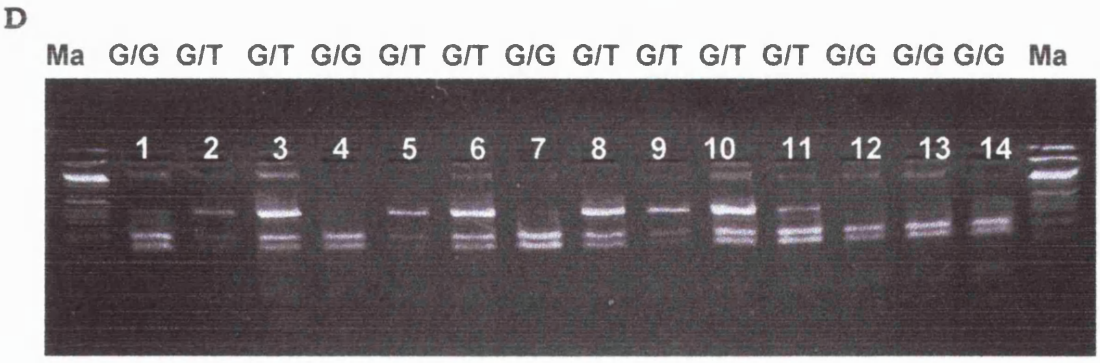

Figure 7.5 C-part of the exon 5 sequence from two samples (4 and 7) shown to have different SSCP patterns in 7.5B, sample 4 is heterozygous for a G/T polymorphism and sample 7 is homozygous for the G allele The sequence shown is highlighted on fig 7.5A. D-the T862 variant loses a Cac 8I restriction enzyme site, this enabled genotyping through restriction enzyme digest.

ET1 exon 5 G862T variant	European	Japanese	African
samples genotyped	78	43	28
G/G	49	26	13
G/T	27	15	11
T/T	2	2	4
frequency G allele (95% CI)[1]	0.80 (0.74-0.86)	0.78 (0.69-0.87)	0.66 (0.54-0.78)
frequency T allele (95% CI)	0.20 (0.14-0.26)	0.22 (0.13-0.31)	0.34 (0.22-0.46)
frequency T allele (Irish)*	*0.26*	n/a	n/a
frequency T allele (French)*	*0.22*	n/a	n/a

Table7.3 Genotypes and allele frequencies calculated for the G/T polymorphism in exon 5 of ET1. Genotypes were determined by Cac8I digests of PCR products. *Allele frequencies determined by Tiret et al (1999) in Irish and French populations.

[1] 95% Confidence interval calculated from standard error calculated as:

$1.96\sqrt{\frac{q(1-q)}{N}}$ where q is frequency of the T allele and N is number of alleles counted.

individuals where the frequency of the T862 allele was 0.22 and 0.34 respectively.

A 95% confidence interval (CI) was calculated for each of the observed allele frequencies. It is interesting to note that although the T862 allele was more common in the African sample than in the other two populations' studied (0.34 in African compared to 0.20 and 0.22 in European and Japanese populations respectively) the 95% CI, overlapped in all three population samples. Thus it is possible this difference is due to small population sample or a heterogeneous population. The African group were UK citizens with African ancestry- a very broad grouping. This polymorphism is the same as that described by Tiret et al (1999) and the allele frequencies calculated here are in agreement with this study.

7.3 SSCP analysis of ETRA

Exons two to eight of ETRA were analysed using exactly the same procedures described for ET1. The same range of banding patterns was seen, three and four banded patterns being particularly common. As exon two was relatively large (491 bp) it was divided by PCR amplification in two overlapping fragments. Amplification of the 5' end was carried out using the primers ETA2AF and ETA2AR and yielded a product of 267 bp. The primers ETA2BF and ETA2BR were used to amplify the 3' end and gave a 277bp product. Fig. 7.6 A shows the entire sequence of exon 2 and indicates the position of the primers.

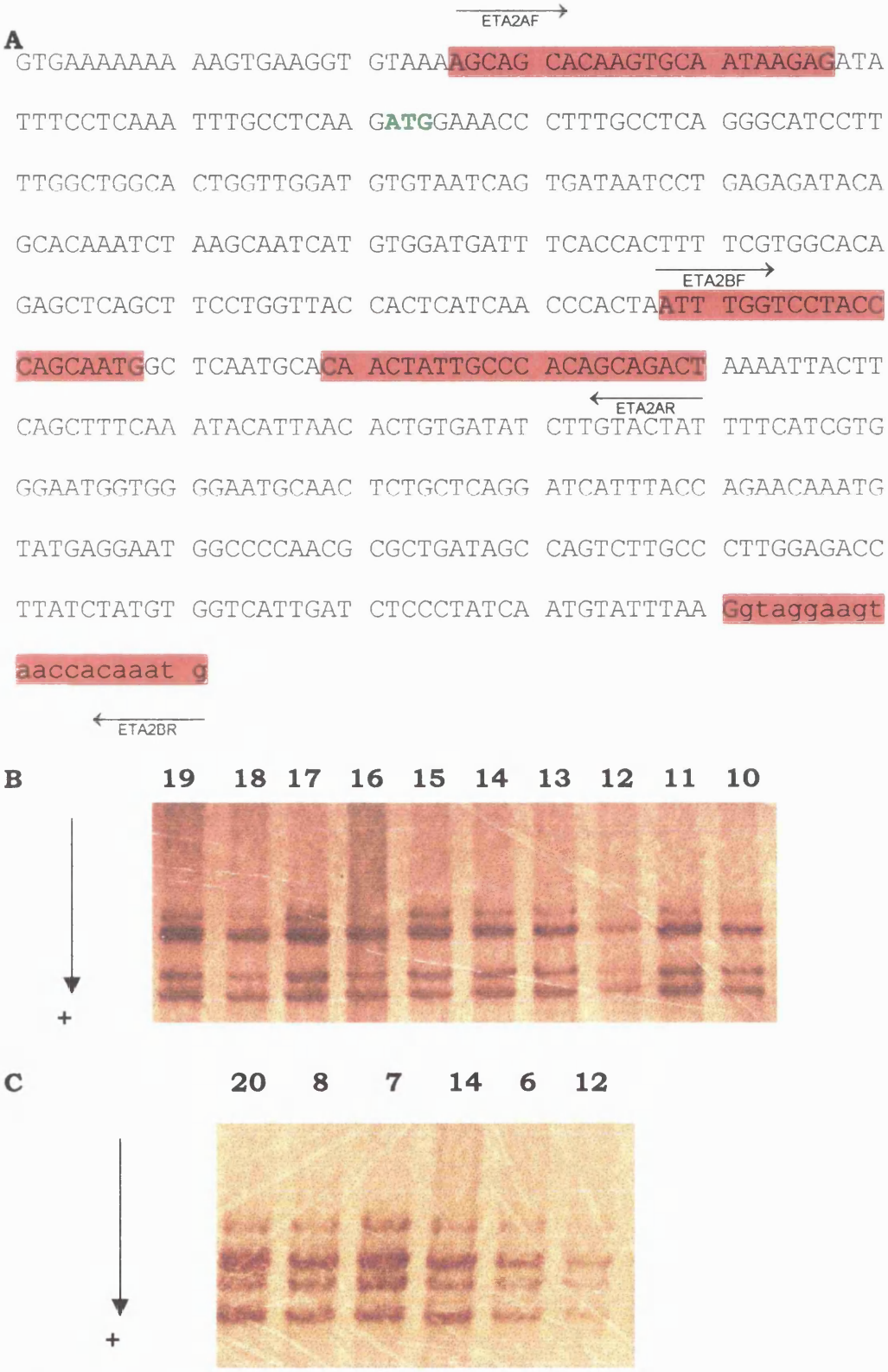

Figure 7.6 SSCP analyses of ETRA exon 2, A-the sequence of exon 2 amplified by two sets of overlapping primers (highlighted in red), the translation initiation codon is typed in green. SSCP gel of 5' exon 2 amplified by primers ETA2AF and ETA2AR, B-12%T 2%C, plus glycerol. C-10%T 1.5%C plus glycerol; both gels were run for 19 hours at 130 volts

Figs 7.6 B and C show typical SSCP analyses using two sets of electrophoretic conditions of the 5' end of exon 2 and D and E the 3' end. Each gel shows four bands indicative of two equally stable conformations for each DNA strand. 44 samples were analysed for exon two and no variants were observed. Similarly SSCP analysis on a panel of samples for exon 3 (n=50); exon 4 (n=38); exon 5 (n=44) and exon 7 (n=50), using electrophoretic conditions which gave the best resolution (exon 3 - 7.7 B, exon 4 - 7.8 C, exon 5 - 7.9 C, exon 7 - 7.10 C), found no variants.

However analysis of exon 6 (Fig 7.11) detected a variant SSCP pattern, in samples 4 and 12. These samples both have a pair of bands of different mobility to that shown by the majority of samples. Samples 3 and 6 show a pattern that appears to comprise a mixture of the two patterns (Fig 7.11B). Sequence analysis of samples 2, 3 and 4 revealed two DNA changes, a C1471T change, and an A1507G change. Sample 4 was homozygous for the T1471 and G1507 alleles and sample 3 was heterozygous (Fig 7.11C). These variants are the same as those identified by Cambien et al (1999), in their study it was shown that the two variant alleles at this locus were in complete association and hence only three genotypes are found. The C 1471 allele is always found with the A 1507 allele and the T 1471 allele is always found with the G 1507 allele. Both variants affect the third nucleotide of a codon and do not cause an amino acid change (histidine 323 and glutamic acid residue 335 remain unchanged).

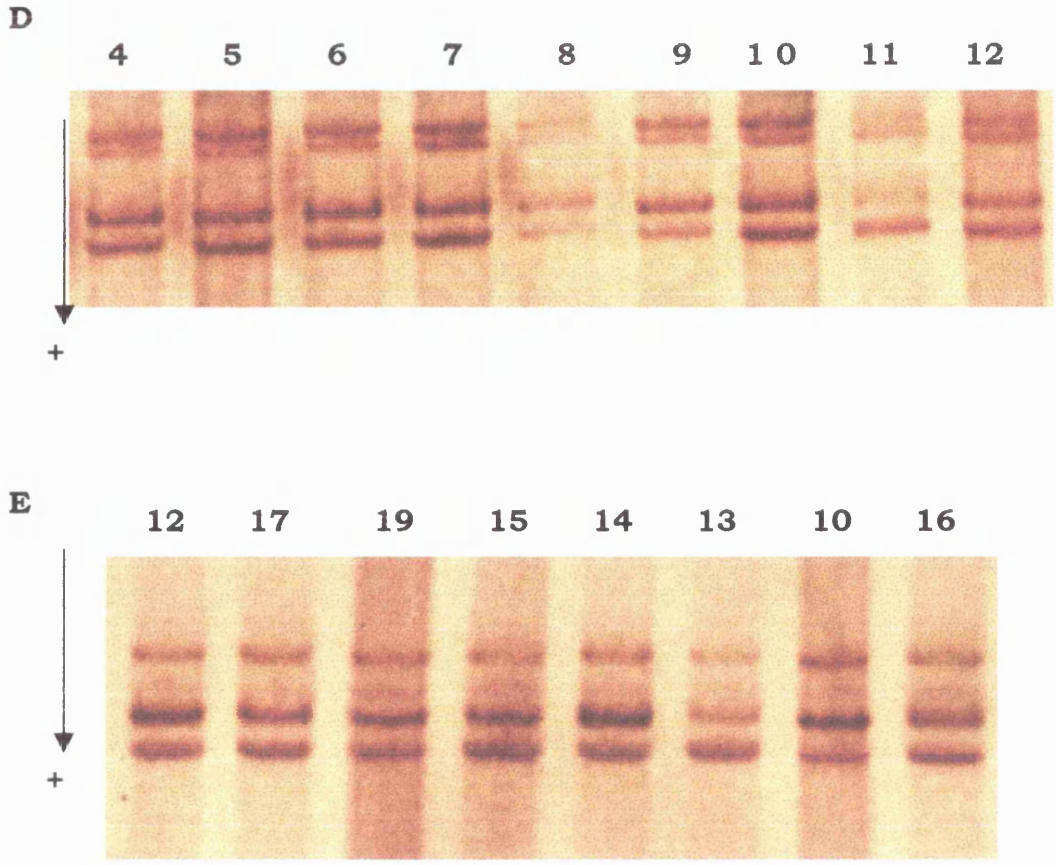

Figure 7.6 SSCP analyses of 3' ETRA exon 2, using the primers ETA2BF and ETA2BR D-12%T 2%C plus glycerol. E-10%T and 1.5%C plus glycerol. Both gels were run for 17.5hrs at 140 volts

A

ETAF3

actgtgtctc cttctttcag CTGCTGGCTG GGCGCTGGCC TTTTGATCAC

AATGACTTTG GCGTATTTCT TTGCAAGCTG TTCCCCTTTT TGCAGAAGTC

CTCGGTGGGG ATCACCGTCC TCAACCTCTG CGCTCTTAGT GTTGACAGgt

aatgtggttc tttccctt

ETAR3

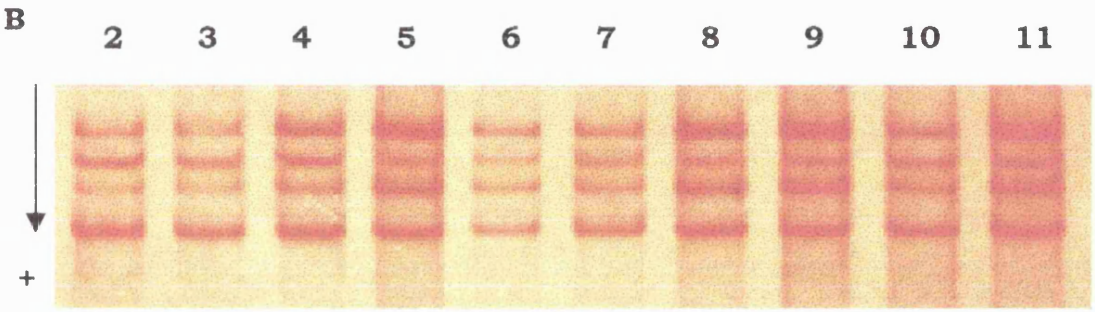

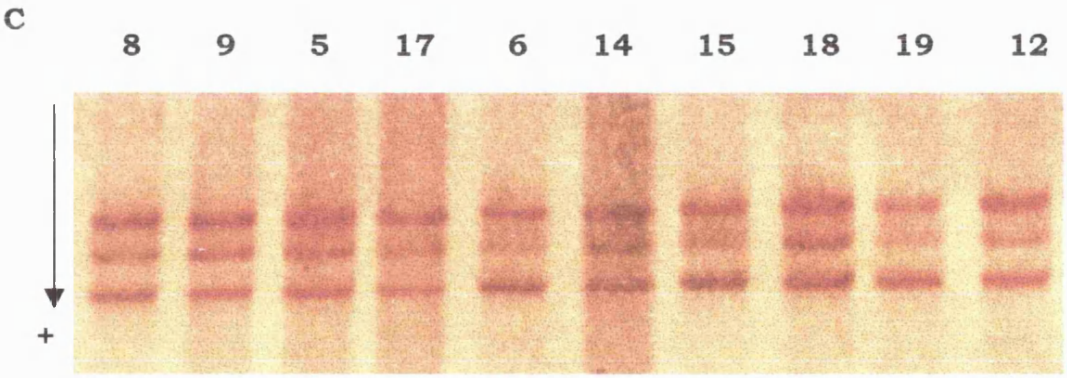

Figure 7.7 SSCP analysis of ETRA exon 3 PCR product, A-the sequence amplified, the primers used are highlighted in red, B- SSCP gel 12%T 2%C, run for 4hrs at 350 volts C-SSCP gel 10%T 1.5%C plus glycerol, run for 4.5hrs at 350 volts.

A

ETA4F →

ttcag GTACAGAGCA GTTGCCTCCT GGAGTCGTGT TCAGGGAATT
GGGATTCCTT TGGTAACTGC CATTGAAATT GTCTCCATCT GGATCCTGTC
CTTTATCCTG GCCATTCCTG AAGCGATTGG CTTCGTCATG GTACCCTTTG
AATATAGGGG TGAACAGCAT AAAACCTGTA TGCTCAATGC CACATCAAAA
TTCATGGAG

← ETA4R

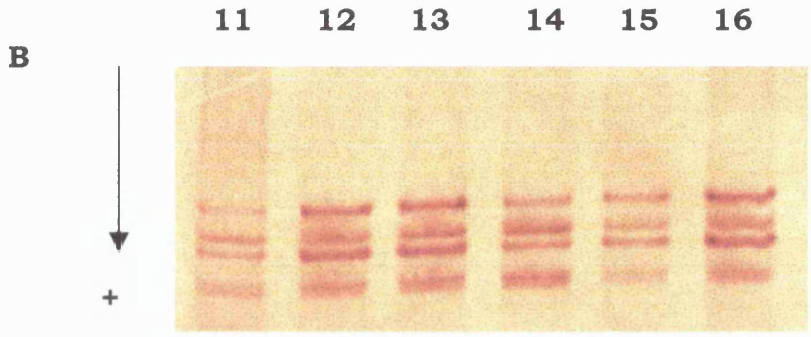

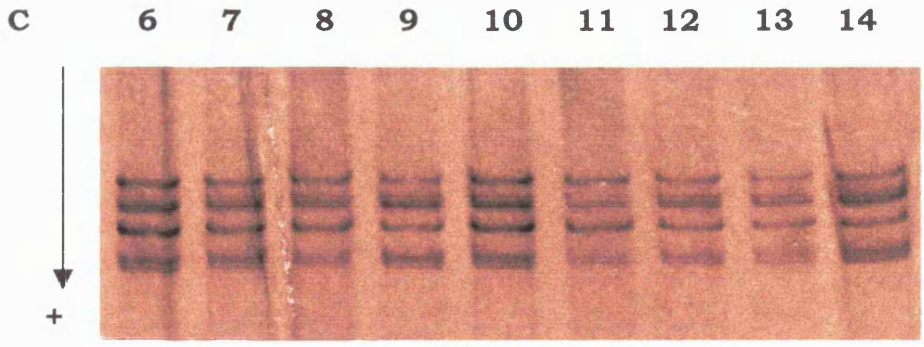

Figure 7.8 SSCP analysis of ETRA exon 4 PCR product A-the sequence of exon 4 amplified by the primers (highlighted in red), B- 12%T 2%C, C- 12%T 2%C plus glycerol. Both gels were run for 4hrs at 350 volts.

A

ETA5F →

t cactttgaag TTCTACCAAG ATGTAAAGGA CTGGTGGCTC

TTCGGGTTCT ATTTCTGTAT GCCCTTGGTG TGCACTGCGA TCTTCTACAC

CCTCATGACT TGTGAGATGT TGAACAGAAG GAATGGCAGC TTGAGAATTG

CCCTCAGTGA ACATCTTAAG CAGgtaaatc ccataacatc atg

← ETA5R

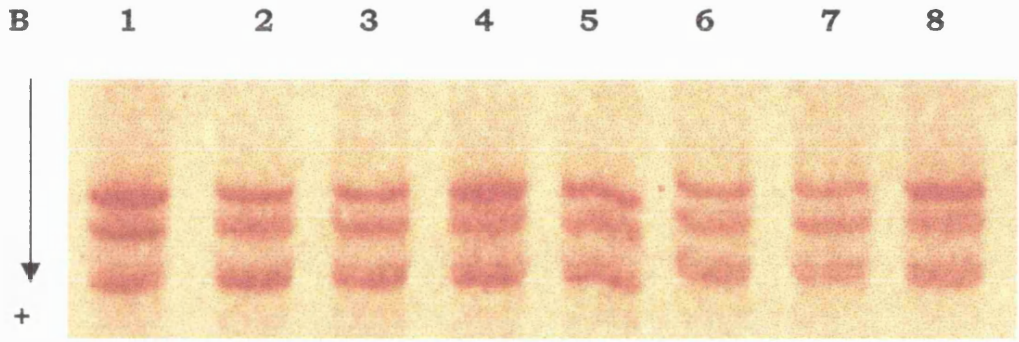

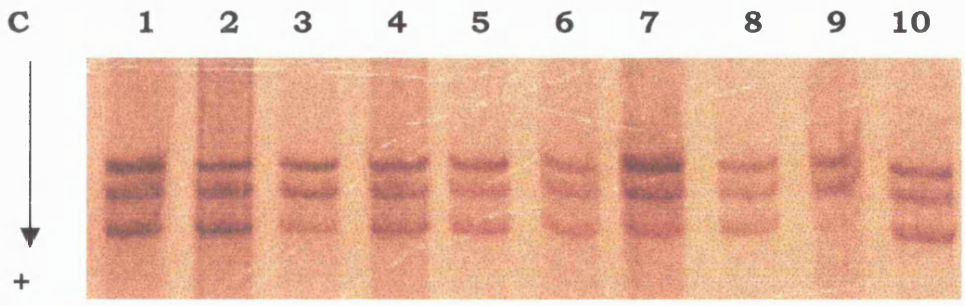

Figure 7.9 SSCP analysis of ETRA exon 5, A- sequence amplified (primers in red), B- 10%T 1.5%C plus glycerol, C- 12%T 2%C, plus glycerol. Both gels were run for 5hrs at 350 volts.

A

ETA7F →

ttgctctag TTTCTTACTG CTCATGGATT ACATCGGTAT TAACTTGGCA

ACCATGAATT CATGTATAAA CCCCATAGCT CTGTATTTTG TGAGCAAGAA

ATTTAAAAAT TGTTTCCAGg taagatgatt tttca

← ETA7R

B

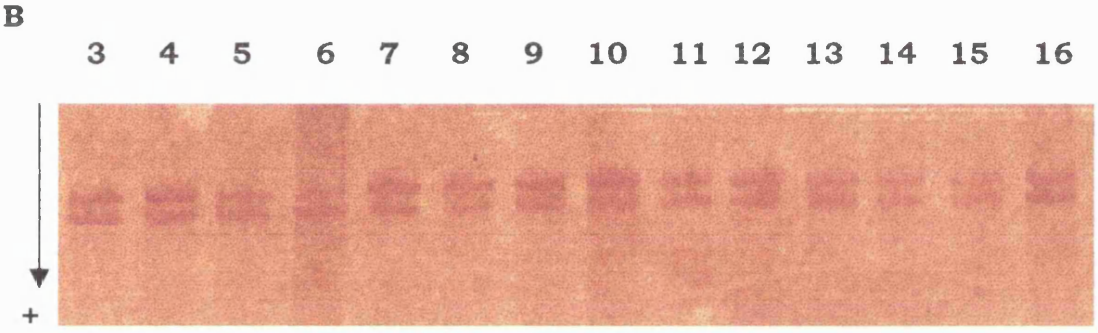

C

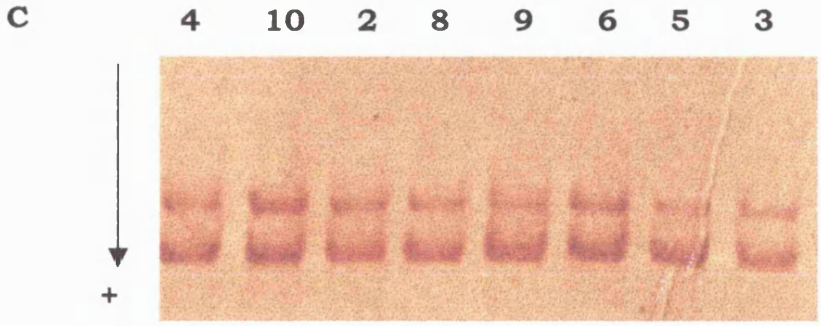

Figure 7.10 SSCP analysis of ETRA exon 7, A-the sequence amplified, the primers used are highlighted in red, B- 12%T 2%C plus glycerol, run for 4hrs at 350 volts. C- 10%T 1.5%C, run for 3hrs at 350 volts.

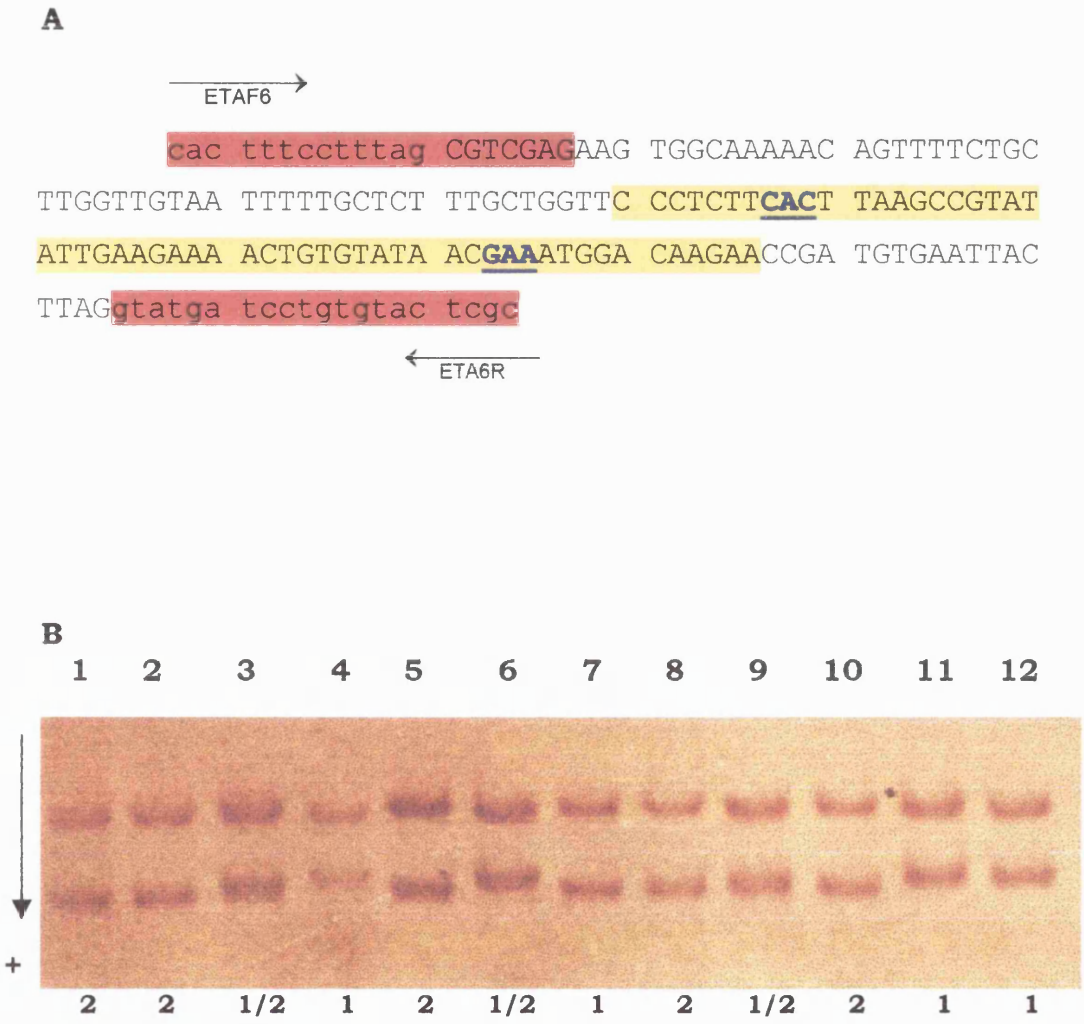

Figure 7.11 Analysis of exon 6 PCR. A-sequence amplified with the primers highlighted in red, the sequence shown in Fig 7.11C is highlighted in yellow. The sequence variants are underlined in blue B- SSCP analysis of exon 6, 12%T 2%C run for 18hrs at 140 volts.

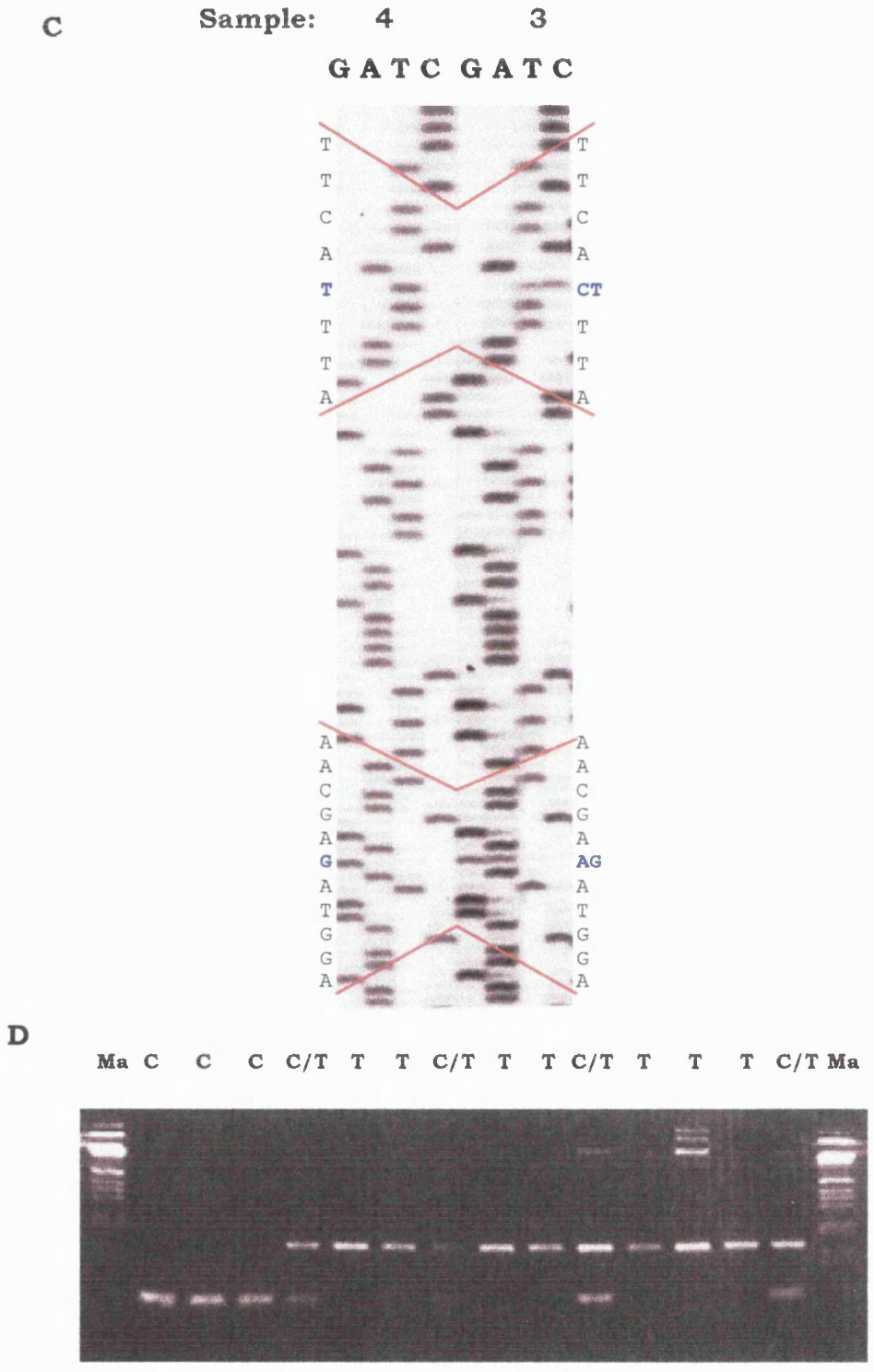

Figure 7.11 analysis of ETRA exon 6, C- sequence across the region containing the C1471T variant and the A1507G variant. Sample 3 is heterozygous and sample 4 is homozygous for both. D- Afl II restriction digest of PCR products showing C/C, C/T and T/T genotypes.

The C1471T variant alters an Afl II restriction enzyme site, the C1471 allele has a site for Afl II where as the T 1471 allele does not. It was possible to genotype the remainder of the panel through restriction enzyme digest (Fig 7.11D). Samples homozygous for the T1471T (and G1507) allele showed one undigested band on the gel. C1471C samples show one broad band, of greater mobility, comprising two bands of approximately 80 base pairs.

Afl II digests were used to genotype 97 European subjects. The T1471 and G1507 allele combination occurred more frequently (0.67) than the C1471 and A1507 allele combination (Table 7.4). Estimated allele frequencies were also calculated in a small population samples of Japanese (n=44) and African (n=26) individuals. A 95% confidence interval (CI) was calculated for the observed allele frequencies and it was found that the European allele frequencies overlapped with the Japanese and African samples, although only slightly in the African sample. However the 95% CI for the Japanese (T1471 =0.75, C1471 = 0.25) and African (T1471=0.48 and C1471 = 0.52) allele frequencies did not overlap. Overall the African sample gave a much higher frequency of the C1471 allele than the other two populations. The allele frequencies found in French (C1471 = 0.27) and Irish (C1471 = 0.22) populations in an independent study (Nicaud et al 1999) are slightly lower but comparable to those found in the European population here. This suggests that the higher frequency of the C

ETRA exon 6 C1471T variant	European	Japanese	African
samples genotyped	97	44	26
T/T	45	25	3
C/T	40	16	19
C/C	12	3	4
frequency T allele (95% CI) [1]	0.67 (0.60-0.74)	0.75 (0.66-0.84)	0.48 (0.35-0.62)
frequency C allele (95% CI)	0.33 (0.26-0.40)	0.25 (0.16-0.34)	0.52 (0.39-0.66)
frequency C allele (Irish)*	*0.22*	n/a	n/a
frequency C allele (French)*	*0.27*	n/a	n/a

Table 7.4 Allele frequencies calculated for the C1471T variant in exon 6 of ETRA. 97 European Caucasian subjects were genotyped through Afl II restriction enzyme digest. Small populations of subjects of Japanese and African origin were also studied and allele frequencies with the 95% confidence interval were calculated, the African sample showed higher frequency of the C allele than the other two populations. *Allele frequencies in French and Irish populations published by Nicaud et al (1999)

[1] 95% Confidence interval calculated from standard error calculated as $1.96\sqrt{\frac{q(1-q)}{N}}$ where q is the frequency of the T allele and N is number of alleles counted

allele in the African population may be genuine and further samples should be analysed to confirm this interesting observation.

Fig. 7.12A shows the sequence of the exon 8 PCR product. Analysis of exon 8 identified three types of SSCP banding pattern (Fig 7.13C). These banding patterns were interpreted as representing a heterozygous and two different homozygous patterns determined by two alleles. In Fig 7.13C sample 11 is one type of homozygote, samples 13 and 15 are the other type of homozygote and samples 16 and 17 are heterozygotes (Fig 7.13 C). These samples were sequenced which revealed a C 1856 G variant; sample 15 was homozygous for the C allele and sample 11 was homozygous for the G allele (not shown). This variable site was 70 basepairs downstream from the translation termination codon and the same polymorphism was identified by Cambien et al (1999).

The C1856G polymorphism caused a Tsp45I restriction enzyme to be altered; the C1856 allele has a Tsp45I RE site where as the G1856 allele does not. Therefore samples homozygous for the G1856 allele showed one, undigested band on the gel of approximately 290bp and individuals homozygous for the C1856 allele show two bands; one of 220bp size one of 70bp (Fig 7.12D).

In total 89 European subjects were genotyped and the allele frequencies were estimated (Table 7.5). The G1856 allele was found more frequently than the C1856 allele (G1856=0.56, C1856=0.44). Estimated allele frequencies were also calculated in a small

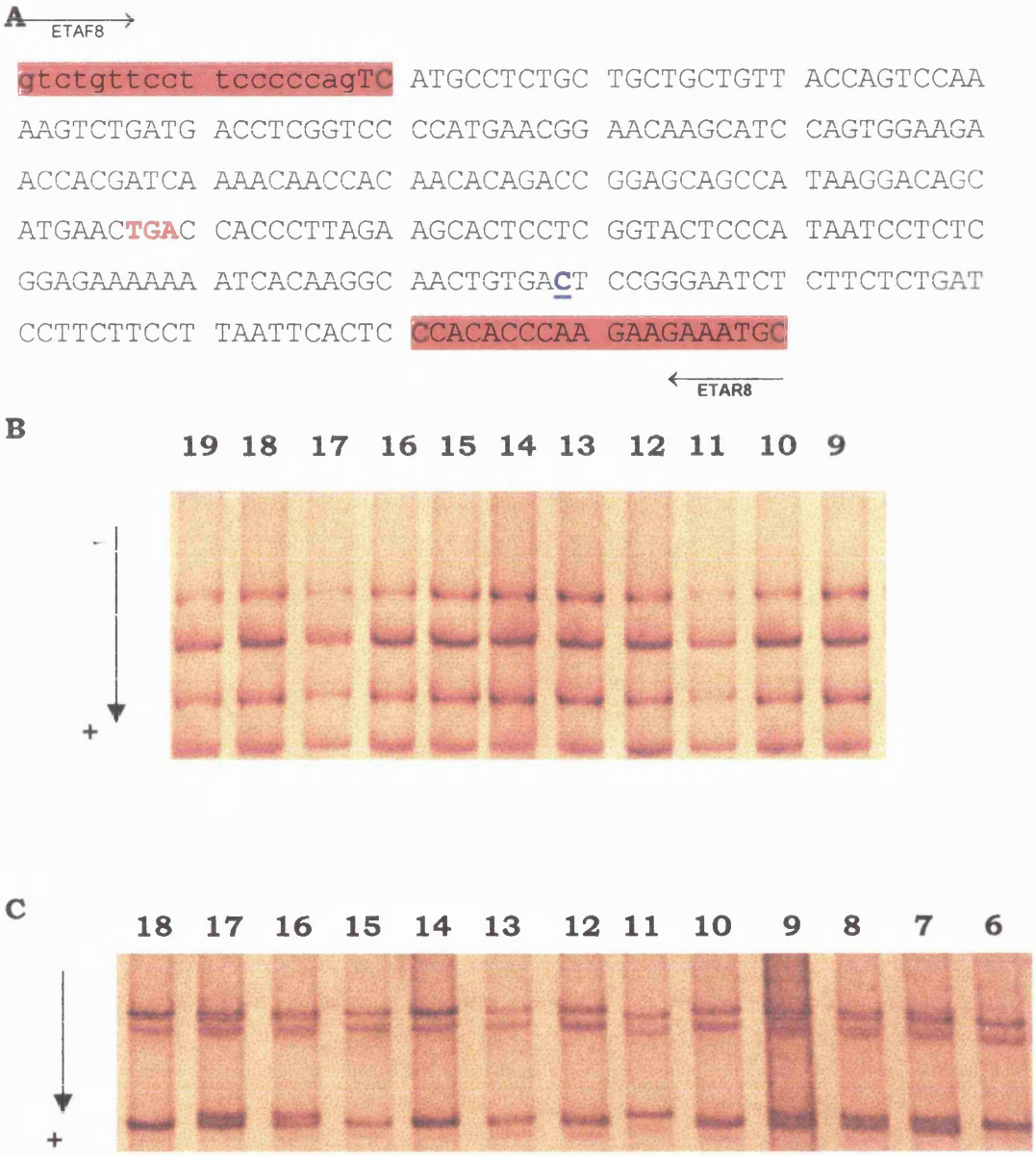

Figure 7.12 Analysis of the ETRA exon 8 PCR product. A-the primers are highlighted in red and the variant is underlined in blue. B-A typical SSCP gel for the exon 8 PCR product, 12%T 2%C run for 18hrs at 180 volts. C-SSCP gel 12%T 2%C plus glycerol run for 18hrs at160 volts.

D

Ma G/G G/G G/G C/C C/C - G/C G/C G/C G/C C/C G/G G/G G/G Ma

Figure 7.12 E -Tsp45I restriction enzyme digest of the exon 8 PCR product, the G1856 allele does not have the restriction site.

ETRA exon 8 C 1856 G variant	European	Japanese	African
samples genotyped	89	44	27
G/G	31	7	2
G/C	37	21	12
C/C	21	16	13
frequency G allele (95% CI) [1]	0.56 (0.49-0.63)	0.40 (0.30-0.50)	0.26 (0.14-0.0.38)
frequency C allele (95% CI)	0.44 (0.37-0.51)	0.60 (0.50-0.70)	0.74 (0.62-0.86)
frequency C allele (Irish)*	0.39	n/a	n/a
frequency C allele (French)*	0.40	n/a	n/a

Table7.5 Genotypes and allele frequencies calculated for the C1856G variant in exon 8 of ETRA. 89 European Caucasian subjects were genotyped through Tsp45I restriction enzyme digest. Small populations of Japanese and African origin were also studied and allele frequencies with the 95% confidence interval calculated. *Allele frequencies generated by a previous study (Nicaud et al 1999).

[1] 95% Confidence interval calculated from standard error calculated as $1.96\sqrt{\frac{q(1-q)}{N}}$ where q is frequency of the T allele and N is number of alleles counted

population samples of Japanese (n=44) and African (n=26) individuals. A 95% confidence interval (CI) was calculated for the observed allele frequencies in each population sample. With the 95% CI the European and Japanese frequencies (G1856=0.40) overlapped and the Japanese and African frequencies (G1876=0.26) overlapped. However, the 95%CI for the African and European frequencies did not overlap and overall the C allele was much more frequent in the African sample (C1876=0.74) compared to the other two populations (C1876 =0.44 and 0.66 in European and Japanese respectively). The C1876 allele frequency was found to be 0.40 and 0.39 in French and Irish populations respectively in a previous study (Nicaud et al 1999), comparable to frequencies found here in the European sample. This also suggests that a significant difference in the frequency of the G1876C polymorphism exists with respect to ethnic origin. Larger African and Japanese population samples should be studied to confirm this observation.

7.4 Summary

Exons one to five of ET1 and two to eight of ETRA were PCR amplified, the products were analysed for variants using SSCP analysis. One polymorphism was found in exon 5 of ET1 and three polymorphisms were found in ETRA, two in exon 6 that were in complete association and one in the 3' un-translated sequence of exon 8 (Table 7.6). All of these variants were identical to those found

Gene		***Total***	***1/1***	***1/2***	***2/2***
ET-1 exon 5 **G862T**			G/G	G/T	T/T
Males	39	78	49	27	2
Females	39				

Allele frequency: G= 0.80; T = 0.20

ETA exon 6 **C1471T**			T/T	T/C	C/C
Males	51	97	45	40	12
Females	46				

Allele frequency: T= 0.67; C = 0.33

ETA exon 8 **C1856G**			G/G	G/C	C/C
Males	45	89	31	37	21
Females	44				

Allele frequency: G= 0.56; C = 0.44

Table 7.6 Summary of allele frequencies of one polymorphism in ET1 and two polymorphisms in ETRA. Where DNA had been collected in either blood or saliva form from scanned unrelated subjects of Caucasian origin these subjects were scored for the chin cleft trait and used to carry out a preliminary association analysis between genotype and phenotype, the results of which are displayed in Table 7.7.

in a large independent study investigating cardiac pathology (Cambien et al 1999).

70-100 European subjects were typed for these three variants using the restriction enzymes Cac8I, Afl II and Tsp45. The other reported polymorphisms are all in non-translated sequence and so not identified in this study. The genotype data generated in this analysis is used in the next section in a preliminary association study in conjunction with the phenotype data generated from Chapters 4 and 5.

7.5 ET1 & ETRA and mandibular phenotypes

7.5.1 Chin cleft

The variants ET-1 G862T, ETRA C1471T and ETRA C1856G were genotyped in individuals analysed for chin cleft type. The Chi-square statistic was used to investigate whether the phenotype frequencies varied significantly in the different genotype categories; subjects heterozygous and homozygous for the rare alleles were grouped together to form a 2 x 3 contingency table with 2 degrees of freedom. There was no significant difference between observed and calculated expected frequencies (ET-1 G862T; $\chi^2 = 4.2$, p= 0.12; 2 d.f, Table 7.7 A; ETRA C1471T; $\chi^2 = 6.85$, p=0.14, 2 d.f. Table 7.7 B; ETRA C1856G; $\chi^2 = 3.56$, p=0.17, 2 d.f Table 7.7 C), but the 2x2 analyses (Table 7.7D-F) suggested there may be a significant association between the ET1 exon 5 G862T genotype and the chin cleft phenotype. However, this must be treated cautiously as the frequency of the rarer allele is quite low and so further analyses must be carried out to see if this trend persists.

Males and females were also analysed separately but neither sex showed association between phenotype and genotype (ET-1

	STRONG		WEAK		NO CLEFT	
A **ET1 exon 5 G862T**	Obs.	Exp.	Obs.	Exp.	Obs.	Exp.
G/G	9	8.7	29	25.4	9	12.9
G/T & T/T	5	5.3	12	15.6	12	8.1
B **ETRA exon 6 C1471T**	Obs.	Exp.	Obs.	Exp.	Obs.	Exp.
T/T	5	7.6	29	24.6	10	11.8
T/C & C/C	11	8.4	23	27.4	15	13.2
C **ETRA exon 8 C1856G**	Obs.	Exp.	Obs.	Exp.	Obs.	Exp.
G/G	8	5	16	17.1	7	8.9
G/C & C/C	6	9.0	32	31.0	18	16.0

D **ET1 exon 5 G862T**

	S	W
G	92	27
T	18	15
Fishers: p=0.01		

E **ETRA exon 6 C1471T**

	S	W
T	50	22
C	86	28
Fishers: p=0.23		

F **ETRA exon 8 C1856G**

	S	W
G	73	26
C	51	24
Fishers: p=0.25		

Table 7.7 χ^2 analysis (2d.f) of the distribution of ET-1 G862T, ETRA C1471T and ETRA C1856G alleles amongst individuals whose chin cleft type has been determined. Individuals carrying one or two copies of the rarer allele were grouped together because of low numbers.

A 2 x 2 analysis was carried out of marker allele frequencies versus cleft (i.e. strong and weak grouped together) and no cleft. Fishers exact test was used to test for significant associations.

G862T: males (n=36); χ^2=0.9, p=0.64, 2 d.f and females (n=38); χ^2=2.55, p=0.28, 2 d.f; ETRA C1471T; males (n=47); χ^2 = 1.16, p=0.56, 2 d.f and females (n=46); χ^2=0.27, p=0.87, 2 d.f; ETRA C1856G: males (n=41); χ^2=9.1, p=0.06, 2 d.f and females (n=42); χ^2=4.18, p=0.38, 2 d.f).

7.5.2 Jaw protrusion

Similarly subjects were scored for jaw protrusion and genotyped for the ET-1 G862T, ETRA C1471T and ETRA C1856G variants. A T-test was used to investigate whether the mean jaw protrusion value was significantly different with respect to allele variation at each of the variant loci. Individuals homozygous for the rare allele and heterozygotes were grouped together and tested against subjects homozygous for the common allele. A two-tail T-test did not find any significant difference in mean jaw protrusion values when comparing the two genotype groups (ET-1 G862T; n=80 p=0.25, ETRA C1471T; n=96 p=0.72 and ETRA C1856G; n=89 p=0.29). The two sexes were also analysed separately, there was no significant difference in mean values in either sex for any of the loci (ET-1 G862T; males p=0.86, females p=0.40, ETRA C1471T; males p=0.89 females p=0.34, and ETRA C1856G males p=0.37 females p=0.31).

CHAPTER 8

Discussion

This thesis describes a pilot study, which attempted to dissect the observed variability in human facial features, with the long-term aim of establishing a connection between facial appearance and genetic constitution. This project was deemed to be timely for two major reasons: the first was the rapid progress made in sequencing the human genome, which has provided a massive increase in the available resources to identify and analyse genome regions of interest as well as candidate genes; the second was the technological advancements made, in generating and processing 3D surface data that enables rapid and accurate collection of data from the whole face.

Although a direct genotype-phenotype link was not established in this study, this by no means suggests that this is an unattainable aim. On the contrary, the work presented here has made significant progress towards reaching this goal through producing accurate and reproducible phenotype classifications suitable for genetic analysis. Use of the optical surface scanners coupled with the surface segmentation software enabled a full survey of the face to be carried out and this initial work identified two polymorphic features which appear to behave as Mendelian traits. This work has also illustrated the feasibility of the process of choosing and analysing candidate

'face' genes for molecular studies to identify polymorphisms and to carry out association studies with facial traits.

Overall, the results generated in this study are exciting for two reasons. First, two facial traits, which clearly segregate in pedigrees, were identified. These are amenable to linkage analysis and, with resources, such as good quality DNA from complete families, could lead to the identification of appropriate chromosomal regions of interest and perhaps to gene identification. There was not sufficient DNA data collected from the complete families in this study in order for linkage analysis to be feasible (Table 4.1) e.g. DNA was only available from 10 complete families; furthermore this was a mixture of blood and saliva samples and hence there was considerable variation in the amount and quality of extracted DNA. The molecular study illustrates the feasibility of screening candidate genes once a candidate region can be identified. Second if these two features follow simple Mendelian patterns of inheritance then it is possible other features could also be relatively simple and the understanding of the associated facial phenotypes and their modes of inheritance could reduce the apparent complexity of the face.

This chapter discusses this project in a general framework. All aspects are considered starting with the technicalities and logistics of the study, including practical considerations on data collection, equipment and reproducibility. The data generated is then discussed with particular relevance to analysis and the features classified and how this approach could be exploited in the future. The genetic aspects of these features is also discussed in the context of gene identification and finally a general appraisal is given of the potential contribution of this work to future attempts to understand the genetic basis of normal facial variation.

A large study of 'normal' variation relies heavily on volunteer participation. The novel concept of the project, coupled with the visual appeal of the 3D data, led to extremely good subject recruitment and over 1000 volunteers were scanned within the three-year period. Two types of optical surface scanner were used to collect the data generated in this study; a fixed system housed in UCL and a portable HLS system. Both scanners were relatively straightforward in terms of their operation. It was easy to train individuals to use either of the scanners and generate data that could not be differentiated from those data generated by other operators. The data generated by the two different scanners was assessed and found to be of comparably high quality.

Although both scanners produced accurate 3D representation of the majority of the facial surface, neither scanner was able to collect adequate data from the very convoluted surface of the ear. This complex shape is very variable over relatively short distances and the occluded surfaces proved to be too difficult to capture. A large amount of ear data (not shown) was collected using a digital camera in an attempt to overcome this problem. However, the inherent complexity of the ear rendered the 2D data generated extremely variable and difficult to reproduce. In some cases for example, it was impossible to match the left and right ears of the same subject let alone identify features suitable for classification.

The fixed and the hand held scanners both produced accurate structural representation of the face with equally high quality. If the project was to start again then the HLS system would be preferred for data collection since it offers portability, speed and convenience especially if data are required from families with young children. The only disadvantage being that the head-band used in the tracking system of the HLS tends to obscure the upper forehead region.

Optical surface scanning was chosen in this study to collect accurate 3D data from the face because the primary concern was with the classification of facial structures. Collecting the data in this manner provided a permanent resource of the whole facial surface that could be repeatedly analysed using different approaches. The alternative methods of data collection applicable to this project would have been photography or direct physical measurements made with callipers. Photography, given excellent equipment and suitable conditions (e.g. control of lighting) has the advantage of being rapid and provides an accurate reproduction of skin tone, eye colour, hair colour, overall face shape and respective location of the principal features. However, the classification of features is very difficult from 2D images, as accurate information on the dimensions of a feature cannot be obtained from a single photo. The main advantage of photography over the scanner is that it captures the personal aspect of the face (including expression, skin tone and colour) that we use to make judgements about a person in every day life. However, this

information is inappropriate for an objective analysis of structural variation and so for this study does not provide additional information. 3D scanning permitted collection of uniform data in terms of facial dynamics as all subjects were scanned with their eyes closed and the face at rest reducing the chance of capturing individual emotion and expression. Furthermore, it was easy to obtain consistent repeat scans with the face 'set at rest'.

Direct physical analysis made on a 'living' subject allows accurate measurements to be recorded but requires lengthy preplanning and experience to ensure reproducibility and does not provide a physical record that can be reanalysed. Prof J. Waddington and his colleagues are carrying out an interesting example of detailed work of this kind in Ireland. They have found, using morphometric techniques, minute variation in an extensive repertoire of head and neck measurements in comparing schizophrenic patients to age and ethnicity matched control subjects (Lane et al 1997). To detect these minor facial differences, exhaustive and lengthy anthropometric analysis of the face of each subject was required. Also, to ensure consistency of measurements, the same experienced individuals have collected this data. Thus the accumulation of data has been a slow and lengthy procedure. Following up on our successful experience with scanning normal faces Waddington's group is now expanding their data set using an HLS system. It will be interesting to see if they are successful in reproducing their previous results obtained by

traditional morphometric analysis and whether additional variation can be detected.

The long-term aim of this study was to identify genes responsible for normal facial variation. In order to achieve this, whole genome linkage analysis combined with candidate region association studies would be a logical approach to take. However, this requires good quality DNA, a disappointing aspect to the current project was the DNA collection. There was a poor uptake of volunteers willing to provide blood samples. A slightly better response was achieved with buccal samples but the quality of the DNA obtained by this method was extremely variable. Aside from the unwillingness of volunteers the other factor that affected collection of genetic material was the facilities we were operating with. DNA collection was impractical in public arenas where the majority of the family data was collected. With hindsight this could have been better prepared for, but there is the added difficulty with a study of normal variation that it will always be difficult to convince each family member to provide a 20ml intravenous blood sample simply 'for the good of research'. Buccal samples were obtained by a non-invasive procedure but whether they provide sufficient good quality genetic material to use for whole genome association studies is doubtful. Perhaps a more realistic approach to take would be to scan families who have already been extensively genotyped for markers throughout the genome as part of another study, such as the extensive series of diabetic families

studied by Todd and his colleagues (Todd and Farrall 1996) or the famous collection of CEPH families.

From the outset it was clear that in this pilot study it was unlikely that a direct genotype-phenotype link would be made. Nevertheless it seemed sensible to test as many different aspects of this project as possible during this pilot study. The main purpose being to facilitate full-scale analysis and follow up in subsequent phases in this study of genes and faces. Thus in addition to collecting 3D face data sets, classifying features and carrying out population and family studies it was decided from the outset to carry out a small scale candidate gene study.

Based on a study of the literature, emerging during the first two years of the project, ET-1 and ETRA were selected as the most suitable 'face gene' candidates. Genetic polymorphisms had not been reported in either of these genes at the time this work began but within a matter of months a number of variants were published. In practice this study has provided a satisfactory test of feasibility and logistics, in other words a good practical run through, helpful for future studies. In terms of identifying a genotype-phenotype link this was a rather optimistic approach to take; there are many of the ~8000 known named genes which could be biologically justified as good candidates, as well as a considerable proportion of the unnamed genes (Wang et al 1998). The chance of selecting a candidate gene and identifying a variant that segregates with a classified phenotype

is pretty slim. However this kind of approach would be logical to employ after a candidate region of the genome had been identified though linkage.

The rapid advance in sequencing the genome has meant that efforts are currently concentrated on identifying single nucleotide polymorphisms (SNPs). It is believed that there are up to 2 million genetic differences between two people (Wang et al 1998). Whole genome SNP association is currently perceived to be the ultimate method of detecting the genetic contribution to a given phenotype. Modelling of different populations has enabled estimates of the minimal number of SNPs needed to be screened in order to detect association. This ranges from the worst scenario of 500 000 (Kruglyak 1999) to 300 000 (Collins et al 1999). While such an immense undertaking is not conceivable for a small-scale research project it is important to take on board population considerations used to generate these estimates. The relative power of association studies can be increased through selection of a population where one might expect to find higher levels of linkage disequilibrium. This could include studies of recently founded population such as Finland or Iceland (Terwilliger et al 1998) where much of the genome is in linkage disequilibrium. Or, alternatively by studying recently admixed populations, such as Hawaii and Brazil, between different ethnic groups where linkage disequilibrium is generated as a consequence of

different allele frequencies in the respective parent populations (Briscoe et al 1994).

The data presented in this thesis was collected in London and as a consequence was a very heterogeneous group with few volunteers actually originating from the local area. Recently the relative merits of gene hunting in metropolitan populations as opposed to more homogenous populations were discussed in an article entitled Manhattan versus Reykjavik (Abbott 2000). The advantages of studying an isolated population is that the homogeneity provides a simple genetic background; an advantage in studies of single gene disorders as well as multifactoral conditions to separate environmental from genetic effect. The merits of studying an urban population are in the identification of the genetic basis of complex traits, where a large number of genes produce a relatively small effect. While an isolated population has the benefits of reducing the effects of genetic background there is also the danger of magnifying the effect of relative rare alleles. Nonetheless, whatever approach or justification for population selection is used the most important factor still remains the accurate and reproducible assignment of the phenotype.

The use of the surface segmentation software in this thesis has demonstrated that at least two aspects of normal human facial variation; chin cleft and nose band, can be classified as discrete traits, which appear to obey Mendelian laws of inheritance. The

family data provided strong evidence to support this rather simplistic model. Nevertheless even these facial traits showed complexities in the data with respect to ethnicity and gender. There were very striking male-female differences in chin cleft phenotype frequencies for example and strong hints that differences in genetic background might also affect the phenotype. It is possible that some of these differences arise because the chin cleft and nose band are secondary sex characteristics. That is, the 'development' of the phenotype could be modified by genes on the sex chromosomes or affected by male-female variations in temporal-spatial gene expression during embryonic development. Interestingly the idea of sex limiting modifying genes was put forward to explain a similar finding in an early study to account for a significant sex bias in an extensive study of diaphyseal aclasia (Harris 1949). Even now it is not clear how such characteristics develop though there is increasing evidence for the existence of such genes. Both oestrogen and androgen receptors have been found in the skeletal muscle of several animals. Recent evidence of sexually dimorphic gene expression comes from evidence that the male hormone, testosterone, plays a role in maintaining myosin heavy chain expression in the adult male mouse masseter, the main jaw muscle for mastication (Eason et al 2000).

The analysis of jaw protrusion also revealed evidence of male-female differences in facial traits. In the population analysis the mean value was significantly different with respect to gender. In the

family analysis the gender difference was effectively magnified, since there was strong evidence of same sex parent-offspring correlation. In this scenario it is difficult to assess the extent to which this observation is due to the inheritance of the degree of jaw protrusion or genetic background, specifically gender. This again could be suggestive of sex-limiting genes that alter the extent of manifestation of a trait or facial form in general. What is also interesting is that in this study the result was quite contrary to that expected in that the extent of apparent jaw protrusion in the females was greater than the males.

Looking at chin cleft and nose band in the small populations of individuals of different ethnic origin there is evidently some variation and this is an interesting general topic to address. For example, can different genetic backgrounds have the effect of 'masking' or 'magnifying' a specific phenotype. It will be of general interest to look at traits in families with interracial marriages to see if parental features are manifest as predicted in offspring. During the course of this study, a small number of 'mixed marriage' couples did come forward but unfortunately none were directly informative for chin cleft or nose band traits.

As well as considering the effects of genetic background on the manifestation of a trait, consideration must also be given to trait heterogeneity, for example whether an observed phenotype is produced by different alleles within a gene or by independent loci.

There are many lessons to be learnt from studies of pathology and these are catalogued in McKusicks massive compendium OMIM (McKusick-Nathans 2000). For example the ocular disorder Retinitis Pigmentosa arises from mutation at many independent loci and there is evidence of multiple allelism at many loci. Similarly 51 different pathogenic mutations have been identified in the TCOF1 gene believed to cause Treacher Collins syndrome (Splendore et al 2000). Such factors need to be considered when analysing the genetic basis of facial features as possible explanations for variability in the phenotype. The detailed analysis of genetically heterogeneous traits can often lead to the recognition of subtle phenotype variations which are genetically distinct, again re-emphasising the importance of accurate and reliable description of phenotype.

At this stage in the project it is quite difficult to present an opinion about covariance of facial features. A great deal more information and classification is required. One way of viewing covariance of facial features is to consider say 10 facial features that are simple polymorphic traits, each determined at one major independent genetic locus. This would constitute the predetermined genetic component of the face. Growth and development, together with epigenetic effects, hormonal environment, gender and ethnic variation etc. then might affect the extent to which these 10 traits integrate together and become manifest as the final form of the face in an individual. A preliminary study of covariance was carried out to

investigate the association between nose band and chin cleft traits. This was carried out on the male data; judged to be the most reliable data, with the assumption that both traits are fully manifest in males. These data are presented in Table 8.1, and there is no significant association between the traits in males.

The method used to generate the classification of these two traits was the surface segmentation software. This provided a colour-coded segmentation file calculated from the raw 3D scan data, independent of orientation and is a novel approach for objective classification of facial features. While surface segmentation is ideally suited to the identification of discretely variable facial traits it is not clear how it could be applied to assess overall aspects of facial morphology, or traits that exhibit a continuous graded variation. There is some scope for varying the patch size used to calculate the surface segmentation and the detail of the patterns produced. Denser data collection using a greater number of sweeps with the HLS for example, coupled with use of a smaller patch size might also facilitate detailed specific feature analysis. Other parameters of surface curvature that might be useful for trait identification and classification, for example the curvedness parameter (R) described by Koenderink and Van Doorn (1992) have been relatively under explored here but might be appropriate for the analysis of the tip of the nose for example. The depth map briefly described in Chapter 4

		Chin Cleft			
		S	SW	W	
Nose band	1	47 (44)	87 (82.4)	34 (41.6)	168
	2	8 (11)	16 (20.6)	18 (10.4)	42
		55	103	52	210

Table 8.1 Association between nose band and chin cleft phenotypes in unrelated European males. The expected frequencies are calculated from the observed. There was no significant association between the two phenotypes ($\chi^2 = 4.49$, $p>0.05$, 2 d.f)

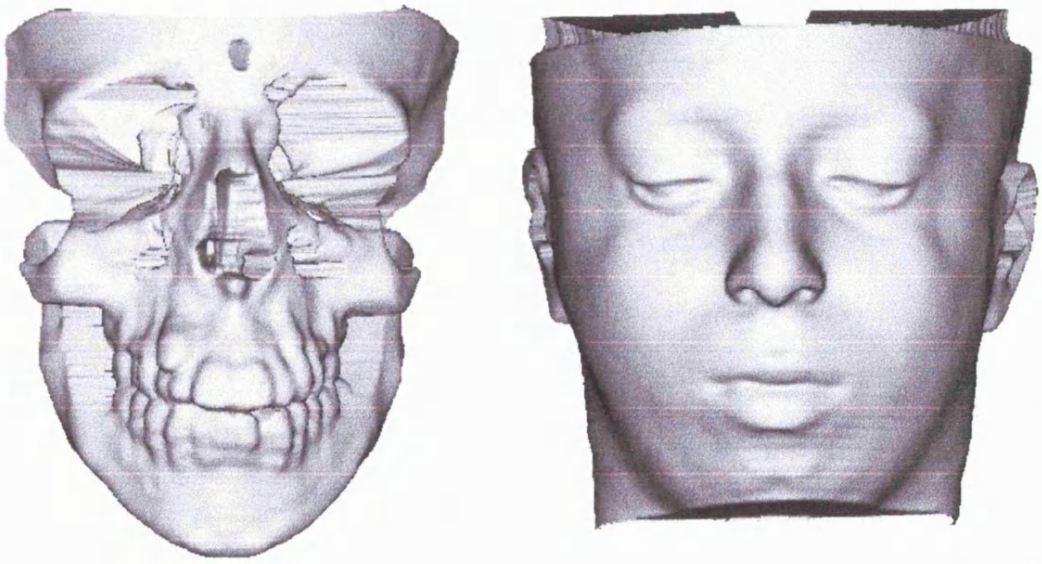

Figure 8.1 Skull and facial surface data generated from a CT scan of a Treacher Collins patient.

might also be very useful if it could be generated in a format independent of orientation of the 3D file.

It would also be interesting to analyse CT scans of the head as the CLOUD software can visualise such data in a similar way to the surface scans and would allow both the underlying skeleton and overlying face to be visualised and analysed. Fig 8.1 illustrates CT data, kindly made available to me by Robin Richards, from a Treacher Collins patient of the skeleton and overlying facial surface. Other possible sources of skeletal information could include archive data of skull x-rays carried out both anterior-posterior and laterally. Under the guidance of Dr J. Deng, Dept Medical Physics, I was able to carry out a preliminary experiment to investigate the use of ultrasound to obtain a representation of the skeletal structure. While this was relatively messy, with the equipment not designed for the face, it did produce some interesting results and could possibly be modified for use on the face.

This thesis has provided basic groundwork and a sizeable resource of more than 1000 3D face scans from which a larger scale initiative into the investigation of the genetic basis of appearance can develop. Looking ahead, more consideration should be given to the substructure of the face, and the specific contribution of skeleton, muscle and cartilage components to facial structures. The surface segmentation of the face has by no means been exhaustive and further detailed feature classifications should be possible.

Heterogeneity also needs to be more widely addressed; both in the context of genetic multilocus and allelic heterogeneity as well as looking at more complex facial traits.

With the acquisition of the HLS system, the opportunities for data collection have been expanded. However it is now clear that in order to collect good scan data, as well as personal information and a DNA sample, more than two investigators are required, particularly in public arena scanning. This must be an important consideration in any future studies especially with the focus moving towards gene identification and the increasing importance of acquiring good quality DNA samples. Future priorities should also aim to increase the family data set; to further support the patterns of inheritance of chin cleft and nose band as well as the analysis of other segregating facial traits. While the possibility of whole genome SNP screening may be possible in the long term, services such as the Linkage Hotel (HGMP) should be explored as a short-term option to gene identification. If a candidate region of the genome could be identified by this approach then the process of screening candidate genes in the specified region would become a more practical procedure to take.

One aim of this thesis was the classification of facial features suitable for genetic analysis with the long-term aim of gene identification. This study has made significant contribution to this aim by breaking down the complexity of the face and identifying qualitative traits for analysis. At this stage of the project I believe it is

very important not to underestimate the strength of simple classifications of the face. Even 10 classified, independent polymorphic traits, each with three phenotypes would generate about 60 000 different facial combinations without considering covariance and other genetic effects.

In a more general biological context it will be interesting to see how much the genes involved in normal facial variation overlap with those responsible for pathological syndromes and dysmorphology. It will be interesting to address questions about the face shape as a measure of genetic fitness, and why so much facial variation exists in humans. It should also be possible to look at the face in the context of wider sociological aspects of human behaviour; for instance, at the simplest level it should be relatively straightforward to assess whether there is assortative mating based on facial phenotypes.

Finally, the long-term aims of this project understandably have generated considerable forensic interest. The accurate description and categorisation of facial features has immediate and obvious practical uses in facial description and 'photo fit' type portraits of suspects where as the possibility of 'face gene' identification has revolutionary implications. Computer reconstruction of a face from a DNA sample may sound suspiciously like the plot from one of the current genre of science fiction films, but it is not inconceivable that in a relatively short time it might be possible to make reasonable

predictions about some distinctive normal facial features from the analysis of DNA.

REFERENCES:

Abbott A, 2000 Manhattan versus Reykjavik. Nature 406: 340-342

Arridge S, Moss JP, Linney AD, James DR. 1985 Three dimensional digitisation of the face and skull. J Maxillofac Surg. 13: 136-43.

Aung SC, Ngim RC, Lee ST. 1995 Evaluation of the laser scanner as a surface measuring tool and its accuracy compared with direct facial anthropometric measurements. Br J Plast Surg. 48: 551-8.

Barni T, Fantoni G, Gloria L, Maggi M, Peri A, Balsi E, Grappone C, Vannelli GB. 1998 Role of endothelin in the human craniofacial morphogenesis. J Craniofac Genet Dev Biol. 18:183-94

Beardsley MC. 1966 Aesthetics from classical Greece to the Present. New York: Macmillan

Bentley DR. 2000 The Human Genome Project-an overview. Med Res Rev. 20: 189-96.

Berry AC and Berry RJ 1967 Epigenetic variation in the human cranium. J. Anat 101:361-380

Besl PJ and Jain RC 1985 Three-Dimensional Object Recognition Computing Surveys 17: 75-145

Besl PJ and Jain RC 1986 Invariant Surface Characteristics for 3D Object Recognition in Range Images. Computer Vision and Image Processing 33: 33-80

Bhanu BV, Malhotra KC. 1972 A population genetic study of cleft chin in India. Am J Phys Anthropol. 37:367-72.

Bishara SE, Cummins DM, Jorgensen GJ, Jakobsen JR. 1995 A computer assisted photogrammetric analysis of soft tissue changes after orthodontic treatment. Part I: Methodology and reliability. Am J Orthod Dentofacial Orthop. 107: 633-9.

Blevins LS Jr, Hall GS, Madoff DH, Laws ER Jr, Wand GS. 1992 Case report: acromegaly and Cushing's disease in a patient with synchronous pituitary adenomas. Am J Med Sci. 304: 294-7.

Bookstein FL. 1977 Orthogenesis of the hominids: an exploration using biorthogonal grids. Science. 197: 901-4.

Bookstein FL. 1997 Landmark methods for forms without landmarks: morphometrics of group differences in outline shape. Med Image Anal.1: 225-43.

Bookstein F, Schafer K, Prossinger H, Seidler H, Fieder M, Stringer C, Weber GW, Arsuaga JL, Slice DE, Rohlf FJ, Recheis W, Mariam AJ, Marcus LF. 1999 Comparing frontal cranial profiles in archaic and modern homo by morphometric analysis. Anat Rec. 257:217-24.

Briscoe D, Stephens JC, O'Brien SJ. 1994 Linkage disequilibrium in admixed populations: applications in gene mapping. J Hered. 85:59-63.

Brown T, Alvesalo L, Townsend GC. 1993 Craniofacial patterning in Klinefelter (47 XXY) adults. Eur J Orthod. 15:185-94.

Bruce V and Young A: 1998 In the Eye of the Beholder: the science of face perception Published: Oxford University Press

Burke PH, Healy MJ. 1993 A serial study of normal facial asymmetry in monozygotic twins. Ann Hum Biol. 20: 527-34.

Burr CW. 1935 Personality and Physiognomy. Dent Cosmos 77; 556-560

Burton AM, Bruce V, Dench N. 1993 what's the difference between men and women? Evidence from facial measurement. Perception. 22: 153-76.

Bush K, Antonyshyn O. 1996 Three-dimensional facial anthropometry using a laser surface scanner: validation of the technique. Plast Reconstr Surg. 98: 226-35.

Butler AB. 2000 Chordate evolution and the origin of craniates: an old brain in a new head. Anat Rec. 261:111-25.

Byard PJ, Poosha DV, Satyanarayana M, Rao DC 1985 Family resemblance for components of craniofacial size and shape. J Craniofac Genet Dev Biol 5:229-38

Cambien F, Poirier O, Nicaud V, Herrmann SM, Mallet C, Ricard S, Behague I, Hallet V, Blanc H, Loukaci V, Thillet J, Evans A, Ruidavets JB, Arveiler D, Luc G, Tiret L. 1999 Sequence diversity in 36 candidate genes for cardiovascular disorders. Am J Hum Genet. 65: 183-91.

Carey JW, Steegmann AT Jr. 1981 Human nasal protrusion, latitude, and climate. Am J Phys Anthropol. 56: 313-9.

Chan DQ. 1999 Fetal alcohol syndrome Optom Vis Sci. 76: 678-85.

Chen LH, Iizuka T 1995 Evaluation and prediction of the facial appearance after surgical correction of mandibular hyperplasia. Int J Oral Maxillofac Surg. 24: 322-6.

Chung CS, Kau MC, Walker GF. 1982 Racial variation of cephalometric measurements in Hawaii. J Craniofac Genet Dev Biol. 2: 99-106.

Clouthier DE, Hosoda K, Richardson JA, Williams SC, Yanagisawa H, Kuwaki T, Kumada M,Hammer RE, Yanagisawa M. 1998 Cranial and cardiac neural crest defects in endothelin-A receptor-deficient mice. Development. 125: 813-24.

Clouthier DE, Williams SC, Yanagisawa H, Wieduwilt M, Richardson JA, Yanagisawa M. 2000 Signalling pathways crucial for craniofacial development revealed by endothelin-A receptor-deficient mice. Dev Biol. 217: 10-24.

Cole J: 1997 About Face. Published by MIT press

Collins A, Lonjou C, Morton NE. 1999 Genetic epidemiology of single-nucleotide polymorphisms. Proc Natl Acad Sci U S A. 96:15173-7.

Coombes AM, Linney AD, Richards R, Moss JP. 1990 A method for the analysis of the 3D shape of the face and changes in the shape brought about by facial surgery. Biostereomatics and Applications, Editor Robin Herron, Proc: SPIE, 1380: 180-189.

Coombes AM, Richards R, Linney A, Bruce V and Fright R 1992, Description and recognition of faces from 3D data Proc. SPIE 1766:180–189.

Corvo G, Tartaro GP, Stoppoloni F, Balzano G. 1998 Cephalometric evaluation of patients with Turner syndrome. Minerva Stomatol. 47: 127-33.

Craw, I.G., Ellis, H., and Lishman, J. 1987. Automatic extraction of facial features. Pattern Recognition Letters 5: 183-187.

Cross J. 1817 An attempt to establish physiognomy upon scientific principles. Glasgow: University Press.

Dean D, Hans MG, Bookstein FL, Subramanyan K. 2000 Three-dimensional Bolton-Brush Growth Study landmark data: ontogeny and sexual dimorphism of the Bolton standards cohort.
Cleft Palate Craniofac J. 37: 145-56.

Devor EJ. 1987 Transmission of human craniofacial dimensions. J Craniofac Genet Dev Biol.7: 95-106.

Dixon, J.; Hovanes, K.; Shiang, R.; Dixon, M. J. 1997: Sequence analysis, identification of evolutionary conserved motifs and expression analysis of murine tcof1 provide further evidence for a potential function for the gene and its human homologue, TCOF1. Hum. Molec. Genet. 6: 727-737.

Dorai C and AK Jain 1997 COSMOS – A Representation Scheme for 3D Free-Form Objects IEEE Transactions on Pattern Analysis and Machine Intelligence 19: 1115 – 1130,.

Driscoll DA. 1994 Genetic basis of DiGeorge and velocardiofacial syndromes. Curr Opin Pediatr. 6:702-6.

Durer A: The Four Books on Human Proportions, published posthumously in 1528.

Eason JM, Schwartz GA, Pavlath GK, English AW. 2000. Sexually dimorphic expression of myosin heavy chains in the adult mouse masseter. J Appl Physiol. 89:251-8.

Eaves L, Heath A, Martin N, Maes H, Neale M, Kendler K, Kirk K, Corey L. 1999 Comparing the biological and cultural inheritance of personality and social attitudes in the Virginia 30,000 study of twins and their relatives. Twin Res. 2: 62-80.

Edwards, S. J.; Gladwin, A. J.; Dixon, M. J. 1997: The mutational spectrum in Treacher Collins syndrome reveals a predominance of mutations that create a premature-termination codon. Am. J. Hum. Genet. 60: 515-524.

Ekman P 1999 Expression of emotions in man and animals by Charles Darwin, published by Fontana Press.

El Ghouzzi V, Legeai-Mallet L, Aresta S, Benoist C, Munnich A, de Gunzburg J, Bonaventure J. 2000 Saethre-Chotzen mutations cause TWIST protein degradation or impaired nuclear location. Hum Mol Genet. 9: 813-9.

Enlow DH and Hans MG. 1996 Essentials of facial growth. Published by W. B. Saunders company, Philadelphia.

Epstein CJ 1990. The consequences of chromosome imbalance. Am J Med Genet Suppl. 7:31-7.

Farkas LG, Bryson W, Klotz J. 1980 Is photogrammetry of the face reliable? Plast Reconstr Surg. 66: 346-55.

Farkas LG and Cheung G 1981 Facial Asymmetry in healthy North American Caucasians. Angle Orthod. 51; 70-77

Farkas LG and Munro IR 1987 Anthropometric facial proportions in medicine. Springfield IL; Charles C Thomas

Farkas LG, Hajnis K, Posnick JC. 1993 Anthropometric and anthroposcopic findings of the nasal and facial region in cleft patients before and after primary lip and palate repair. Cleft Palate Craniofac J. 30: 1-12.

Farkas L. J 1994 Anthropometry of the head and face: 2nd edition Raven Press: New York

Ferrario VF, Sforza C, Poggio CE, Serrao G, Miani A Jr. 1994 A three-dimensional study of sexual dimorphism in the human face. Int J Adult Orthodon Orthognath Surg. 9: 303-10.

Galton, F 1869. Hereditary genius. London: MacMillan

Galton, F. 1875 The history of twins, as a criterion of the relative powers of nature and nurture Pop. Sci. Monthly 8: 345-357

Galton, F 1878 'Composite portraits' Journal of the anthropological institute, 8: 134

Galton, F 1884. Record of Family Faculties. London: MacMillan

Galton, F 1889 ' Feasible experiments on the possibility of transmitting acquired habits by means of inheritance' Nature 40: 610 and Brit. Ass. Report 59: 620-621

Galton, F 1891 'Method of indexing finger marks' Proc. Roy. Soc. 49, 540-48

Galton, F. 1909 Essays in eugenics / London: The Eugenics Education Society.

Galton, F. 1910 Numeralised Profiles for classification and recognition Nature 83: 125-129

Golomb, B.A., Lawrence, D.T., and Sejnowski, T.J. 1991. SEXNET: A neural network identifies sex from human faces. Advances in Neural Information Processing Systems 3, Editors; Touretzky, Lippman, San Mateo, CA, Morgan Kaufmann.

Gotoda Y, Wakamatsu N, Kawai H, Nishida Y, Matsumoto T. 1998 Missense and nonsense mutations in the lysosomal alpha-mannosidase gene (MANB) in severe and mild forms of alpha-mannosidosis. Am J Hum Genet. 63: 1015-24.

Graves JA. 1998 Evolution of the mammalian Y chromosome and sex-determining genes. J Exp Zool. 281:472-81.

Grays anatomy 38th Edition 1995 Henry Gray : Churchill Livingstone :medical division of Pearson professional ltd

Grimberg J, Maguire S, Belluscio L. 1989 A simple method for the preparation of plasmid and chromosomal E. coli DNA. Nucleic Acids Res. 17:8893.

Gripp KW, Zackai EH, Stolle CA. 2000 Mutations in the human TWIST gene. Hum Mutat.15: 150-5.

Hall JG, Froster-Iskenius UG, Allanson J. 1989 Handbook of normal physical measurements, , Oxford university press

Hanihara T. 1997 Craniofacial affinities of Mariana Islanders and circum-Pacific peoples. Am J Phys Anthropol.104: 411-25.

Harris H 1949 A sex limiting modifiying gene in diaphysial aclasis (multiple exostoses). Annals of Eugenics 14: 165-170.

Hassin R, Trope Y. 2000 Facing faces studies on the cognitive aspects of physiognomy. J Pers Soc Psychol. 78: 837-52.

Haxby JV, Hoffman EA, Gobbini MI. 2000 The distributed human neural system for face perception. Trends Cogn Sci. 4: 223-233.

Hodge GP. 1977 A medical history of the Spanish Habsburgs. As traced in portraits. JAMA. 238: 1169-74.

Howard, T. D.; Paznekas, W. A.; Green, E. D.; Chiang, L. C.; Ma, N.; Ortiz De Luna, R. I.; Delgado, C. G.; Gonzalez-Ramos, M.; Kline, A. D.; Jabs, E. W.: 1997 Mutations in TWIST, a basic helix-loop-helix transcription factor, in Saethre-Chotzen syndrome. Nature Genet.15: 36-41.

Hrdlicka, A. Anthropometry 1920 Philadelphia: The Wistar institute of Anatomy and biology.

Huang WJ, Taylor RW, Dasanayake AP. 1998 Determining cephalometric norms for Caucasians and African Americans in Birmingham. Angle Orthod. 68:503-11

Humphrey LT. 1998 Growth patterns in the modern human skeleton. Am J Phys Anthropol. 105: 57-72.

Indridason OS, Thomas L, Berkoben M. 1996 Medullary sponge kidney associated with congenital hemihypertrophy. J Am Soc Nephrol. 7:1123-30.

Inoue A, Yanagisawa M, Takuwa Y, Mitsui Y, Kobayashi M, Masaki T. 1989 The human preproendothelin-1 gene. Complete nucleotide sequence and regulation of expression. J Biol Chem. 264:14954-9.

Jabs EW, Muller U, Li X, Ma L, Luo W, Haworth IS, Klisak I, Sparkes R, Warman ML, Mulliken JB, et al 1993. A mutation in the homeodomain of the human MSX2 gene in a family affected with autosomal dominant craniosynostosis. Cell. 75: 443-50.

Jamison PL, Ward RE. 1993 Brief communication: measurement size, precision, and reliability in craniofacial anthropometry: bigger is better. Am J Phys Anthropol. 90:495-500.

Johnson M and Morton J 1991 Biology and Cognitive Development: The Case of Face Recognition. Published by Blackwell, Oxford UK.

Johnson D, Iseki S, Wilkie AO, Morriss-Kay GM. 2000 Expression patterns of Twist and Fgfr1, -2 and -3 in the developing mouse coronal suture suggest a key role for twist in suture initiation and biogenesis. Mech Dev. 91: 341-5.

Kaye, C. I.; Martin, A. O.; Rollnick, B. R.; Nagatoshi, K.; Israel, J.; Hermanoff, M.; Tropea, B.; Richtsmeier, J. T.; Morton,N. E. 1992.: Oculoauriculovertebral anomaly: segregation analysis. Am. J. Med. Genet. 43: 913-917

Keen JA 1950 Study of differences between male and female skulls. Am J Phys Anthropol 8:65-79

Koenderink and AJ Van Doorn 1992. Surface shape and curvature scales. Image Vision Computing 10: 557-565

Kohout MP, Aljaro LM, Farkas LG, Mulliken JB. 1998 Photogrammetric comparison of two methods for synchronous repair of bilateral cleft lip and nasal deformity. Plast Reconstr Surg. 102: 1339-49.

Kruglyak L. 1999 Prospects for whole-genome linkage disequilibrium mapping of common disease genes. Nat Genet. 22: 139-44.

Kukita Y, Tahira T, Sommer SS, Hayashi K. 1997 SSCP analysis of long DNA fragments in low pH gel. Hum Mutat.10:400-7.

Kurihara Y, Kurihara H, Suzuki H, Kodama T, Maemura K, Nagai R, Oda H, Kuwaki T, Cao WH, Kamada N, et al. 1994 Elevated blood pressure and craniofacial abnormalities in mice deficient in endothelin-1. Nature. 368: 703-10.

LaBonne C, Bronner-Fraser M. 1999 Molecular mechanisms of neural crest formation. Annu Rev Cell Dev Biol.15: 81-112.

Lajeunie E, Cameron R, El Ghouzzi V, de Parseval N, Journeau P, Gonzales M, Delezoide AL, Bonaventure J, Le Merrer M, Renier D. 1999 Clinical variability in patients with Apert's syndrome. J Neurosurg. 90: 443-7.

Lander ES. 1996 The new genomics: global views of biology. Science. 274: 536-9.

Lane A, Kinsella A, Murphy P, Byrne M, Keenan J, Colgan K, Cassidy B, Sheppard N, Horgan R, Waddington JL, Larkin C, O'Callaghan E. 1997 The anthropometric assessment of dysmorphic features in schizophrenia as an index of its developmental origins. Psychol Med. 27:1155-64.

Larsen, William J. Human embryology 1997 2nd edition. New York ; London : Churchill Livingstone ,

Laveter JC. 1789 Essays on physiognomy, vols. 1-3. London: GGJ and J Robinson

Lebow, M. R.; Sawin, P. B. 1941 Inheritance of human facial features: a pedigree study involving length of face, prominent ears and chin cleft. J. Hered. 32: 127-132.

Le Douarin NM, Dupin E, Ziller C. 1994 Genetic and epigenetic control in neural crest development. Curr Opin Genet Dev. 4:685-95.

Lele, S 1993 Euclidean Distance Matrix analysis (EDMA): estimation of mean form and mean form difference. Mathematical Geology, 25:573-602

Liggett J 1974 The Human Face published by Constable, London

Liu YH, Tang Z, Kundu RK, Wu L, Luo W, Zhu D, Sangiorgi F, Snead ML, Maxson RE. 1999 Msx2 gene dosage influences the number of proliferative osteogenic cells in growth centers of developing murine skull: a possible mechanism for MSX2-mediated craniosynostosis in humans. Dev Biol. 205: 260-74.

Lombruso C. 1911 5th ed., 3 vol., 1896–97; partial tr. as Criminal Man,

Mao XQ, Gao PS, Roberts MH, Enomoto T, Kawai M, Sasaki S, Shaldon SR, Coull P, Dake Y, Adra CN, Hagihara A, Shirakawa T, Hopkin JM. 1999 Variants of endothelin-1 and its receptors in atopic asthma. Biochem Biophys Res Commun. 262:259-62.

Marsh KL, Dixon J, Dixon MJ. 1998 Mutations in the Treacher Collins syndrome gene lead to mislocalization of the nucleolar protein treacle. Hum Mol Genet. 7:1795-800.

Masterson TJ, Hartwig WC. 1998 Degrees of sexual dimorphism in Cebus and other New World monkeys. Am J Phys Anthropol. 107: 243-56.

McAlarney ME, Chiu WK. 1997 Comparison of numeric techniques in the analysis of cleft palate dental arch form change. Cleft Palate Craniofac J. 34:281-91.

McKusick-Nathans 2000: Online Mendelian Inheritance in Man, OMIM (TM). Institute for Genetic Medicine, Johns Hopkins University (Baltimore, MD) and National Center for Biotechnology Information, National Library of Medicine (Bethesda, MD). World Wide Web URL: http://www.ncbi.nlm.nih.gov/omim/

McNeil D: 1998 The Face a guided tour: Hamish Hamilton Group: London

McPherson EW, Clemens MM, Gibbons RJ, Higgs DR. 1995 X-linked alpha-thalassemia/mental retardation (ATR-X) syndrome: a new kindred with severe genital anomalies and mild hematologic expression. Am J Med Genet. 55:302-6.

Melnick M. J Craniofac Genet Dev Biol. 1997 17:65-79 Cleft lip and palate etiology and its meaning in early 20th century England: Galton/Pearson vs.Bateson; polygenically poor protoplasm vs. Mendelism.

Meyers, G. A.; Day, D.; Goldberg, R.; Daentl, D. L.; Przylepa, K. A.; Abrams, L. J.; Graham, J. M., Jr.; Feingold, M.;Moeschler, J. B.; Rawnsley, E.; Scott, A. F.; Jabs, E. W. 1996. FGFR2 exon IIIa and IIIc mutations in Crouzon, Jackson-Weiss, and Pfeiffer syndromes: evidence for missense changes, insertions, and a deletion due to alternative RNA splicing. Am. J. Hum. Genet. 58: 491-498

Miyajima K, McNamara JA Jr, Kimura T, Murata S, Iizuka T 1996 Craniofacial structure of Japanese and European-American adults with normal occlusions and well-balanced faces. Am J Orthod Dentofacial Orthop. 110:431-8.

Moorrees CF, uan Venrooij ME, Lebret LM, Glatky CG, Kent rl, Reed RB. 1976 New norms for the mesh diagram analysis.
Am J Orthod. 69: 57-71.

Mosier, C I 1939 Determining a simple structure when loading for certain tests are known Pschometrika, 4:149-162

Moss JP, Grindrod SR, Linney AD, Arridge SR, James D. 1988 A computer system for the interactive planning and prediction of maxillofacial surgery. Am J Orthod Dentofacial Orthop. 94: 469-75.

Moss JP, Coombes AM, Linney AD, Campos J 1991 Methods of three-dimensional analysis of patients with asymmetry of the face.
Proc Finn Dent Soc. 87: 139-49.

Nakajima E, Maeda T, Yanagisawa M. 1985 The Japanese sense of beauty and facial proportions II; the Beautiful face and the √2 rule.
Quintessence Internat. 9:629-637

Nance, M. A.; Berry, S. A. 1992: Cockayne syndrome: review of 140 cases. Am. J. Med. Genet. 42: 68-84.

Nanni, L.; Ming, J. E.; Bocian, M.; Steinhaus, K.; Bianchi, D. W.; de Die-Smulders, C.; Giannotti, A.; Imaizumi, K.; Jones,K. L.; Del Campo, M.; Martin, R. A.; Meinecke, P.; Pierpont, M. E. M.; Robin, N. H.; Young, I. D.; Roessler, E.; Muenke, M. 1999. The mutational spectrum of the Sonic hedgehog gene in holoprosencephaly: SHH mutations cause a significant proportion of autosomal dominant holoprosencephaly. Hum. Molec. Genet. 8: 2479-2488,

Nanni L, Schelper RL, Muenke MT. 2000 Molecular genetics of holoprosencephaly. Front Biosci. 5:D334-42

Nechala P, Mahoney J, Farkas LG. 1999 Digital two-dimensional photogrammetry: a comparison of three techniques of obtaining digital photographs. Plast Reconstr Surg. 103: 1819-25.

Nguyen BN, Johnson JA. 1998 The role of endothelin in heart failure and hypertension. Pharmacotherapy.18: 706-19

Nicaud V, Poirier O, Behague I, Herrmann SM, Mallet C, Troesch A, Bouyer J, Evans A, Luc G, Ruidavets JB, Arveiler D, Bingham A, Tiret L, Cambien F. 1999 Polymorphisms of the endothelin-A and -B receptor genes in relation to blood pressure and myocardial infarction: the Etude Cas-Temoins sur l'Infarctus du Myocarde (ECTIM) Study. Am J Hypertens. 12: 304-10.

Nichols EM. 1973 Pigment spotting in man and the number of genes determining skin and eye colour. Hum Hered. 23: 1-12.

Northcutt RG, Gans C. 1983 The genesis of neural crest and epidermal placodes: a reinterpretation of vertebrate origins. Q Rev Biol. 58: 1-28.

Osborne R.H and De George F. V 1959 Genetic Basis of Morphological variation published for The Commonwealth Fund by Harvard University Press, Cambridge Massachusetts.

Parigi, Appresso Giacomo Langlois: Trattato della pittura di Lionardo da Vinci, nouamente dato in luce, con la vita dell'istesso autore, Published: 1651.

Park, W.J.; Theda, C.; Maestri, N. E.; Meyers, G. A.; Fryburg, J. S.; Dufresne, C.; Cohen, M. M., Jr.; Jabs, E. W. 1995: Analysis of phenotypic features and FGFR2 mutations in Apert syndrome. Am. J. Hum. Genet. 57: 321-328

Perrett DI, Lee KJ, Penton-Voak I, Rowland D, Yoshikawa S, Burt DM, Henzi SP, Castles DL, Akamatsu S. 1998 Effects of sexual dimorphism on facial attractiveness. Nature. 394: 884-7.

Qiu M, Bulfone A, Ghattas I, Meneses JJ, Christensen L, Sharpe PT, Presley R, Pedersen RA, Rubenstein JL. 1997 Role of the Dlx homeobox genes in proximodistal patterning of the branchial arches: mutations of Dlx-1, Dlx-2, and Dlx-1 and -2 alter morphogenesis of proximal skeletal and soft tissue structures derived from the first and second arches. Dev Biol. 185: 165-84.

Quaderi, N. A.; Schweiger, S.; Gaudenz, K.; Franco, B.; Rugarli, E. I.; Berger, W.; Feldman, G. J.; Volta, M.; Andolfi, G.;Gilgenkrantz, S.; Marion, R. W.; Hennekam, R. C. M.; Opitz, J. M.; Muenki, M.; Ropers, H. H.; Ballabio, A. 1997: Opitz G/BBB syndrome, a defect of midline development, is due to mutations in a new RING finger gene on Xp22. Nature Genet. 17: 285-291.

Ras F, Habets LL, van Ginkel FC, Prahl-Andersen B. 1996 Quantification of facial morphology using stereophotogrammetry-demonstration of a new concept. J Dent. 24: 369-74.

Rao CR and Suryawanshi S. 1998 Statistical analysis of shape through triangulation of landmarks: A study of sexual dimorphism in hominids. Proc Natl Acad Sci U S A. 95: 4121-5.

Rhodes H. 1956 Biography of Alphonse Bertillon.

Richardson ER. 1980 Racial differences in dimensional traits of the human face. Angle Orthod. 50: 301-11.

Richtsmeier JT, Baxter LL, Reeves RH. 2000 Parallels of craniofacial maldevelopment in Down syndrome and Ts65Dn mice. Dev Dyn.217:137-45

Richtsmeier JT, Lele S. 1990 Analysis of craniofacial growth in Crouzon syndrome using landmark data. J Craniofac Genet Dev Biol. 10 : 39-62.

Ricketts RM. 1982 The biologic significance of the divine proportion and Fibonacci series. Am J Orthod.81: 351-70

Robin, N. H.; Feldman, G. J.; Aronson, A. L.; Mitchell, H. F.; Weksberg, R.; Leonard, C. O.; Burton, B. K.; Josephson, K.D.; Laxova, R.; Aleck, K. A.; Allanson, J. E.; Guion-Almeida, M. L.; Martin, R. A.; Leichtman, L. G.; Price, R. A.; Opitz, J. M.;Muenke, M. : 1995 Opitz syndrome is genetically heterogeneous, with one locus on Xp22, and a second locus on 22q11.2. Nature Genet. 11: 459-461.

Robins AH. 1973 Skin melanin content in blue-eyed and brown-eyed subjects. Hum Hered.; 23:13-8.

Robins G. 1994 Proportion and style in ancient Egyptian Art. London: Thames and Hudson

Sanger F, Nicklen S, Coulson AR. 1977 DNA sequencing with chain-terminating inhibitors. Proc Natl Acad Sci U S A. 74:5463-7.

Shalhoub SY, Sarhan OA, Shaikh HS. 1987 Adult cephalometric norms for Saudi Arabians with a comparison of values for Saudi and North American Caucasians. Br J Orthod. 14:273-9.

Shaner DJ, Peterson AE, Beattie OB, Bamforth JS. 2000 Assessment of soft tissue facial asymmetry in medically normal and syndrome-affected individuals by analysis of landmarks and measurements. Am J Med Genet. 93: 143-54.

Singh GD, McNamara JA Jr, Lozanoff S. 1998 Morphometry of the midfacial complex in subjects with class III malocclusions: Procrustes, Euclidean, and cephalometric analyses. Clin Anat.; 11:162-70.

Splendore A, Silva EO, Alonso LG, Richieri-Costa A, Alonso N, Rosa A, Carakushanky G, Cavalcanti DP, Brunoni D, Passos-Bueno MR. 2000 High mutation detection rate in TCOF1 among treacher collins syndrome patients reveals clustering of mutations and 16 novel pathogenic changes. Hum Mutat. 16:315-22.

Sprengelmeyer R, Young AW, Calder AJ, Karnat A, Lange H, Homberg V, Perrett DI, Rowland D 1996 Loss of disgust. Perception of faces and emotions in Huntington's disease. Brain. 119: 1647-65.

Stokely, E.M. & Wu, S.S. 1992 Surface Parameterisation and Curvature Measurement of Arbitrary 3-D Objects: Five Practical Methods. IEEE Transactions on Pattern Analysis and Machine Intelligence 14, 833 – 840.

Terrazas A, McNaughton BL. 2000 Brain growth and the cognitive map. Proc Natl Acad Sci U S A. 97:4414-6.

Terwilliger JD, Zollner S, Laan M, Paabo S. 1998 Mapping genes through the use of linkage disequilibrium generated by genetic drift: 'drift mapping' in small populations with no demographic expansion. Hum Hered. 48:138-54.

Thomas BL, Liu JK, Rubenstein JL, Sharpe PT 2000. Independent regulation of Dlx2 expression in the epithelium and mesenchyme of the first branchial arch. Development. 127:217-24.

Thompson, D. 1917 On growth and form: Cambridge University Press

Thompson EM, Winter RM. 1988 Another family with the 'Habsburg jaw'. J Med Genet. 25: 838-42.

Tiret L, Poirier O, Hallet V, McDonagh TA, Morrison C, McMurray JJ, Dargie HJ, Arveiler D, Ruidavets JB, Luc G, Evans A, Cambien F. 1999 The Lys198Asn polymorphism in the endothelin-1 gene is associated with blood pressure in overweight people. Hypertension 33:1169-74

Todd JA, Farrall M. 1996 Panning for gold: genome-wide scanning for linkage in type 1 diabetes. Hum Mol Genet.5: 1443-1448

Trainor P, Krumlauf R. 2000 Plasticity in mouse neural crest cells reveals a new patterning role for cranial mesoderm. Nat Cell Biol. 2: 96-102.

Tucker AS, Yamada G, Grigoriou M, Pachnis V, Sharpe PT. 1999 Fgf-8 determines rostral-caudal polarity in the first branchial arch. Development 126:51-61.

Turk M, Pentland 'Eigenfaces for recognition' 1991 A. J Cognitive Neurosci; 3: 71-86.

Tyrrell AJ, Evison MP, Chamberlain AT, Green MA. 1997 Forensic three-dimensional facial reconstruction: historical review and contemporary developments. J Forensic Sci. 42:653-61.

Valverde P, Healy E, Jackson I, Rees JL, Thody 1995 Variants of the melanocyte-stimulating hormone receptor gene are associated with red hair and fair skin in humans. Nat Genet. 11:328-30.

Veraksa A, Del Campo M, McGinnis W. 2000 Developmental patterning genes and their conserved functions: from model organisms to humans. Mol Genet Metab. 69: 85-100.

Wang DG, Fan JB, Siao CJ, Berno A, Young P, Sapolsky R, Ghandour G, Perkins N, Winchester E, Spencer J, Kruglyak L, Stein L, Hsie L, Topaloglou T, Hubbell E, Robinson E, Mittmann M, Morris MS, Shen N, Kilburn D, Rioux J, Nusbaum C, Rozen S, Hudson TJ, Lander ES, et al. 1998 Large-scale identification, mapping, and genotyping of single-nucleotide polymorphisms in the human genome. Science. 280:1077-82.

Ward RE, Jamison PL. 1991 Measurement precision and reliability in craniofacial anthropometry: implications and suggestions for clinical applications. J Craniofac Genet Dev Biol. 11: 156-64.

Wilkie, A. O. M.; Slaney, S. F.; Oldridge, M.; Poole, M. D.; Ashworth, G. J.; Hockley, A. D.; Hayward, R. D.; David, D. J.; Pulleyn, L. J.; Rutland, P.; Malcolm, S.; Winter, R. M.; Reardon, W. 1995 Apert syndrome results from localized mutations of FGFR2 and is allelic with Crouzon syndrome. Nature Genet. 9: 165-172.

Wilkie AO. 1997 Craniosynostosis: genes and mechanisms. Hum Mol Genet.6: 1647-56.

Wilkie AO, Tang Z, Elanko N, Walsh S, Twigg SR, Hurst JA, Wall SA, Chrzanowska KH, Maxson RE Jr. 2000 Functional haploinsufficiency of the human homeobox gene MSX2 causes defects in skull ossification. Nat Genet. 24: 387-90.

Wilson, D. I.; Burn, J.; Scambler, P.; Goodship, J. 1993. DiGeorge syndrome, part of CATCH 22. J. Med. Genet. 30: 852-856

Winter RM. 1996 What's in a face? Nat Genet. 12: 124-9.

Winter R and Baraitser M 1998 Oxford Medical Database: London Dysmorphology Database, Oxford University Press electronic publishing: version 2.10.

Wise, C. A.; Chiang, L. C.; Paznekas, W. A.; Sharma, M.; Musy, M. M.; Ashley, J. A.; Lovett, M.; Jabs, E. W. 1997 TCOF1 gene encodes a putative nucleolar phosphoprotein that exhibits mutations in Treacher Collins syndrome throughout its coding region. Proc. Nat. Acad. Sci. 94: 3110-3115.

Wolff G, Wienker TF, Sander H. 1993 On the genetics of mandibular prognathism: analysis of large European noble families. J Med Genet. 30: 112-6.

Zhang XT, Wang SK, Zhang W, Wang XF. 1990 Measurement and study of the nose and face and their correlations in the young adult of Han nationality. Plast Reconstr Surg. 85: 532-6.

Zhao LP, Aragaki C, Hsu L, Quiaoit F. 1998 Mapping of complex traits by single-nucleotide polymorphisms. Am J Hum Genet. 63: 225-40.

Zumpano MP, Carson BS, Marsh JL, Vanderkolk CA, Richtsmeier JT. 1999 Three-dimensional morphological analysis of isolated metopic synostosis. Anat Rec. 256:177-88

Refs:

Kruglyak L. 1999 Prospects for whole-genome linkage disequilibrium mapping of common disease genes. Nat Genet. 22: 139-44.

Collins A, Lonjou C, Morton NE. 1999 Genetic epidemiology of single-nucleotide polymorphisms. Proc Natl Acad Sci U S A. 96:15173-7.

Wang DG, Fan JB, Siao CJ, Berno A, Young P, Sapolsky R, Ghandour G, Perkins N, Winchester E, Spencer J, Kruglyak L, Stein L, Hsie L, Topaloglou T, Hubbell E, Robinson E, Mittmann M, Morris MS, Shen N, Kilburn D, Rioux J, Nusbaum C, Rozen S, Hudson TJ, Lander ES, et al. 1998 Large-scale identification, mapping, and genotyping of single-nucleotide polymorphisms in the human genome. Science. 280:1077-82.

Schafer A J & Hawkins J R 1998 DNA variation and the future of human genetics. Nature Biotech. 16: 33-39

Whittemore AS, Halpern J 2001 Problems in the definition, interpretation, and evaluation of genetic heterogeneity.
Am J Hum Genet ;68:457-65

Lander ES. 1996 The new genomics: global views of biology. Science. 274: 536-9.

Reed P, Cucca F, Jenkins S, Merriman M, Wilson A, McKinney P, Bosi E, Joner G, Ronningen K, Thorsby E, Undlien D, Merriman T, Barnett A, Bain S, Todd J. 1997 Evidence for a type 1 diabetes susceptibility locus (IDDM10) on human chromosome 10p11-q11. Hum Mol Genet. 6 1011-6.

Spielman RS, McGinnis RE, Ewens WJ.The transmission/disequilibrium test detects cosegregation and linkage. 1994
Am J Hum Genet.; 54, 559-63

Lander ES, Schork NJ.Genetic dissection of complex traits. 1994
Science. 265, 2037-48.

Spence MA and Hodge SE. 1996 Segregation analysis In: Emery and Rimoin's Principles and practice of medical genetics. Rimoin, D L ,Connor J M &Pyeritz R E eds. 3rd edition Edinburgh, Churchill Livingstone.

Lathrop GM, Terwilliger JD &Weeks DE 1996 Multifactorial inheritance and genetic analysis of multifactorial disease In: Emery and Rimoin's Principles and practice of medical genetics *ibid*

Mueller RF &Cook J 1996 Mendelian inheritance In: Emery and Rimoin's Principles and practice of medical genetics *ibid*

Wang M C K 2000 Linkage analysis with qualitative trait In: Introduction to statistical methods in modern genetics. Vol 3 Asian Mathematics Series Ed Yang C-C.Gordon &Breach,Amsterdam.

Wright AF,Carothers AD & Pirastu M 1999 Population choice in mapping genes for complex diseases Nat Genet 23 397-404

Schork NJ, Fallin D, Thiel B, Xu X, Broeckel U, Jacob HJ, Cohen D 2001The future of genetic case-control studies.Adv Genet. 42:191-212.

Urbanek M, Legro RS, Driscoll DA, Azziz R, Ehrmann DA, Norman RJ, Strauss JF Spielman RS & Dunaif A 1999 Thirty seven candidate genes for polycystic ovary syndrome :strongest evidence for linkage is with follistatin, Proc Natl Acad Sci 96 8573-8578.

Clerget-Darpoux F, Bonaiti-Pellie C (1992) strategies on marker information for the study of human diseases. Ann Hum Genet 46: 145-153